The Role of Human Papillomaviruses and their Replication in Nonmelanoma Skin Cancer

Lorna J. Mackintosh

MBChB, MRCP (UK).

This thesis is submitted to the University of Glasgow in accordance with the requirements for the degree of Doctor of Philosophy in the Faculty of Medicine

MRC-University of Glasgow Centre for Virus Research,
Institute of Infection, Immunity and Inflammation,
College of Medical, Veterinary and Life Sciences,
Garscube Estate, Bearsden Road,
Glasgow,
United Kingdom

Submitted October 2011

Abstract

Nonmelanoma skin cancer (NMSC) is the commonest cancer worldwide and is a significant and increasing burden on health care resources. NMSC aetiology is fundamentally linked to sun exposure although infection with oncogenic viruses including Human Papillomaviruses (HPV) is thought to be a cofactor. Fair skinned populations residing in geographical areas with high sun exposure have an increased incidence of NMSC and an excess of NMSC is also observed in certain patient groups including immunosuppressed organ transplant recipients.

This thesis describes the epidemiology of NMSC in the immunosuppressed renal transplant population in the West of Scotland. Clinical samples from this population were investigated for the presence of HPV utilising a PCR reverse hybridisation technique. This assay specifically examined for HPV of the genus Beta that have been previously linked to NMSC.

The effect of presence of HPV in these samples was evaluated through an investigation of the expression of cellular biomarkers. A biomarker expression pattern specific to HPV infected lesions would add further support to the link between HPV and NMSC. Samples were probed for Ki67, p16, p53, MCM2 and MCM5 antigens in addition to novel antigen, Topoisomerase II Beta Binding Protein 1 (TopBP1). TopBP1 is a host cellular protein that is involved in the DNA damage response and is an interacting partner for HPV thus making it a likely candidate for involvement in cutaneous carcinogenesis. A biomarker expression pattern specific to HPV infected NMSC was not identified although aberrant expression of TopBP1 was identified in a subset of skin cancers.

To investigate this novel observation, a molecular investigation of the interaction between TopBP1 and the viral replication factor E2 was carried out, firstly in HPV-16 before extending the work to the cutaneous virus HPV-8. A mutant of HPV-16E2 that failed to bind TopBP1 was generated. Failure to bind TopBP1 resulted in a phenotype exhibiting compromised viral replication. The equivalent mutation generated in HPV-8E2 resulted in an even more compromised replicative phenotype. In addition to this work, gene targets of TopBP1 were also identified by a microarray analysis. This was carried out using MCF7 cells untreated or damaged by ultraviolet radiation (UVR) with endogenous

TopBP1 depleted by SiRNA treatment. These studies showed that TopBP1 is involved in a number of cellular processes and is likely to be involved in controlling DNA damage targets following UVR induced DNA damage.

The work described in this thesis provides further evidence supporting the role of HPV in the aetiology of nonmelanoma skin cancer. Generation of an E2 mutant that fails to bind TopBP1 and exhibits a compromised replication phenotype provides further evidence to support the hypothesis that the E2-TopBP1 interaction is essential for viral replication and therefore the viral life cycle. This work may facilitate the development of anti-viral therapies for HPV-associated disease by targeting HPV DNA replication through disruption of the E2/TopBP1 interaction.

Table of Contents

List of Tables

List of Figures

List of Accompanying Material

Presence of Beta Human Papillomaviruses in non melanoma skin cancer from organ transplant recipients and immunocompetent patients in the West of Scotland. LJ Mackintosh, MNC de Koning, WGV Quint, J ter Schegget, IM Morgan, RM Herd and MS Campo. *Br J Dermatol*. 2009 Jul; 161(1):56-62. Epub 2009 Mar 30

Preface

For Colin, Calum and Iona.

Acknowledgements

I would like to thank my supervisors Saveria Campo, Robert Herd and Iain Morgan for all their support and guidance.

I also thank the members, past and present, of the Papillomavirus Group and the Alan Lyell Centre for Dermatology who have assisted me along the way.

Finally, I thank Colin for his unwavering support and encouragement throughout.

This work was supported by a Clinical Research Training Fellowship from the Medical Research Council, funding from the Chief Scientist Office and the University of Glasgow.

Author's Declaration

I declare that the work described in this thesis was carried out personally unless otherwise stated and has not been submitted in full or in part for consideration for any other degree or qualification.

Lorna J. Mackintosh

October 2011

Definitions

AK	Actinic Keratosis
A (Ala)	Alanine
aa	Amino Acid
N (Asn)	Asparagine
D (Asp)	Aspartic Acid
ATM	Ataxia Telangiectasia Mutated
ATR	ATM Rad3-related
ATRIP	ATR Interacting Protein
Aza	Azathioprine
BCC	Basal Cell Carcinoma
bp	Base Pair
BCA	Bicinchoninic acid
BSA	Bovine serum albumin
BRCT	Breast Cancer susceptibility gene 1 (BRCA1) Carboxyl Terminus
CO_2	Carbon dioxide
Cic	Ciclosporin
CR1	Conserved Region 1
CR2	Conserved Region 2
CMV	Cytomegalovirus
°C	Degree centigrade
DNA	Deoxyribonucleic Acid
DMSO	Dimethyl sulphoxide
DBD	DNA Binding Domain
ddH_2O	Double distilled water
EV	Epidermodysplasia Verruciformis
FT	Full thickness
alphaPV	Genus Alpha Papillomaviruses
betaPV	Genus Beta Papillomaviruses
E (Glu)	Glutamic Acid
GST	Glutathione-S-Transferase
g	Gram
H&E	Haematoxylin and Eosin
HHV-8	Human Herpes Virus 8
HLA	Human Leucocyte Antigen
HPV	Human Papillomaviruses
hTERT	Human Telomerase Reverse Transcriptase
IC	Immunocompetent
IS	Immunosuppressed
IPA	Ingenuity Pathway Analysis
IEC	Intra-epidermal Carcinoma
J/cm^2	Joules per centimetre squared
KS	Kaposi's sarcoma
KC	Keratinocyte Cancers
Kb	Kilobase pairs
KDa	Kilodaltons
LM	Lentigo maligna
LMM	Lentigo maligna melanoma
LCR	Long control region
MHC	Major Histocompatibilty Complexes
MM	Malignant Melanoma

mTORi	Mammalian target of Rapamycin inhibitors
MIS	Melanoma in situ
mRNA	Messenger RNA
μl	Microlitre
Mg	Milligram
Ml	Millilitre
Mm	Millimetre
mM	Millimolar
MCM	Minichromosome maintenance protein
M	Molar
MMF	Mycophenolate Mofetil
nM	Nanometres
NMSC	Nonmelanoma skin cancer
PM-PCR/RHA	One step polymerase chain reaction - reverse hybridisation assay
OTRs	Organ transplant recipients
PV	Papillomavirus
PBS	Phosphate buffered saline
pmol	Picomole
PAGE	Polyacrylamide gel electrophoresis
PCR	Polymerase Chain Reaction
Pred	Prednisolone
PDZ	PSD-95/discs large/ZO-1
qPCR	Quantitative polymerase chain reaction
RTRs	Renal transplant recipients
pRb	Retinoblastoma protein p105Rb
RNA	Ribonucleic Acid
Ser	Serine
siRNA	Small interfering RNA
SCC	Squamous Cell Carcinoma
SBCC	Superficial Basal Cell Carcinoma
TopBP1	Topoisomerase II Beta Binding Protein 1
p53	Tumour suppressor protein, p53
Y (Tyr)	Tyrosine
UV	Ultraviolet
UVR	Ultraviolet Radiation
UVA	Ultraviolet wave length A
UVB	Ultraviolet wave length B
UK	United Kingdom
V (Val)	Valine
Ori	Viral origin of replication
VLPs	Virus Like Particles
V	Volts
v/v	Volume per unit volume
VIN III	Vulval intraepithelial neoplasia III
w/v	Weight per unit volume
XP	Xeroderma Pigmentosum

Chapter 1: Introduction

1.1 Nonmelanoma skin cancer

The incidence of skin cancer in the UK has risen steadily over the last decade and this is largely attributed to changes in the pattern of sun exposure of the population(1). Skin cancer is subdivided into cutaneous Malignant Melanoma (MM) and nonmelanoma skin cancer (NMSC). Nonmelanoma skin cancer accounts for approximately 85% of all skin cancers and of these, the keratinocyte derived cancers, basal cell carcinoma (BCC) and squamous cell carcinoma (SCC) account for at least 80%. The remainder are made up of rarer tumours such as appendageal tumours, cutaneous lymphomas, sarcomas and neuroendocrine tumours.

Skin cancer is very common and accounts for over 20% of all cancer registrations. It is difficult to obtain accurate skin cancer incidence figures, particularly for NMSC, due to underreporting of these cancers. In England and Wales in 2001, the age-standardised incidence rates for NMSC were 65 for females and 96 for males per 100,000 population(1). Although skin cancers are the most common cancers, they account for only 2% of all cancer deaths and of those MM is responsible for over 80%. While NMSC results in few cancer deaths overall, the management of NMSC is a significant and increasing burden on health care resources and is the focus of this thesis.

1.1.1 Aetiology and pathogenesis of NMSC

Exposure to ultraviolet radiation (UVR) results in damage to the DNA of the keratinocytes and is the principal contributing factor to NMSC. Evidence for this is clinical, with the majority of NMSC appearing on photo-exposed skin(2); epidemiological with studies demonstrating an excess of NMSC in areas of high UVR exposure(2) and molecular as demonstrated by the finding of UVR signature mutations in skin cancers(3).

Host susceptibility to NMSC plays a major role in its aetiology. NMSC is associated with increasing age and male sex. Those who are exposed to high levels of UVR through outdoor occupations or through recreational sun exposure are at increased risk. Those with fair skin and poor tanning ability, fair or red hair and light coloured eyes are at greater risk than darker skinned populations.

Migration of populations with these characteristics to geographical areas with high UVR exposure such as Australia has led to elevated skin cancer incidence rates in these patient groups (2). Individuals with certain inherited conditions have specific host genetic mutations associated with an excess of skin cancer. Xeroderma Pigmentosum (XP) is an autosomal recessive condition characterised by defects in DNA repair resulting in severe photosensitivity and increased risk of MM, SCC and BCC (reviewed in (4)).Gorlins syndrome is an autosomal dominant condition characterised by mutations in the tumour suppressor gene PTCH1 and results in the development of multiple basal cell carcinomas (BCC) in childhood and early adulthood with associated skeletal deformities (reviewed in(5)).

There is an interplay between these host determined factors and UVR as well as other environmental factors such as exposure to chemical carcinogens, ionizing radiation, immunosuppression and Human Papillomaviruses (HPV).

The role of both immunosuppression and HPV will be discussed in further detail later.

1.1.1.1 Actinic Keratoses, Intra-epidermal Carcinoma and Squamous Cell Carcinoma

SCC originate from the suprabasal epidermal keratinocytes and the epidermal appendages. SCC may arise *de novo* or from precursor lesions. Actinic Keratoses (AK) are epidermal dysplastic lesions, pre-malignancies that may progress to invasive SCC. Intra-epidermal carcinoma (IEC), also known as Bowen's disease or Bowenoid AK on photo-protected/exposed sites respectively, are considered by most to be a more advanced precursor lesion, again with the ability to progress to invasive SCC.

SCC usually occur on sun-exposed sites in fair-skinned patients and are associated with a chronic UVR exposure pattern, therefore appearing most commonly in the elderly and those with outdoor occupations. SCC typically appear as crusted or keratinising nodules or ulcers on sun exposed skin and may develop in isolation or on a background of actinic keratoses and Bowen's disease. The multiplicity of lesions at differing stages of development reflects field damage to the skin from UVR. SCC may grow rapidly and have the potential to metastasise.

SCC may be associated with germline mutations in patients with XP as discussed above. Somatic mutations may be found in tumour tissue and such mutations are typically UVR signature mutations comprising C-T and CC-TT substitutions. Such mutations have been found in several key genes; tumour suppressor genes p53(6), p16INK4a(7;8) and the oncogene, Ha-*ras* (9).

1.1.1.2 Basal Cell Carcinoma

BCC are thought to arise from the hair follicles. BCC are slow growing tumours which arise *de novo* and metastasise rarely; they cause morbidity as a result of local tissue invasion and destruction. There are a number of clinical subtypes of BCC including nodular, superficial, pigmented and morphoeic /sclerosing. The nodular subtype are the most common, accounting for approximately 80% of BCC, 80-90% of which occur on the head and neck and typically appear as pearly nodules with prominent telangiectasia, rolled edges and central ulceration. Superficial BCC (SBCC) account for approximately 15% of all BCC, they appear as scaly, indurated plaques and occur on the trunk in approximately 50% of cases and are seen with increasing frequency in younger patients (10). The morphoeic/sclerosing subtype typically arises on the head and neck and is the most destructive to local tissue due to invasion of the sub-cutis. BCC appear to be related to a different pattern of UVR exposure than SCC with exposure in childhood and intermittent burning exposure thought to be most significant.

XP patients who have defective DNA repair have an increased rate of BCC as well as other skin cancers. Patients with Gorlins syndrome have a specific increase in BCC as well as associated deformities of the skeleton such as bone cysts. In Gorlins syndrome there is a mutation in the PTCH gene, part of the Sonic Hedgehog pathway, a pathway crucial for normal embryonic development. A variety of mutations in this pathway have been found in up to 70% of sporadic BCC (11).The next most common mutations found in BCC are mutations of the tumour suppressor gene p53 (p53) and these are predominantly UVR signature mutations (12). A mutation at codon 177 has been identified as specific to BCC whereas in SCC there is a specific p53 mutation at codon 278 (13).

Nonmelanoma skin cancers are illustrated in Figure 1.

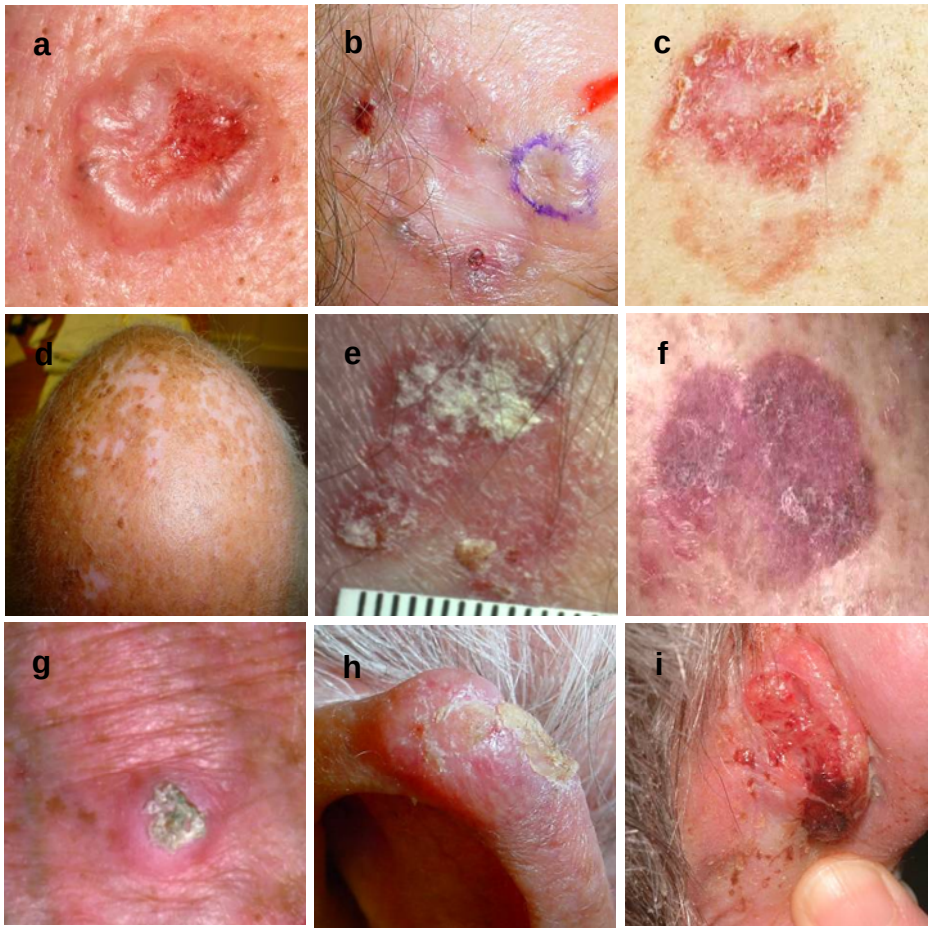

Figure 1 Nonmelanoma skin cancers.

Upper panels demonstrate different types of basal cell carcinomas; (a) nodular, (b) morphoeic and (c) superficial.

Middle panels illustrate premalignant lesions (d) diffuse actinic keratosis on a male scalp (e) close up of actinic keratosis (f) intra-epidermal carcinoma.

Lower panels show a spectrum of invasive squamous cell carcinomas at different stages of development; early keratinising lesion on the (g) dorsum of hand (h) pinna and (i) advanced ulcerated lesion behind the ear.

1.2 Skin cancer and organ transplantation

Patients who are immunosuppressed are at increased risk of skin cancer and one patient group in whom skin cancer is a major clinical problem are organ transplant recipients (OTRs).

There are over one million OTRs worldwide and that number is increasing (14). Patients are now transplanted at an older age and are surviving longer, resulting in an ageing transplant population. Improvements in immunosuppressive regimens and transplant techniques have led to better graft survival both in the short and long term (15) hence the number of patients on long term immunosuppression is increasing. It is now well established that a consequence of long term immunosuppression is an increased risk of cancer.

1.2.1 Epidemiology of skin cancer in organ transplant recipients.

Transplant recipients are reported to have a two to six fold overall increased risk of cancer and the highest risks are for skin cancers, predominantly the keratinocyte cancers (KC) SCC and BCC, Kaposi's sarcoma (KS), anogenital cancers and post transplant lymphoproliferative disorders (16-18). There is also an increased risk of MM and rarer tumours such as Merkel Cell Carcinoma (19;20), sarcomas and appendageal tumours.

This section will focus on the epidemiology of NMSC in OTRs with brief mention of KS and MM.

1.2.1.1 Nonmelanoma skin cancer

SCC and BCC are the most common malignancies occurring in Caucasian transplant recipients(21). In immunocompetent populations, BCC outnumber SCC four fold. The incidence of both SCC and BCC is increased post transplant. The risk is increased two to ten fold for BCC (22-25) and 65-250 fold for SCC (22;26;27). There appears to be an exponential rise in the incidence of SCC post transplantation but a linear rise in BCC (28;29). This has resulted in a reversal of the BCC: SCC ratio in the transplant population. In a study from the Netherlands, the ratio was reversed to 3.6 SCC: 1 BCC (22). Some studies from Southern Europe however report lower SCC: BCC ratios (30-33).

There is variability of risk across reported studies and this appears to reflect differences in ethnicity and skin type of the study population and the climate within which they reside. The highest post transplant KC incidences have been reported from Australia (28;34;35) with cumulative incidence of 75% for patients transplanted for over 20 years (28). Studies from Europe with a similar length of follow up report lower cumulative incidence rates of 30% and 35% in the UK(29) and the Netherlands(22). The incidence of KC increases with the duration of time since transplantation – the cumulative incidence rising from 7% at one year post transplant to 82% after 20 years in one Australian study (36). Following the development of a first SCC, subsequent lesions are common; the cumulative incidence of a second skin cancer being approximately 60-70% in studies from France and the Netherlands (37;38). A Scandinavian study reported that 50% of OTRs will have a second lesion within 3.5 years (27) whilst Liddington et al reported a mean interval of 15 months between first and second cancers in British OTRs and 11 months between second and third lesions (39). Approximately 30-50% of patients with SCC will also have BCC(28;40), many patients have multiple tumours and the number of tumours per patient can be very high; a study from Scandinavia reported two patients with over 100 lesions (41). Whilst the majority of NMSC are curable, in transplant patients, cancers may behave more aggressively and recur more frequently than in immunocompetent patients. SCC recur locally in 13% of OTRs and the risk of metastasis is increased from approximately 3.6 % at three years in the immunocompetent population (42) to 7% in OTRs (43).

1.2.1.2 Cutaneous Melanoma

Most but not all studies report an increased risk for MM in OTRs although the increase is of lower magnitude than that seen for KC. The relative risk of MM is increased by approximately 2-3 fold (17;25;26) although a study in 2006 by Le Mire et al reported an eight fold increased risk of MM in a UK transplant population, the highest reported increased risk in the literature (44).

1.2.1.3 Kaposi's sarcoma

KS are cutaneous and extra-cutaneous tumours associated with Human Herpes Virus-8 (HHV-8) (45) which occur sporadically in populations where HHV-8

infection is prevalent and with increased frequency in immunosuppressed patients. The incidence of KS in OTRs is highest in areas where HHV-8 infection is prevalent. Data published by Penn from the Cincinnati Transplant Tumour Registry found a KS prevalence of 4.3% (46). Further single country studies have found variable prevalence ranging from 0.02 % in the USA(47) to 1.4% in Italy(48) and 5.3% in Saudi Arabia (49). Although the numbers of KS affected OTRs are low in absolute terms the risk is significantly elevated when compared to the immunocompetent population: for example the risk was estimated to be 54 fold higher in the USA and 100 fold higher in Italian OTRs (47;48).

1.2.2 The aetiology of post-transplant skin cancer

The aetiology of post transplant skin cancer is multi factorial and includes host factors such as skin type and environmental factors including sun exposure, immunosuppression and infection with oncogenic viruses.

1.2.2.1 Immunosuppression

Immunosuppressive regimens are highly effective in the prevention of allograft rejection following solid organ transplantation; however potent immunosuppression is associated with an increased risk of malignancy. Immunosuppression contributes to carcinogenesis through a number of mechanisms.

Immunosuppressants prevent allograft rejection by suppressing host immune recognition of allograft antigens but they also cause global dysfunction of cellular and humoral immunity leading to reduced immune surveillance. This may alter the immune systems ability to recognise altered proteins in/on cells that are the consequence of DNA damage and mutation.

Immunosuppressants also have a direct carcinogenic effect. Ciclosporin aids growth of tumours and metastases via increased expression of transforming growth factor ß (50). Azathioprine increases the frequency of tumours in UVR treated mice (51) while its metabolites act as photosensitisers by absorbing light in the UVA spectrum and generating mutations (52). In contrast, the mammalian

Target of Rapamycin inhibitors (mTORi), sirolimus and everolimus exhibit both anti-neoplastic and immunosuppressive properties and regimens incorporating these agents may confer a reduced risk of skin cancer. Sirolimus has been shown to reduce growth and proliferation of cancer cells *in vitro* and inhibit angiogenesis via vascular endothelial growth factor pathways (53). Furthermore sirolimus reduces the pro-carcinogenic effects of ciclosporin when the two agents are combined (54). Everolimus has similar antineoplastic properties to sirolimus however currently available data on mTORi and post transplant malignancy pertain to sirolimus.

1.2.2.2 Oncogenic viruses

Immunosuppressants render the immunosuppressed host vulnerable to infection with oncogenic viruses. OTRs have and increased prevalence of virus- associated cancers including Kaposi's sarcoma (HHV-8) (45), post-transplant lymphoproliferative disorder (Epstein Barr Virus), Merkel's cell carcinoma (Merkel cell polyomavirus) (55) and anogenital cancers (mucosal HPV). NMSC has been associated with genus beta HPV (betaPV) and further discussion on the role of viruses in the aetiology of NMSC will focus on HPV.

1.3 Human papillomaviruses

Papillomaviruses are small, circular, epitheliotropic double-stranded DNA viruses which selectively infect the cutaneous or mucosal epithelia of humans and animals. There are over 100 types of papillomaviruses known to infect humans, HPV.

1.3.1 HPV and Disease

HPV are causative or implicated in a wide variety of benign and malignant diseases. In general, the disease state is closely linked to the virus type and relates to the target epithelia of each virus and its ability to transform infected cells. Over half of the known HPV types infect the genital mucosa and certain types are associated most commonly with disease. HPV may be termed high or low risk in accordance with their prevalence in cancers (56).

1.3.1.1 Benign disease and HPV

A variety of benign conditions have been associated with HPV. The genital HPV types are the cause of condyloma acuminata or genital warts and the most commonly associated types are HPV-6 and -11 (57). These low-risk genital HPV types also cause benign papillomas on other mucosal surfaces. HPV-11 is the most common type found in the childhood condition recurrent respiratory papillomatosis (58) and HPV-6 and -11 are also found in conjunctival papillomas (59).

Infection with low risk cutaneous HPV results in cutaneous warts of which there are a number of clinical types. Certain HPV-types are most closely associated with each disease. Common cutaneous warts are associated with HPV-2, -4, -7, -26, -27, -28 and -29. Butchers warts, occurring on the hands of workers dealing with raw meat and poultry are usually associated with HPV-1, -2, -3, -4 and -7 (60). Filiform warts are associated with HPV-1, -2 or -7 (61) whereas plane warts with HPV-2, -3, -10, -26, -27, -28, -29, -41 (62). On the foot, plantar warts are associated with HPV-1, -2, -60, -63 and -65 (63;64).

1.3.1.2 Cancers and HPV

The high-risk mucosal types HPV-16 and HPV-18 are established causative agents of cervical and other ano-genital cancers. Other high risk types such as HPV-31, HPV-33, HPV-45, HPV-52 and HPV-58 are also found in cervical cancers. These high-risk types have also been isolated from other cancers of the anogenital tract. HPV-16 and -18 have been associated with cancers of the oral cavity, oropharynx and tonsil (64).

On the skin, periungal tumours have been associated with high risk-mucosal types HPV-16 and -18 and it is suggested that these may represent cross-infections from the genital tract (65). Cutaneous HPV types have been found in skin cancers and this will be discussed in greater detail below.

1.3.2 Classification of HPV

HPV belong to the family *Papillomaviridae* and are further classified into genera, species and types(66). The phylogenetic tree of 118 known HPV is illustrated in Figure 2. HPV infecting the genital mucosa, including HPV-16, belong to the genus alpha. HPV implicated in NMSC belong to the genus beta and are known as the betaPV types.

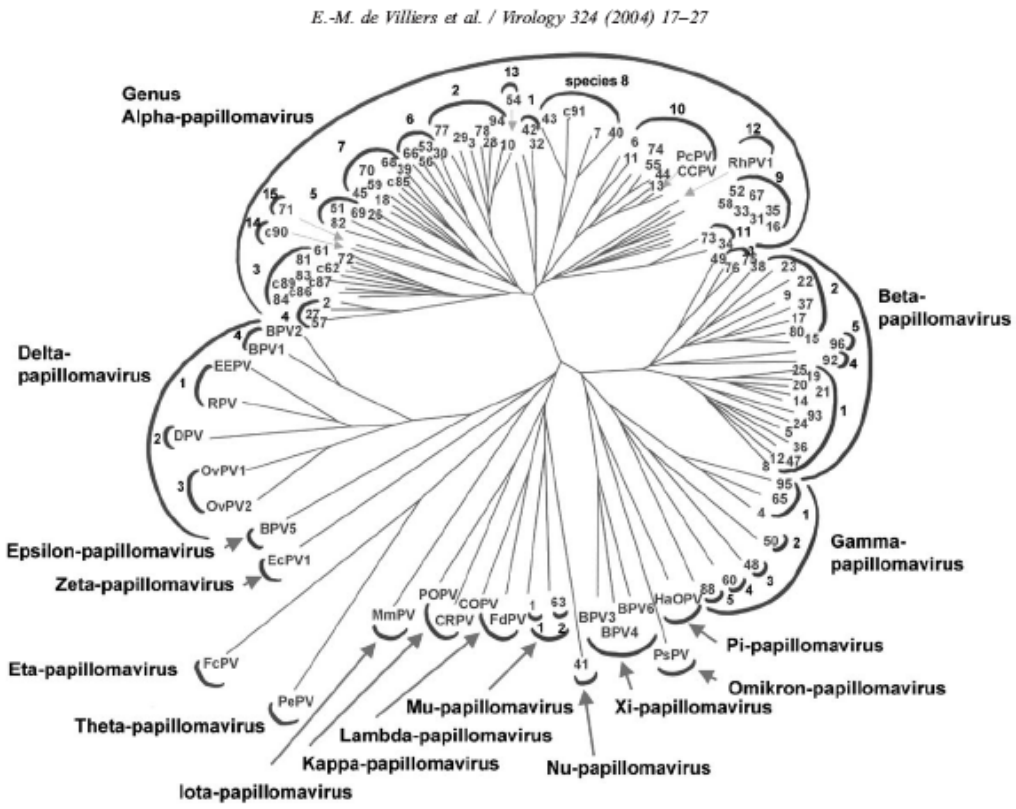

Figure 2 Phylogenetic tree of 118 papillomavirus (PV) types.

The outermost semicircular symbols identify the genera, the inner one the PV species and the PV types are numerical. Abbreviations including letters refer to animal PV types.

From "Classification of papillomaviruses" by de Villiers E.M., Fauquet, C., Broker T.R., Bernard H.U. and zur Hausen H. Virology, 324, 17-27(2004).

1.4 BetaPV and nonmelanoma skin cancer

The main HPV types studied in this project were genus beta papillomaviruses. There are 25 betaPV types (HPV-5, -8, -9, -12, -14, -15, -17, 19, -20, -21, -22, -23, -24, -25, -36, -37, -38, -47, -49, -75, -76, -80 and candidate types -92, -93, -96).

1.4.1 BetaPV were first isolated from patients with Epidermodysplasia Verruciformis

Epidermodysplasia Verruciformis (EV) is a rare inherited skin disease; patients have a defect in cell-mediated immunity which renders them susceptible to infection with HPV. Recently, EV patients have been found to have mutations in two genes – EVER1 and EVER2 (67). EV patients develop multiple flat-topped warts which, on sun-exposed sites, progress to cutaneous SCC in 30% of patients by the third decade (68;69). Specific HPV types have been isolated from both warts and SCC from EV patients. Originally known as the EV-types these HPV are now known as betaPV following the 2004 taxonomic classification of papillomaviruses (66). The clinical features coupled with isolation of betaPV from lesions suggested that betaPV might act as a co-carcinogen in combination with UVR. It is well recognised that transplant recipients have an increased risk of skin cancer and these cancers, similar to EV patients, often develop on a background of numerous warts and keratoses(70) typically on sun-exposed skin. This patient group was therefore of particular interest when a link was sought between betaPV and NMSC not just in EV patients but in the wider population.

1.4.2 Epidemiology of BetaPV infections and nonmelanoma skin cancer

1.4.2.1 BetaPV DNA is found in NMSC from both immunosuppressed and immunocompetent patients.

BetaPV DNA has been isolated extensively in premalignant and malignant skin biopsies from both Immunocompetent (IC) and immunosuppressed (IS) patients. In published studies, there is much variability in the number and type of samples examined, their collection method and the method utilised to detect HPV DNA.

Some methods detect HPV from all genera, others detect only betaPV whilst others detect only specific HPV types and these methods vary in sensitivity. Lack of a consistent method of betaPV DNA detection renders comparison between studies difficult.

There are a number of studies comparing HPV prevalence within SCC biopsies from renal transplant recipients (RTRs) and IC controls within the same study hence using the same detection methods. In these studies, the prevalence of HPV has been consistently higher in RTRs (43%-75%) (71-75) than in IC controls (22-47%) (71-75). Many of these studies have also examined HPV prevalence in IEC, AK, BCC, warts and normal skin; a summary of the results is shown in Table 1.

Similarly, there are a number of studies examining HPV prevalence in SCC biopsies from either RTRs or IC patients and whilst direct comparison between studies is difficult for the reasons discussed above, in RTRs, HPV was detected in 20.8%-91% of SCC (76-82) whilst in IC controls, HPV prevalence appeared lower, ranging from 13%-59.7% (83-88). A summary of the results of these studies is shown in Table 2.

Newer methods for detection of betaPV however such as the broad spectrum, one step, polymerase chain reaction (PCR) reverse hybridisation assay (PM-PCR-RHA) method for detecting all 25 known betaPV types as described by de Koning et al have been used in more recent studies (89). The use of such highly sensitive techniques for detection of betaPV has resulted in detection of betaPV in 81% and 83.7% of SCC samples from IC patients (90;91).

1.4.2.2 BetaPV DNA is isolated in plucked hair and healthy skin samples from both immunosuppressed and immunocompetent patients.

The high prevalence of betaPV in SCC samples lends support to the hypothesis that betaPV is involved in cutaneous carcinogenesis; however betaPV DNA is also detected in normal skin samples.

There are several studies of plucked hair samples, swabs or biopsies of normal skin, where direct comparison is made between RTRs and IC patients. In these studies HPV prevalence is 71%- 94% in RTRs with the highest prevalence in

plucked hair samples (92-95) and is lower in samples from IC patients (35%-80%) with the highest prevalence in normal skin swabs (92-95).

Studies examining HPV prevalence in skin swabs and eyebrow hairs of IC patients only have detected HPV in 35-66% of samples (96-100), again rising to 89%-96% of samples when highly sensitive detection methods are employed (101;102)(Table 3).

These studies demonstrate that HPV is ubiquitous in both immunocompetent and immunosuppressed populations.

1.4.2.3 Serological studies

The link between betaPV and NMSC is also supported by evidence from serological studies of antibodies against betaPV. Most of these studies detect antibodies to the L1 capsid protein of betaPV types. The results of studies until 2006 are reviewed by Casabonne et al (103). These studies looked at the prevalence of antibodies to betaPV types in cases (immunocompetent patients with SCC) and controls (no SCC). Briefly, positive associations were found between SCC cases and seroreactivity to HPV-5(104-106), HPV-8(87;103;105-110), HPV-9(106), HPV-15(87;105;106;108), HPV-20(87;105;106), HPV-23(108), HPV-24(87;105;106), HPV-36(106;108) and HPV-38 (87;105;106).

Recently it has been shown that positive betaPV serology is common in IC patients both with and without SCC. A study across the Netherlands, Italy and Australia of IC patients demonstrated positive betaPV serology in 68% of patients with SCC and 57% in controls, seropositivity was significantly associated with SCC in the Australian cohort. A serological response to HPV-8 was the most frequent and seropositivity to multiple betaPV types was common but the risk of SCC was not significantly associated with the number of positive serotypes(102). Conversely, Struijk et al previously demonstrated that the highest risk of SCC was in those patients with seroreactivity to multiple betaPV types (106).

Similarly positive HPV serology is also common in OTRs. A study of HPV serology in OTRs without skin cancer in two UK centres demonstrated that seropositivity to HPV was common in these patients with 86% of OTRs seropositive for at least one HPV(111). This study detected antibodies to 34 HPV types including alpha

mucosal, alpha cutaneous, beta, gamma and other types; 56% of patients were seropositive to betaPV types, the commonest being HPV-8, HPV-15, HPV-17, HPV-38 and HPV-49(111).

There are two studies in which reactivity to the viral proteins E6 and E7 (discussed in detail later) are reported (87;112). Struijk et al demonstrated that antibodies to both E6 and L1 proteins rarely co-exist and that while L1 positivity was associated with the presence of AK and SCC, E6 positivity inversely correlated to the presence of AK perhaps suggesting that E6 antibodies might protect against SCC or that SCC patients had difficulty in mounting an antibody response to E6 proteins (87). Dang et al examined multiple skin biopsies from four immunosuppressed OTRs comparing tissue betaPV DNA with serological antibodies to the L1, E6 and E7 proteins of betaPV types but found no correlation between the two(112).

1.4.2.4 Summary of the epidemiology of betaPV infections and link to NMSC.

There is a high prevalence of betaPV in SCC from RTRs and IC controls. The seemingly higher prevalence in RTRs may reflect higher infection rates in immunosuppressed patients however use of more sensitive detection methods has led to similarly high levels of betaPV detection in IC patients. It may be that both groups have equally high levels of betaPV infection, it is also possible that viral loads are lower in IC patients and low levels of infection may have been missed by older less sensitive assays.

While these findings might suggest a role for betaPV in NMSC, the high prevalence of betaPV DNA in normal skin suggests that these viruses are ubiquitous. It has been suggested that the hair follicles act as a reservoir for infection and betaPV could be viewed as merely a commensal on the skin. The presence of viral DNA in skin biopsies does not indicate active infection – viral messenger ribonucleic acid (mRNA) would be required for this and if skin samples are stripped to remove the surface layers prior to sampling, reduced HPV DNA is detected in biopsy samples compared to skin swabs again suggesting that HPV may be a contaminant (113).

However it has been shown that the presence of betaPV is significantly associated with NMSC. Prevalence of betaPV DNA in plucked eyebrow hairs is

higher in patients with actinic keratoses than controls (93;97;98) and patients with SCC (99;102) than controls. Additionally, persistence of betaPV infection in eyebrow hairs is associated with an increased risk for the future development of actinic keratoses (114). A comparative study of betaPV DNA prevalence in healthy skin in patients with or without NMSC demonstrated that NMSC is significantly associated with the presence of betaPV types (94).

While HPV-5 and -8 predominate in SCC from EV patients (115), in non-EV patients no high risk betaPV types have yet been identified although there is a suggestion that HPV-5, HPV-8 and HPV-38 are found more commonly in SCC. This is in distinct contrast to alpha mucosal HPV associated with cervical cancer where several high risk types have been identified including HPV-16 and HPV-18.

Clearly the epidemiology of betaPV infection in relation to NMSC differs greatly to the relationship between the high risk mucosal HPV types and cervical cancer. Furthermore, in cervical cancer, high risk mucosal HPV DNA is frequently found integrated into the host genome whereas in cutaneous SCC, betaPV DNA is found in only 1 in 14,000 cells (116). As the major aetiological factor for NMSC is undoubtedly UVR, it may be that betaPV plays a role in potentiating the effects of UVR early in carcinogenesis but is not required for maintenance of the malignant phenotype. This might be supported by the finding of higher betaPV prevalence and viral DNA loads in AK than in SCC (86;116).

HPV is ubiquitous and detection of DNA in normal skin and skin cancers in both immunocompetent and immunosuppressed populations has failed to establish a hierarchy of risk for different betaPV types and their relationship to cutaneous SCC. Furthermore, detection of antibodies to betaPV has also failed to reliably identify high risk betaPV types across studies. Serological responses to betaPV may suggest a clinically significant past or present infection whereas detection of betaPV DNA may be a reflection of the ubiquitous nature of betaPV DNA and not represent active infection. However, the factors which predict a serological response to betaPV are not known. It is possible that development of an SCC may lead to a positive serological response as could a cancer related event such as severe sunburn, a concept known as reverse causality. Recently a study combined both approaches; DNA detection, utilising the skin beta HPV prototype research assay (Diassay BV, Rijswijk, The Netherlands) to detect betaPV DNA in

eyebrow hairs and multiplex serology to detect antibody responses. Using concordant DNA detection and antibodies, this study identified a significant association HPV-36 infection and cutaneous SCC in OTRs and a trend towards positive associations for HPV-5, -9 and -24(117). Future large epidemiological studies utilising this combined approach may be helpful in determining the association between betaPV and SCC.

Author Year/REF	Patients	Method	Predominant HPV genera/ types present	Lesions	Prevalence
Stark 1994(74)	RTR	Southern Blot and type specific PCR, HPV-1,-2,-5,-6,-11,-16,-18		SCC IEC/AK/Warts/NS	43% 33%/42%/79%/16%
	IC			SCC IEC/AK/Warts/NS	22% 23%/25%/100%/8%
Shamanin 1996(73)	RTR	Degenerate PCR		SCC, n=20 IEC/BCC	65% 50%/60%
	IC			SCC, n=26 KA/BCC	31% 50%/36%
Harwood 2000(71)	RTR	Degenerate PCR	betaPV	SCC, n=44 AK+IEC/BCC	84.1% 88.2%/75%
	IC			SCC, n=22 AK+IEC/BCC	27.2% 54.4%/36.7%
Meyer 2003(72)	RTR	Degenerate PCR	betaPV, HPV-1, -2, -4	SCC, n=16 AK+ IEC/NS/Warts	75% 38%/17%/91%
	IC			SCC, n=15 AK+ IEC/NS/Warts	47% 36%/16%/88%
Stockfleth 2004(75)	RTR	Degenerate PCR	betaPV, mucosal PV, (HPV-8 and -18 predominate in SCC from RTR)	SCC, n=16 BCC	75% 50%
	IC			SCC, n=19 BCC	37% 48%

Table 1 List of studies of prevalence of Human Papillomavirus in benign, premalignant and malignant skin lesions.

Inter-study comparison of RTR and IC patients.

Abbreviations:, RTR, renal transplant recipient; IC, immunocompetent; HPV, Human Papillomavirus; SCC, squamous cell carcinoma; IEC, intraepidermal carcinoma; AK, actinic keratoses; NS, normal skin; BCC, basal cell carcinoma; PCR, polymerase chain reaction.

Author Year/REF	Patients	Method	Predominant HPV genera /types present	Lesions	Prevalence
Barr 1989(76)	RTR	Southern Blot	HPV-5, -8	SCC, n=25	60%
Tieben 1994(81)	RTR	Consensus PCR	betaPV	SCC, n=24 IEC/AK/BCC	20.8% 33.3%/28.6%/0%
deJong Tieben 1995(78)	RTR	Broad spectrum PCR	betaPV	SCC AK/BCC	80% 93%/50%
de Villiers 1997(80)	RTR	Nested PCR	betaPV + HPV-1, -2, -4, -10, -27, -57, -63	SCC, n=22 IEC/Keratoses/Warts	91% 91%/65%/100%
Berkhout 2000(77)	RTR	MaHa PCR	betaPV + HPV-2, -3, -10, -27, -28, -29, -57	SCC, n=81 AK/BCC/ Papillomas/Benign/N/S	77.8% 67.9%/35.7% 77.5%/38.5%/32.3%
deJong Tieben 2000(79)	RTR	Nested PCR	betaPV	Keratoses/NS (with vs. without NMSC)	55%/13% vs 53%/0%
Forslund 2007(82)	RTR	Nested PCR	betaPV, species 2 predominate (HPV-15, -23, -38, -80, -17)	SCC, n=82 AK/BCC/Benign/NS	25.6% 22.5%/17.5%/26.1%/12%
Biliris 2000(83)	IC	Degenerate PCR	HPV-8, -18	SCC, n=23 AK/IEC/BCC	13% 25%/40%/31%
Iftner 2003(85)	IC	Degenerate PCR	mucosal, betaPV and cutaneous PV	SCC, n=72 AK+IEC/BCC/Warts/NS	59.7% 60.4%/27.8%/90.9%/4.7%
Pfister 2003(86)	IC	Nested PCR	betaPV	SCC, n=20 IEC/AK, n=114	45% 33%/75%
Caldeira 2003(84)	IC	Type-specific PCR (HPV-38)	HPV-38	SCC, n=26 BCC/AK/NS	46% 55%/32%/10%
Struijk 2006(87)	IC	Type-specific PCR	HPV-5, -8, -15, -20, -24, -38	SCC, n=64 AK/NS	44% 54%/40%
Asgari 2008 (88)	IC	Nested PCR	betaPV	SCC, n=85 Perilesional/NS	54% 53%
Patel 2008(90)	IC	PM-PCR/RHA	betaPV	SCC, n=98 BCC	83.7% 77.6%
Plasmeijer 2010 (91)	IC	PM-PCR/RHA	betaPV	SCC, n=21 Eyebrow hairs/Perilesional/NS	81% 86%/95%/81%

Table 2 List of studies of prevalence of Human Papillomavirus in benign, premalignant and malignant lesions.

Separate studies of RTR and IC patients. Abbreviations: PM-PCR/RHA, one step polymerase chain reaction/reverse hybridisation assay (other abbreviations as for Table 1).

Author Year/REF	Patients	Method	Predominant HPV genera /types present	Lesions	Prevalence
Boxman 1997(93)	RTR IC	Degenerate PCR	betaPV	Eyebrow/arm/leg hairs	92% 53%
Antonsson 2000(92)	RTR IC	FAP PCR	alpha/beta/gamma HPV	Skin swabs (NS)	94% 80%
Harwood 2004(94)	RTR IC	Degenerate/nested PCR	betaPV	Biopsies (NS)	87% 35%
Hazard 2007(95)	RTR IC	FAP PCR	betaPV/gamma PV	Skin swabs (NS)	71-90% 69-71%
Boxman 2000(97)	IC	Nested PCR	betaPV	NMSC/eyebrow hairs	39%/66%
Boxman 2001(98)	IC	Nested PCR	betaPV	Eyebrow hairs males/females	49%/44%
Struijk 2003(99)	IC	Type-specific PCR	HPV-2, -5, -8, 15-, 16-, 20, -24, -38	Eyebrow hairs	63.10%
Antonsson 2003(96)	IC	FAP59/64	alpha/beta/gamma HPV	Skin swabs (NS)	35.70%
Termorshuizen 2004(100)	IC	Type-specific PCR	HPV-5, -8, -15, -20, 24-, 38	Eyebrow hairs/(controls/SCC patients)	44.8%/60.4%
De Koning 2007(101)	IC	PM-PCR/RHA	betaPV	Eyebrow hairs	96%
Bouwes Bavinck 2010(102)	IC	PM-PCR/RHA	betaPV	Eyebrow hairs/ (controls/SCC patients)	89%/93%

Table 3 List of studies of prevalence of HPV in normal skin biopsies, swabs and hairs.

Abbreviations as for Table 1 and 2.

1.5 The Biology of Human Papillomaviruses

1.5.1 The HPV genome

The HPV genome is a double stranded, circular DNA molecule approximately 8 kilobases (Kb) in size. The genome is divided into three regions (i) a region coding for the Early genes E1, E2, E4, E5, E6 and E7, (ii) a region coding for the Late genes L1 and L2 which code for the structural proteins L1 and L2, and (iii) a non-coding region, the long control region (LCR) containing the regulatory elements necessary for the control of viral replication and transcription.

All HPV have a similar genomic organisation as illustrated in Figure 3, except for the E5 gene which is not present in the majority of betaPV (118).

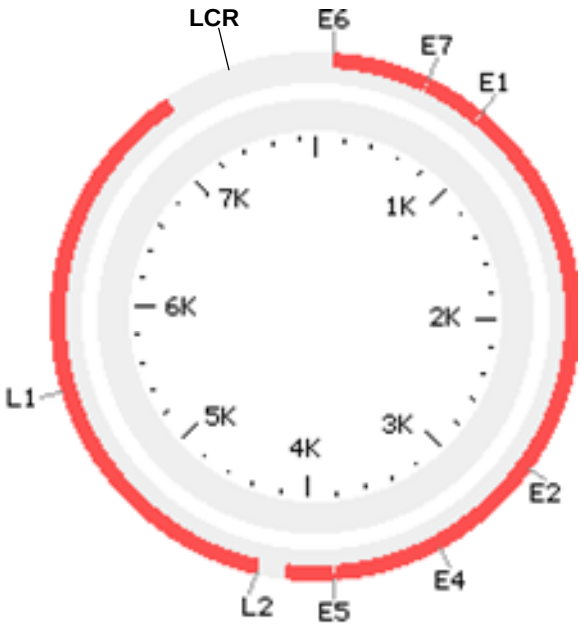

PROTEIN	FUNCTION
EARLY PROTEINS	
E1	Replication
E2	Replication and Transcription
E4	Disruption of cytokeratin networks/cell growth arrest
E5	Transformation
E6	Transformation
E7	Transformation
LATE PROTEINS	
L1	Major capsid protein
L2	Minor capsid protein

Figure 3 The HPV genome.

The HPV genome is a double stranded, circular DNA molecule approximately 8 Kilobases (K) in size. The early region encodes the early genes E1, E2, E4, E5, E6 and E7, the functions of which are summarised in the box on the right. The late region encodes the late genes L1 and L2. The non-coding region known as the long control region (LCR) of upstream regulator region is necessary for control of viral replication and transcription.

1.5.2 HPV life cycle

The HPV life cycle begins when HPV infect the epithelial stem cells by entering the cutaneous or mucosal epithelia via cuts or abrasions (reviewed in (119)). Infected basal cells move into the upper layers of the epithelium where they divide and undergo differentiation. During this phase viral DNA is amplified and the viral genomes are packaged into infectious virions before being released as cells are shed from the upper terminally differentiated layers.

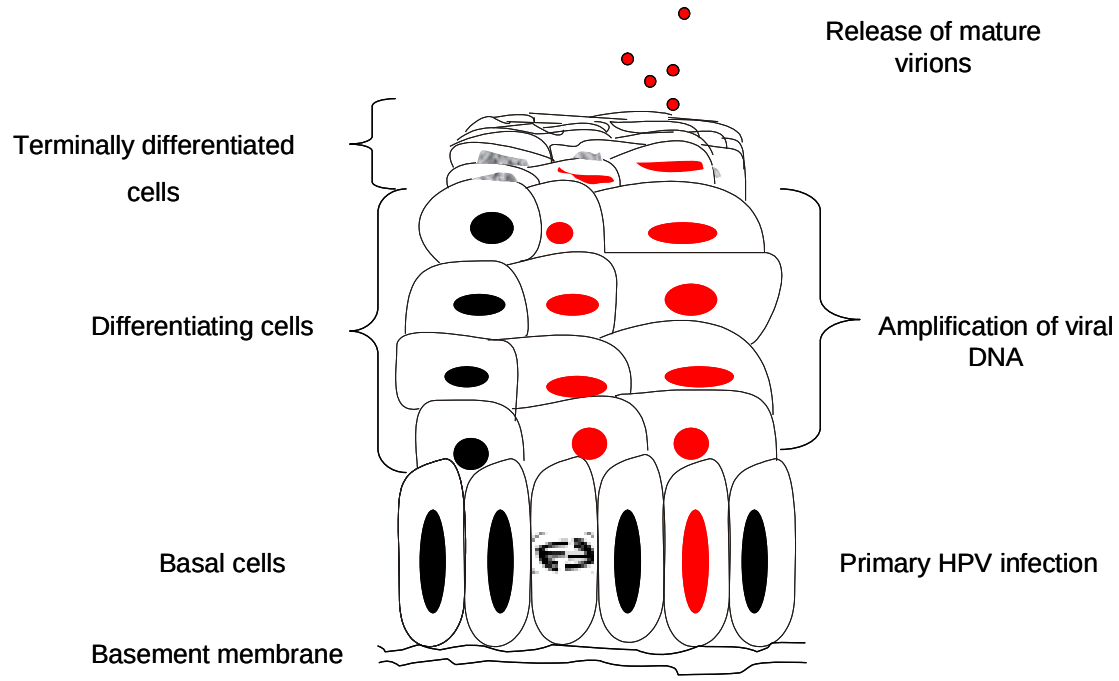

Figure 4 HPV life cycle.

Schematic representation of the HPV life cycle in infected epithelium. Infected basal cells (red) move up through the epithelium, the cells are differentiating, and viral DNA is amplified. In the terminally differentiated uppermost layers, viral genomes are packaged into infectious virions and released as the uppermost cells are shed. Figure adapted from image courtesy of IM Morgan.

1.5.3 Integration of high risk HPV into the host genome

In the normal viral life cycle, HPV genomes are present in a circular or episomal state in the basal cells and there are approximately 50-100 copies per cell (120;121). In the episomal state, expression of the viral oncogenes E6 and E7 is tightly regulated, occurs in the supra-basal cells and allows activation of the host replication machinery such that the viral genomes may be amplified prior to production of virions. As the viral genome is retained in its episomal state, it is destined to be shed from the uppermost epithelial layers and does not pose a carcinogenic threat (reviewed in (122) . If viral oncogenes are expressed in the basal epithelial cells however, this inhibits cell differentiation and induces chromosomal instability that can drive carcinogenesis. In the vast majority of cervical carcinomas, this de-regulation of viral oncogene expression is seen in cells in which the viral genome has become integrated into the host DNA (122). Comparative analysis of HPV DNA status in low and high grade pre-malignant lesions shows that the frequency of viral DNA integration increases with the severity of the disease (123). Integration of the HPV genome occurs only with the high-risk HPV types, and is seen in 100% of HPV-18 positive cervical carcinomas (124-126) and up to 80% of HPV-16 positive cases (125-127).

Integration into the host genome is not a normal part of the viral life cycle. When the viral genome is integrated, several key features are consistently observed, loss of the viral E2 gene (128) and increased expression of E6 and E7 (129). Previous studies have demonstrated that E2 can repress the expression of the E6/E7 genes, therefore integration and loss of E2 results in elevated E6/E7 expression. This increased expression can contribute to the transformation of the infected cell.

1.6 The Biology of Human Papillomaviruses

1.6.1 The major transforming proteins of high risk mucosal HPV

The E6 and E7 gene products are the major transforming proteins. E6 and E7 have developed a number of strategies to evade host immunosurveillance thus allowing viral persistence and to alter control of the cell cycle and apoptosis thus allowing the accumulation of DNA damage and mutations. Often the two proteins target the same pathways albeit by different mechanisms thus the two proteins act synergistically to promote cellular transformation (reviewed in (118)).

While some properties of E6 and E7 are shared between different virus types, some are exclusively associated with the carcinogenic HPV types (130). Of these, the best studied is HPV-16.

In cervical cancer cells, viral DNA is often integrated into the cellular genome and the E6 and E7 proteins are consistently actively expressed (129). Continuous E6 and E7 expression is necessary for maintenance of the malignant phenotype as silencing both genes in cervical cancer cell lines results in cell death due to the reactivation of the p53 and retinoblastoma protein p105Rb (pRb) pathways (reviewed in (131)).

1.6.1.1 The E6 protein

The HPV-16 E6 gene encodes a 151 amino acid protein. E6 has two atypical zinc fingers at the base of which are two motifs containing two cysteines each which are conserved in all E6 types (118). One of the major actions of E6 is its ability to moderate the action of p53 (132).

The role of p53 is to ensure integrity of the cellular genome by delaying the cell cycle and cellular division until DNA damage has been repaired or preventing further cell division by inducing apoptosis. Levels of p53 within the cell increase following stress such as UVR radiation and hypoxia (133). p53 is a transcription factor, and transactivation of target genes by p53 results in arrest of the cell cycle at G1, or apoptosis (134). One of the best known targets of p53 is p21, activation of which results in cell cycle arrest by the inhibition of cyclin

dependent kinases that are necessary for entry into the S phase of the cell cycle (134). Activation of p53 induces apoptosis through many pathways such as transactivation of pro-apoptotic genes such as Bax and PUMA (135).

HPV-16E6 inactivates p53 by accelerating its proteolytic degradation thereby removing its restrictions on the cell cycle and control of apoptosis. This is achieved by forming a complex with the cellular ubiquitin-protein ligase E6AP (136-138). Ubiquitination results in targeting of p53 for proteasomal degradation. Induction of p53 degradation by E6 appears to occur exclusively with E6 from high-risk HPV types (139;140). The ability of E6 to degrade p53 is likely to be a key event in malignant transformation and this has been demonstrated *in vivo* by the expression of E6-binding peptides in HPV-16 positive cells which resulted in the abrogation of p53 degradation and thus induction of apoptosis (141).

HPV-18E6 can also interfere with apoptosis independently of p53 by its association with Bak, a member of the Bcl-2 family. Cellular stress leading to apoptotic signals causes Bak to form pores in the mitochondrial membrane. This results in release of cytochrome C from the mitochondria and induction of the caspase apoptotic cascades (142). HPV-18E6 induces the degradation of pro-apoptotic factor Bak via the ubiquitin –mediated pathway similarly to p53 (143;144).

HPV-16E6 induces activation of telomerase by activating transcription of the hTERT (human Telomerase Reverse Transcriptase) gene (145). Normal somatic cells have very little or no telomerase activity, telomeres shorten as the cell divides until they reach a critical size and the cell reaches senescence (146). High telomerase activity therefore allows HPV-16 infected cells to maintain telomere length and thus proliferate indefinitely leading to cell immortalisation (145).

Another important function of E6 proteins is their ability to interact with proteins containing PDZ (PSD-95/ discs large/ZO-1) domains. PDZ proteins such as DLG, MAGI and MUPP I have all been shown to have tumour suppressor functions (147) and are involved in cell signalling and cell-cell adhesion(148). HPV-18 and HPV-16E6 have been shown to bind and degrade many of the PDZ proteins(149-151).

1.6.1.2 The E7 protein

The HPV-16E7 gene encodes for a 98 amino acid protein. The amino acid terminus has two conserved regions, CR1 and CR2 and a Leu-X-Cys-X-Glu (LXCXE) motif that is necessary for the association between E7 and pRb (152).

One of the main functions of E7 as a transforming protein occurs via its interaction with pRb and its relatives, p107 and p130, a family of proteins also known as the pocket proteins of which pRB is the most studied and this leads to disruption of the cell cycle. This function of HPV-16E7 assists in the viral life cycle; by deregulating the cell cycle, basal epithelial cells begin proliferating and are now able to support viral DNA replication (reviewed in (153)), however disruption of the cell cycle potentially allows the accumulation of DNA damage/mutations.

The Rb proteins act as tumour suppressors by regulating entry into S phase and progression of the cell cycle via modulation of the transcriptional activities of the E2F transcription factors (reviewed in(154)). The active form of pRb is hypophosphorylated. During a normal cell cycle, pRb is cyclically phosphorylated/dephosphorylated. In G1 hypophosphorylated pRb binds to E2F repressing its transcriptional activity. As the cell cycle progresses, pRb is sequentially phosphorylated by cyclin D/cdk4 and cyclin E/cdk2 and cyclin A/cdk2 complexes. By late G1, pRb is hyperphosphorylated, no longer interacts with E2F1, therefore E2F1 is free to act as a transcriptional activator and activates the transcription of many genes that allow progression of the cell cycle through S phase (reviewed in (155)).

HPV-16E7 forms complexes with hypophosphorylated (active) pRB resulting in functional inactivation of pRb and permits the cell to enter S phase thus contributing to the transforming activities of E7(156). HPV-16E7 also destabilises pRb by promoting its proteolysis (157). Furthermore, HPV-16E7 has the ability to directly associate with and activate E2F1 independent of pRb (158).

In addition to targeting the pocket proteins, HPV-16E7 can alter the cell cycle through its interactions with cell kinases that normally have an inhibitory effect on the cell cycle (reviewed in (118)).

1.6.1.3 The E6 and E7 proteins generate genomic instability.

The functions of the E6 and E7 proteins allow the accumulation of DNA damage/mutations. Additional host genomic mutations are necessary however for progression to a malignant phenotype and the development of aneuploidy is specifically associated with high-risk HPV infection *in vivo* (159). Cytogenetic abnormalities have been detected in HPV-immortalized keratinocytes suggesting that HPV oncogene expression may facilitate genomic destabilisation (160) and expression of high risk E6 and or E7 in primary human cells increases genomic instability (161;162). Aneuploidy arises as a consequence of gains or losses of chromosomes during mitosis due to mitotic abnormalities such as lagging chromosomal material, anaphase bridges and multipolar mitoses (163). Multipolar mitoses are hallmarks of high-risk HPV associated cancers (164) and are induced by supernumerary centrosomes that arise during abnormal chromosome segregation during cell division (165). HPV-16E7 induces supernumerary centrosomes by uncoupling centriole synthesis from the cell division cycle causing abnormal centriole synthesis and hence multipolar mitoses (166).

1.6.1.4 E6 and E7 and immune evasion

The majority of women with genital HPV infections clear the infection within 12-18 months however, in a small number, infection persists and these women are at high risk for development of cervical carcinoma (167). There is evidence that E6 and E7 can modulate the host immune response to HPV infection by disruption of the interferon pathway. Type I interferons (alpha and beta) are cytokines secreted by virally infected cells that start a signalling cascade via the Jak-Stat pathway to initiate genes with a range of anti-viral effects (168). Microarray studies have shown that HPV-16 and HPV-31 downregulate the expression of interferon inducible genes (169;170). HPV-16E6 and HPV-16E7 have been shown to interact with Interferon regulatory factor 3 and 1 respectively, interfering with interferon-mediated signalling (171;172).

1.6.2 The transforming proteins of the beta papillomaviruses

In contrast to the extensively studied mucosal HPV types, little is known about the functions of early proteins of the cutaneous HPV types. However there is

emerging evidence to suggest that E6 and E7 of some cutaneous types have some ability to interfere with cell cycle regulation and apoptosis and as such may also act as transforming proteins. It is likely that they act in co-operation with UVR.

1.6.2.1 The E6 protein

To date, none of the cutaneous HPV types studied are able to promote p53 degradation (173-175). However E6 may be able to interfere with p53 functions via other mechanisms. HPV-77E6 selectively attenuates UV induced transactivation of p53 regulated pro-apoptotic genes Fas, PUMA, APAF-1 and PIG-3 leaving other p53 target genes such as those involved in cell cycle regulation unaffected (176). Furthermore the E6 protein from HPV-5 and HPV-77 inhibits UV-induced apoptosis in conditions where p53 is strongly stabilised and activated (175). HPV-38 E6 and E7 expression in keratinocytes induces stabilisation of p53 by promoting the up regulation of an isoform of p73, ΔNp73 which induced transcriptional repression of p53 thus inhibition of p53-responsive gene expression (177).

E6 can interfere with apoptosis via p53 independent mechanisms by association with the pro-apoptotic protein Bak. Bak is a member of the Bcl-2 family. In normal skin, in response to UVR irradiation, Bak is highly stabilised and activated in the epidermis. In the presence of HPV-5, -10 and -77 E6, following UVR, stabilisation of Bak and apoptosis are not observed(144). HPV E6 proteins can stimulate the ubiquitin–ligase mediated degradation of Bak and this interaction has been shown for high risk mucosal HPV-18, low-risk genital mucosal types HPV-11 and -6 and for the betaPV types HPV-5 and -8, and cutaneous types HPV-10 and -77 (143;175;178).

Other functions of cutaneous HPV E6 proteins include interference with DNA repair pathways. HPV-5 E6 has been shown to compromise the repair of UVB induced cyclobutane pyrimidine dimers in epidermal cells (179). HPV-8 E6 binds the XRCC1 protein which is involved in repairing UVR induced single strand breaks in DNA. Failure to repair these can lead to the formation of double strand DNA breaks during DNA replication and thus is a step towards chromosomal instability (180).

1.6.2.2 The E7 protein

The E7 proteins of the mucosal high risk HPV interfere with the regulation of the cell cycle via binding and degradation of pRb. Little is known about the biological properties E7 of the cutaneous viruses. Thus far the only betaPV to have been shown to have similar properties is HPV-38E7 which binds pRb in vitro with the same efficiency as HPV-16E7, promotes destabilisation of pRb in rodent and primary human cells and consistent with this, HPV-38E7 induced transformation in rodent cells. These properties were not shared by HPV-10 and HPV-20 in the same assays (84).

1.6.2.3 Immortalization of primary keratinocytes and mouse models

Further data to support a role for betaPV in cutaneous carcinogenesis comes from studies in primary human keratinocytes and mouse models. Expression of HPV-38E6 and E7 in primary human keratinocytes resulted in an extended lifespan and disruption of senescence and these cells were found to have detectable telomerase activity (84). Primary human keratinocytes expressing HPV-8E7 grown on an organotypic raft were able to migrate and invade into underlying dermis suggesting that HPV-8 may promote an invasive phenotype by degradation of components of the basement membrane and extra-cellular matrix by induction of the extra-cellular proteinases MMP-1, MMP-8 and MT1-MMP. (181).

In studies of transgenic mice expressing the complete early genome of HPV-8, 91% developed benign tumours and 6% developed SCC, in the absence of any treatment with UVR or chemical carcinogens providing evidence of the carcinogenic effect of HPV-8 in vivo(182). The same group then generated transgenic mice expressing HPV-8E2 and 60% developed ulcerated/dysplastic skin lesions in the absence of any UVR/carcinogen and following a single dose of UVR, 87% developed skin tumours with histology similar to aggressive spindle cell SCC suggesting that HPV-8E2 has intrinsic oncogenic potential in vivo (183). Transgenic mice expressing HPV-38E6 and E7 developed epidermal hyperplasia and dysplasia, loss of UVR-induced cell cycle checkpoints and developed a high incidence of papillomas, keratoacanthomas following chemical carcinogenesis compared to controls (184). Transgenic mice expressing betaPV, HPV-20 E6/E7 or genus alpha PV (alpha PV, associated with benign cutaneous warts), HPV-

27E6/E7 were exposed to chronic UVR. Both HPV-20E6/7 and HPV-27E6/7 mice developed epidermal proliferation compared to controls however there was a higher rate of malignant progression to SCC in HPV-20 expressing mice, suggesting that betaPV may play a role in enhancing the carcinogenic potential of UVR (185).

1.6.3 E4 and E5

The HPV-16E5 protein has an additive effect to the transforming properties of E6 and E7 (186;187) and, in conjunction with E7, has the ability to transform mouse fibroblasts (188;189). E5 has also been implicated in immune evasion via alteration of antigen presentation by virally infected cells, via the major histocompatibility complexes (MHC) (Human Leucocyte Antigen (HLA) pathway in humans), to T cells for viral recognition and clearance. In primary cells, expression of BPV-1E5 down regulates MHC Class I complexes (190;191). In the presence of HPV-16E5, cells display decreased levels of surface HLA-A and HLA-B and MHC II molecules are down regulated (192;193).

The E4 protein is translated from spliced mRNA transcripts forming an E1^E4 fusion protein containing the first five residues of E1 fused to the remainder of E4(194). The exact role of E4 in the virus life cycle is not clearly understood. Induction of high levels of E4 is associated with the switch from maintenance of the viral genome in the basal differentiating cells to vegetative genome amplification (195). E4 appears to be essential for viral genome amplification of HPV types -16, -18 and -31(196-198) but may not be necessary for all types such as HPV-11(199). Other functions of E4 include inhibition of the G2 to M transition of the cell cycle (200-202) and promotion of apoptosis by alteration of mitochondrial function (203). E4 is also associated with the collapse of cellular cytokeratin networks and this may facilitate viral release late in the viral life cycle (204-206).

1.6.3 Late capsid proteins

The structure of the viral capsid or virion is consistent across HPV types and is a non-enveloped icosahedral structure of 55nm diameter made up of 72 pentameric capsomeres (207). The capsid is made up of the two late proteins, L1

and L2 which encapsulate the viral genome. L1 is the major structural (capsid) protein of papillomaviruses while L2 is the minor capsid protein. L1 and L2 are expressed in the highly differentiated suprabasal cells of the epithelium (208).

1.6.4 The replication proteins

HPV DNA is replicated within the nuclei of infected epithelial cells using the host cellular proteins that form part of the host replication machinery and the viral early proteins E1 and E2. Viral replication is initiated at the viral origin of replication (ori). HPV ori sequences are approximately 80-140 bp in length and are located in the LCR region of the HPV genome. Ori sequences consist of an E1 protein binding site flanked by multiple E2 binding sites and A/T rich sequences (209).

In order to initiate replication of double stranded DNA, the two DNA strands have to be separated to expose the bases and this process is known as melting. Once the double stranded DNA is melted, DNA helicases unwind the double stranded DNA in front of the replication fork(210). E1 is the viral DNA helicase; it is the only HPV enzyme and is essential for viral DNA replication. E1 melts the DNA and binds and hydrolyses Adenosine Triphosphate (ATP) to unwind the DNA (210).

E2 is the primary ori recognition protein and recruits E1, the viral helicase protein, to the ori (209).

1.6.4.1 Structure and functions of the E1 protein

The HPV-16E1 protein is 649 amino acids in length and forms a dihexameric replicative helicase (211). The E1 protein has three domains; (i) the N-terminal domain, (ii) a central hinge domain and (iii) the carboxyl terminal DNA binding domain (DBD). The carboxyl terminal of the E1 protein has ATPase/helicase activities, interacts with the E2 protein and with the host cellular replication machinery proteins such as DNA polymerase (212;213). The DBD allows E1 to bind to the E1 binding site on the ori. E1 is recruited to ori by E2 where it binds to an E1 binding site in the AT rich region of the ori.

In order to initiate viral replication and elongate the replication fork, E1 also interacts with several proteins that are part of the cellular replication machinery. E1 interacts with DNA polymerase α primase. Polymerase α is the only polymerase able to initiate DNA synthesis so it is essential at the replication fork (212;214). E1 also interacts with the single stranded DNA binding protein complex, replication protein A, a complex essential for the correct initiation and elongation of the DNA replication forks (215). E1 also interacts with Topoisomerase I, proliferating cell nuclear antigen, replication factor C and polymerase δ.

1.6.4.2 Structure and functions of the E2 protein

The E2 protein is approximately 360 amino acids in length and contains three functional domains, (i) the carboxyl terminus DBD, (ii) a central hinge region and (iii) the amino acid terminus (N terminal domain) (216).

The DBD forms homodimers that recognise and bind to palindromic DNA sequences within the ori region of the LCR (217). The N terminal domain is essential for interaction with E1, and a number of host cellular transcription factors and for the transcriptional control of E6 and E7; reviewed in (216).

E2 has important function for both replication and transcription of the virus. There are four E2 binding sites within the LCR of the HPV genome. Following expression E2 binds to these sites and recruits E1 to the ori via a physical interaction between the amino terminus of E2 and the E1 protein. Thus E1 is recruited to ori by E2 and initiates viral DNA replication (218).

E2 regulates the expression of other HPV genes by acting as a transcriptional activator and repressor. It does so by binding, via its DBD, to target DNA sequences on the LCR then activating or repressing transcription from adjacent promoters (reviewed in (216)). The target DNA sequences on the LCR are highly conserved between PV species suggesting that the organisation of the E2 target sequences plays an important role in the regulation of the virus life cycle. E2 interacts with Topoisomerase II β Binding Protein 1 (TopBP1) and this interaction and its consequences for viral DNA replication will be discussed in greater detail later (219).

When the viral genome is integrated into the host genome, this leads to loss of E2 expression and the loss of control of E2 mediated control of E6 and E7 expression (128). Reintroduction of E2 into cervical carcinoma cells lines can repress the expression of E6 and E7 thereby inducing growth arrest and apoptosis via the restoration of the normal functions of p53 and pRb (128;220;221). There is also evidence to suggest that the E2 proteins of high-risk HPV types can induce apoptosis via p53 independent mechanisms (222;223).

E2 also has important functions in the segregation of HPV genomes between daughter cells after cell division. Episomal viral genomes are retained in the nucleus of infected keratinocytes and are segregated between daughter cells during cell division as they are attached to cellular chromosomes in mitotic cells via the E2 transactivator protein which tethers viral DNA onto the mitotic chromosomes (224-227).

A summary of diagram of the main interactions involved in the initiation of viral DNA replication is illustrated in Figure 5.

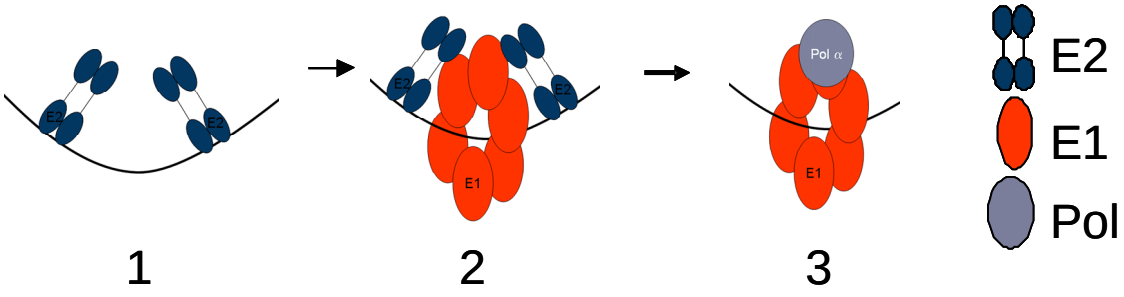

Figure 5 Diagram of initiation of HPV replication.

1. The E2 protein forms homodimers and binds to 12bp palindromic sequences surrounding the A/T rich origin of replication.

2. E1 is recruited to the origin via a protein-protein interaction with E2 whereupon it forms di-hexamers (only one shown for simplicity).

3. E1 has helicase activity and binds to DNA polymerases in order to replicate the viral genome.

Abbreviations; Pol, Polymerase α

1.7 Therapeutic targets for HPV

There are over one hundred types of HPV and these HPV are implicated in many diseases ranging from conditions such as genital and cutaneous warts which whilst benign have implications for healthcare provision, to cervical cancer which is a leading cause of mortality in young women worldwide.

1.7.1 Prophylactic HPV vaccines

1.7.1.1 L1 prophylactic vaccines

The major capsid protein, L1 assembles into virus-like particles (VLPs) and it was this discovery that led to the development of prophylactic vaccines against HPV, potentially one of the most significant public health developments of recent years. VLPs present the epitopes for generating high titre neutralizing antibodies against HPV, they do not contain any viral DNA and they can be produced on a large scale making them ideal candidates for the development of prophylactic vaccines (228). Trials of vaccination with L1 VLPs have been shown to be both immunogenic and safe when administered to women (229-231).

Two prophylactic vaccines have been developed and tested in large multicentre trials. The first is a quadrivalent vaccine, Gardasil® produced by Merck which protects against HPV-6, -11, -16 and -18 (232-234). The other is a bivalent vaccine, Cevarix®, produced by GlaxoSmithKline which protects against HPV-16 and -18 (232;235;236). Both vaccines have proven to be nearly 100% effective in protecting against the virus types to which they are directed, there is a certain degree of cross protection against virus types although the degree of cross protection remains debatable, both vaccines were fully licensed in 2006 (237). In the UK, a national programme to vaccinate girls ages 12-13, along with a catch up programme vaccinating girls ages 14-17, commenced in September 2007. The vaccine used in the UK programme is Cevarix ®.

1.7.1.2 L2 prophylactic vaccines

Whilst L1-VLP based vaccines are type specific, vaccines based on the minor capsid protein, L2 have been shown to elicit antibody responses against a broad

spectrum of HPV types (238;239). As these vaccines are directed against linear L2 epitopes, such vaccines are peptide based and are likely to be cheaper to produce with longer shelf lives(240). It remains to be seen whether these vaccines prove useful in clinical development and trials.

1.7.2 Limitations of available L1 prophylactic HPV vaccines

While it is anticipated that the introduction of prophylactic vaccination programmes should lead to a reduction in the incidence of HPV-related genital diseases including cervical, vulvar and vaginal cancers, it is clear that the currently available prophylactic HPV vaccines have several limitations.

Prophylactic vaccines are type specific and therefore do not protect against all high risk HPV types. Over time other high risk mucosal HPV types may become more prevalent and take over from HPV-16 and HPV-18 as the leading causes of cervical cancer. There is ongoing work into the development of a prophylactic vaccine against all high risk mucosal types (207).

The production of VLPs occurs in eukaryotic cells and is very expensive and the vaccine must be transported and stored at low temperatures. Both these factors are likely to impact on the delivery of these vaccines in developing countries where the burden of HPV disease is highest and there are no cervical cancer screening programmes (207).

Prophylactic vaccines do not treat existing HPV infections. Women already infected with HPV-16 and HPV-18 are still vulnerable to cervical cancer and will remain so for the rest of their lives. Strategies for the treatment of those already infected with HPV, such as therapeutic vaccines and other anti-viral agents must be explored.

Finally, the prevention and treatment of other HPV associated diseases including head and neck cancers and nonmelanoma skin cancers is not addressed by the currently available prophylactic vaccines. In the case of NMSC, where no predominant HPV type has been implicated, then prophylactic vaccines may not be the answer; instead a therapeutic approach may be needed.

1.7.3 Therapeutic vaccines

Therapeutic vaccines against HPV-associated cancers would in theory reduce the incidence of such cancers immediately while it will take some time before a fall in the incidence of cervical cancer is observed as a result of prophylactic vaccination programmes. Potential targets for therapeutic vaccines would be E6 and E7 which are expressed in both pre-malignant and malignant lesions.

HPV-16E6/E7 derived therapeutic vaccines have been tested in a small group of patients with cervical cancer in whom they led to expansion of HPV-16 specific CD4+ and CD8+ T cells (241). These vaccines have also been tested in women with high grade HPV-16 associated vulval intraepithelial neoplasia and induced a HPV-16 specific immune response as well as a promising clinical response (242).

A number of other strategies for the development of therapeutic vaccines are being developed (reviewed in (240)) but as yet there are no available licensed therapeutic HPV vaccines.

1.7.4 Anti-viral therapies for HPV associated disease

There are currently no drugs for HPV related disease that directly target the viral life cycle. One way to therapeutically target HPV would be to interfere with viral replication.

There are inhibitors of E1 but they do not work well and they do not work across types (243). Disruption of the E1/E2 interaction by small molecule inhibitors has proven successful for HPV-6 and HPV-11 but the usefulness of such inhibitors is limited as they do not work effectively against different HPV types due to subtle differences in the interaction of the E1/E2 proteins and therefore have not been developed for clinical use (244). Therefore one way to identify novel targets to disrupt the virus life cycle is to focus on the interactions between the viral replication proteins and host interacting proteins. In comparison with the viral E1/E2 interaction, it is likely that interactions between viral and host proteins should be conserved across HPV types suggesting that targets studied in HPV-16 for example may also be effective in disrupting the virus life cycle of cutaneous types. Little is known about the cellular proteins that interact with E1/E2 to initiate viral replication. TopBP1 was identified as a novel interacting partner for

HPV-16E2 in the Morgan laboratory (245). Subsequently this laboratory has shown that TopBP1 also interacts with HPV-16E1 (unpublished data) making the TopBP1/E1/E2 interaction a potential target for disruption of HPV replication.

TopBP1 is studied in this thesis as an interacting partner for HPV using HPV-16 as a model system and extending that work to the cutaneous type HPV-8.

The structure and functions of TopBP1 are described below.

1.8 Topoisomerase II β Binding Protein 1 (TopBP1)

Topoisomerases are enzymes that catalyze structural changes of DNA. Topoisomerase II is essential for replication and segregation of chromosomes in yeast and Topoisomerase IIβ performs similar functions in mammalian cells. TopBP1 is an essential nuclear protein which was identified as an interacting partner for Topoisomerase II β using a yeast two hybrid assay (246).

Much of what is known of the function of TopBP1 comes from studies of TopBP1 homologues in other organisms namely the fission yeast *Schizosaccaromyces Pombe* (Rad4), budding yeast *Saccharomyces Cerevisiae* (Dbp11), *Drosophila melanogaster* (Mus101), *Xenopus laevi* (XTopBP1) and *Caernohabitis elegans* (F37D6.1).

1.8.1 Structure of TopBP1

TopBP1 is a large (1435 amino acid (aa)) nuclear protein which contains eight BRCT domains (Breast Cancer susceptibility gene 1 (BRCA1) Carboxyl Terminus) (247). BRCT domains are found in proteins involved in DNA repair and cell cycle checkpoints. No other protein has as many as eight BRCT domains suggesting that TopBP1 is an important DNA repair protein and aberrant expression of TopBP1 protein has been identified in breast cancers (248) whilst polymorphisms in the TopBP1 gene have been associated with familial breast and ovarian cancers (249).

1.8.2 Functions of TopBP1

1.8.2.1 TopBP1 and DNA damage repair

A number of cellular proteins function to sense DNA damage and initiate the DNA damage cascade such as BRCA1, PML and Rad9. The nuclear protein TopBP1 is recruited to sites of DNA damage (250) possibly by direct interaction with damaged DNA or by recruitment via Rad9 (251;252). Having localised to DNA damage sites, TopBP1 signals that damage has been detected in order to initiate the cellular DNA damage cascade. To do this, TopBP1, interacts with the ATR (ATM and Rad3-related)-ATRIP (ATR interacting protein) complex, activating ATR and allowing phosphorylation of downstream targets such as Chk1 (253-257). The ATR pathway is activated by UVB (reviewed in (258)) thus it is likely that TopBP1 is involved in regulating the response of keratinocytes to UV.

1.8.2.2 TopBP1 and DNA replication initiation

TopBP1 plays a role in the initiation of DNA replication. The Xenopus homologue of TopBP1, Xmus 101 is essential for the initiation of DNA replication in Xenopus nuclear extracts where it plays a role in loading the initiation complex onto DNA (259). In mammalian cells, there is some evidence to suggest that TopBP1 is essential for an intact S phase and that it plays a key role in monitoring genome integrity through S phase(260). However it appears that TopBP1 depletion by small interfering RNA (siRNA) does not inhibit replication in all cells (255;261).

1.8.2.3 TopBP1 as a transcription factor

There is also evidence to suggest that TopBP1 may act as a regulator of transcription. The transcription factor E2F1 coordinates cell cycle progression; TopBP1 directly interacts with E2F1 via BRCT6 following DNA damage thereby repressing E2F1 transcriptional activity, induction of S-phase entry and apoptosis (262;263). TopBP1 also acts as a transcriptional repressor for the Miz1 protein therefore regulating the function of c-Myc(264). TopBP1 can also act as a transcriptional activator. TopBP1 can co-activate the transcription of the HPV-16E2 protein (219) and also with the c-Ets protein (265). Studies have identified several TopBP1 domains that can both activate or repress transcription(266).

1.9 Research Aims

The scope of this thesis is wide ranging and will look at several aspects of HPV-associated non-melanoma skin cancer from delineating the extent of the clinical problem, identifying the extent of betaPV infection in our population and looking at ways in which the role of betaPV in NMSC could be further clarified.

The work of this thesis will then take a molecular approach looking at potential therapeutic targets to disrupt the virus life cycle using HPV-16 as a model system before extending the work to the betaPV type, HPV-8.

This thesis has five main aims:

(i) To investigate the epidemiology of nonmelanoma skin cancer in the West of Scotland renal transplant population.

(ii) To identify the spectrum of betaPV found in NMSC from the West of Scotland renal transplant population.

(iii) To identify whether expression of cellular biomarkers in NMSC biopsies differentiate between HPV-associated and non HPV-associated NMSC.

(iv) To characterise the interaction between E2 and TopBP1 a potential target for interruption of the viral life cycle in HPV-associated disease.

(v) To investigate the relationship between UVR and TopBP1.

Chapter 2: Materials and Methods

2.1 Materials

The materials used in this thesis including the manufacturer and distributors details where applicable are given in this section.

2.1.1 Tissue samples

The methods used to collect the tissue samples are described in detail in section 2.2.2.

2.1.2 Materials for HPV genotyping

DDL Diagnostic Laboratories, Voorburg, the Netherlands

Reverse hybridisation assay for the identification of skin (beta) human papillomavirus genotypes - KI00062 v 0.5 RHA KIT skin (beta) HPV

2.1.3 Materials for Immunohistochemistry

2.1.3.1 Antibodies

Dako UK LTD (Cambridgeshire, United Kingdom)

Envision + System-HRP labelled polymer, Anti-Rabbit – Catalogue Number: K4003

Envision + System-HRP labelled polymer, Anti-Mouse – Catalogue number: K4001

KI67 Monoclonal mouse Anti-Human Ki-67 antigen, clone MIB-1 - Catalogue Number: M724001-2

Novocastra (Newcastle, United Kingdom)

p53, rabbit, polyclonal anti-human p53, clone CM-1 – Catalogue Number: NCL-p53-CM1

Panomics (California, United States of America)

MCM2 – Mouse anti-human MCM2, Clone SPM196 – Catalogue Number: E5184

MCM5 – Mouse anti-human MCM5, Clone SPM197 – Catalogue number: E5194

TopBP1 polyclonal antibody R1180 against amino acids 861-1287 was raised in a rabbit. The methods of preparation of the antibody and the pre-immune have been described by Boner *et al* 2002(219).

2.1.3.2 Chemicals and reagents

Institute of Comparative Medicine (University of Glasgow, United Kingdom)

Haematoxylin – Gills Haematoxylin (Triple Strength) 500ml - (345ml distilled H_2O, 125ml Ethylene Glycol, 3g Haematoxylin, 0.3g Sodium Iodate, 26.40g Aluminium Sulphate, 30ml Glacial Acetic Acid)

Eosin – Potts Eosin - (25g Eosin, 250ml saturated aqueous pioric acid, 2000ml distilled H_2O, 12.5g potassium dichromate, 250ml Absolute Alcohol)

Sigma- Aldrich Company Ltd. (Dorset, UK)

Tween 20 (Polyoxethylene sorbitan nonolaurate) - Catalogue Number: P1379

Tris Base (2-Amino-2-(hydroxymethyl)-1, 3-propanediol) – Catalogue Number: T6066

Vector Laboratories Ltd (Peterborough, United Kingdom)

Vectabond™ Reagent – Catalogue Number: SP1800

2.1.3.3 Kits

Dako UK LTD (Cambridgeshire, United Kingdom)

CINtec ™ p16INK4a Histology Kit – Catalogue Number: K533611-2

DakoCytomation Envision® + System-HRP (DAB) Kit (Mouse) – Catalogue Number: K4007

DakoCytomation Envision® + System-HRP (DAB) Kit (Rabbit) – Catalogue Number: K4011

Washbuffer, Concentrated X 10 for Immunocytochemistry- Catalogue Number: S300685-2

2.1.3.4 Miscellaneous

Leitz Wetzlar microscope

Prestige

Prestige microwave pressure cooker

Sharp

Microwave oven

Thermo (Cheshire, United Kingdom)

Glass coverplates and microscope slides– Catalogue Number: 72110013

2.1.4 Materials for Molecular Biology

2.1.4.1 Antibodies

Abcam (Cambridge, United Kingdom)

Anti-c-myc antibody, mouse monoclonal antibody – Catalougue Number: ab32

Amersham Biosciences (part of GE Healthcare, Buckinghamshire, United Kingdom)

Anti-mouse IgG peroxidase-linked whole antibody developed in sheep - Catalogue Number: NXA931

Anti-rabbit IgG, peroxidase-linked species specific whole antibody (from donkey) - Catalogue Number: NA934

Cell Signalling Technology (New England Biolabs UK Ltd, Hertfordshire, United Kingdom)

Phospho-Chk1 (ser317) polyclonal antibody developed in rabbit – Catalogue Number: 2344

Phosphor-Chk1 (ser 345) polyclonal antibody developed in rabbit – Catalogue Number: 2341

Cancer Research UK (CRUK, London, United Kingdom)

TVG 261 anti-HPV16E2 antibody developed in mouse was purchased from CRUK.

Sigma- Aldrich Company Ltd. (Dorset, UK)

Anti-Rabbit IgG (whole molecule) peroxidase developed in goat – Catalogue Number: A6154

Monoclonal Anti-γ-Tubulin antibody produced in mouse, clone GTU-88 – Catalogue Number: T6557

Anti-FLAG polyclonal IgG antibody developed in rabbit – Catalogue Number: F7425

TopBP1 polyclonal antibody R1180 against amino acids 861-1287 was raised in a rabbit. The methods of preparation of the antibody and the pre-immune have been described by Boner *et al* 2002(219).

2.1.4.2 Bacteriology

Becton Dickinson Labware (Oxford, United Kingdom)

15ml polypropylene tubes – Catalogue Number: 348206

50ml polypropylene tubes - Catalogue Number: 358206

20ml sterile syringes - Catalogue Number: 301031

BD Bacto™ Agar - Catalogue Number: 214010

Bibby Sterlin Ltd (Staffordshire, United Kingdom)

90mm bacteriology petri dishes - Catalogue Number: 502014

Invitrogen Ltd (Paisley, United Kingdom)

Subcloning efficiency ™ DH5α™ chemically competent cells - Catalogue Number: 18265

S.O.C medium – Catalogue Number: 15544-034

Sigma Chemical Co. Ltd. (Dorset, United Kingdom)

Ampicillin - Catalogue Number: 10047

Luria Broth (LB-Broth) (1 litre: 20g dissolved in ddH_2O) – Catalogue Number: L3022

Luria Bertai agar (LB agar) (1 litre: 35g dissolved in ddH_2O) – Catalogue Number: L2897

2.1.4.3 Cell Lines

HaCaT cells are spontaneously immortalised human adult keratinocytes as described in (267)**.**

Human Embryonic Kidney 293T (HEK293T) are derived from the 293 cell line in which the SV40 T-antigen was inserted. These cells were a kind gift from Dr. Brian Willet, University of Glasgow.

MCF7 cells derived from a human Caucasian breast adenocarcinoma were purchased from Cancer Research UK (CRUK, London, United Kingdom).

U2OS are an osteosarcoma cell line, expressing wild type p53 and were purchased from Cancer Research UK (CRUK, London, United Kingdom).

U2OS B3 are U2OS cells that stably express HPV-16E2. The method used to prepare this cell line has been described by Taylor et al 2003 (268).

U2OS 4.1 are U2OS cells that stably express HPV-16E2N89YE90V and were prepared using the methods described to prepare the B3 cell line (268).

2.1.4.4 Chemicals and Reagents

Amersham International PLC (Buckinghamshire, UK)

Enhanced Chemiluminescence (ECL) Plus™ Western Blotting detection reagents – Catalogue Number: RPN2133

Hyperfilm X-ray film – Catalogue Number: 93184

Applied Biosystems (Warrington, United Kingdom)

Hi-Di™ Formadide - Catalogue Number: 4440753

Eurogentec Ltd (Southampton, United Kingdom)

Agarose - Catalogue Number: EP-0010-05

GE Healthcare (Buckinghamshire, United Kingdom)

Glutathione Sepharose 4 Fast Flow, Catalogue Number: 28104

Thrombin, 500U – Catalogue Number: 27-0846-01

Isopopyl-β-D-1-thiogalactosidase (IPTG) - Catalogue Number: 15502

Promega (Southampton, United Kingdom)

Deoxynucleotide Triphosphates (dNTPs)

dATP, 100mM - Catalogue Number : U120A

dGTP, 100mM - Catalogue Number: U121A

dCTP, 100mM - Catalogue Number: U122A

dTTP 100mM - Catalogue Number: U123A

Roche Applied Science (Hertfordshire, United Kingdom)

Complete Protease Inhibitor Cocktail Tablets - Catalogue Number: 11836145001

TritonX-100, Catalogue Number - 10789704001

Sigma-Aldrich (Dorset, United Kingdom)

3',5',5"-Tetrabromophenolsulfophethalein (Bromophenol Blue) – Catalogue Number: B0126

4-(2-hydroxyethyl) piperazine-1-ethanesulfonic acid (HEPES) – Catalogue Number: H4034

3-Hydroxy-4-(2-sulfo-4-[4-sulfophenylazo] phenylazo)-2, 7-naphthalenedisulfonic acid sodium salt (Ponceau S) – Catalogue Number: P7170

Acetic acid sodium salt (Sodium acetate) – Catalogue Number: S2889

Bicinchonoinic Acid (BCA) solution - Catalogue Number: B9643

Boric Acid – 99% - Catalogue Number: B9643

Copper (II) sulphate (pentahydrate 4% (w/v) solution) - Catalogue Number: C2284

Cycloheximide ready made 100mg/ml solution– Catalogue Number: C4859

Ethidium Bromide 10mg/ml - Catalogue Number: E-1510

Nonidet P-40 (NP40) – Catalogue Number: I8896

Phenol: Chloroform: Isoamyl Alcohol 25:24:1 saturated with 10mM Tris, pH8.0, 1mM EDTA - Catalogue Number: P3803

Tween 20 (Polyoxethylene sorbitan nonolaurate) - Catalogue Number: P1379

Tris Base (2-Amino-2-(hydroxymethyl)-1,3-propanediol) – Catalogue Number: T6066

University of Glasgow Stores (Glasgow, United Kingdom)

Crude Ethanol

VWR International (Leicestershire, UK)

Absolute 99.7-100% AnalaR® ethanol - Catalogue Number: 10107EP

AnalaR® D-(+)-Glucose – Catalogue number: 101176K

AnalaR® Methanol - Catalogue Number: 10158FK

AnalaR® Potassium Chloride – Catalogue Number: 437023F

AnalarR® Sodium dodecyl sulphate (SDS) - Catalogue Number: 108073J

Crystal Violet - Catalogue Number: 340245L

Dimethyl sulfoxide (DMSO) - Catalogue Number: 8029122500

Ethylene diamine tetra acetate (EDTA) disodium salt – Catalogue number: 30031.294

Hydrochloric acid – Catalogue Number: 101252F

Propan-2-ol (Isopropanol) Molecular Biology Grade - Catalogue Number: 437423R

2.1.4.5 Enzymes and Buffers

Cambrex Bioscience (Wokingham, United Kingdom)

Takara DNA Ligation Kit (version V) - Catalogue Number: 6022

Invitrogen Ltd (Paisley, United Kingdom)

*Bam*H1 and REact® 3 Buffer – Catalogue Number: 15201-023 and Y9004

*Eco*R1 and REact® 3 Buffer – Catalogue Number: 15202-013 and Y9004

Xho1 and REact® 2 Buffer – Catalogue Number: 1523-012 and Y92500

Magnesium Sulphate - 50mM Catalogue Number: 52044

Platinum ® P*fx* DNA polymerase - Catalogue Number: 11708-013

P*fx* Amplification Buffer (10x) - Catalogue Number: 52806

New England Biolabs (Hertfordshire, United Kingdom)

Bovine Serum Albumin 100x - Catalogue Number: B9001S

Dpn1, 20,000U/ml - Catalogue Number: R0176L

Exonuclease III, 100,000U/ml – Catalogue Number: M0206L

NEBuffer 1 – Catalogue Number: B7001S

NEBuffer 3 - Catalogue Number: B7003S

Roche Products Ltd (Hertfordshire, United Kingdom)

Shrimp Alkaline Phosphatase – Catalogue Number: 11370400

Shrimp Alkaline Phosphatase Dephosphorylation Buffer (10x) – Catalogue Number: 70092921

2.1.4.6 Kits

Ambion (Applied Biosystems, Warrington, United Kindom)

DNA-free™ Kit – Catalogue Number: AM1906

RNase-Zap – Catalogue Number: AM9780

Applied Biosystems (Warrington, United Kingdom)

ABI Prism BigDye Terminator v 3.1 Cycle sequencing kit - Catalogue Number: 4336915

Invitrogen (Paisley, United Kingdom)

Purelink® HiPure plasmid maxiprep kit – Catalogue Number: K210006

NuPage® 4-12% Bis-Tris 12 well 1.0 mm gels – Catalogue Number: NP0302BOX

NuPage® 4-12% Bis-Tris 10 well 1.0 mm gels – Catalogue Number: NP0301BOX

NuPage® Antioxidant – Catalogue Number: NP0005

NuPage® MES SDS Running buffer (20X) – Catalogue Number: NP0002

NuPage® Sample Reducing Agent (10X) – Catalogue Number: NP0009

NuPage® LDL Sample Buffer (4x) – Catalogue Number: NP0007

NuPage® Transfer Buffer (20X) – Catalogue Number: NP0006

Novagen (Merck Chemicals Ltd., Nottingham, United Kingdom)

KOD DNA Polymerase Kit (containing KOD DNA Polymerase 2.5U/µl, 10X KOD DNA polymerase buffer, 25mM $MgCl_2$, 2mM dNTPs) - Catalogue Number: 71085

Promega Ltd (Southampton, United Kingdom)

Luciferase assay system – Catalogue Number: E1500

Reporter Lysis Buffer (5x solution) – Catalogue Number: E3971

Qiagen Ltd (Crawley, United Kingdom)

Qiaquick PCR purification Kit (50) – Catalogue Number: 28104

QiaPrep Spin Miniprep Kit (50) - Catalogue Number: 27104

QIAquick Gel Extraction Kit - Catalogue Number: 28704

RNeasy® Mini Kit (50) - Catalogue Number: 74104

Stratagene (Agilent Technologies UK Ltd, Cheshire, United Kingdom)

Brilliant® QPCR Master Mix – Catalogue Number: 600549

2.1.4.7 Miscellaneous

Applied Biosystems (Cheshire, United Kingdom)

7500 Real time PCR system and sequence detection software, Version 1.2.2 – Catalogue Number: 4351104

3130X1 Genetic Analyzer, 16 capillary DNA sequencer

MicroAmp optical 8 cap strip – Catalogue Number: 4323032

Astec Microflow Ltd (Hampshire, United Kingdom)

Microflow PCR workstation – Model: OMN-007

Elkay International (Basingstoke, United Kingdom)

1.5ml microcentrifuge tubes with attached cap – Catalogue Number: MICR050

0.5ml microcentrifuge tubes with attached cap – Catalogue Number: MICR051

Plastic Pasteur Pipettes – Catalogue Number: P511

Invitrogen Ltd (Paisley, UK)

iBlot® Gel Transfer Device – Catalogue Number: IB1001UK

iBlot® Gel Transfer Stack Mini (Nitrocellulose) – Catalogue Number: IB301002

iBlot® Gel Transfer Stack regular (Nitrocellulose) – Catalogue Number: IB301001

Kimberley Clark (Brighton, United Kingdom)

Safeskin Disposable Purple Nitrile Exam Gloves – Catalogue Number: 014602

Morrisons Supermarket (Anniesland, United Kingdom)

Marvel dried skimmed milk

Nunc™ Part of Thermo Fisher Scientific (Hereford, UK)

96 well Fluoro flat bottom microplate – Catalogue Number: 236108

Scientific Laboratory Suppliers (Lanarkshire, United Kingdom)

Syngene GeneFlash System Complete – Catalogue Number: MOL5380

Sigma-Aldrich (Dorset, United Kingdom)

Albumin from bovine serum lyophilized powder, ≥96% (agarose gel electrophoresis) – Catalogue Number: A9647

Protein A Sepharose® 4B, Fast Flow Beads – Catalogue Number: P9424

Thermo Labsystems Corporation (Warwickshire, United Kingdom)

Luminoskan Ascent Luminometer and Ascent Software (version 2.4.2)

Multiskan Acent Reader and Software.

ThermoScientific (Hampshhire, United Kingdom)

ABgene® PCR plates – Catalogue Number: AB-0600

2.1.4.8 Molecular weight markers

Invitrogen Ltd (Paisley, UK)

100bp DNA Ladder - Catalogue Number: 15628-050

1Kb DNA Ladder – Catalogue Number: 15615

See Blue® Pre-stained protein standard – Catalogue Number: LC5925

2.1.4.9 Plasmids

pGL3 control contains the SV40 promoter and enhancer sequences driving the expression of firefly luciferase (Promega Ltd Southhampton, United Kingdom).

pGL3 basic lacks promoter and enhancer sequences (Promega Ltd Southhampton, United Kingdom).

ptk6E2luc contains the thymidine kinase promoter from HSV-1 cloned into the pGL3 luciferase vector upstream of 6 HPV-16E2 binding sites(269).

pTopBP1 expresses the full length TopBP1 under control of the cytomegalovirus promoter and was a kind gift from Dr Kazuhiko Yamane.

pTopBP1 2-258ΔBRCT1 expresses nucleotides 2-258 of the TopBP1 gene with a deletion mutation of the BRCT1 binding site.

pGEX-4T-2 expressed glutathione S transferase and contains a thrombin cleavage site , and multiple cloning site including BamH1 and Xho1 restriction sites (GE Healthcare, Catalogue Number : 27-4581-01)

p16E1myc (clone3) is a myc tagged vector expressing HPV16E1 in mammalian cells. It was previously made in the laboratory (Mr E. Dornan) by taking the multiple cloning site of pGBKT7 (a vector expressing the myc tag in yeast) and cloning it into pCDNA3, a mammalian vector. The E1 gene was then cloned into this vector between the EcoR1 and BamH1 restriction sites.

p16E2 contains the full length HPV-16E2 sequence (nucleotides 2755-3853) cloned into the pJ4Ω plasmid as described in (270).

p16E1 contains the full length HPV-16E1 ORF (nucleotides 865-3210) as described in (271).

p16E1Ha contains the HPV-16 genome (nucleotides 83-2814) containing the E1 ORF with the influenza haemagglutinin epitope tag (Ha) inserted in-frame into the E1 coding sequence within the QM-Ntag/Ai vector (as described in (272)).

p16oriM contains the HPV-16ori plasmid (as described in (271)) with a point mutation at nucleotide 115 (C to T) of the HPV genome creating a Dpn1 site (method described in (273)).

The following HPV-8 plasmids were a kind gift from Dr Baki Akgul and are described in detail in (274).

p8-1 contains the HPV-8 origin of replication

pCE1 contains HPV-8E1 in pCB6

pCE2 contains HPV-8E2 in pCB6

pCMV2-HPV8-E2-Flag contains the HPV-8E2 open reading frame, amplified with specific primers and ligated to the EcoR1 and BamH1 sites of pCMV2-Flag

2.1.4.10 Primers, DNA probes and Oligonucleotides

Dharmacon

2.1.4.10.1 Oligonucleotides for siRNA

Oligo name		
SiTopBP1	Target sequence	GUGGUUGUAACAGCGCAUC
	Sense strand 5'-3'	GUGGUUGUAACAGCGCAUCdTdT
	Anti-sense strand 3'-5'	dTdTCACCAACAUUGUCGCGUAG
SiLuciferase	Target sequence	CGUACGCGGAAUACUUCGA
	Sense strand 5'-3'	CGUACGCGGAAUACUUCGAdTdT
	Anti-sense strand 3'-5'	dTdTGCAUGCGCCUUAUGAAGCU

Eurogentec, (Southampton, United Kingdom)

2.1.4.10.2 Probe and primer set for HPV-16 qPCR

	Sequence 5'-3'
Probe OriM	ACC AAA AGA GAA CTG CAA TGT TTC AGG ATC C
Forward Primer oriFwd	ATC GGT TGA ACC GAA ACC G
Reverse Primer oriRev	TAA CTT TCT GGG TCG CTC CTG

2.1.4.10.3 Probe and primer set for HPV-8 qPCR

	Sequence 5'-3'
Probe HPV-8Ori	CGG TAA GTT TCA TCA GTG TAC CAG GTG CG
Forward Primer HPV-8oriFwd	GCA TCT CCA ACG GAC CGT TA
Reverse Primer HPV-8oriRev	AGA CGA TGG TTG TTG GCA ATA A

Integrated DNA Technologies, Leuven, Belgium

2.1.4.10.4 Primers for HPV-16E2 site directed mutagenesis

Mutant	Primer	Sequence 5'- 3'
N89Y	MDP264 (Forward)	5' CAATATATAACTCACAATATAGTTATGAAAAGTGGACATTACAAG 3'
	MDP265 (Reverse)	5' CTTGTAATGTCCACTTTTCATAACTATATTGTGAGTTATATATTG 3'
E90A	MDP262 (Forward)	5' CAATATATAACTCACAATATAGTAATGCAAAGTGGACATTACAAG 3'
	MDP263 (Reverse)	5' CTTGTAATGTCCACTTTGCATTACTATATTGTGAGTTATATATTG 3'
E90V	MDP260 (Forward)	5' CAATATATAACTCACAATATAGTAATGTAAAGTGGACATTACAAG 3'
	MDP261 (Reverse)	5' CTTGTAATGTCCACTTTACATTACTATATTGTGAGTTATATATTG 3'
N89YE90V (template 16E2E90A)	LMP9 (Forward)	5' CAATATATAACTCACAATATAGTGCTGCAAAGTGGACATTACAAG 3'
(template 16E2E90A	LMP10 (Reverse)	5' CTTGTAATGTCCACTTTGCAGCACTATATTGTGACTTATATATTG 3'

2.1.4.10.5 Primers for sequencing HPV-16E2 plasmids

Primer	Sequence 5'- 3'
MDP233 (Forward)	5' GTTGTGCTGTCTCATCATTTTG 3'

2.1.4.10.6 Primers for HPV-8E2 site directed mutagenesis

Mutant	Primer	Sequence 5'- 3'
E90V	MDP270 (Forward)	5' CAGAAATCTGAGTTTGCAGATGTGCCTTGGACATTAGTGGACAC 3'
	MDP271 (Reverse)	5' GTGTCCACTAATGTCCAAGGCACATCTGCAAACTCAGATTTCTG 3'
E90A	MDP272 (Forward)	5' CAGAAATCTGAGTTTGCAGATGCGCCTTGGACATTAGTGGACAC 3'
	MDP273 (Reverse)	5' GTGTCCACTAATGTCCAAGGCGCATCTGCAAACTCAGATTTCTG 3'
D89A	LMP11 (Forward)	5' CAGAAATCTGAGTTTGCAGCTGAGCCTTGGACATTAGTGGACAC 3'
	LMP12 (Reverse)	5' GTGTCCACTAATGTCCAAGGCTCAGCTGCAAACTCAGATTTCTG 3'
D89AE90V	LMP13 (Forward)	5' CAGAAATCTGAGTTTGCAGCTGTGCCTTGGACATTAGTGGACAC 3'
	LMP14 (Reverse)	5' GTGTCCACTAATGTCCAAGGCACAGCTGCAAACTCAGATTTCTG 3'

2.1.4.10.7 Primers for sequencing HPV-8E2 plasmids

Primer	Sequence 5'- 3'
MDP271 (Reverse)	5' GTGTCCACTAATGTCCAAGGCACATCTGCAAACTCAGATTTCTG 3'
LMP5 (Forward)	5' GAG AAT CTC AGC GAG CGT 3'

2.1.4.10.8 Primers for moving HPV-8E2 into pE1myc clone 3

Primer	Sequence 5' – 3'	Restriction sites
LMP7 (Forward)	5' TGA GAA TTC ATG GAG AAT CTC AGC GAG C 3'	EcoR1
LMP8 (Reverse)	5' TGA GGA TCC TTA CCA TAA GAT GTA TCA ACT C 3'	BamH1

2.1.4.10.9 Primers for cloning TopBP1 into pGEX-4T-2

Primer	Sequence 5'-3'	Restriction sites
LMP1	CGG GGATCC CAC CAC CAG CGA TGT GTC	BamH1
LMP2	CGG GGATCC GCA AGT GTT CAA GAA TAC	BamH1
LMP3	CGG GGATCC CCA CTC TCA GAA GTT ATT G	BamH1
MDP50	CGG CTC GAG TTC TAG ATT TTC AAG TGT	Xho1
MDP41	TTC CTC GAG CTG AAA GCG GTT CAT ATC TAA AGG	Xho1
MDP37	TTC CTC GAG TGG CGT ACT CGG TTT CC	Xho1
LMP4	CGG CTC GAG AGA CAC AGC TGA GAG TAG	Xho1

2.1.4.11 Tissue Culture

Corning incorporated (Leicestershire, UK)

100mm x 20mm non-pyrogenic cell culture dishes – Catalogue Number: 3296

60mm x 15mm non-pyrogenic cell culture dishes – Catalogue Number: 4301

25ml disposable serological polystyrene pipettes – Catalogue Number: 4251

10ml disposable serological polystyrene pipettes – Catalogue Number: 4101

5ml disposable serological polystyrene pipettes – Catalogue Number: 4135

Cell scraper – Catalogue Number: 3010

Greiner Bio-one Ltd (Stonehouse, UK)

50ml polypropylene centrifuge tubes – Catalogue Number: 210201

15ml polypropylene centrifuge tubes – Catalogue Number: 188261

96 well ELISA microplates – Catalogue Number: 072003

Invitrogen Ltd (Paisley, UK)

Dulbecco's Modified Eagle Medium (DMEM) (1x) +w/GlutaMAX™/Glucose NaPyr – Catalogue Number: 31966

Dulbecco's Modified Eagle Medium (DMEM) (1X) High Glucose – Catalogue Number: 21068

Fœtal Bovine Serum – Catalogue Number: 16141

L-Glutamine 200mM 100x – Catalogue Number: 25030

Opti-MEM® I Reduced-Serum medium (1X), liquid - Catalogue Number: 11058

Penicillin–Streptomycin Solution (5000:5000) liquid – Catalogue Number: 15070

Trypsin-EDTA (1x) 0.05% trypsin 0.53mM EDTA Na – Catalogue Number: 25300

Nunc™ Part of Thermo Fisher Scientific (Hereford, UK)

25cm tissue culture flasks with filtered caps- Catalogue Number: 136196

80cm tissue culture flasks with filtered flasks – Catalogue Number: 178905

175cm tissue culture flasks with filtered flasks – Catalogue Number: 178883

Promega Ltd (Southampton, UK)

Phosphate buffered saline (PBS) tablets – Catalogue Number: P4417

Thermo Scientific Dharmacon (Leicestershire, United Kingdom)

SiLuciferase 0.05μmol – Custom SiRNA synthesis

SiTopBP1 0.05μmol – Custom SiRNA synthesis

2.1.4.12 Microarray

Array name: Human Gene 1.0 ST

Array/chip type: HuGene-1_0-st-v1

Organism: Homo sapiens

NetAffx release: 31 (2009-11-16).

2.2 Methods

The protocols used in this thesis are described in the following section. The manufacturers and distributors details for materials used are given in the previous section.

2.2.1 Epidemiology

A specialist Dermatology clinic for renal transplant recipients (RTRs) was established at the Western Infirmary Glasgow. All patients with a functioning renal transplant in the West of Scotland were invited to attend for Dermatology review. All new RTRs from this date forward received an appointment to attend the Dermatology clinic and referrals were taken from all sources for any RTRs requiring Dermatology review. The study period was from September 2005 to November 2008 (38 months). 610 individuals attended during the study period. The number and frequency of follow up visits varied according to clinical need.

Data on all RTRs were entered into the West of Scotland renal electronic patient record. A Dermatology section was added to this database to collect data on risk factors for and episodes of skin cancer. The Dermatology section was designed to be intrinsically linked to the renal database in order to allow correlation between skin cancer data and transplant data such as immunosuppressive drugs.

A clinical history and full dermatological examination was carried out for each patient. Data collected for each patient included skin type, occupation and use of sun beds. Previous UVR exposure was graded to be low, medium or high based on the patient's occupation, leisure activities and sunbathing habits. The presence of viral warts and/or epidermal dysplasias (actinic keratoses and Bowen's disease) was recorded. All skin cancers diagnosed on the first and any subsequent patient visits were recorded. Additionally, data were collected for all retrospectively diagnosed skin cancers. Only histologically diagnosed tumours were recorded. For each cancer the date of diagnosis, tumour type, anatomical location and management were recorded. All tumour recurrences and management of recurrences were recorded. The use of oral retinoids (dose and duration of treatment) was recorded.

2.2.2 HPV genotyping

2.2.2.1 Collection of patient samples

Patient samples were collected from both IC patients and IS RTRs. Samples from IC patients were identified from the Western Infirmary Pathology database by searching under the diagnoses of interest. Samples from IS patients were identified by cross-referencing the patients from the West of Scotland Renal Transplant database with the Western Infirmary Pathology database to identify patient samples with the diagnoses of interest.

Once samples were identified, all pathology reports were examined. Patient hospital numbers from the IC group were cross-referenced with the renal transplant database to ensure no RTRs were included in this group. Samples were excluded from the study if the diagnosis was uncertain.

2.2.2.1.1 Paraffin-embedded samples

Archival, formalin-fixed, paraffin-embedded skin biopsy specimens of AK, IEC and SCC (including Keratoacanthomas from IS group only) were collected.

Normal skin controls were collected prospectively from IC patients who were having dermatological surgery to remove any lesion (benign or malignant). Patients consented to donate either a 3mm punch biopsy from clinically normal photo-protected skin from the inner arm or clinically normal peri-lesional skin. Tissue was placed directly into formalin and was processed at the Department of Histopathology, Institute of Comparative Medicine.

2.2.2.1.2 Frozen samples

Frozen tissue samples, both lesional and normal skin, were obtained from IC and IS patients with consent. Where patients were donating more than one sample, normal skin was taken first and any subsequent surgery was performed using a new sterile biopsy kit to avoid cross-contamination between specimens.

Frozen tissue was taken from any lesion where the clinical diagnosis was suspected SCC. A core of tissue was taken from the excised lesion placed in a

labelled, sterile 1.5ml microcentrifuge tube and placed directly into liquid nitrogen before storing at -80°C until further use. The remainder of the lesion was processed by the Department of Pathology, Western Infirmary and the histological diagnosis recorded.

A number of patients consented to donate an additional 3mm punch biopsy of normal skin from the photo-protected inner arm. A 3mm punch biopsy was taken, placed in a labelled, sterile 1.5ml microcentrifuge tube and placed directly into liquid nitrogen before storing at -80°C.

2.2.2.2 Processing of tissue sections for DNA extraction

All tissue blocks were sectioned at the Department of Histopathology, Institute of Comparative Medicine. This work was carried out by Mr Colin Nixon and Mrs Lynne Stevenson.

First, several sections were removed from the surface of the block and discarded to avoid surface contamination. Thereafter, two 10 micron thick, sections were placed into a 1.5 ml sterile screw cap microcentrifuge tube. The blade was sterilised between each sample and sterile gloves and forceps used for each sample.

2.2.2.3 DNA isolation

DNA isolation was performed at DDL Diagnostic Laboratory, Voorburg, the Netherlands. The work was carried out by Dr Maurits de Koning, technical staff from DDL Diagnostic Laboratory and by Dr Lorna Mackintosh.

Skin biopsy specimens (10µm) were incubated in 250 µl of 1 mg/ml proteinase K in 50mM Tris, pH8.0, 1mM EDTA, and Tween-20 at 56˚C for 16 h to release the DNA, after which, proteinase K was inactivated at 95˚C for 10 min. The samples were then centrifuged at 13,000-x g for 5 minutes and the supernatant stored at -20°C or used directly for PCR. A negative control sample containing only the proteinase K solution was processed with each batch of 10 samples and analysed in parallel to the other samples.

2.2.2.4 PCR-reverse hybridisation assay

The PCR-reverse hybridisation assay (PM-PCR-RHA) was performed at DDL Diagnostic Laboratory, Voorburg, the Netherlands. The work was carried out by Dr Maurits de Koning, technical staff from DDL Diagnostic Laboratory and assisted by Dr Lorna Mackintosh.

BetaPV detection and genotyping was performed with the PM-PCR RHA method according to the instructions of the manufacturer (The skin (beta) HPV prototype research assay; Diassay BV, Rijswijk, The Netherlands). This method was designed for the amplification and identification of 25 established betaPV types, namely betaPV genotypes 5, 8, 9, 12, 14, 15, 17, 19, 20, 21, 22, 23, 24, 25, 36, 37, 38, 47, 49, 75, 76, 80, 92, 93 and 96(89).

2.2.2.4.1 PCR protocol

DNA isolated from the tissue samples as described (2.2.2.3) was amplified by a broad spectrum PCR using biotinylated consensus primers (two forward and seevn reverse) to amplify a 117 base pair region from the E1 gene of the betaPV types according to the protocol described by de Koning et al(89).

10µl of target DNA was mixed with 5µl GeneAmp 10xPCR II buffer(Applied Biosystems), 1.5 units AmpliTaq Gold DNA polymerase (Applied Biosystems), 2.5mM $MgCl_2$ (Applied Biosystems), 200µM each dNTP (Amersham Biosciences), 10µl Primer mix (PM) (KI00062 v0.5 RHA KIT skin (beta) HPV genotyping assay) and distilled water to a total volume of 50µl.

The PCR was carried out with precautions to avoid contamination. The PCR was performed by a nine minute pre-heating step at 94ºC, followed by 35 cycles of amplification comprising 30seconds at 94ºC, 45 seconds at 52ºC and 45 seconds at 72ºC. A final elongation step at 72ºC of five minutes ends the PCR.

2.2.2.4.2 Reverse Hybridisation Assay (RHA) protocol

The RHA allows the simultaneous identification of multiple HPV types in a single hybridisation step. Biotinylated amplimers generated by the PCR protocol were

hybridised to nitrocellulose strips containing probes based on sequence alignments from the 117 bp amplimers.

Each nitrocellulose strip contains a conjugate probe, a universal probe and 27 genotype specific probes.

2.2.2.4.2.1 Conjugate Probe

The top line of each nitrocellulose strip contained a positive control of biotinylated DNA. This serves as a positive control for the enzymatic colouring reaction (described below).

2.2.2.4.2.2 Universal Probe

A relatively conserved region permitted the design of additional general probes for broad spectrum betaPV detection. These probes detected the established genotypes with the exception of types 38, 92 and 96. A positive reaction on the universal probe in the absence of a positive reaction or pattern of reaction on the genotype specific probes therefore indicates presence of a known genotype at low copy number or detection of a new genotype that would only be determined by sequencing of the amplimers.

2.2.2.4.2.3 Genotype specific probes

Sequences from the PM amplimers shows a relatively variable region allowing the deduction of 27 genotyping probes. Twenty-three probes are genotype specific, the four remaining probes are used in pattern recognition of genotypes. HPV genotypes 5, 9, 12, 14, 15, 17, 19, 23, 24, 25, 36, 37, 38, 49, 75, 76, 80, cand92, 93 and cand96 are recognised by hybridisation to a single probe line. Types 8 and 21 yield a specific hybridisation pattern on the RHA, types 20, 22 and 47 are identified by a single probe line as well as by a specific reaction pattern (89).

The RHA assay was performed using the strips and reagents contained in the KI00062 v0.5 RHA KIT skin (beta) HPV genotyping assay kit. 10µl of biotin-labelled amplimer was mixed with 10µl of denaturation solution and 10µl of 3B buffer in a plastic trough containing the betaPV strip. The mix was incubated at room temperature for 5 minutes before adding 2ml of pre-warmed (37ºC) hybridisation buffer and incubated at 50ºC for one hour. All incubation and washing steps were performed automatically in an Auto-LiPA. The strips were washed twice for 30 seconds and once for 30 minutes with 2ml of hybridization

solution. The strips were then incubated with 2ml of alkaline phosphatase-streptavidin conjugate for 30 minutes at room temperature, the streptavidin attaches to the biotinylated amplimers. The strips were then washed twice with 2ml of rinse solution and once with 2ml of substrate buffer.

Two ml of substrate (5-bromo-4-chloro-3-indolylphosphate and nitroblue tetrazolium) were added and incubated for 30 minutes at room temperature. The reaction was stopped by washing for 3 minutes and 10 minutes and by a wash with 2ml of water. The strips were dried and the purple bands visually analysed against a reference sheet.

2.2.3 Immunohistochemistry

2.2.3.1 Tissue samples

The patient samples used were paraffin-embedded samples collected and processed as described earlier (2.2.2).

2.2.3.2 Processing of samples for immunohistochemical staining.

The work was performed at the Department of Histopathology, Institute of Comparative Medicine and was carried out by Dr Lorna Mackintosh, Mr Colin Nixon and Mrs Lynne Stevenson.

Sections were cut from tissue blocks transferred to glass microscope slides. For each sample, sections were prepared for each antibody under investigation (Ki67, p53, p16, MCM2, MCM5, and TopBP1), as well as Haematoxylin and Eosin, and positive and negative control slides.

2.2.3.2.1 Heat-mediated antigen retrieval

Slides were placed in an oven at 60°C for a minimum of 12 hours to melt the wax. Wax was then removed from the slides by placing in a slide rack and immersing in Citroclear (National Diagnostics, Charlotte, NC, USA) for 3-5 minutes. The slides were then dehydrated by immersing 10 times in each of three sequential alcohol baths before placing in water for a final minute.

A slide box was filled with antigen retrieval buffer (25ml sodium citrate buffer, pH6.0), 225 ml de-ionised H_2O), placed in the centre of a microwave pressure cooker containing 600ml of de-ionised H_2O before pre-heating in the microwave for ten minutes at maximal temperature. Slides were then transferred to the pre-heated antigen retrieval buffer; the pressure cooker sealed and heated in the microwave at maximal temperature for 3-4 minutes until the correct pressure was reached, then heated for a further 2 minutes at the correct pressure before cooling for 20 minutes. Once cooled antibodies were applied.

(For sections to be stained with p16 antibody, heat mediated antigen retrieval was carried out in a boiling bath according to the manufacturer's instructions (Dako, UK, Ltd).

2.2.3.2.2 Immunohistochemical staining of slides

Sections from each specimen were processed for routine Haematoxylin and Eosin staining (H&E).

Cooled slides were transferred to staining chambers and washed in de-ionised H_2O for 5 minutes. Endogenous peroxidise was blocked with 2 drops of peroxidise block from the appropriate EnVision Kit (Dako) (mouse kit for mouse primary antibodies and rabbit kit for rabbit primary antibodies). The reaction was allowed to proceed for 5 minutes then terminated by adding buffer Tris/Tween and the slides washed for 7 minutes.

Sections from each specimen were then probed with primary antibodies (150μl) against the following antigens; Ki-67 (mouse, monoclonal anti-human Ki-67 antigen, clone MIB-1, Dako), p53, (rabbit, polyclonal anti-human p53, clone CM-1, Novocastra), p16 (mouse, anti-human p16, CINtec ™ p16INK4a Histology kit, Dako), MCM2 and MCM5 (mouse, anti-human MCM2, clone SPM196; mouse anti-human MCM5, clone SPM197, Panomics), and TopBP1 (rabbit, polyclonal anti-human TopBP1, R1180). Antibodies were diluted in buffer TRIS to the correct dilution and were used at the following concentrations - Ki67 1:2000; p53 1:500; p16 (ready to use); MCM2 1:50; MCM5 1:500; TopBP1 1:1000. A positive control was included for each antibody and was a section of archival tissue previously shown to have a strongly positive reaction to that antibody. Serial sections in each run of slides tested, where the primary antibody was omitted, acted as negative controls. For mouse primary antibodies (Ki67, p16, MCM2 and MCM5), normal rabbit serum applied to the slide instead of antibody as a negative control. For rabbit primary antibodies (p53 and TopBP1), normal mouse serum was used as a negative control.

Following one hours incubation, slides were washed with Tris/Tween for 7 minutes, before applying two drops of the appropriate mouse or rabbit secondary antibody (Dako, UK Ltd). The secondary antibody was left on for 50

minutes before washing with tris/Tween for 7 minutes then washing with distilled water for three minutes before a final wash for seven minutes.

100μl of 3,3'-diaminobenzidine (DAB)/substrate-Chromogen mix was applied to each slide [1ml of (DAB + substrate buffer) + 1 drop of (DAB+ chromogen), EnVision™ Kit, Dako, UK, Ltd] and the reaction allowed to proceed for ten minutes.

The slides were then counter-stained with Haematoxylin for one minute and then re-hydrated by dipping in acid alcohol and transferred to a water bath then to Citroclear prior to mounting. Coverslips were attached with Vectabond™ Reagent and left to dry on a hot plate overnight.

Sections were analysed using a Leitz Wetzlar microscope.

2.2.4 Molecular Biology

2.2.4.1 Agarose Gel Electrophoresis

Agarose gel electrophoresis was carried out in 1- 1.5% agarose gels depending on the predicted size of the sample DNA. The appropriate weight of electrophoresis grade agarose (Eurogentec Ltd) was dissolved by heating in1xTBE Buffer (10x TBE: 900mM Tris base, 900mM boric acid, 25mM EDTA, pH8.0). The solution was cooled to approximately 50ºC then, for a 100ml solution, 2.5ul of Ethidium Bromide (10mg/ml) was added before pouring into a gel cast and cooling to set. Once set the gel was placed into an electrophoresis tank and submerged in 1xTBE buffer (see above). 5μl of sample was mixed with 0.5 - 1μl of 10x loading buffer (65% (w/v) sucrose, 10mM Tris-HCl, pH7.5, 10mM EDTA, pH8, 0.3% (w/v) bromophenol blue). The samples were then loaded into wells alongside a 100bp ladder (Invitrogen) as a molecular weight marker. The sample DNA was separated by electrophoresis at 100V for sufficient time to allow bands and sizes to be easily distinguishable. The DNA was then visualised by UV light and photographed using a UV gel documentation system (Syngene GeneFlash).

2.2.4.2 DNA/RNA Concentration Determination

To measure the DNA or RNA concentration, samples were measured on a Nanodrop (ND-1000 Spectrophotometer) according to the manufacturer's instructions.

2.2.4.3 DNA Purification using Phenol Chloroform

2.2.4.3.1 Replication assays

500μl of Phenol Chloroform was added to each sample before vortexing to produce an emulsion then centrifuging for 20 minutes, 15000g at 4°C. The upper aqueous layer was removed to a fresh 1.5ml microcentrifuge tube, the lower organic layer and interface discarded and the above steps repeated before precipitating DNA with ethanol.

2.2.4.3.2 Site directed mutagenesis

Small volume samples volumes were completed to 200µl with distilled water before adding one volume of Phenol Chloroform. The sample was vortexed well to produce and emulsion before centrifuging for 10 minutes, 15000g at room temperature. The upper aqueous layer was removed to a fresh microcentrifuge tube and the lower organic layer and interface discarded before precipitating DNA with ethanol.

2.2.4.4 Ethanol precipitation of DNA

After DNA purification with Phenol Chloroform, DNA was precipitated with Ethanol. To each sample, one tenth the sample volume of 3M Sodium Acetate pH5.2 and 2.5 x the sample volume of 100% ethanol were added and the sample incubated at -20ºC for 10 minutes to two hours. Samples were then centrifuged at 15000g for 20 minutes at 4ºC, the ethanol removed and the pelleted DNA washed with 2x the sample volume of 70% Ethanol. Samples were centrifuged a final time at 15000g for 10 minutes at 4ºC before removing the ethanol and drying the DNA pellet. The pelleted DNA was then re-suspended in distilled water.

2.2.4.5 Cloning

2.2.4.5.1 Platinum Pfx DNA polymerase PCR

DNA was amplified by PCR using the Platinum Pfx DNA polymerase protocol. PCR reactions were carried out in a reaction volume of 50µl. For each reaction, 2ng of template DNA was added to 10µl of 10x P*fx* amplification buffer, 10mM dNTP mixture (dATP, dGTP, dCTP and dTTP), 3µl of forward primer (1:10), 3µl of reverse primer (1:10), 0.6µl of Platinum® P*fx* DNA polymerase and 28.4µl of distilled water. Amplification was carried out using a MJ research PT200 gradient cycler. The cycle conditions were 94 ºC for 5 minutes (denaturation step), 94ºC for 25 seconds (denaturation step), 55 ºC for 30 seconds (annealing step) and 68 ºC for 3 minutes (elongation step). After repeating the cycle 28 times the reaction underwent 68ºC for 10 minutes before being maintained at 4 ºC.

The PCR product was cleaned up using the QIAquick PCR Purification kit (Qiagen) before digesting with restriction digest enzymes.

2.2.4.5.2 Restriction Enzyme Digests

The DNA insert and the vector were digested with restriction enzymes. 10μl of the insert or vector to be digested was mixed with 1μl of each restriction enzyme, 5μl of the appropriate restriction enzyme buffer, 0.5μl of bovine serum albumin (BSA) and distilled water to a final volume of 50μl and incubated for three hours at 37ºC. The insert was then cleaned up again (QIAquick PCR Purification kit (Qiagen)) and the vector was gel purified as described below.

2.2.4.5.2 Gel Extraction

Restriction digest products were purified using the QIAQuick Gel Extraction Kit (Qiagen). Restriction digest products were separated over 2 hours at 50V by Agarose gel electrophoresis. The gel was visualised under low UV light and the area of gel containing the DNA to be purified was cut out, placed in a sterile microcentrifuge tube and weighed. Three volumes of Buffer QG were added to the gel before incubating at 50°C for 10 minutes, vortexing every two to three minutes, until the gel had dissolved. One gel volume of isopropanol was added to the sample and mixed. The sample was then applied to a QIAquick column in a 2ml collection tube and centrifuged for one minute at 13000g, the flow through was discarded, 0.5ml of Buffer QG was added and the column centrifuged again for 1 minute. The column was then washed by the addition of 0.75ml of Buffer PE and centrifuging again for one minute. The flow through was discarded and the centrifugation step repeated before placing the column in a clean 1.5ml microcentrifuge tube. To elute the DNA, 50μl of Buffer EB was added and the column centrifuged for one minute at 13000g. The purified DNA was then stored at -20°C until further use.

2.2.4.5.3 Phosphatase Treatment

After restriction digest, cut vectors were de-phosphorylated to prevent vector re-ligation. 2μl of Shrimp Alkaline Phosphatase (SAP) (Roche) and 10μl of 10xSAP Buffer (Roche) was added to the restriction digest and incubated at 37ºC for 30 minutes before heat inactivating the Phosphatase at 65ºC for 10 minutes. The

samples were then purified with the QiaQuick PCR Purification Kit (Qiagen) as described.

2.2.4.5.4 Ligation of DNA

After restriction enzyme digests and dephosporylation of the vector, DNA inserts and vector were ligated. 1μl of DNA insert, 3μl of dephosporylated vector, 5μl of ligase (Takara DNA ligation kit solution 1) and 1μl of distilled H_20 was added to a sterile 1.5ml microcentrifuge tube. The reaction was incubated at 16°C overnight. The next day, DH5α™ chemically competent bacterial cells (Invitrogen) were transformed with 5μl of the ligation reaction and controls. Colonies were picked the following day and small scale preparation of plasmid DNA (miniprep) carried out using the QiaPrep Spin Miniprep Kit. DNA was then amplified (ABI cycle sequencing protocol) and sequenced with the appropriate primers.

2.2.4.6 Transformation of Chemically Competent Bacterial Cells

DH5α™ chemically competent bacterial cells (Invitrogen) were transformed. 5μl of a ligation reaction was added to 50μl of bacterial cells in a sterile 1.5ml microcentrifuge tube and incubated on ice for 30 minutes. Cells were then heat shocked at 42ºC for 1 minute then incubated on ice for a further 1 minute. 200μl of S.O.C. medium (Invitrogen) (25ml bactotyrptone, 0.5% yeast extract, 10mM NaCl, 2.5mM KCl, 10mM $MgCl_2$, 10mM $MgSO_4$ and 20mM glucose) was added to each sample before incubating at 37ºC shaking for 1 hour. After incubation, samples were plated onto Ampicillin containing agar plates, inverted and incubated overnight at 37ºC. Single colonies were picked the following day and grown in 3-5ml of Ampicillin containing L-Broth for 6-8 hours at 37ºC whilst shaking. One ml of the bacterial culture was transferred to a conical flask containing 100ml Ampicillin containing L-Broth overnight and incubated at 37ºC whilst shaking prior to preparation of plasmid DNA.

2.2.4.7 Large Scale Preparation of Plasmid DNA (Maxiprep)

Plasmid DNA was purified using the PureLink™ HiPure Plasmid DNA purification Kit (Invitrogen) according to the manufacturer's instructions. Briefly, bacterial

colonies containing plasmid DNA were picked and grown for eight hours in 5ml of Ampicillin containing L-Broth at 37ºC whilst shaking (200rpm). 1ml of a 5ml bacterial culture was used to inoculate a 200ml conical flask containing 200ml of Ampicillin containing L-Broth and incubated overnight at 37ºC whilst shaking (200rpm). The HiPure Maxi column was equilibrated with 30ml of Equilibration buffer (EQ1). Bacterial cells were pelleted by centrifugation at 5000g for 10 minutes at room temperature and the resultant supernatant discarded. The bacterial pellet was re-suspended in 10ml of Resuspension Buffer (R3) containing RNase by pipetting before adding 10ml of Lysis Buffer (L7) and gently mixing by inverting the capped tube five times. The lysis reaction continued for five minutes at room temperature before adding 10ml of Precipitation Buffer (N3) and mixed gently by inversion until the solution was homogeneous. The solution was then centrifuged at 5000g for 30 minutes at room temperature and the supernatant loaded onto the equilibrated column and allowed to drain by gravity. The column was then washed with 60ml of wash Buffer (W8) and allowed to drain again by gravity. The column was then placed into a 50ml centrifuge tube, 15ml of Elution Buffer (E4) (pre-warmed to 37ºC) was added to the column and the eluted DNA drained by gravity into the centrifuge tube. 10.5ml of isopropanol was then added to the elution tube and mixed well to precipitate the DNA before centrifuging at 5000g for one hour at 4°C. The supernatant was removed and 5ml of 70% Ethanol added to the pellet before centrifuging again at 5000g for 30 minutes. Most of the supernatant was removed then the pellet and any residual ethanol transferred to a sterile 1.5ml Eppendorf tube before centrifuging at 15000g for 30 minutes. Any residual supernatant was removed and the pellet allowed to air dry before re-suspending in 200-500µl of TE buffer according to the size of the pellet. Plasmid DNA was stored at -20°C until further use.

2.2.4.8 Small Scale Plasmid Purification (Miniprep)

Small scale plasmid DNA was purified using the QiaPrep Spin Miniprep Kit (Qiagen). Bacterial colonies containing plasmid DNA were picked and grown overnight in 5ml of Ampicillin containing L-Broth at 37ºC whilst shaking (200rpm).1ml of bacterial culture was transferred to a 1.5ml Eppendorf tube and centrifuged at 15000g for 5 minutes at room temperature. The supernatant was removed and the pelleted cells were re-suspended by pipetting in 250µl of

buffer P1. To lyse the cells, 250µl of buffer P2 was added and the sample mixed by inverting the tube five times then incubating at room temperature for 5 minutes. To precipitate the sample, 350µl of buffer P3 was then added, the sample mixed by inversion again before centrifuging again at 15000g for 10 minutes at room temperature. The supernatant was applied to a QIAprep spin column centrifuged for 60 seconds, the flow through discarded before washing the column with 750µl of buffer PE and centrifuging again for 60 seconds. The flow through was discarded and the centrifugation step repeated to remove residual wash buffer before placing the column into a clean 1.5ml microcentrifuge tube and eluting the DNA by adding 50µl of buffer EB to the centre of the column, allowing to stand for one minute before centrifuging for one minute at 15000g then discarding the spin column.

2.2.4.9 Quantitative PCR

To analyse the replication assays by quantitative PCR (qPCR), a standard curve was prepared using plasmids containing the HPV-16 or HPV-8 origin of replication (pOri). The following serial dilutions of pOri prepared: 10pg/µl, 1pg/µl, 0.1pg/µl, 0.01pg/µl, 0.001pg/µl, 0.0001pg/µl and 0.00001 pg/µl. 10µl of each standard was added to each well thereby creating a standard curve ranging from 100pg to 0.0001pg of DNA per well. 100pg of DNA per well on the standard curve equated to 1.8×10^7 viral copies and the lowest dilution of 0.0001pg DNA per well equated to 1.8 viral copies.

The probe and primer set for HPV16 had previously been determined in the Morgan Laboratory using the Primer Express software. The probe and primer set for HPV was designed using the primer express software by L. Mackintosh and E. Dornan. Probes and primers were designed using Primer Express. Probes were stored at a concentration of 100µM and were diluted to a concentration of 5µM before use. Primers were stored at a concentration of 100pmol/ml and reverse primers were diluted 1:10 before use to a final concentration of 10pmol/ml. All reactions were prepared in a Microflow PCR workstation with UV decontamination (Astec Microflow Ltd). A master mix was prepared containing 12.5µl Brilliant® QPCR Master Mix (Stratagene), 0.5µl Reference dye 15µM (Stratagene), 0.25µl forward primer, 0.25µl reverse primer, 0.5µl probe DNA and

6µl distilled water. 5µl of sample DNA, standard or no template control (distilled H_2O) was used per reaction giving a final sample volume of 25µl. Each sample was analysed in triplicate, each standard in duplicate and one non-template control (distilled H_20) in quadruplicate. Each triplicate, duplicate or quadruplicate was prepared in a single tube and the appropriate amount of master mix added to each tube thereby eliminating a source of variability. Each sample was then pipetted into individual wells on a PCR plate.

Samples were then run on an ABI 7500 machine and the results analysed against the standard curve using the Applied Biosystems 7500 sequence detection systems version 1.2.2 software.

2.2.4.10 PCR Purification

PCR products were purified with the QIAquick PCR Purification kit (Qiagen). To 100µl of PCR product, 500µl of buffer PBI was added and mixed. All centrifugation steps were carried out at 15000g at room temperature. The sample was applied to a QIAquick column in a 2 ml collection tube and centrifuged for 1minute. The flow through was discarded and the column washed by adding 750µl of buffer PE and centrifuging for 1 minute before discarding the flow through and centrifuging for a further 1 minute. The column was placed in a clean 1.5ml microcentrifuge tube and the DNA eluted from the column by adding 30µl of buffer EB to the QIAquick membrane and centrifuging the column for 1 minute. The purified DNA was then stored at -20ºC.

2.2.4.11 Site Directed Mutagenesis

In a sterile 0.5ml PCR reaction tube, 1µl of 100ng/µl template DNA and 1µl 10µM each of the forward and reverse primers was mixed with 5µl 10x KOD Buffer number 1, 5 µl 2mM dNTPs, 4µl 25mM $MgCl_2$, 1µl DMSO, 1µl KOD polymerase and the reaction was completed to 50µl with distilled H_2O. PCR was carried out on a MJ research PT200 gradient cycler with the following conditions: 94 ºC for 5 minutes (denaturation step), 94ºC for 15 seconds (denaturation step), 60 ºC for 30 seconds (annealing step) and 72ºC for 20 seconds per Kilobase (Kb) (elongation step). After repeating the cycle a further 17 times, a final step of 72ºC for 5 minutes was performed before being maintaining the reaction at 4 ºC.

The PCR product was then transferred to a clean 1.5ml microcentrifuge tube. To digest the DNA, 1µl of Dpn1 was added and the sample incubated at 37ºC for 90 minutes. 150µl of distilled H_2O was added to them sample before carrying out Phenol Chloroform extraction and Ethanol precipitation of DNA as described earlier. The pelleted DNA was re-suspended in 15µl of distilled H_2O.

5µl of the resultant mutated DNA was then transformed into 100µl of DH5α™ chemically competent bacteria (Invitrogen) using the method described above. Single colonies were picked after 16 hours and placed in a sterile 5ml Bijoux container with 3-5ml of Ampicillin containing L-Broth solution. Samples were incubated at 37ºC whilst shaking (200rpm) for 16 hours. 1ml of the sample was then transferred to a sterile 1.5ml microcentrifuge tube and centrifuged at 15000g for 30minutes at 4ºC to pellet the bacteria. The supernatant was removed and small scale preparation of plasmid DNA (miniprep) procedure carried out as described above.

DNA was then amplified and sequenced to check for mutations (described below).

2.2.4.12 DNA Sequencing

DNA was amplified using the ABI Prism BigDye Terminator v 3.1 Cycle sequencing kit (Applied Biosystems). For each sample of plasmid DNA a primer complementary to the area of interest was used. 6µl of the DNA to be sequenced was placed in a 1.5ml PCR tube and 2µl BigDye, 4µl BigDye Buffer, 2µl of the appropriate primer and 6µl distilled water were added. After an initial step of 95ºC for 4 minutes the samples were heated to 95 ºC for 10 seconds, 50ºC for 5 seconds and 60 ºC for 4 minutes and the cycle was repeated 25 times before heating to 60 ºC for 4 minutes. The samples were then held at 4 ºC until required.

Cell cycle reactions were purified by adding each sample to a 1.5ml microcentrifuge tube containing 16µl of distilled water and 64µl of 95% ethanol before mixing and incubating at room temperature for 15 minutes. Each sample was then centrifuged at 15000g for 20 minutes at 4ºC. The supernatant was removed and discarded before adding 250µl of 70% ethanol to the pelleted DNA.

Samples were centrifuged at 15000g for 10 minutes at 4 ºC, the resultant supernatant aspirated and discarded and the pelleted DNA dried for 1-2 minutes on a heating block at 70ºC. The DNA pellet was re-suspended in 25µl of HiDi Formadide and transferred to a PCR plate. Plasmids were sequenced using an Applied Biosystems 3100 automated sequencer and the sequences analysed with the Chromas Lite version 2.01 software (Technelysium Pty Ld).

2.2.4.13 BCA/$CuSO_4$ Assay

To assess the concentration of protein extracts, BSA protein standard solutions were prepared from powdered BSA to the following concentrations – 2000, 1000, 500, 400, 200, 100, 80, 50µg/ml. 10µl of each standard, 10µl of ddH_2O, 10µl of each protein lysate to be measured (both neat lysate and at a 1:10 dilution) were loaded into a 96 well Elisa plate. 200µl of developing solution (5ml Bicinchonic Acid (BCA) (Sigma) and 100µl Copper II Sulphate pentahydrate 4% (V/V) solution (Sigma)) was added to each occupied well. The plate was then incubated at 37ºC for 30 minutes before the absorbance was measured at 562nm (Multiskan Acent reader and software, Labsystems). The absorbance readings for the BSA standards were used to derive a standard curve from which the protein concentrations of the lysates were calculated.

2.2.4.14 Western Blotting

The protein concentrations of the lysates to be assessed were determined using a BCA/CuSO4 assay as described. Equal amounts of protein (typically 15-30µg) from each lysate was added to a micro-centrifuge tube before adding 4µl NuPage™ sample loading buffer (4X) and 2µl NuPage™ sample reducing agent (10X) (Invitrogen). Samples were heated to 70ºC for 10 minutes. Pre-cast, 4-12% gradient SDS-PAGE gels (Invitrogen) (either 10 or 12 wells) were placed into a gel tank filled with 1xMES running buffer. 400µl of 10X antioxidant (Invitrogen) was added to the running buffer before loading the samples. 8µl of See-Blue® kDa marker (Invitrogen) was added to the first well as a marker and the samples loaded into the wells using fine pipette tips. Gels were run at 200V for one hour. The buffer was then discarded and the gel cast carefully cracked open and the top plate removed leaving the gel in place. The gel was washed in transfer buffer while gently shaking at room temperature for 10 minutes (8ml NuPage®

Transfer Buffer (20X) (Invitrogen), 20ml methanol and 172ml distilled water). The gel was then transferred to a nitrocellulose membrane using the Iblot dry transfer method (Invitrogen) according to the manufacturer's instructions.

Following transfer, the membrane was incubated with 5% milk- PBS-T (5% non-fat milk, 1xPBS 0.1% Tween) whilst gently shaking at room temperature for 1 hour to remove any non-specific bands. The milk – PBS-T solution was removed and the primary antibody prepared to an appropriate dilution in 5% milk- PBS-T was applied and the membrane incubated for one hour at room temperature while gently shaking. The antibody was removed and the membrane washed in PBS-T for 15 minutes followed by three five minute washes at room temperature whilst gently shaking. The secondary antibody at an appropriate dilution in 5% milk- PBS-T was added to the membrane and incubated for one hour at room temperature whilst gently shaking. The secondary antibody was removed and the membrane washed as above. The proteins were detected using ECL-plus (GE Healthcare). 2ml of detection reagent A and 50µl of detection reagent B were mixed, added to the membrane and incubated for 5 minutes at room temperature. The excess developing solution was removed and the membrane wrapped in Saran wrap, placed into a film cassette and developed with x-ray hyperfilm (Amersham).

2.2.4.15 Stripping Membranes

Nitrocellulose membranes were stripped to remove traces of previously used antibody before re-probing. 10mls of 0.2M NaOH was added to the membrane and incubated for 15 minutes at room temperature whilst gently shaking. The NaOH was removed and the membrane washed in PBS-T for 15 minutes then 5 minutes three times. The membrane was then blocked in 5% milk-PBS-T for one hour at room temperature whilst gently shaking before the new primary antibody was applied.

2.2.4.16 Immunoprecipitation

Cell lysates were harvested as described (2.2.5.3). All centrifugation steps described below were carried out at 80g at 4°C.

Protein A Sepharose beads (Sigma) were transferred to a sterile 1.5ml microcentrifuge tube and centrifuged for 1 minute. The supernatant was removed and the beads were washed in 1 volume of Lysis buffer (0.5% NP40, 150mM NaCl, 50mM Tris pH 8.0). This step was repeated four times. Beads were stored at 4°C until further use (unblocked beads). The procedure was repeated with a second microcentrifuge tube of beads and, after the final wash, one volume of 1% BSA (Sigma) in PBS was added to the beads which were then incubated whilst rotating, overnight at 4°C. Beads were then washed with an equal volume of Lysis buffer four times and re-suspended in one volume of lysis buffer after the final wash and stored at 4°C until further use (blocked beads).

Lysis buffer was chilled to 4°C, samples and beads were kept on ice unless otherwise stated. 100μl of cell extract containing 200μg of protein was added to a sterile 1.5ml microcentrifuge tube, 10μl of unblocked beads were added and the bead/protein mixture incubated for one hour rotating at 4°C. The sample was centrifuged and the supernatant removed to a fresh microcentrifuge tube. 2μl the appropriate antibody was added and incubated whilst rotating at 4°C for one hour. 20μl of blocked beads were then added to each sample before incubating for one hour whilst rotating at 4°C. Beads were then washed with 500μl of Lysis Buffer four times. After the final wash, lysis buffer was removed leaving a residual 5μl. 2μl of NuPage sample reducing agent and 5μl of NuPage LDS sample buffer (Invitrogen) was added to the beads before heating at 70°C for ten minutes. Samples were then separated on a SDS-PAGE gel, 200V for 1 hour and the proteins detected by Western Blotting.

2.2.4.17 Preparation and purification of GST Fusion Proteins

To induce GST fusion proteins, 3ml of Ampicillin containing L-Broth was inoculated with a single bacterial colony containing the plasmid DNA and grown overnight at 37ºC whilst shaking. Next morning 1ml of bacterial culture was inoculated into 100ml of Ampicillin containing L-Broth and grown for 3 hours at 37ºC whilst shaking following which the optical density was measured. Incubation continued until the optical density reached the desired level. IPTG was added to give a final concentration of 1mM and the culture was incubated for a further 1hour at 37ºC whilst shaking before spinning the culture at 5000g

for 5 minutes and discarding the supernatant. The bacterial pellet were then stored at -80º until further use.

To lyse the bacteria, pellets were then re-suspended in 2ml of ice-cold 1% triton-X-100 in PBS containing one protease inhibitor tablet per 10ml of solution. The sample was then subjected to 10 cycles of sonication (30seconds on, 30 seconds off) at the high setting keeping the samples on ice throughout. Following sonication, 3mls of ice-cold 1% Triton-X-100 in PBS was added to each sample to bring the sample volume to 5mls before spinning for 10 minutes at 12000g at 4ºC. The resultant supernatant was transferred to a fresh 15ml falcon tube and the cell debris discarded. 500µl of GST-Fast Sepaharose beads were added to each sample and incubated for 1 hour at 4ºC whilst the rotating the sample. The samples were spun at 500g at 4ºC for 2 minutes to bring the beads to the bottom of the tube than the supernatant was discarded and the beads washed with 10ml of 1% Triton-X-100. This step was repeated 5 times. 1ml of 1% Triton-X-100 was added to the final pellet and the beads were transferred to a clean 1.5ml Eppendorf tube. 100ul of beads from each sample was then transferred to a second clean 1.5ml micro-centrifuge tube. GST fusion proteins were cleaved from the beads by adding 3 X volume of Thrombin (80µl in 920µl PBS) to the beads and incubating overnight whilst rotating at 4°C. The remaining beads were spun at 80g for 2 minutes, the supernatant removed and 500µl of glycerol was added to the sample before storing at -80ºC.

2.2.4.18 Coomassie Blue Staining

To assess the quantity of protein induced, 100µl of beads retained from each sample was spun at 80g, 4ºC for 2 minutes, the supernatant removed before adding 2µl of sample reducing agent and 5µl off LDS sample buffer. Samples were then heated at 70ºC for 10 minutes to separate the proteins from the beads. The sample was spun briefly before loading the supernatant onto a 4-12% gradient SDS gel. To separate the proteins the gel was run for 1 hour at 200V then transferred to a gel tank and covered with Coomassie Blue. The gel/Coomassie Blue solution was then heated in the microwave until the solution reached boiling point then incubated shaking at room temperature for 1 hour. The Coomassie Blue was removed, the gel rinsed briefly with water twice, then immersed in 20% NaCl solution to de-stain and incubated at room temperature

whilst gently shaking overnight. The gel was then visualised and photographed on a light box.

2.2.5 Tissue Culture

2.2.5.1 Maintenance of cells in culture

All cell culture work was carried out in a tissue culture laboratory under strict sterile conditions. Cell culture work was performed inside a flow hood (Class II Microbiology Safety cabinets, Gelaire, BSB4).

293T, MCF7, and U2OS cell lines were grown in DMEM (1x) +w/GlutaMAX™/Glucose NaPyr, 10%FCS, 1% Penicillin/Streptomycin. U2OS B3 and 4.1 cell lines were grown in DMEM (1x) +w/GlutaMAX™/Glucose NaPyr, 10%FCS, G418 (600μg/ml). HaCaT cells were grown in calcium free DMEM (1X) High Glucose, 10%FCS, 5ml L-Glutamine 200mM (100x), 1% Penicillin/Streptomycin.

All cell lines were grown in an atmosphere containing 5% CO_2 (v/v) (Napco model 5410, Napco Scientific). Cell lines were split 1/10 twice weekly.

2.2.5.2 Transient Cell Transfection

Cells were plated in monolayer at the appropriate density and transient transfection performed 24 hours later.

2.2.5.2.1 Calcium Phosphate Transient Transfection

The appropriate amount of the DNA of interest was added to a sterile 1.5ml microcentrifuge tube and completed to 375μl with distilled water. 125μl of 1M Calcium Chloride was added and vortexed for one minute to mix. This 500μl solution was then added drop wise whilst vortexing to a sterile 5ml Bijoux containing 500μl of 2x HEPES buffered saline (2xHBS) (8g NaCl, 0.37g KCl, 0.135g 1.5mM Na2HPO4.2H2O, 1g Dextrose, 5g HEPES, completed to 500ml with distilled H_2O and adjusted to pH 7.05 with a few drops of 0.1M NaOH). The solution was left to incubate at room temperature for approximately 15 minutes until a precipitate was formed. The solution was then added to the cell monolayer drop wise and the cells returned to the incubator. After 16 hours, the media was removed from the cells which were then washed twice with 5-10mls

of PBS before adding an appropriate volume of fresh media and returning the cells to the incubator for a further 24 hours.

2.2.5.2.2 Lipofectamine 2000™ Transient Transfection

For siRNA treatment of HaCaT and MCF7 cells, transient transfection was carried out with Lipofectamine 2000™.

Cells were trypsinised and washed twice in PBS. Cells were re-suspended in antibiotic free media and counted. In sterile 1.5 ml microcentrifuge tubes, two transfection solutions were prepared; firstly 2.5μl of the desired oligonucleotides (siTopBP1 or siLuciferase, Dharmacon) was added to 497.5μl of Optimem (Invitrogen) and secondly, 15μl of Lipofectamine 2000™ (Invitrogen) was added to 485μl of Optimem. The two separate cocktails were incubated at room temperature for 5 minutes before mixing and incubating for a further 20 minutes at room temperature. For mock transfected cells, the oligonucleotide was omitted. For no treatment plates, both the oligonucleotide and Lipofectamine 2000™ were omitted.

Following the incubation, the desired volume of cells were added to the Optimem/Lipofectamine 2000™/oligonucleotide solution, and seeded onto tissue culture plates then incubated at 37°C 5% CO2 (v/v). The next day, media was aspirated, the plates washed with 1xPBS 5-10mls twice and fresh antibiotic containing media applied.

2.2.5.3 Preparation of Protein Extracts

For the detection of protein by Western Blotting, cells grown in monolayer were washed with 10ml of PBS twice before adding 1ml/4ml of Trypsin to a 60mm/100mm cell culture plate and incubated at 37.5ºC 5% CO_2 (v/v) for 5-15 minutes. 5/10ml of fresh cell culture medium was added to the plate before aspirating and transferring to a 15ml centrifuge tube and spinning at 80g for 5 minutes at room temperature. The resultant cell pellet was washed with 10ml of PBS and spun at 80g for 5 minutes at room temperature. The PBS was aspirated and the pellet re-suspended in 100-150μl of lysis buffer (0.5% NP40, 150mM NaCl, 50mM Tris pH 8.0 containing 1/10 volume protease inhibitor cocktail tablet). The lysate was transferred to a microcentrifuge tube and incubated on

ice for 30 minutes before centrifuging at 15000g for 30 minutes at 4ºC. The resultant supernatant containing the cell proteins was then transferred to a new microcentrifuge tube and stored at -80ºC until required.

2.2.5.4 Replication Assays

293T cells were plated onto 100mm tissue culture plates at a concentration of $6x10^5$ cells per plate. After 24 hours, cells were transiently transfected with the DNA(s) of interest by calcium phosphate transfection. Sixteen hours following transfection, cells were washed twice with 10ml of 1xPBS and fresh media applied. On day four post transfection cells were harvested by washing each plate twice with 5mls of PBS then adding 800µl of HIRT solution (0.6% SDS, 10mM EDTA) to each plate to lyse the cells. After a 10 minute incubation at room temperature the resultant lysate was scraped into a clean 1.5 ml microcentrifuge tube containing 200µl of 5M NaCl. The samples were gently vortexed and stored at 4ºC overnight. Next day samples were centrifuged for at 15000g at 4ºC for 30mins and the supernatant removed to a fresh 1.5 ml microcentrifuge tube. Samples were then extracted with Phenol Chloroform (2.2.4.3.1) twice before ethanol precipitation was carried out (2.2.4.4).

Pelleted DNA was re-suspended in 20µl of distilled H_2O. DNA was digested with Dpn1. To each 20µl DNA sample, 5µl of NEB Buffer1, 0.5µl BSA, 2µl Dpn1 and 22.5µl of distilled H_2O water was added and the samples incubated at 37°C overnight.

The next day, samples were digested with EXO III by adding 1µl of EXO III to each sample and incubating at 37°C for 90 minutes. EXO III was then heat inactivated at 70°C for 30 minutes and the samples allowed to cool before analysis by qPCR (2.2.4.9).

2.2.5.5 Luciferase Assay

Luciferase assays were carried out in 293T cells. All assays were carried out in duplicate on 60mm cell culture plates. $3x10^5$ 293T cells were seeded onto each plate and transiently transfected with the DNA(s) of interest 24 hours later by the $CaPO_4$ method (2.2.5.2.1). After 16 hours cells were washed twice with 5ml

of 1xPBS and fresh media applied. 48 hours following transfection, cell culture media was aspirated and the cells washed twice with 2ml of sterile PBS. The PBS was removed by aspiration. 300µl of 1 x reporter lysis buffer (Promega) was added to each plate and incubated at room temperature for 10 minutes. Cells were scraped off the culture plate with a cell scraper directly into a 1.5ml microcentrifuge tube. The lysates were centrifuged at 15000g at 4ºC for 10 minutes to pellet the cell debris. The resultant supernatant was transferred to a fresh 1.5ml microcentrifuge tube.

Luciferase activity was determined using a luminometer with an automatic injection (Luminoskan Ascent- Thermo Labsystems). 80µl of each lysate was added to a 96 well Fluoro flat bottom microplate (Nunc) and 80µl of Luciferase assay buffer (Promega) used at a 1:2 dilution was automatically injected into each well.

2.2.5.6 Cycloheximide Treatment Time Course

For time course experiments, 293T ($6x10^5$ cells) or U2OS ($6x10^5$ cells) cells were plated onto 10cm cell culture plates containing 10mls of cell culture medium and incubated at 37.5ºC 5% CO_2 (v/v) for 24 hours.

Cycloheximide ready made solution 1mg/ml (Sigma) was diluted with cell culture media to a concentration of 100µg/ml. Cell culture media was aspirated from cells plates and replaced with 10mls of the Cycloheximide/cell culture media mix at different time points. Cell plates were harvested in unison. Protein extracts were prepared as described and analysed by Western Blotting.

2.2.5.7 Irradiation of Cells with UVB

Cells were plated in monolayer in cell culture plates. Twenty-four hours later, the media was aspirated and the cells washed with 10mls of PBS twice. Cells were then treated with UVB (312nM) with varying doses from 0 to 0.050 Joules/cm^2 (J/cm2). Fresh cell culture media was applied and plates were incubated at 37ºC 5% CO_2 (v/v) for 30 minutes before the cells were harvested and protein or RNA extracts prepared as described.

2.2.5.8 Crystal Violet Colony Survival Assay

The colony survival assay provides a measure of cell viability over a 14 day period. The cell lines to be assayed and controls were siRNA treated as described (2.2.5.2.2). 24 hours following transfection, the cells were washed twice with 10ml of PBS and fresh medium applied. 48 hours following transfection, cell plates were trypsinised, harvested and counted. 500 cells from each cell line and controls were plated out in triplicate on a 10cm cell culture plate containing 10mls of media. The plates were incubated and the media was replaced twice weekly. 14 days following transfection, the media was removed and the cells washed twice with 10mls of PBS. The surviving colonies were visualised by staining with 2mls of 0.5% crystal violet solution (25% methanol, ddH_2O) for 20 minutes at room temperature whilst gently rocking. The plates were then washed in tap water until the solution ran clear and the plates were left to dry overnight at room temperature. The colonies were then counted.

2.2.5.9 Cell Growth Assay

The cell growth assay provided a measure of cell viability. Cell lines and controls to be assayed were transfected using Lipofectamine 2000™ as described then seeded onto cell culture plates. 24 hours following transfection, cells were washed with 5-10mls of 1xPBS twice and fresh media applied. 48 hours following transfection, cells were trypsinised, harvested and counted. Each plate was counted twice and the average of two counts determined. $2x10^5$ cells from each experiment were then plated out in triplicate onto a 60mm cell culture containing 5ml of cell culture medium. Following further 48 hours incubation, cell plates were again trypsinised, harvested and counted and $2x10^5$ cells plated out as described above. After a further 48 hours incubation, cells were trypsinised, harvested and counted for the final time. The number of growing cells for each cell line and controls was then determined by plotting the mean counts of each triplicate set of plates on a graph. At each time point the residual cells were retained and protein extracts prepared. The extracts were then analysed by Western Blotting to ensure that the gene knockdown persisted at each time point.

2.2.5.10 Preparation of RNA

For the gene expression microarray experiments, $6x10^5$ MCF7 cells were transfected or mock transfected with si-RNA and seeded onto 60mm tissue culture plates. 48 hours later plates were treated or mock treated with UVB and harvested by trypsinisation 30 minutes following irradiation. The resultant pellets were stored at -80 ºC until required. RNA was extracted from the cell pellets using the RNAeasy kit (Qiagen) according to the manufacturer's instructions. Briefly, the cell pellets were thawed, 350µl of buffer RLT was added to each pellet, mixed and the resultant lysate pipetted onto a Qiashredder spin column in a 2ml collection tube before centrifuging for 2 minutes at 15000g. 350µl of 70% Ethanol was added to each sample and mixed before applying 700µl of the sample to an RNeasy mini column in a 2ml collection tube and centrifuging at 15000g for 15 seconds. The flow through was discarded, 700µl of buffer RW1 was added to the column before centrifuging at 10000g for 15 seconds. The flow through was discarded and the column transferred to a new 2ml collection tube. 500µl of buffer RPE was added to the column, incubated for two minutes before centrifuging at 10000g for 15 seconds. The flow through was discarded and a further 500µl of buffer RPE added before centrifuging at 15000g for 2 minutes. The RNeasy colum was transferred to a new 2ml collection tube and centrifuged for 1minute at 15000g. The column was then transferred to a sterile 1.5ml microcentrifuge tube, 50µl of RNase free water pipetted directly onto the membrane and the column centrifuged at 15000g for 1 minute.

The column was discarded and the RNA treated with DNase to remove any residual traces of DNA.

2.2.5.11 DNAse treatment of RNA samples

RNA samples were treated to remove any contaminating DNA with the DNA-free™ kit (Ambion) according to the manufacturer's instructions. Briefly, 30µl of the RNA sample was taken into 1.5ml microcentrifuge tube. 3µl of TurboDNase buffer (10x) and 1µl of TurboDNase was added to the RNA and gently mixed before incubating at 37ºC for 30 minutes. 3.4µl of DNase inactivation reagent was added to the sample and mix well before incubating at room temperature

for 2 minutes then centrifuging at 15000g for 2 minutes. The resulting supernatant was removed to a fresh 1.5ml microcentrifuge tube before centrifuging again at 15000g for 2 minutes and again the resultant supernatant was removed to a fresh 1.5 ml microcentrifuge tube and stored at -80ºC until further use.

2.2.6 Microarray

The raw data in the form of Affymetrix CEL files were generated with Affymetrix GCOS software. The further analysis was done with the Partek Genomics Suite (http://www.partek.com/). A full description of the methodology used for generating and analysing the microarray data is given in chapter 3.5.

2.2.7 Statistics

2.7.1 Epidemiology

SPSS software package for Windows version 14 (SPSS Chicago, IL, USA) was used to analyse the data. The log rank test was used to show significance for the Kaplan Meier plots giving an estimate of probability that the three groups are not random samples from the same population with respect to actuarial survival. A p value of <0.05 was regarded as statistically significant.

2.7.2 HPV Genotyping

SPSS software package for Windows version 15 was used to analyse the data by logistic regression analysis. The Chi-squared test was used on the overall analysis to show significance. *P* <0.05 was considered to be statistically significant

2.7.3 Immunohistochemistry

SPSS software package for Windows version 15 (SPSS Chicago, IL, USA.) was used to analyse the data. Fisher's exact test was used to show significance. P< 0.05 was considered to be statistically significant.

2.7.4 Molecular Biology

2.7.4.1 Mean and standard error

The mean +/- the standard error of the mean (S.E.M.) are shown in several experiments as a control for experimental reproducibility. The S.E.M. gives a measure of the precision of the mean giving a representation of the spread of the data, indicating how far the mean of the sample is from the true mean.

$$\text{S.E.M.} = \frac{\text{Standard Deviation}}{\sqrt{[\text{sample number } (n)]}}$$

2.7.4.2 Statistical Significance

Statistical significance for the experimental data in this thesis (unless stated otherwise) was typically calculated using a Students-T-test to give a significance value (p). This was carried out using Microsoft Excell (T-test function). The cut off for all experiments was taken as 0.05, therefore if two sets of data return a p value of <0.05 there is a less than 5% chance that the observed result is due to chance and the two groups are therefore statistically significantly different.

Chapter 3: Results

Chapter 3.1 Nonmelanoma Skin Cancer in the West of Scotland Renal Transplant Population

OTRs are now being transplanted at an older age and are surviving longer, resulting in an ageing transplant population. Improvements in immunosuppressive regimens and transplant techniques have led to better graft survival in the short and long term (15) and hence the number of patients on long-term immunosuppression is increasing. It is well established that one of the consequences of long-term immunosuppression is an increased risk of cancer. Transplant patients are reported to have a two to six fold increased risk of cancer and the highest risks are for skin cancers(16-18). Skin cancers in transplant recipients may be multiple, evolve rapidly, recur and metastasise more frequently and exhibit unusual clinical appearances when compared with immunocompetent patients. Transplant recipients therefore have an increased need for access to Dermatology services. The 2006 document from The National Institute for Health and Clinical Excellence (NICE), *Improving Outcomes for people with Skin Tumours including Melanoma*, recommends that transplant patients who have pre-cancerous skin lesions or who have developed a skin cancer should be seen in a dedicated "transplant patient skin clinic"(1).

A specialist Dermatology clinic for RTRs was established at the Western Infirmary, Glasgow which is the transplant centre for the West of Scotland, in 2005. The primary aims were to provide a dedicated Dermatology clinic offering skin cancer surveillance and education to all RTRs, to provide rapid access to Dermatology services for RTRs and to establish close links with transplant surgeons and renal physicians to allow for optimal patient management. The secondary aim was to collect data on skin cancer within the West of Scotland renal transplant population. While data exist for other UK transplant populations, few data pertain specifically to the Scottish transplant population. The results of this investigation are presented here.

3.1.1 Age and sex distribution

610 (374 male, 236 female) patients attended the clinic on at least one occasion. The mean age of the population was 50 years (median 49, range 18-83). The mean age was similar for both male and female patients being 50 and 49 years respectively. The mean follow up time since first renal transplantation was 5 years (median 10, range 0-37 years).

3.1.2 Skin type and sun exposure

Four hundred and twenty-six patients (69.8%) had Fitzpatrick's skin type I-III (I-106; II-199; III-121). Of the remaining 184 (30.2%) patients, 20 (3.3%) had skin type IV, 29(4.8%) type V and skin type was not recorded in 135 (22.1%). Eleven (1.8%) patients had previously used sun beds. Sixty-nine (11.3%) patients had lived outwith the United Kingdom for a period of six months or more. On the basis of previous and current occupational and recreational sun exposure and behaviour patterns in the sun, 314 (51.5%) patients were deemed to have had low, 144 (23.6%) patients medium and 80 (13.1%) patients high UVR exposure. In the remaining 72 (11.8%) patients, UVR exposure was not recorded.

3.1.3 Clinical examination

On examination at the screening visit, 169 (27.7%) patients had viral warts. Only palmo-plantar and classical cutaneous warts were documented, plane warts were not recorded. 112(18.4%) patients had actinic keratoses or Bowen's disease. The presence of actinic keratoses or Bowen's disease was associated with non-melanoma skin cancer. Forty-four (47.8%) of patients with skin cancer had actinic keratoses present on initial examination compared with 69(13.4%) of the non-skin cancer group.

3.1.4 Skin cancers

All retrospectively diagnosed skin cancers were recorded as well as those diagnosed at the first clinic visit and any subsequent tumours that developed within the study period. Of the 610 patients who attended the clinic, 95(15.6%) patients had a cutaneous malignancy of whom 68(72%) were male and 27(28%) female. 370 cutaneous malignancies were diagnosed, a mean of 3.9 tumours per patient (median 2, range 1-40).

BCC were the most frequently diagnosed tumours. 74(12.1%) of all patients had a BCC. There were 208 BCC in total (181 nodular and 27 superficial, mean 2.8 tumours per patient (range 1-26)). SCC were less common than BCC (42 (7%) of all patients had an SCC). There were 151 SCC in total (including 8 Keratoacanthoma – like SCC), mean 3.6 SCC per patient (range 1-40).

The overall SCC: BCC ratio was 0.7. To determine whether the SCC: BCC ratio varied with length of follow up, patients with skin cancer were grouped according to the era in which they were transplanted (1970-1984, 1985-1994 or 1995 onwards) (Table 4). There were 10 patients with skin cancer transplanted from 1970-1984, the SCC: BCC ratio was 1.1 (mean number of tumours per patient 8.5, mean follow up 28.2 years). From 1985-1994 there were 37 patients with skin cancer, the SCC: BCC ratio was 0.8 (mean number of tumours per patient 3.3, mean follow up 17.2 years). From 1995 onwards there were 43 patients with skin cancer, the SCC: BCC ratio was 0.5 (mean number of tumours per patient 3.5, mean follow up 8.0 years).

Era of renal transplant	Patients	SCC	BCC	SCC:BCC ratio	Mean tumours per patient (median, range)	Mean follow up (years) (median, range)
1970-1984	10	45	40	1.1	8.5 (3.5, 1-40)	28.2 (27, 24-37)
1985-1994	37	56	67	0.8	3.3 (2, 1-15)	17.2 (16, 14-23)
1995 onwards	43	50	101	0.5	3.5 (2, 1-40)	8.0 (9, 0-13)

Table 4 The SCC: BCC ratio by era of renal transplantation.

All patients with skin cancer (n=95) were grouped according to the era in which they were transplanted. Five patients who had neither SCC nor BCC were excluded from the analysis. SCC and BCC are the number of each tumour per group. The mean number of tumours per patient (SCC and BCC only) and mean length of follow up are shown for each era (median, range).

Abbreviations: SCC, squamous cell carcinoma; BCC, basal cell carcinoma.

There were eight MM in total including one Lentigo Maligna (LM), one Lentigo Maligna Melanoma (LMM) and one Melanoma *in situ* (MIS). Five (0.8%) patients had a melanoma. One patient had four MM, the remaining four patients each having a single lesion.

There were three other skin malignancies; one cutaneous B cell lymphoma which had occurred prior to transplantation, and two cases of vulval intraepithelial neoplasia III (VIN III). There were no cases of KS, neuroendocrine or appendageal tumours. The number and distribution of tumours is summarised in Figure 6.

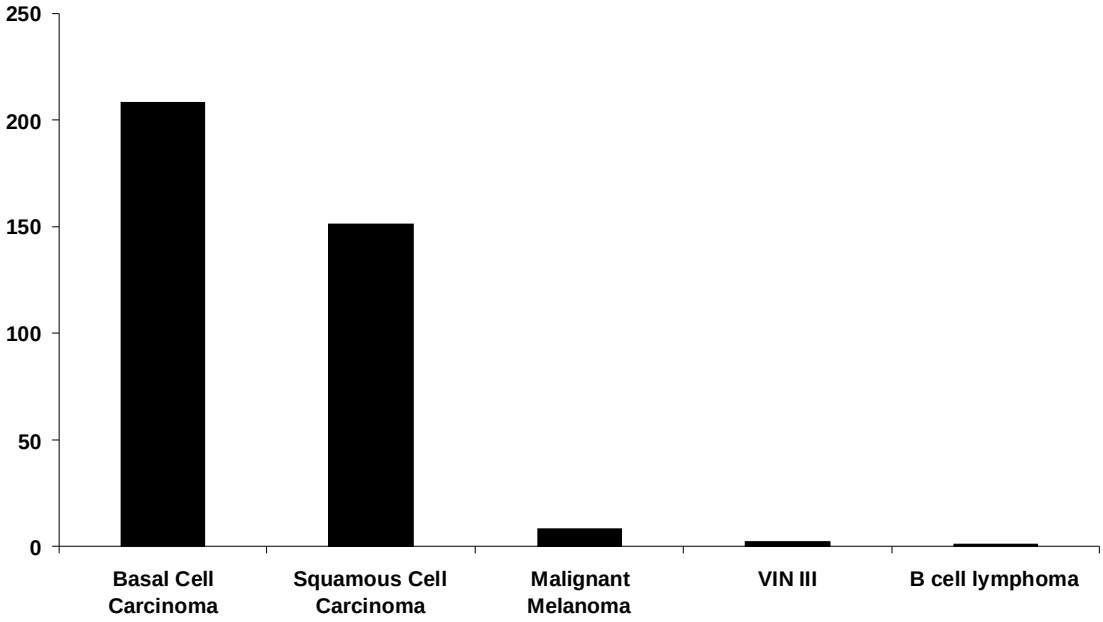

Figure 6 Number and distribution of cutaneous malignancies.

Abbreviations: VIN III, vulval intraepithelial neoplasia III.

Thirty-seven (38.9%) patients had a single tumour. Twenty-five patients having a single BCC, eight patients a single SCC, two patients had a MM and two patients had VIN III. Fifty-eight (61.1%) patients had multiple tumours. Twenty-two patients had multiple BCC, seven had multiple SCC, one had multiple MM, 25 had a combination of BCC and SCC and three had BCC and/or SCC with MM or cutaneous B cell lymphoma.

3.1.5 Location of tumours

Two hundred and thirty-one tumours (62.4%) were located on the head and neck area, of which 17 (5.5%) lesions were at high risk sites on the ears (9 BCC and 5 SCC) and lips (2 BCC and 1 SCC). Fifty tumours (13.5%) were located on the trunk, 47 (12.7%) on the upper limbs, 14 (3.8%) on the lower limbs, 2 (0.5%) on the vulva. The site was not recorded in the remaining eight (2.2%) lesions. The location of skin tumours is summarised in Figure 7.

Nodular BCC were predominantly located on the head and neck (132 (72.9%) head and neck, 24 (13.2%) trunk, 18 (9.9%) limbs, 7 (3.9%) site not recorded). Superficial BCC (SBCC) were more likely to be located on the trunk (ten (37.0%) head and neck, 16 (59.2%) trunk, one (3.7%) limbs).

SCC were predominantly located on the head and neck (87 (57.6%), five (3.3%) trunk, 58 (38.4%) limbs (47 upper, 11 lower limb), one (0.7%) site not recorded). SCC was the only tumour located on the hands.

Of the eight MM, one (12.5%) was located on the head and neck, five (62.5%) on the trunk and two (25.0%) on the limbs.

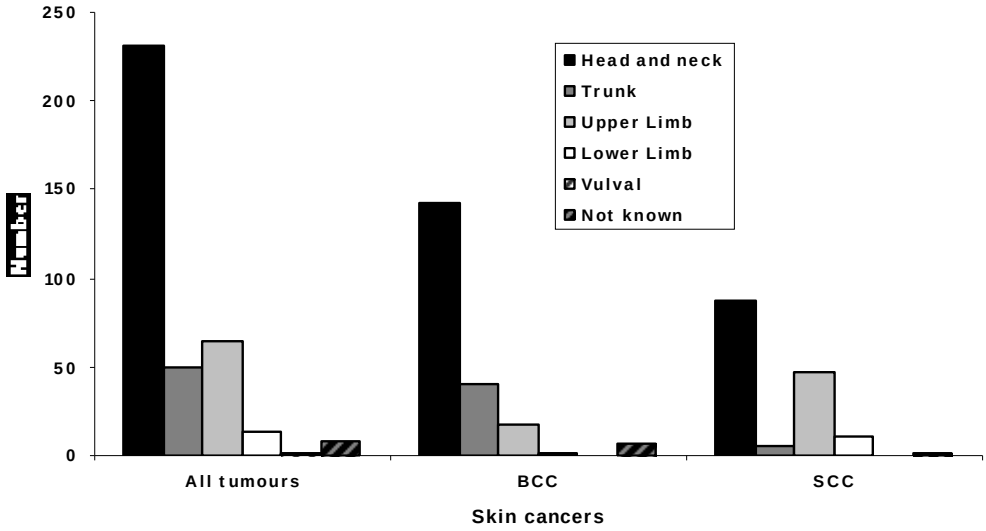

Figure 7 Location of skin tumours.

Abbreviations, BCC: basal cell carcinoma; SCC, squamous cell carcinoma.

3.1.6 Recurrences and metastases

Within the study period there have been three recurrent SCC. One SCC recurred locally and was treated by wide local re-excision. Two patients both with SCC occurring on the pre-auricular skin have had tumours metastasising to local lymph nodes. Both patients have required extensive surgical excision, lymph node clearance, radiotherapy and reduction of immunosuppression.

3.1.7 Clinical course

Of the 610 patients, the date of their first renal transplant was recorded on the database for 608 patients (the data were incomplete for the remaining 2 patients who all had transplants elsewhere and in whom the date of transplant was not recorded). Accurate length of follow up data was therefore available for 608 patients and was taken as date of first transplant to date of death or November 2008. Follow-up data was rounded up or down to the nearest year. This gave us follow up data for patients on immunosuppression for 5957 patient years. The mean follow up time post transplantation was 5 years (median 10, range 0-37 years).

Four patients who had skin cancer before first kidney transplant were excluded from the analyses of time to first skin cancer. For the remaining 604 patients the number of patients who had developed skin cancer was calculated at various time points following transplantation and the results are shown in Figure 8. In those who had been immunosuppressed for less than 3 years, 5.4% of patients had skin cancer. This figure rose to 12.7% by 3-7 years, 26.1% by 8-15 years and was 25.0% in those patients who had been immunosuppressed for over 15 years. The prevalence of skin cancer increased as time from transplantation increased but appeared to plateau after 15 years.

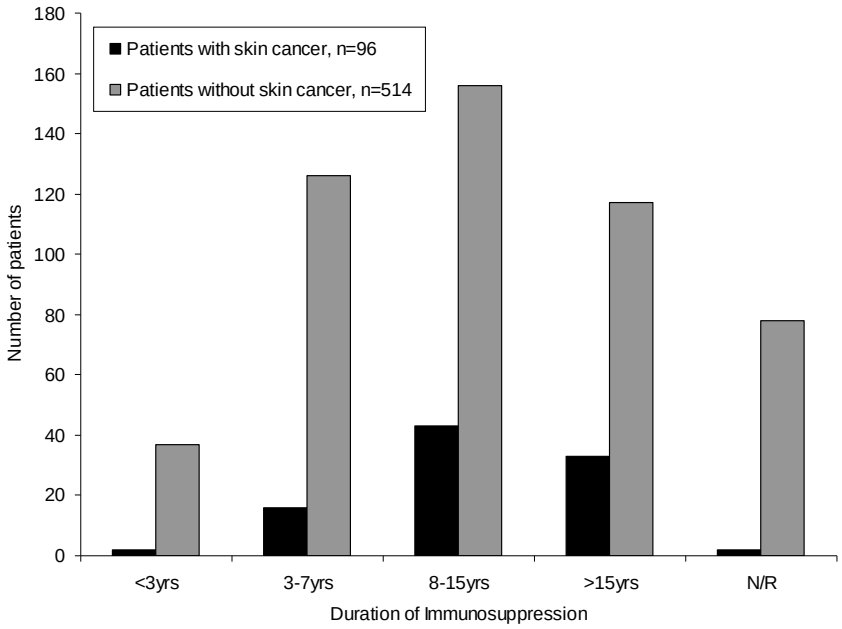

Figure 8 Number of patients with skin cancer and duration of immunosuppression.

3.1.8 Transplantation to first cancer

The mean time between transplantation and the development of a first skin cancer varied with the age of the patient at transplantation (Figure 9). In patients transplanted between the ages of 15 and 29 years, the mean time to development of first skin cancer was 17.2 years. The mean time to develop cancer fell as the age of the patient at transplantation increased (30-39 yrs – 10.5 yrs; 40-49 yrs – 9.1 yrs; 50-59 yrs – 7.7 yrs; 60-70yrs – 4.5yrs).

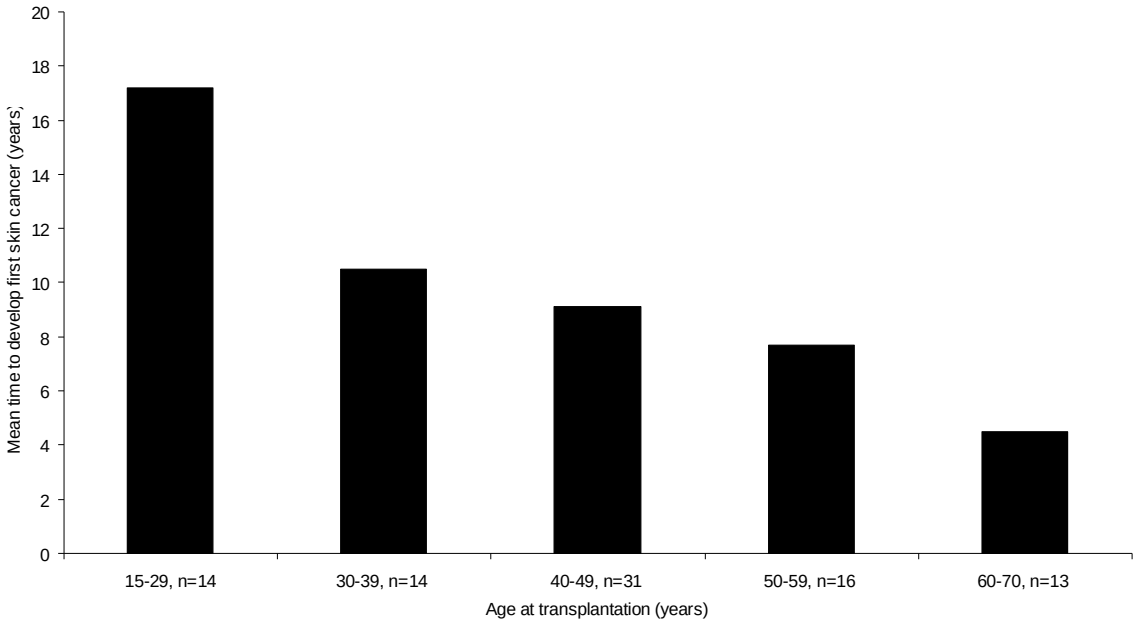

Figure 9 Time between transplant and development of first skin cancer.

The mean time in years between transplantation and the development of a first skin cancer is shown for age groups 15-29, 30-39, 40-49, 50-59 and 60-70 years. Excluded from the analysis were six patients in whom the first skin cancer pre-dated transplantation and two patients in whom the date of first transplant was not recorded.

3.1.9 Immunosuppression

Alterations in immunosuppressive therapy regimens over time may influence the development of skin cancer. In our centre between 1970 and 1985 all patients received prednisolone and azathioprine. From 1985 patients were immunosuppressed with prednisolone, azathioprine and ciclosporin, weaning off either azathioprine or ciclosporin at one year post transplant. From 1990 patients stayed on triple therapy unless major side effects. From 1995

mycophenolate mofetil (MMF) was increasingly used instead of azathioprine and tacrolimus instead of ciclosporin for any patients who had acute rejection or ciclosporin associated side effects. From 2007 all patients were started on prednisolone, tacrolimus and MMF. Sirolimus has been used in a small minority of patients since 2000 mainly as a way of minimising exposure to calcineurin inhibitors when mycophenolate was not tolerated.

To determine whether the type of immunosuppression used influenced the development of skin cancer, a survival analysis was performed. Patients were divided into three groups according to the era in which they were transplanted; 1970 -1984 (n=66), 1985-1994 (n=195) or 1995 onwards (n=343).

The percentage of patients surviving without skin cancer was plotted against the years since transplant. The results are shown in Figure 10. In the 1970-1984 group, it was 25 years post transplantation before 20% of patients developed skin cancer. However this fell to 15 years and 10 years in the 1985-94 and 1995- groups respectively. The differences between the groups was significant, $p<0.0001$.

Multivariate analysis demonstrated that the effect of era was independent of age at transplant and sex (table 5).

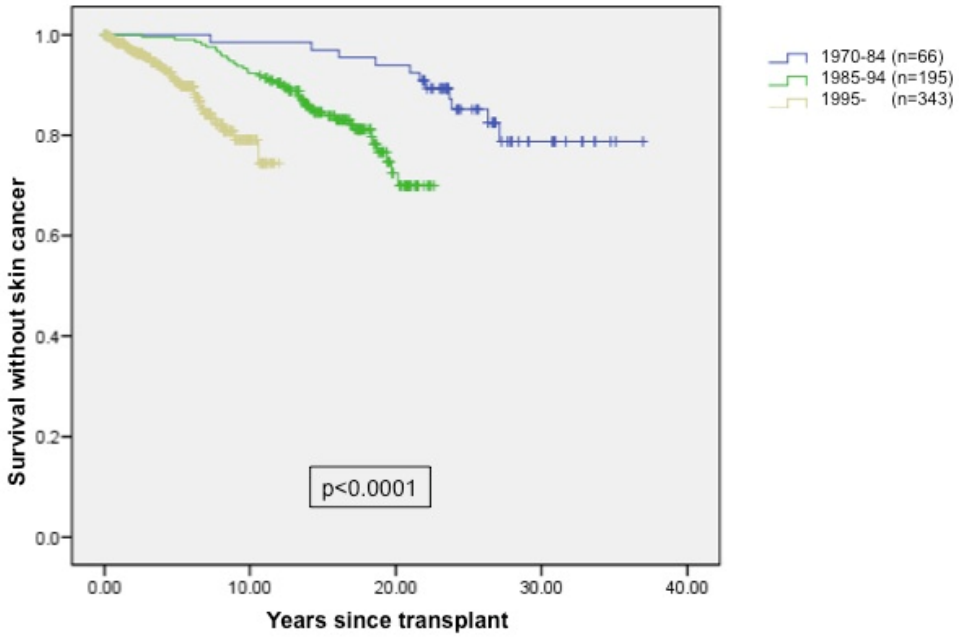

Figure 10 Time to first skin cancer by era of transplantation.

Kaplan Meier analysis of survival without skin cancer over time since transplantation. Patients transplanted between 1970 and 1984 are represented by the blue line, between 1985 and 1994 by the green line and after 1995 by the yellow line. The differences between the three groups were significant, p<0.0001.

	Hazard ratio	p	95% Confidence Interval for Hazard ratio	
			Lower	Upper
Age at transplant (per year)	1.061	0.000	1.042	1.080
Male	1.853	0.013	1.141	3.009
First transplant 1985-94*	2.605	0.044	1.025	6.616
First transplant 1995-*	6.952	0.000	2.372	20.379

Table 5. Cox proportional hazards model with time from first transplant to first skin cancer as the independent variable. (* transplant 1970-84 as reference).

To compare the effect of dual therapy versus triple therapy regimens on the development of skin cancer a comparison was made between patients on prednisolone and azathioprine with those on prednisolone, azathioprine and ciclosporin at one year post transplant. A survival analysis was performed determining survival without skin cancer over time since transplantation. The results are illustrated in Figure 11. It was 25 years post transplantation before 20% of patients on dual therapy developed skin cancer however for patients on triple therapy, 20% of patients developed skin cancer within 15 years. The difference between the groups were significant, $p<0.0001$. The data were similarly analysed according to immunosuppression immediately and two years post transplantation (data not shown), and results were similar to the analysis at one year post transplantation.

Multivariate analysis of these 213 patients who were either on prednisolone and azathioprine or prednisolone, azathioprine and ciclosporin at one year after transplant demonstrated that the effect of era was not statistically significant independent of age at transplant and sex (Table 6).

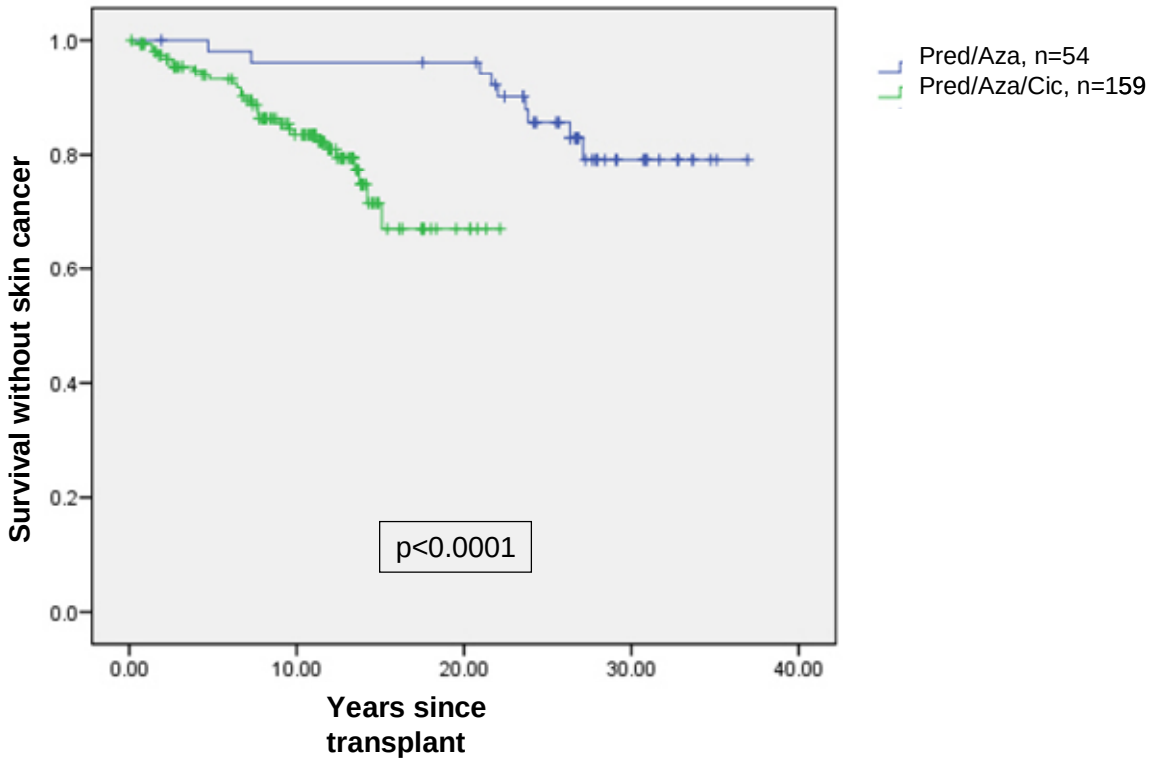

Figure 11 Time to first skin cancer by immunosuppression at one year post transplant.

Kaplan Meier analysis of survival without skin cancer over time since transplantation. Patients on dual therapy, consisting of prednisolone and azathioprine are represented by the green line. Those on triple therapy with prednisolone, azathioprine and ciclosporin are represented by the blue line. The difference between the groups were significant, p<0.0001.

Abbreviations; Pred, prednisolone; Aza, azathioprine; Cic, ciclosporin.

			95% Confidence interval for Hazard ratio	
	Hazard ratio	**p**	**Lower**	**Upper**
Age at transplant (years)	1.065	0.000	1.037	1.092
Male	1.875	0.073	0.942	3.730
Pred/Aza/cic at 1 year*	3.347	0.071	0.903	12.405

Table 6. Cox proportional hazards model with time from first transplant to first skin cancer as the independent variable.

To compare triple therapy regimens based on azathioprine with those based on MMF or sirolimus, a survival analysis was performed determining survival without skin cancer over time since transplantation. The results are illustrated in Figure 12. In this analysis, 20% of patients on triple therapy regimens incorporating Azathioprine developed skin cancer within 12 years whereas 20% of patients on MMF based regimens developed skin cancer within 10 years. The differences between the three groups did not reach statistical significance (p=0.43).

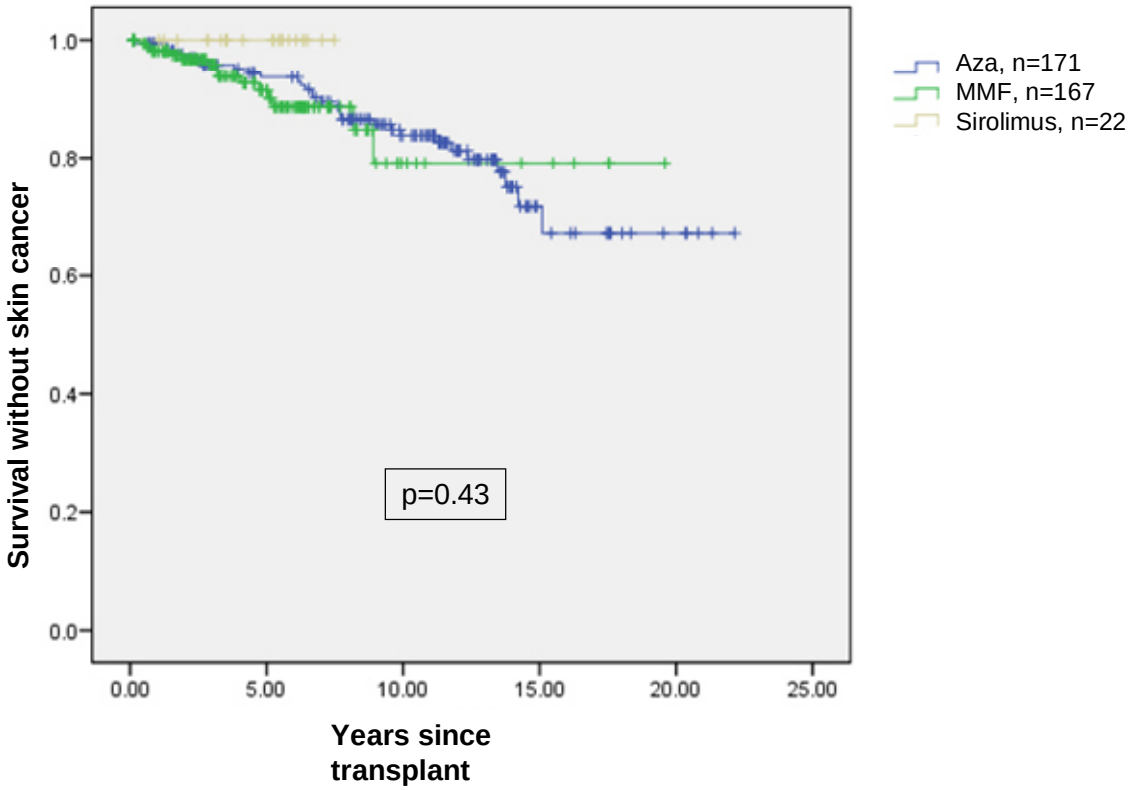

Figure 12 Time to first cancer by immunosuppression at one year post-transplant- comparison of triple therapy regimens.

Kaplan Meier analysis of survival without skin cancer over time since transplantation. The blue line represents triple therapy with Azathioprine (with prednisolone and either tacrolimus or ciclosporin). The green line represents triple therapy with Mycophenolate Mofetil (with prednisolone and either tacrolimus or ciclosporin. The yellow line represents patients on sirolimus in combination with any two other agents. The differences between the groups did not reach statistical significance, p=0.43.

Abbreviations; Aza, azathioprine; MMF, mycophenolate mofetil.

3.1.10 Discussion

Keratinocyte cancers comprising SCC and BCC are the most common malignancies occurring in Caucasian transplant recipients(21). The data from this population of Scottish renal transplant recipients are interesting as lower cancer incidence rates and a different pattern of skin cancer, with fewer SCC than BCC, are observed in comparison with other geographical areas.

3.1.10.1 Incidence of NMSC

The incidence of NMSC is greater in countries at lower latitude with cumulative incidences of 70 – 82% at 20 years post transplantation in Australian cohorts (28;36) compared to 30-52% in groups from the UK and The Netherlands (22;29). In this study the incidence of skin cancer was 15.6%, the mean follow up period post transplantation being five years. This may be a reflection of smaller numbers of patients or incomplete data e.g. patients who did not come to this clinic could have already been attending elsewhere and may have had skin cancers. It may also reflect a shorter follow up period; it is possible that over time incidence rates will rise to be in keeping with reports from elsewhere in the UK. Alternatively the lower skin cancer incidence rates could be a reflection of the immunosuppression regimens used or relatively lower UV exposure in this location.

3.1.10.2 SCC: BCC ratio

Following transplantation, the risk of BCC is increased two to ten fold (22-25) and for SCC the risk is increased 65-250 fold SCC (22;26;27). In immunocompetent populations, BCC outnumber SCC four fold however in transplant recipients a reversal in the BCC: SCC ratio is observed. The magnitude of reversal varies across studies with SCC to BCC ratios of 1.7 to 3.6 reported in studies from South Africa 1.7(275); Australia 2.0(36), 2.9(28) and 3.1(276); France 2.4(40); Italy 2.6(277); Ireland 2.6(278); the UK 3.2(279), 3.6(39) and The Netherlands 3.6(36).

In this study, there was no reversal of the BCC: SCC ratio - the SCC: BCC ratio was 0.7. There are reports of similar SCC: BCC ratios in Spanish renal transplant

populations; Fuente et al reported a SCC: BCC ratio of 0.7 (30) and Marcen et al reported a SCC:BCC ratio of 1(31).

Based on skin type and sun exposure patterns similar SCC: BCC ratios to those reported from elsewhere in the UK and Ireland were expected in this study. Based on differences in the SCC:BCC ratio seen at different latitudes within Australia (280), it has been suggested that the level of sun exposure influences the proportion of BCC and SCC observed following transplantation with increasing SCC related to increased sun exposure (281). The relative paucity of UVR exposure in Scotland might therefore explain the low SCC: BCC ratio in this study compared to elsewhere in Europe and Australia however it does not explain the differences between our patients and those elsewhere in the UK and Ireland. SCC are typically associated with chronic UVR exposure whereas BCC are related to short intense bursts of UVR such as that obtained on sunny holidays, the type of sun exposure typically received by our patients and perhaps explaining our higher BCC rates. It has been postulated that the low SCC: BCC ratios seen in transplant recipients in southern Europe such as those reported by Fuente and Marcen, might be due to the darker skin type in such populations being relatively protective against SCC but less so against BCC (281). The similarities in SCC: BCC ratio between our population and those of southern Europe would not be readily explained by either skin type or sun exposure patterns; in our Scottish RTRs the majority of patients had fairer skin types I-III.

In transplant recipients there appears to be an exponential rise in the incidence of SCC but a linear rise in BCC (28;29). Fuente et al(30) noted that the exponential increase in SCC increased over time post transplantation, thereby a gradual increase in SCC: BCC ratio was noted over time. The mean follow up time in this study (all patients) was five years. To determine if the SCC:BCC ratio increased over time in our study it was calculated according to the era of transplantation revealing a SCC:BCC ratio of 1.1, 0.8 and 0.5 associated with follow up lengths of 28.2, 17.2 and 8.0 years respectively (skin cancer patients only). It is possible that as this study continues prospectively an increase in the overall SCC: BCC ratio may be observed.

An alternative explanation might lie in reporting bias as it is recognised that there is variability in recording of NMSC. Some cancer registries combine BCC

and SCC as NMSC whereas some will record each SCC but only the first BCC. These reporting methods might lead to under-reporting of BCC in many registry based studies and subsequently alter the reported SCC: BCC ratio. In this study, a history was taken from each patient included in the study and each tumour recorded separately.

3.1.10.3 Time between transplantation and first cancer

The mean time between transplantation and development of a first skin cancer varied with age from a mean of 17 years in those transplanted between age 15 and 29 to six years in those transplanted between ages 60 and 70 years. A shorter interval between transplantation and first cancer in older patients has been previously reported (29).

3.1.10.4 Immunosuppressive regimens

The results of this investigation suggest that patients who were transplanted in the era 1970 – 1984 were immunosuppressed for a longer duration before developing skin cancer and a similar effect was seen between 1985-1994 and 1995 onwards. This may suggest that the introduction of ciclosporin from 1985 onwards resulted in skin cancers appearing sooner than in the pre-ciclosporin era. Ciclosporin is a potent immunosuppressant that has a direct carcinogenic effect aiding growth of tumours and metastases via transforming growth factor ß (50). Lower doses of ciclosporin have been associated with reduced incidence of skin cancer; a single centre randomised control trial by Dantal and colleagues compared azathioprine and normal dose ciclosporin to azathioprine and low dose ciclosporin. After 66 months of follow-up, significantly fewer patients in the low dose ciclosporin group developed skin cancer (282).

Similarly the results showed a shorter duration of time between transplantation and first cancer between the eras 1985-1995 and 1995 onwards. Over time increasing numbers of patients tended to stay on triple therapy rather than be weaned onto two agents at one year post transplant. A number of studies have shown that dual therapy is associated with a lower incidence of skin cancer (283;284). Over time there has been increasing use of MMF instead of

azathioprine and although there was a trend for shorter time between transplant and first cancer in the MMF group, this did not reach statistical significance.

Newer immunosuppressive agents, the mammalian target of Rapamycin inhibitors (mTORi), sirolimus and everolimus, exhibit both immunosuppressive and anti-neoplastic properties and regimens incorporating these agents may confer a lower risk of skin cancer(53;54). Our results showed that patients on sirolimus at one year post transplant had not developed any skin cancers however the numbers were too few and the period of follow up too short to allow further interpretation of this finding.

3.1.10.5 Strengths and Limitations of the study

3.1.10.5.1 Strengths

Patients included in the study were all examined by Dermatologists in one centre, a careful history taken from each patient and data on skin cancer collected and entered onto the renal electronic patient record. All data from 2005 onwards are collected prospectively.

3.1.10.5.2 Limitations

Not all patients with a functioning transplant at the start of the study period have attended our clinic. These patients who are not included in this study could be attending Dermatology clinics elsewhere. Whilst an effort has been made to ensure that all West of Scotland RTRs attend the specialist clinic at the Western Infirmary, due to the large geographical area that the transplant centre serves, some patients prefer to attend Dermatology services local to their area.

Data on skin tumours diagnosed prior to September 2005 were collected retrospectively and in some instances the data were incomplete. Retrospective data is subject to survivor bias. We do not know the skin cancer incidence in those patients transplanted prior to 2005 who either died or returned to dialysis. The effect of immunosuppressive regimens on any retrospectively collected data must therefore be interpreted with caution.

3.1.10.6 Conclusion

A dedicated Dermatology clinic for the West of Scotland renal transplant population with close links to the renal transplant centre has been established. Development of a skin cancer database for this population incorporated in the West of Scotland renal electronic patient record has facilitated the study of skin cancer in this population. To our knowledge, this is the largest reported survey of skin cancer in Scottish renal transplant recipients. Our data reveal lower skin cancer incidence rates than are seen in transplant populations elsewhere in the UK and there is no reversal of the BCC: SCC ratio. Ongoing studies of this population will reveal whether these differences are intrinsic to our population, reflect local immunosuppression practices or are a reflection of the length of post transplant follow up in this study.

Chapter 3.2 HPV Genotyping of Nonmelanoma Skin Cancers

The epidemiology of nonmelanoma skin cancer in the West of Scotland renal transplant population is described in Chapter 3.1. The investigation examined the association between NMSC, age, skin type, sun exposure and immunosuppression. Infection with carcinogenic viruses including betaPV may also play a role in the development of NMSC in the immunosuppressed transplant population and the wider immunocompetent population.

Skin biopsies from West of Scotland skin cancer patients, both immunocompetent patients and immunosuppressed renal transplant recipients were examined for the presence of betaPV. This was achieved utilising a recently described PCR reverse hybridisation technique that uses primers specifically designed to detect betaPV . The results of this investigation are presented here.

One hundred and twenty one paraffin-embedded and 13 frozen skin tumours were collected along with 11 paraffin-embedded and seven frozen normal skin samples. The results from the series of paraffin-embedded samples are presented first.

3.2.1 Paraffin-embedded samples

One hundred and twenty one skin tumours from 103 patients were examined [27 AK, 41 IEC and 53 SCC]. 59 tumours were from IC patients and 62 from IS RTRs. 73 tumours were from male patients and 48 were from females. Patient ages ranged from 37-94 years with a mean of 65.4 years. The IC patient group was older (mean age 73.8 years) vs. the IS group (mean age 57.4 years).

Eleven normal skin samples from ten patients were examined, all from IC patients. Nine samples were of normal peri-lesional skin and two were from photo-protected normal inner arm skin. One was from a male patient, the remainder from females. The patient ages ranged from 25-80 with a mean age of 50.2 years.

The different attributes of the paraffin-embedded samples are summarised in Table 7.

	AK	IEC	SCC	Total tumours	Normal skin
Total No. of samples (patients)	27 (24)	41 (35)	53 (44)	121 (103)	11 (10)
IC samples (patients)	16 (14)	20 (19)	23 (22)	59 (55)	11 (10)
IS samples (patients)	11(10)	21 (16)	30 (22)	62 (48)	0
Male/Female	13/14	22/19	38/15	73/48	1/10
Mean age of all patients (range)	65.4 (37-93)	67.4 (48-89)	63.8 (35-94)	65.4 (37-94)	50.2 (25-80)
IC patients (range)	72.9 (58-93)	74.4 (48-89)	73.9 (38-94)	73.8 (38-94)	50.2 (25-80)
IS patients (range)	54.4 (37-69)	60.8 (49-75)	56.1 (35-74)	57.4 (35-75)	N/A

Table 7 Characteristics and origin of the paraffin-embedded lesions.

AK, Actinic keratoses; IEC, intraepidermal carcinoma; SCC, squamous cell carcinoma; IC, immunocompetent; IS, immunosuppressed

3.2.2 BetaPV genotyping – paraffin-embedded samples

Overall betaPV DNA was detected in 57 (47.1%) out of 121 skin tumours but in only 2 (18.2%) out of 11 normal skin samples. In IC patients, betaPV was detected in 30 (50.8%) out of 59 tumours but in only two (18.2%) out of 11 normal skin samples. This was statistically significant as tested by the Chi-squared test, p=0.046. In IS patients, betaPV was found in 27 (43.5%) out of 62 samples. No normal skin samples from IS patients were available as control samples.

3.2.2.1 Beta PV and immune status

BetaPV infection appeared to be more common in tumours from IC patients 30 (50.8%) out of 59 samples compared to IS patients 27 (43.5%) out of 62 samples (Table 6) but the difference between IC and IS patients was not statistically significant.

3.2.2.2 BetaPV and tumour type

Overall, betaPV infection was detected in 15/27 (55.6%) AK, 15/41 (36.6%) IEC and 27/53 (50.9%) SCC. In tumours from IC patients betaPV was detected in 10/16 (62.5%) AK, 8/20 (40%) IEC and 12/23 (52.2%) SCC. In tumours from IS patients in 5/11 (45.4%) AK, 7/21 (33.3%) IEC and 15/30 (50%) SCC (Table 6).

The results of betaPV genotyping in paraffin-embedded samples are summarised in Table 8.

	AK	IEC	SCC	Total Tumours	Normal skin
Paraffin-embedded samples, n	**27**	**41**	**53**	**121**	**11**
BetaPV positive samples, n (%)	15/27 (55.6)	15/41 (36.6)	27/53 (50.9)	57/121 (47.1)	2/11 (18.2)
BetaPV positive samples Immunocompetent, n (%)	10/16 (62.5)	8/20 (40.0)	12/23 (52.2)	30/59 (50.8)	2/11 (18.2)
BetaPV positive samples Immunosuppressed, n (%)	5/11 (45.4)	7/21 (33.3)	15/30 (50.0)	27/62 (43.5)	N/A

Table 8 Results of betaPV genotyping in paraffin-embedded tumours and normal skin.

AK, Actinic keratoses; IEC, intraepidermal carcinoma; SCC, squamous cell carcinoma

3.2.2.3 Spectrum of BetaPV

There were 126 betaPV detections from 57 tumours as many lesions harboured more than one genotype**.** All 25 genotypes were detected with the exception of HPV-21, HPV-25, HPV-47 and HPV-96. Overall, the most frequently detected genotypes were HPV-24 (14 samples), HPV-15 (12 samples) and HPV-38 (11 samples) (Figure 13). The spectrum of betaPV genotypes isolated in each tumour type is summarised in Table 11. The most common genotypes found in SCC were HPV-36 (8 samples), HPV-24 (7 samples) and HPV-38 (6 samples). HPV-36 was only identified in SCC. In thirteen samples, betaPV was detected but the genotype was uncharacterised.

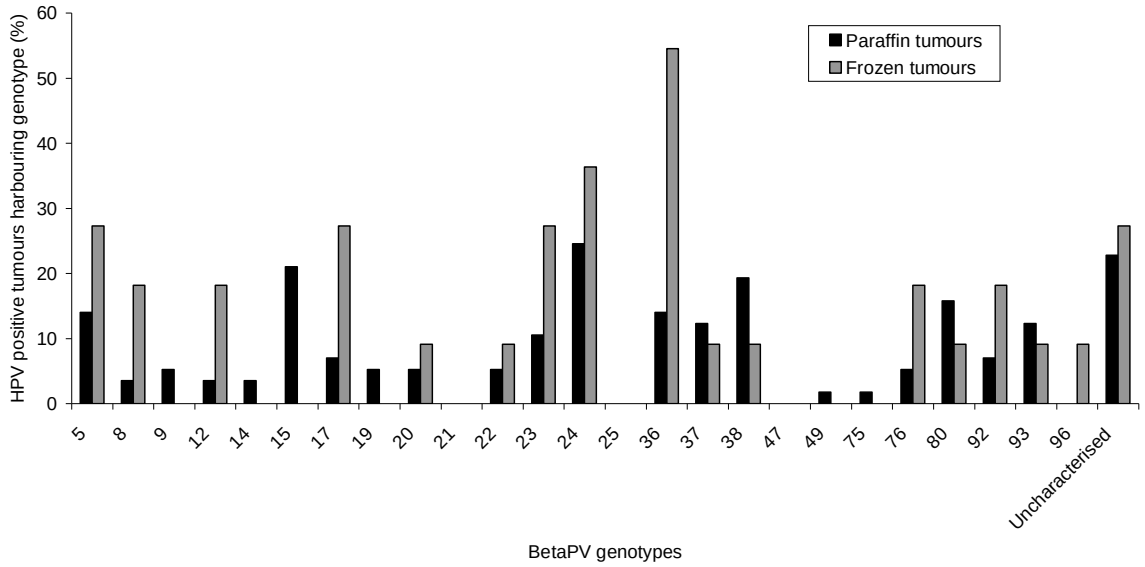

Figure 13 The spectrum of betaPV detected in paraffin-embedded and frozen tumours.

One hundred and twenty one paraffin-embedded and thirteen frozen skin tumours were tested for the presence of 25 known betaPV types. 57paraffin samples and 11 frozen samples were positive for betaPV. The percentage of positive lesions harbouring each genotype is illustrated. Many tumours contained more than one genotype.

3.2.2.4 BetaPV and age

Tumours from IS patients were from a younger age group than those from IC patients and accordingly, betaPV were detected more frequently at a younger age in this group as shown in Figure 14.

3.2.2.5 Multiple infections

Of those tumours infected with betaPV, 28/57 (49.1%) were infected with more than one genotype (range 2-8). Overall, infection with multiple genotypes was found in 14/27 (51.9%) SCC, 5/15 (33.3%) IEC and 9/15 (60.0%) AK. Multiple infections were more common in tumours from IC patients than those from IS patients ($P < 0.001$). Adjustment for age did not change this association. In IC patients, overall 21/30 (70.0%) of tumours were multiply infected [7/10 (70%) AK, 4/8 (50.0%) IEC, 10/12 (83.3%) SCC] compared with 7/27 (25.9%) of tumours from IS patients [2/5 (40.0%) AK, 1/7 (14.3%) IEC, 4/15 (26.7%) SCC] (Figure 15).

Uncharacterised betaPV DNA was detected in two of eleven normal skin samples. There were no multiple infections in normal skin.

A.

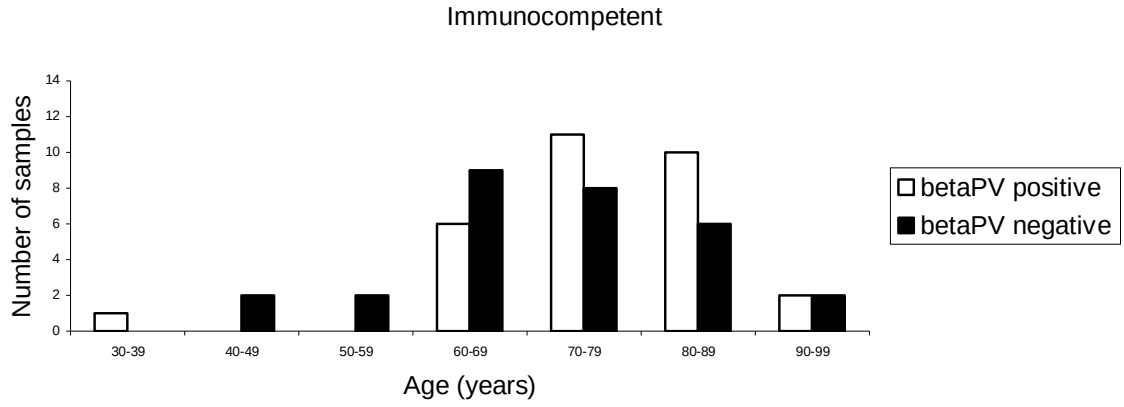

B.

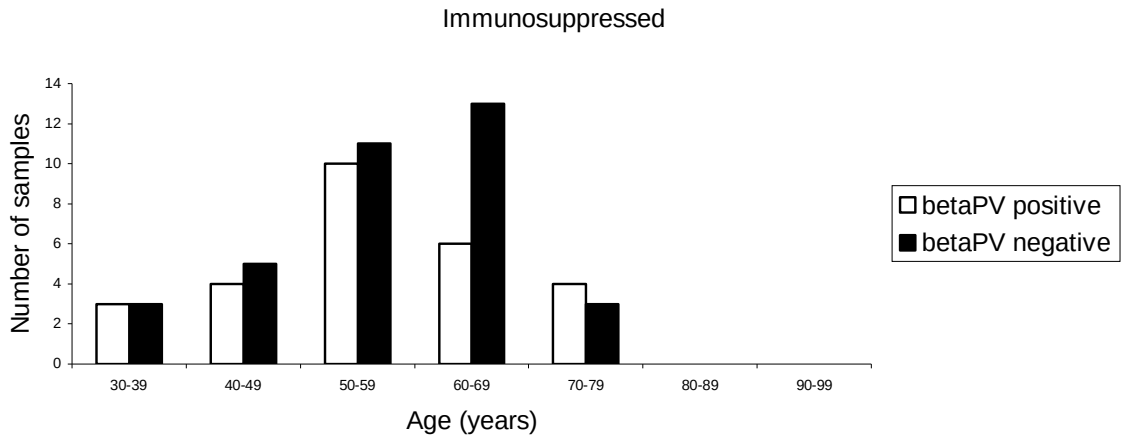

Figure 14 BetaPV infection and age

The distribution of samples according to age in (A) immunocompetent and (B) immunosuppressed patients.

A.

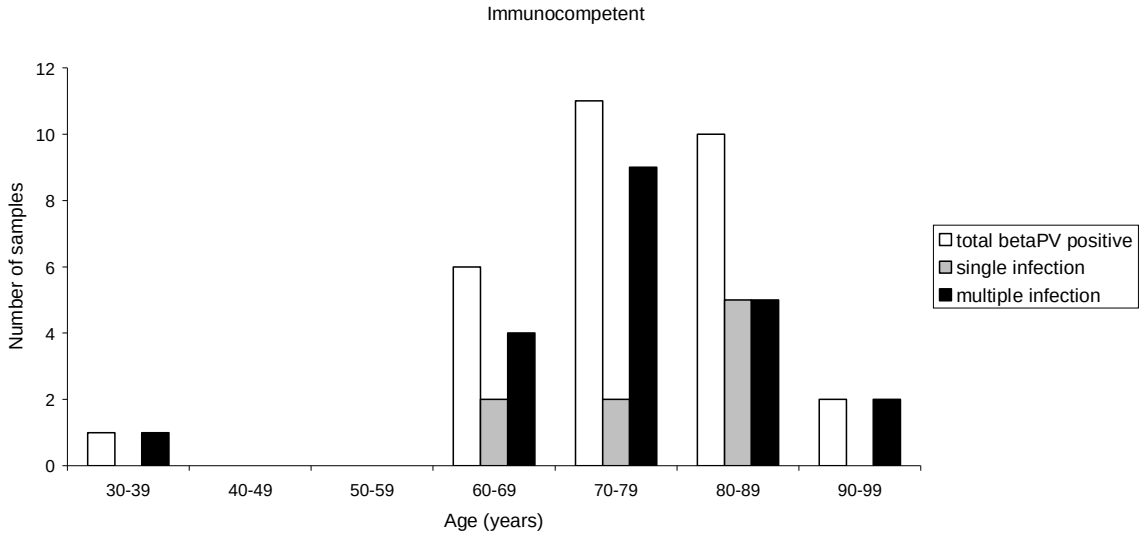

B.

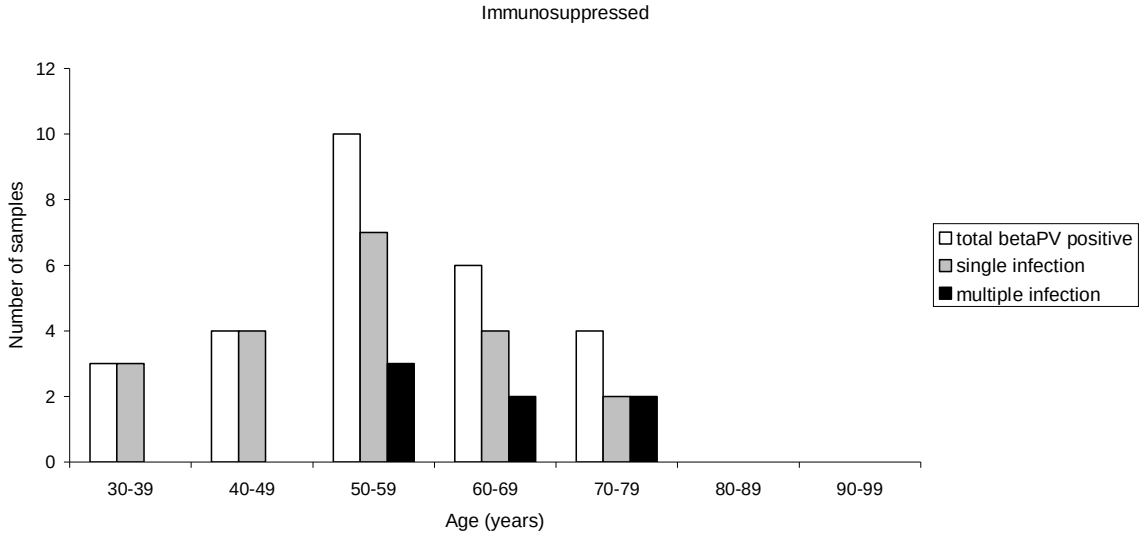

Figure 15 BetaPV infection and age.

Total number of betaPV positive samples, number of single infections and multiple infections in immunocompetent (A) and immunosuppressed (B) patients.

3.2.3 Frozen samples

A small number of frozen tumours and normal skin was collected and similarly analysed. The attributes of the lesions are summarised in Table 9.

Thirteen tumours from 11 patients were examined (2 AK, 4 IEC and 7 SCC). Seven were from IC patients and six were from IS organ transplant recipients (3 renal and 1 liver). Eight tumours were from male patients and five from females. The patient ages ranged from 38-81 years (mean 62.7). Again the IC patients were older with a mean age of 75.0 years (range 67-81) compared to the IS patients whose mean age was 50.4 years (range 38-73).

Seven normal skin samples were examined; all samples were taken from normal, photo-protected skin from the upper inner arm. Six samples were from IC patients and one from an IS renal transplant recipient. Five samples were from male patients and two from females. Overall, the patient ages ranged from 67-81 years (mean 75.0). The IC patient ages ranged from 67-81 years (mean 75.2), the IS patient age was 74 years.

	AK	IEC	SCC	Total tumours	Normal skin
Total No. of samples (patients)	2 (2)	4 (4)	7 (6)	13 (12)	7 (7)
IC samples (patients)	2 (2)	2 (2)	3 (3)	7 (7)	6 (6)
IS samples (patients)	0	2 (2)	4 (3)	6 (5)	1 (1)
Male/Female	0/2	2/2	6/1	8/5	5/2
Mean age of all patients (range)	73.5 (73-74)	67.8 (59-76)	65.4 (38-81)	62.7 (38-81)	75.0 (67-81)
IC patients (range)	73.5 (73-74)	74.5 (73-76)	76.3 (67-81)	75.0 (67-81)	75.2 (67-81)
IS patients (range)	NA	61.0 (59-63)	57.2 (38-73)	50.4 (38-73)	74.0 (1 patient)

Table 9 Characteristics and origin of the frozen lesions.

AK, Actinic keratoses; IEC, intraepidermal carcinoma; SCC, squamous cell carcinoma; IC, immunocompetent; IS, immunosuppressed

3.2.4 BetaPV genotyping of frozen tissue

BetaPV was detected in 11 (84.6%) out of 13 tumours and 4 (57.1%) out of 7 normal skin samples (Table 10). BetaPV infection was found in 5 (71.4%) out of 7 tumours from IC patients compared to 6 (100%) out of 6 tumours from IS patients. The results according to immune status and lesion type are summarised in Table 9. Of those tumours harbouring betaPV, 6 (54.5%) out of 11 harboured more than one genotype (range 2-9). There were 3 (60.0%) out of 5 lesions multiply infected in IC patients and 3 (50.0%) out of 6 in IS patients.

	AK	IEC	SCC	Total Tumours	Normal skin
Frozen samples, n	**2**	**4**	**7**	**13**	**7**
BetaPV positive frozen samples, n (%)	1/2 (50.0)	3/4 (75.0)	7/7 (100.0)	11/13 (84.6)	4/7 (57.1)
BetaPV positive samples Immunocompetent, n (%)	1/2 (50.0)	1/2 (50.0)	3/3 (100.0)	5/7 (71.4)	3/6 (50.0)
BetaPV positive samples Immunosuppressed, n (%)	NA	2/2 (100.0)	4/4 (100.0)	6/6 (100.0)	1/1 (100.0)

Table 10 Results of betaPV genotyping in frozen tumours and normal skin.

AK, Actinic keratoses; IEC, intraepidermal carcinoma; SCC, squamous cell carcinoma

There were 37 HPV detections in total from the tumours. The majority of the 25 betaPV genotypes were detected (Figure 13). The spectrum of betaPV genotypes detected in each lesion type is summarised in Table 11b. The most frequently detected genotypes were HPV-36 (6 samples), HPV-24 (4 samples), HPV-5, HPV-12 and HPV-23 (3 samples each). There were three samples containing uncharacterised betaPV.

Four out of seven frozen normal skin samples were positive: three were from IC patients and one was from an IS patient. Of the three IC samples, one was infected with HPV-15, one with an uncharacterised betaPV and one was infected with both HPV-23 and HPV-75. The single IS sample was positive for HPV-12 (Table 11b). The number of frozen samples was too small for meaningful statistical analysis.

	(a) Paraffin-embedded Tumours				(b) Frozen Tumours				All Tumours
BetaPV Genotype	**AK (n=27)**	**IEC (n=41)**	**SCC (n=53)**	**No. of detections**	**AK (n=2)**	**IEC (n=4)**	**SCC (n=7)**	**No. of detections**	**Total No. of detections**
HPV-5	2	2	4	8	1	1	1	3	**11**
HPV-8		2		2			2	2	**4**
HPV-9	1		2	3				0	**3**
HPV-12		2		2		1	1	2	**4**
HPV-14		1	1	2				0	**2**
HPV-15	3	4	5	12				0	**12**
HPV-17	1		3	4		1	2	3	**7**
HPV-19		1	2	3				0	**3**
HPV-20	1	1	1	3			1	1	**4**
HPV-21				0				0	**0**
HPV-22	1		2	3			1	1	**4**
HPV-23	3	1	2	6			3	3	**9**
HPV-24	4	3	7	14		2	2	4	**18**
HPV-25				0				0	**0**
HPV-36			8	8	1	1	4	6	**14**
HPV-37	1	1	5	7			1	1	**8**
HPV-38	3	2	6	11			1	1	**12**
HPV-47				0				0	**0**
HPV-49			1	1				0	**1**
HPV-75			1	1				0	**1**
HPV-76	1		2	3	1		1	2	**5**
HPV-80	3	1	5	9			1	1	**10**
HPV-92		1	3	4			2	2	**6**
HPV-93	2	2	3	7	1			1	**8**
HPV-96				0			1	1	**1**
U	4	4	5	13		1	2	3	**16**
Total Isolates				**126**				**37**	163

Table 11 BetaPV genotypes found in (a) paraffin-embedded and (b) frozen skin tumours.

The number of infections can add up to more than the numbers of samples due to the presence of multiply infected samples.

AK, Actinic keratoses; IEC, intraepidermal carcinoma; SCC, squamous cell carcinoma; U, uncharacterised

3.2.5 Discussion

There is a growing body of evidence to link betaPV to NMSC. Early investigations of the presence of HPV in NMSC were based on Southern blotting and found HPV DNA infrequently. Subsequent development of broad range, genus and type specific PCR primers has led to HPV detection in 35-85% of AK and IEC and 30-50% of SCC in IC patients and up to 88% of AK and 54-91% of SCC in renal transplant recipients. (64). The presence of betaPV is associated with the development of NMSC and detection of antibodies against the EV type HPV-8 is greater in SCC patients than in controls and has a significant association with presence of AKs (285-288).

However, despite the frequent finding of HPV DNA in tumour biopsies, the biological significance of this observation remains unclear as betaPV DNA is also present in 32-87% of normal skin biopsies with higher detections in IS patients (287),(289).

In this study, NMSC in a cohort of IC and IS patients from the West of Scotland were analysed. Similar investigations had not been conducted in this area of the UK.

AK, IEC and SCC but not benign lesions or BCC were examined for the following reasons. AK, IEC and SCC are considered to represent the spectrum of one disease from epidermal dysplasia through intra-epidermal SCC to invasive malignancy. Moreover in renal transplant recipients the risk of SCC is increased 65-250 fold whereas the risk for BCC is increased only 10 fold compared to the immunocompetent population. This represents an exponential rise in the risk of SCC and a reversal of the normal SCC to BCC ratio (22;26-29;290).

Overall betaPV DNA was present in 57/121 (47.1%) of paraffin-embedded skin tumours and 2/11 (18.2 %) of paraffin-embedded normal skin samples. In our small number of frozen samples the proportion of positive tumours remained higher than that in normal skin [11/13 (84.6%) and 4/7 (57.1%) respectively]. These findings add support to the hypothesis that betaPV has a role in development of NMSC.

The mean age of the IS patient group was 54.4 years whereas the mean age of the IC group was 72.9 years. It is well recognised that IS renal transplant recipients develop NMSC at a younger age than IC patients (29). UVR is the major aetiology for NMSC, the risk of NMSC is highest in countries with highest UVR exposure (28) and ciclosporin used in immunosuppressive regimes may contribute a direct neoplastic effect (50). However, the increased incidence of tumours at an earlier age in IS patients also suggests a role for an infective agent such as HPV. This hypothesis is supported by the high incidence of cancers induced by infection or reactivation of oncogenic viruses in OTRs including high-risk mucosal HPV and anogenital cancers, HHV-8 associated KS and Epstein Barr Virus associated lympho-proliferative malignancies (18;26;291-293).

A wide spectrum of betaPV types was detected in our samples. Within the genus beta there are five species of closely linked types - species 1 (HPV-5, 8, 12, 14, 19, 20, 21, 24, 25, 36, 47, 93,); species 2 (HPV-9, 15, 17, 22, 23, 37, 38, 80); species 3 (HPV-49, 75, 76); species 4 (HPV-92) and species 5 (HPV-96)(66). The most common genotypes we detected were HPV-24, HPV-36, HPV-38, HPV-15, HPV-5 and HPV-80. Sixteen betaPV were detected that could not be characterised. This may be due to either presence of a known genotype at low copy number or detection of a new genotype that would only be determined by sequencing.

A recent study of lesional and normal skin in IC patients found that betaPV species 2 predominate in SCC whereas betaPV species 1 predominated in benign lesions (294). In this study genotypes from both species 1 and 2 predominated in tumours. The most frequent genotype in SCC was HPV-36, a species 1 genotype. In EV patients, HPV-5 and HPV-8 are the most common types found in SCC and are regarded as high-risk types(295). However, in agreement with previous results, in this study, no single type prevails in NMSC in non-EV patients (296-298).

The lowest detection of betaPV was in samples of IEC compared to AK and SCC both in IC and IS patients (36.6% overall). These figures are comparable to previous studies that found EV-HPV DNA in 33% of paraffin–embedded IEC from IC patients and 40% of IEC from RTRs (299;300).

More multiple betaPV infections in tumours from IC patients 21/30 (70.0%) than from IS patients 7/27 (25.9%) (p<0.001) were present.

Some of the results from this study differ from what has previously been reported in the literature. Firstly, the detection of betaPV DNA in 47.1% of paraffin embedded NMSC samples was lower than expected. This may reflect poor quality of DNA extracted from the samples as the samples utilised were archival. The DNA detection was similar in both IC and IS patients and a higher detection rate may have been expected from IS patient samples. Again, this may reflect the use of archival samples. More multiple infections were found in IC than IS patients and previous reports have found the opposite. This may be because this study only examined for betaPV whereas previous studies have included all PV types including mucosal perhaps leading to detection of greater numbers of multiple infections. Alternatively it may be related to the assay. The assay used in this investigation is highly sensitive and specific and can detect HPV DNA at low copy numbers however, one potential disadvantage of any broad-spectrum PCR primer mediated method is the competition between the different HPV types present in a single sample. If one type is present in a higher molar concentration than other type it is possible that the type at lower concentration will be out competed and escape detection in this assay (89). This could then potentially lead to under detection of multiple infections.

One disadvantage of BetaPV DNA detection in samples is the difficulty in distinguishing between a clinically relevant infection and a passenger role for betaPV as it has been shown that betaPV DNA is ubiquitous. It has been suggested that detection of an antibody response to betaPV may represent a more clinically relevant infection. One study of betaPV detection in eyebrow hairs combined with multiplex serology identified that concordant DNA detection of HPV-36 and antibodies to HPV-36 was significantly associated with cutaneous SCC(117) It may be that by employing combined approaches of DNA detection and serological detection in future large scale studies will lead to identification of betaPV types which are important for the development of SCC.

Further characterisation of betaPV in vivo is needed in order to determine the mechanisms by which the virus contributes to cutaneous carcinogenesis. Large-scale epidemiological studies are needed to determine which betaPV types are

primarily associated with NMSC; future in vitro studies should focus on these HPV-types.

Chapter 3.3 Immunohistochemical Analysis of Biomarker Expression in Nonmelanoma Skin Cancers

The results presented in Chapter 3.2 demonstrated the presence of betaPV in skin biopsy specimens from both immunosuppressed and immunocompetent patients. Overall betaPV DNA was present in 57/121 (47.1%) of paraffin-embedded skin tumours and 2/11 (18.2 %) of paraffin-embedded normal skin samples. In the small number of frozen samples investigated, the proportion of positive tumours remained higher than that in normal skin [11/13 (84.6%) and 4/7 (57.1%) respectively]. These findings add support to the hypothesis that betaPV has a role in development of NMSC. It remains unclear however whether betaPV infection is causative of skin cancers in both immunosuppressed patients and the wider immunocompetent population.

One way to gather evidence supporting a causative role of betaPV in NMSC is to identify betaPV infected lesions, and determine whether they have a different expression pattern for a variety of cell cycle markers that have been associated with increased proliferation and cancers in other organs and locations. In cervical lesions, it has been shown that immunohistochemical staining with p16 antibody can aid the diagnosis of cervical cancer associated with alpha-papillomaviruses such as HPV-16 (301). MCM proteins have been proposed as diagnostic markers to identify HPV induced proliferative disease in the cervix while Ki67 is also associated with the risk of HPV associated disease in the cervix (302;303). Although there have been several studies examining the relationship between NMSC and immunohistochemical markers of cell cycle regulatory proteins, previous studies have been limited either in the number of markers examined, or the histological grades and number of lesions examined. In addition there are limited datasets in which these markers are studied in association with HPV and no datasets in which lesions have been comprehensively screened for betaPV. A biomarker pattern particular to betaPV positive skin cancers would support the hypothesis that these viruses are causative agents of disease.

Skin tumours and normal skin samples from IC and IS patients, typed for the presence of betaPV as described in Chapter 3.2, were examined by immunohistochemistry. The objective was to determine if the presence or absence of betaPV altered cell cycle biomarker expression in nonmelanoma skin cancers. The results of this investigation are presented here.

3.3.1 Case distribution and presence of beta papillomaviruses

Due to difficulties in processing frozen tissue for immunohistochemistry, of those specimens previously genotyped, only paraffin-embedded samples were included in this part of the investigation.

One hundred and twenty one paraffin-embedded skin tumours and eleven normal skin samples were genotyped for betaPV. Twenty-one skin tumours were not suitable for analysis due to loss of tissue during processing or inadequate size of sample. The remaining one hundred skin tumours and eleven normal skin samples were included in the study.

The samples were from 67 IC patients and 59 IS OTRs. Of the IC patients, 28 were male and 29 female with a mean age of 69.7 years (range 25-94). Of the IS patients, 39 were male and 20 female with a mean age of 55.4 years (range 22-94).

Forty four NMSC and two normal skin samples harboured betaPV. The results are summarised in Table 12.

	BetaPV negative			**BetaPV positive**		
	IC	IS	**Total (%)**	IC	IS	**Total (%)**
Normal Skin, n=11	9	0	**9 (81.8)**	2	0	**2 (18.2)**
Actinic Keratoses, n=24	6	6	**12 (50.0)**	7	5	**12 (50.0)**
Intra-epidermal Carcinoma, n=37	11	12	**23 (62.2)**	8	6	**14 (37.8)**
Squamous Cell Carcinoma, n=39	11	10	**21 (53.8)**	11	7	**18 (46.2)**
Totals, n=111	**37**	**28**	**65 (58.6)**	**28**	**18**	**46 (41.4)**

Table 12 Results of betaPV genotyping

IC, immunocompetent; IS, immunosuppressed; BetaPV, beta papillomavirus

Of those 46 betaPV positive samples, the range of betaPV genotypes isolated is summarised in Table 13. Many lesions harboured more than one betaPV genotype. Some samples harboured betaPV but the genotype was uncharacterised, this may be due to the presence of a known genotype at low copy number or detection of a new genotype that could only be determined by cloning and sequencing.

BetaPV genotype	Normal skin (n=2)	Actinic keratosis (n=12)	Intra-epidermal carcinoma (n=14)	Squamous cell carcinoma (n=18)	No. of detections
HPV-5		2	2	4	8
HPV-8			2		2
HPV-9		1		2	3
HPV-12			2		2
HPV-14			1	1	2
HPV-15		2	3	3	8
HPV-17		1		2	3
HPV-19			1	1	2
HPV-20			1	1	2
HPV-21					
HPV-22		1		1	2
HPV-23		2	1	2	7
HPV-24		3	3	7	13
HPV-25					
HPV-36		1		4	5
HPV-37		2	1	3	6
HPV-38		1	2	5	8
HPV-47					
HPV-49				1	1
HPV-75				1	1
HPV-76				2	2
HPV-80		2	1	4	7
HPV-92		1	1	2	4
HPV-93		1	2	3	6
HPV-96					
Uncharacterised	2	3	4	2	11
Total isolates	2	23	27	51	103

Table 13 BetaPV genotypes present in HPV positive samples.

46/111 samples investigated were betaPV positive; the specific genotypes isolated in the 46 positive samples are shown. The number of detections is greater than the number of BetaPV positive lesions as many were infected with multiple genotypes.

HPV, human papillomavirus

3.3.2 Results of Immunohistochemical staining

Sections from each sample were probed with antibodies directed against the following proteins: Ki67, MCM2, MCM5, p53, p16 and TopBP1. For each antibody, the expression pattern was categorised according to the intensity and distribution of staining (summarised in Table 14). Each section was examined and the expression patterns for each protein recorded.

Antibody	Distribution of staining within samples	Abbreviation
Ki67	Basal layer to mid layers of the epidermis	basal/mid
	Extending beyond the mid layers of the epidermis up to full thickness	mid/FT
MCM2/5	Basal layer to mid layers of the epidermis	basal/mid
	Extending beyond the mid layers of the epidermis up to full thickness	mid/FT
p53	Negative	negative
	Restricted to the basal layer +/- foci of full thickness staining	basal/focal
	Full thickness staining	FT
p16	Negative/occasional positive cells	negative
	Patchy focal staining	focal
	Intense staining in a band-like distribution through the full thickness	FT
TopBP1	Exclusively nuclear full thickness staining	nuclear
	Nuclear staining in association with intense cytoplasmic staining	cytoplasmic

Table 14 Summary of the observed staining patterns.

MCM2, minichromosome maintenance protein 2; MCM5, minichromosome maintenance protein 5; p16, $p16^{INK4a}$; TopBP1, Topoisomerase IIβ Binding Protein 1

To illustrate the observed staining patterns, representative betaPV positive and negative samples of normal skin (Figures 16 and 17), actinic keratoses (Figures 18 and 19), intra-epidermal carcinoma (Figures 20 and 21), and SCC (Figures 22 and 23) are shown.

3.3.2.1 Biomarker expression in normal skin vs. NMSC and correlation with the presence of BetaPV

3.3.2.1.1 Ki67, MCM2 and MCM5

In normal skin, Ki67 and MCM2 and MCM5 expression was restricted to the basal and mid layers of the epidermis. Fewer nuclei expressed MCM2 than MCM5 and staining was less intense with MCM2 than MCM5 (Figure 16a-c and Figure 17 a-c).

Ki67 expression was similar to normal skin and restricted to the basal and mid layers of the epidermis in 36/100 NMSC (Figures 19a, 22a). In the remaining 64/100 NMSC Ki67 was over-expressed extending beyond the mid layers of the epidermis up to full thickness as shown in Figures 18, 20, 21 and 23a. This increase in Ki67 expression, suggesting an increase in replicating cells in tumours compared to normal skin was significant (64/100 vs. 0/11, $P<0.001$) however it was not influenced by the presence of betaPV (Table 15a).

MCM2 expression was similar to normal skin and restricted to the basal and mid layers of the epidermis in 52/100 NMSC. In the remaining 48/100 NMSC, MCM2 was over-expressed as demonstrated in Figures 18, 20, 21 and 23b.

MCM5 expression was similar to normal skin in 13/100 NMSC and was over-expressed in the remaining 87/100 NMSC as shown in Figures 18, 20, 21 and 23c.

Over expression of MCM antigens was more pronounced in samples stained with MCM5 (87/100 vs. 0/11, $P<0.002$) compared to MCM2 (48/100 vs. 0/11, $P<0.001$). This may suggest that MCM5 antibody is a more sensitive detector of replicating cells. Similar to Ki67, expression patterns of MCM proteins did not differ significantly between betaPV positive and negative lesions (Table 15b and c).

3.3.2.1.2 p53

p53 staining was restricted to the basal layer +/- foci of full thickness (FT) staining (basal/focal) in two normal skin samples and throughout the full epidermal thickness in the remaining nine as seen in Figure 16d and 17d. In normal skin, there was no correlation between p53 distribution and presence of betaPV.

In NMSC, p53 expression was negative in three samples (example not shown) and was basal/focal in 31/100 NMSC (Figure 23d) and throughout the full epidermal thickness in the remaining 65/100 NMSC (Figure 18, 19, 20, 21 and 22d). Expression of p53 did not differ significantly between normal and lesional skin. There was no difference in p53 expression when comparing betaPV positive and negative lesions (Table 15d).

3.3.2.1.3 p16

11/11 normal skin samples were negative for p16 staining as shown in Figures 16 and 17 e.

Similar to normal skin, 6/100 NMSC samples were also negative for p16 staining (not shown). The remaining 94/100 NMSC exhibited over-expression of p16. 51/100 NMSC showed focal p16 over-expression (Figures 18 and 19 e) and 43/100 NMSC showed full thickness p16 over-expression (Figures 20, 21, 22 and 23e). In NMSC, p16 was clearly over-expressed in comparison with normal skin samples; however p16 expression patterns did not correlate with presence of betaPV (Table 15e).

3.3.2.1.4 TopBP1

TopBP1 expression was exclusively nuclear through the FT of the sample (nuclear) in 11/11 normal skin samples as shown in Figures 16 and 17f.

In 76/100 NMSC, TopBP1 expression was exclusively nuclear and similar to that seen in normal skin (Figures 18-22 f). In a 24/100 NMSC, nuclear ToPBP1 staining was present in association with intense cytoplasmic staining as shown in Figure 23 f. This aberrant TopBP1 expression pattern did not correlate with the presence of betaPV (Table 15 f).

	All samples Normal Skin vs. NMSC		Normal skin BetaPV-ve vs. BetaPV+ve		NMSC BetaPV-ve vs. BetaPV+ve	
	Normal Skin	NMSC	Normal Skin -ve	Normal Skin +ve	NMSC -ve	NMSC +ve
	n=11(%)	n=100 (%)	n=9 (%)	n=2 (%)	n=56 (%)	n=44 (%)
(a) Ki67						
basal/mid	11 (100.0)	36 (36.0)	9 (100.0)	2 (100.0)	22 (39.3)	14 (31.8)
mid/FT	0 (0.0)	64 (64.0)	0 (0.0)	0 (0.00)	34 (60.7)	30 (68.2)
(b) MCM2						
basal/mid	11 (100.0)	52 (52.0)	9 (100.0)	2 (100.0)	28 (50.0)	24 (54.6)
mid/FT	0 (0.0)	48 (48.0)	0 (0.0)	0 (0.0)	28 (50.0)	20 (45.4)
(c) MCM5						
basal/mid	11 (100.0)	13 (13.0)	9 (100.0)	2 (100.0)	8 (14.3)	5 (11.4)
mid/FT	0 (0.0)	87 (87.0)	0 (0.0)	0 (0.0)	48 (85.7)	39 (88.6)
(d) p53						
negative	0 (0.0)	3 (3.0)	0 (0.0)	0 (0.0)	1 (1.8)	2 (4.6)
basal/focal	2 (18.2)	31 (31.0)	2 (22.2)	0 (0.0)	18 (32.1)	13 (29.6)
FT	9 (81.8)	66 (66.0)	7 (77.8)	2 (100.0)	37 (66.1)	29 (66.0)
(e) p16						
negative	11(100.0)	6 (6.0)	9 (100.0)	2 (100.0)	2 (3.6)	4 (9.1)
focal	0 (0.0)	51 (51.0)	0 (0.0)	0 (0.0)	28 (50.0)	23 (52.3)
FT	0 (0.0)	43 (43.0)	0 (0.0)	0 (0.0)	26 (46.4)	17 (38.6)
(f) TopBP1						
nuclear	11 (100.0)	76 (76.0)	9 (100.0)	2 (100.0)	45 (80.4)	31 (70.4)
cytoplasmic	0 (0.0)	24 (24.0)	0 (0.0)	0 (0.0)	11 (19.6)	13 (29.56)

Table 15 Results of immunohistochemical staining.

The observed staining patterns and associated abbreviations are described in detail in Table 14. Abbreviations: NMSC, nonmelanoma skin cancer; MCM2, minichromosome maintenance protein 2; MCM5, minichromosome maintenance protein 5; p16, $p16^{INK4a}$; TopBP1, Topoisomerase IIβ Binding Protein 1

3.3.3 Biomarker expression in NMSC – correlation between different stages of carcinogenesis

To determine whether progression through the different stages of carcinogenesis influenced the biomarker expression pattern seen, a comparison of the observed staining patterns was made in normal skin, AK, IEC and SCC. The results are summarised in Table 16.

The results suggest that markers of cell proliferation (Ki67, MCM2 and MCM5) are up-regulated in IEC compared to AK and SCC however the numbers in each group are too small to allow for meaningful statistical analysis.

Similarly, there is a trend for FT p16 staining in IEC compared to both AK and SCC but again, the numbers in each group are too small to allow for meaningful statistical analysis.

		BetaPV negative samples, n=65					BetaPV positive samples, n=46				
		Normal Skin n=9	**AK**	**IEC**	**SCC**	**Total NMSC n=56**	**Normal Skin n=2**	**AK**	**IEC**	**SCC**	**Total NMSC n=44**
(a)	**Ki67**										
	basal/mid	**9 (100.00%)**	7	5	10	**22 (39.29%)**	**2 (100.00%)**	6	1	7	**14 (31.82%)**
	mid/FT	**0 (0.00%)**	5	18	11	**34 (60.71%)**	**0 (0.00%)**	6	13	11	**30 (68.18%)**
(b)	**MCM2**										
	basal/mid	**9 (100.00%)**	7	6	15	**28 (50.00%)**	**2 (100.00%)**	6	1	17	**24 (54.55%)**
	mid/FT	**0 (0.00%)**	5	17	6	**28 (50.00%)**	**0 (0.00%)**	6	13	1	**20 (45.45%)**
(c)	**MCM5**										
	basal/mid	**9 (100.00%)**	1	2	5	**8 (14.29%)**	**2 (100.00%)**	1	0	4	**5 (11.36%)**
	mid/FT	**0 (0.00%)**	11	21	16	**48 (85.71%)**	**0 (0.00%)**	11	14	14	**39 (88.64%)**
(d)	**p53**										
	negative	**0 (0.00%)**	0	1	0	**1 (1.79%)**	**0 (0.00%)**	0	1	1	**2 (4.55%)**
	basal/focal	**2 (22.22%)**	4	8	6	**18 (32.14%)**	**0 (0.00%)**	3	4	6	**13 (29.55%)**
	FT	**7 (77.78%)**	8	14	15	**37 (66.07%)**	**2 (100.00%)**	9	9	11	**29 (65.91%)**
(e)	**p16**										
	negative	**9 (100.00%)**	1	0	1	**2 (3.57%)**	**2 (100.00%)**	3	1	0	**4 (9.09%)**
	focal	**0 (0.00%)**	8	7	13	**28 (50.00%)**	**0 (0.00%)**	8	1	14	**23 (52.27%)**
	FT	**0 (0.00%)**	3	16	7	**26 (46.43%)**	**0 (0.00%)**	1	12	4	**17 (38.64%)**
(f)	**TopBP1**										
	nuclear	**9 (100.00%)**	10	15	20	**45 (80.36%)**	**2 (100.00%)**	11	7	13	**31 (70.45%)**
	cytoplasmic	**0 (0.00%)**	2	8	1	**11 (19.64%)**	**0 (0.00%)**	1	7	5	**13 (29.55%)**

Table 16 Immunohistochemical staining in normal skin and NMSC.

NMSC is the sum of all AK, IEC and SCC lesions. The observed staining patterns are described in detail in Table 10. MCM2, minichromosome maintenance protein 2; MCM5, minichromosome maintenance protein 5; p16, $p16^{INK4a}$; TopBP1, Topoisomerase IIβ Binding Protein 1

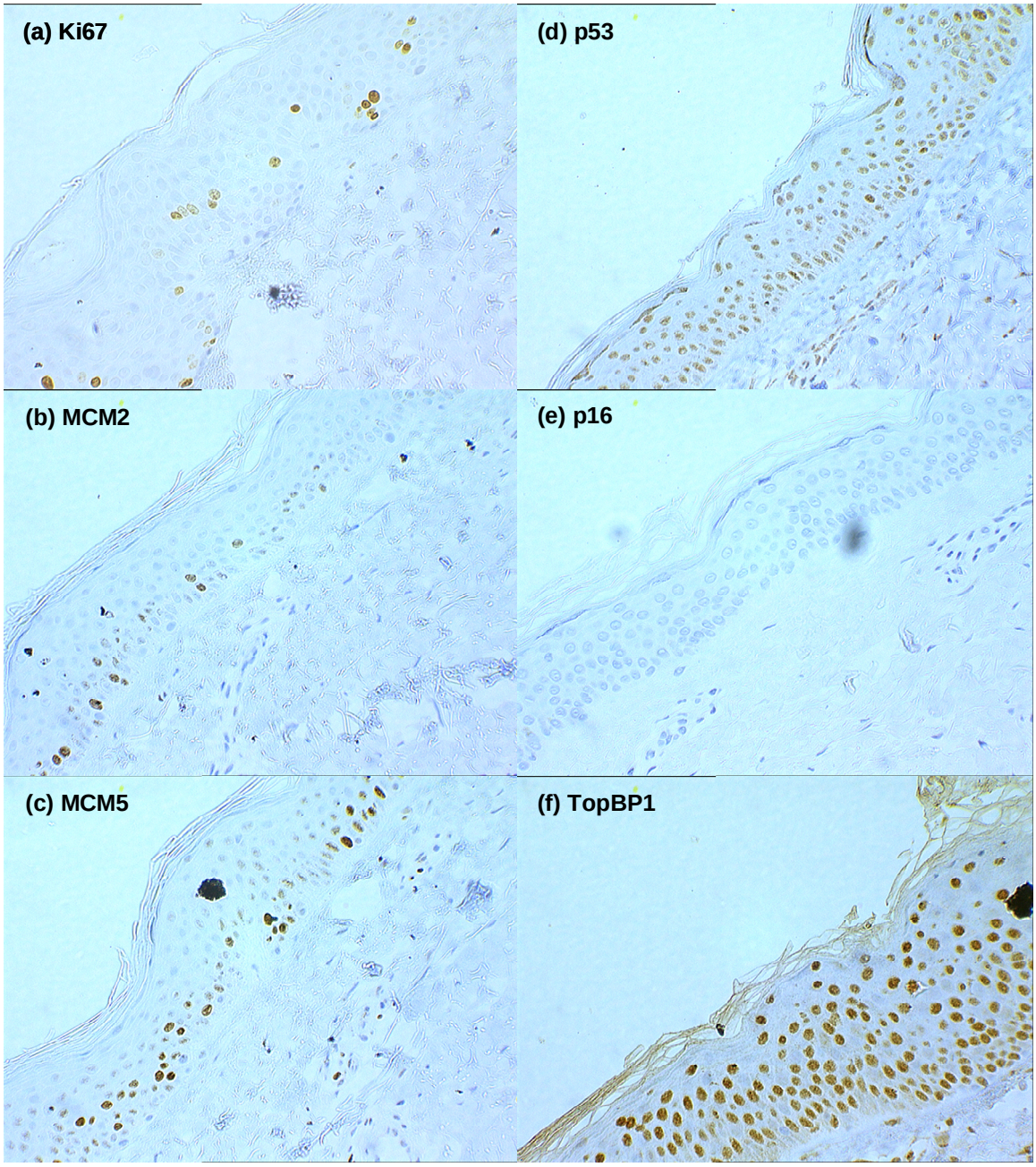

Figure 16 BetaPV positive normal skin.

Normal skin stained for (a) Ki67, (b) MCM2, (c) MCM5, (d) p53, (e) p16 and (f) TopBP1. Ki67, MCM2 and MCM5 expressing cells are present from the basal layers to the mid layers of the epidermis. Nuclei stained with p53 and TopBP1 are present through the full thickness of the epidermis. P16 staining is absent. Original magnification x 20.

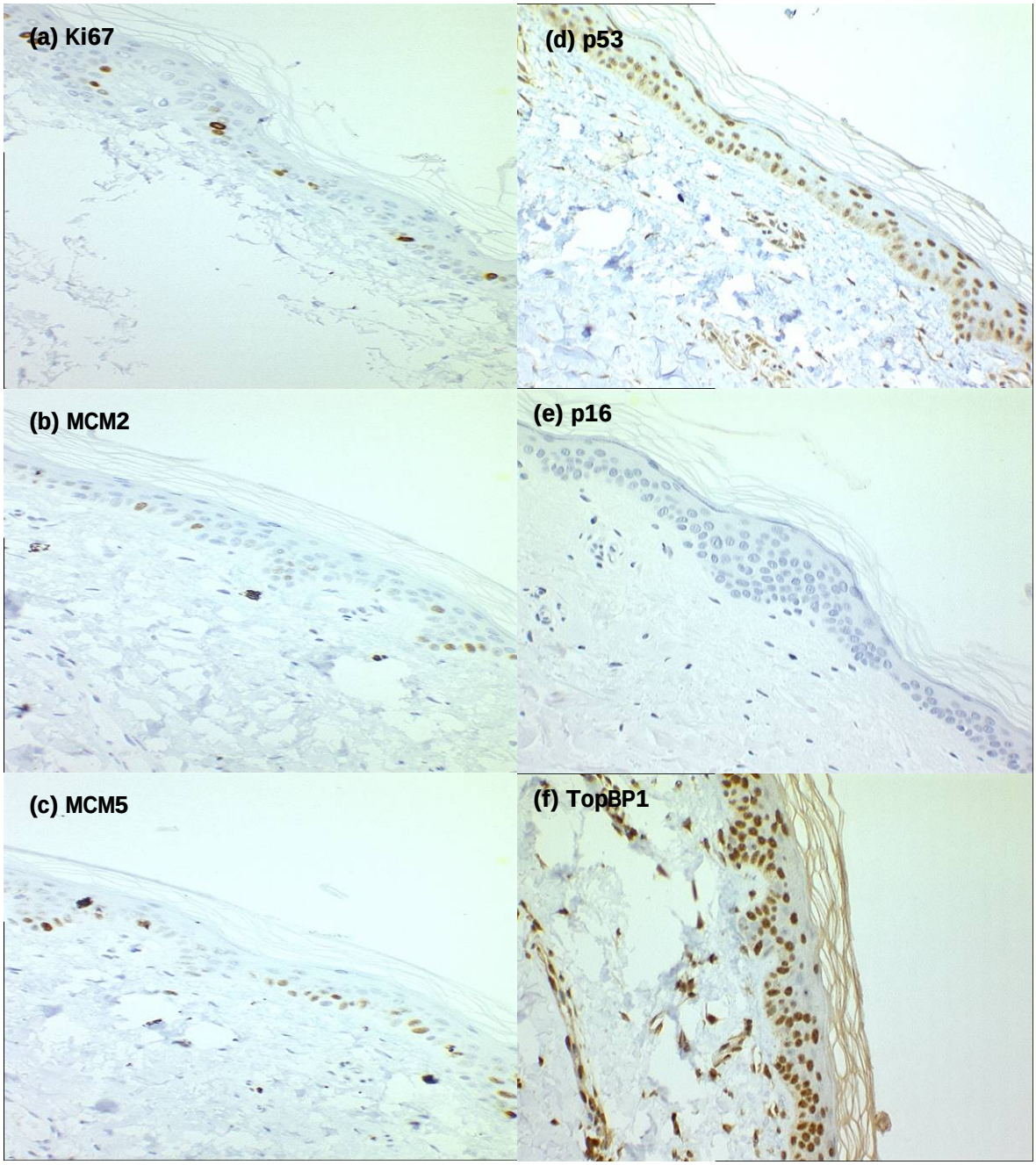

Figure 17 BetaPV negative normal skin.

Normal skin stained for (a) Ki67, (b) MCM2, (c) MCM5, (d) p53, (e) p16 and (f) TopBP1. Original magnification x 20.

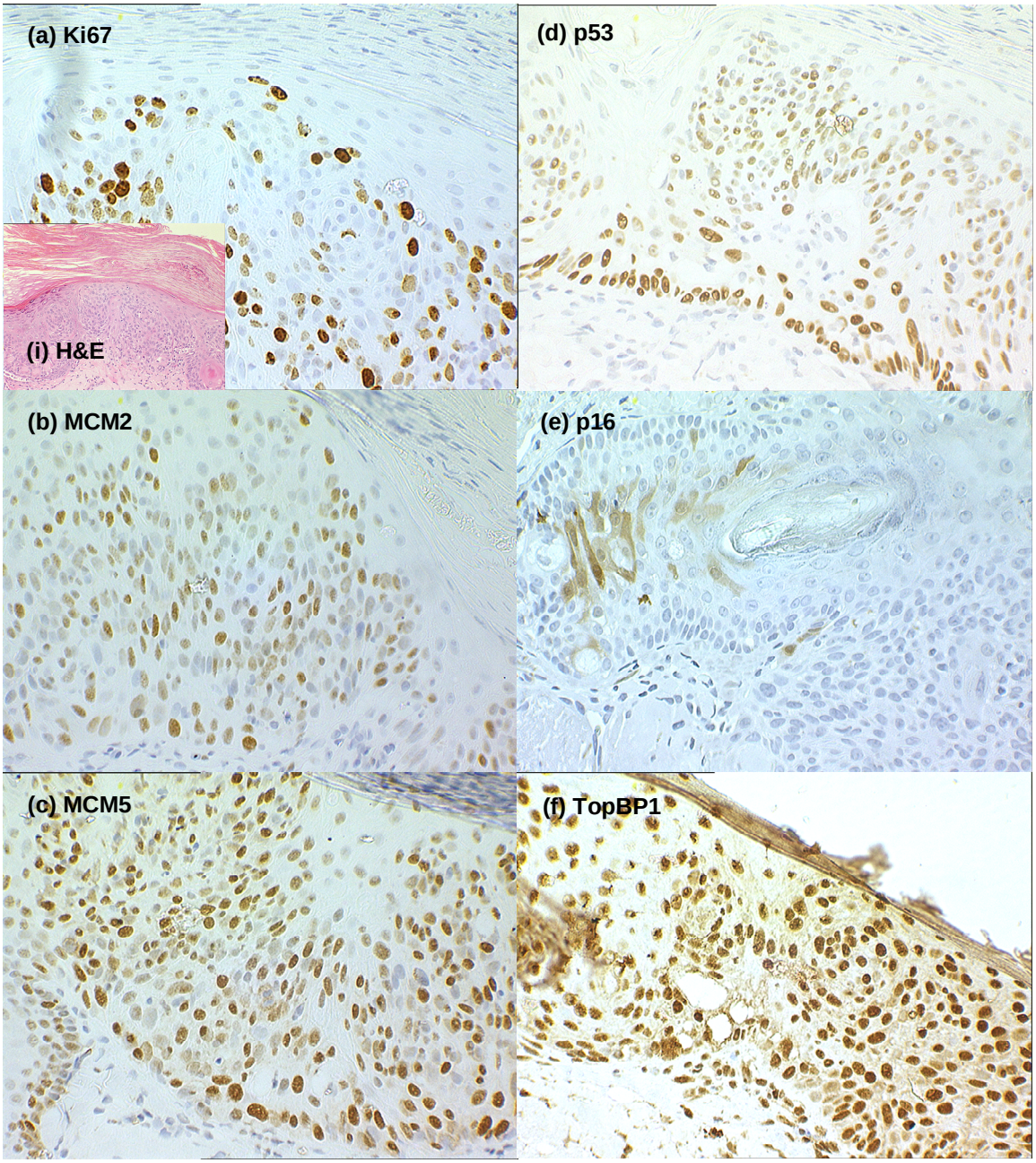

Figure 18 BetaPV positive Bowenoid actinic keratosis.

Sections stained with (i) H&E and antibody directed against (a) Ki67, (b) MCM2, (c) MCM5, (d) p53, (e) p16 and (f) TopBP1. Ki67, MCM2, MCM5, P53 and TopBP1 staining is present through the full thickness of the lesion. Focal p16 staining is present. Original magnification (i) x 5; (a)-(f) x 20.

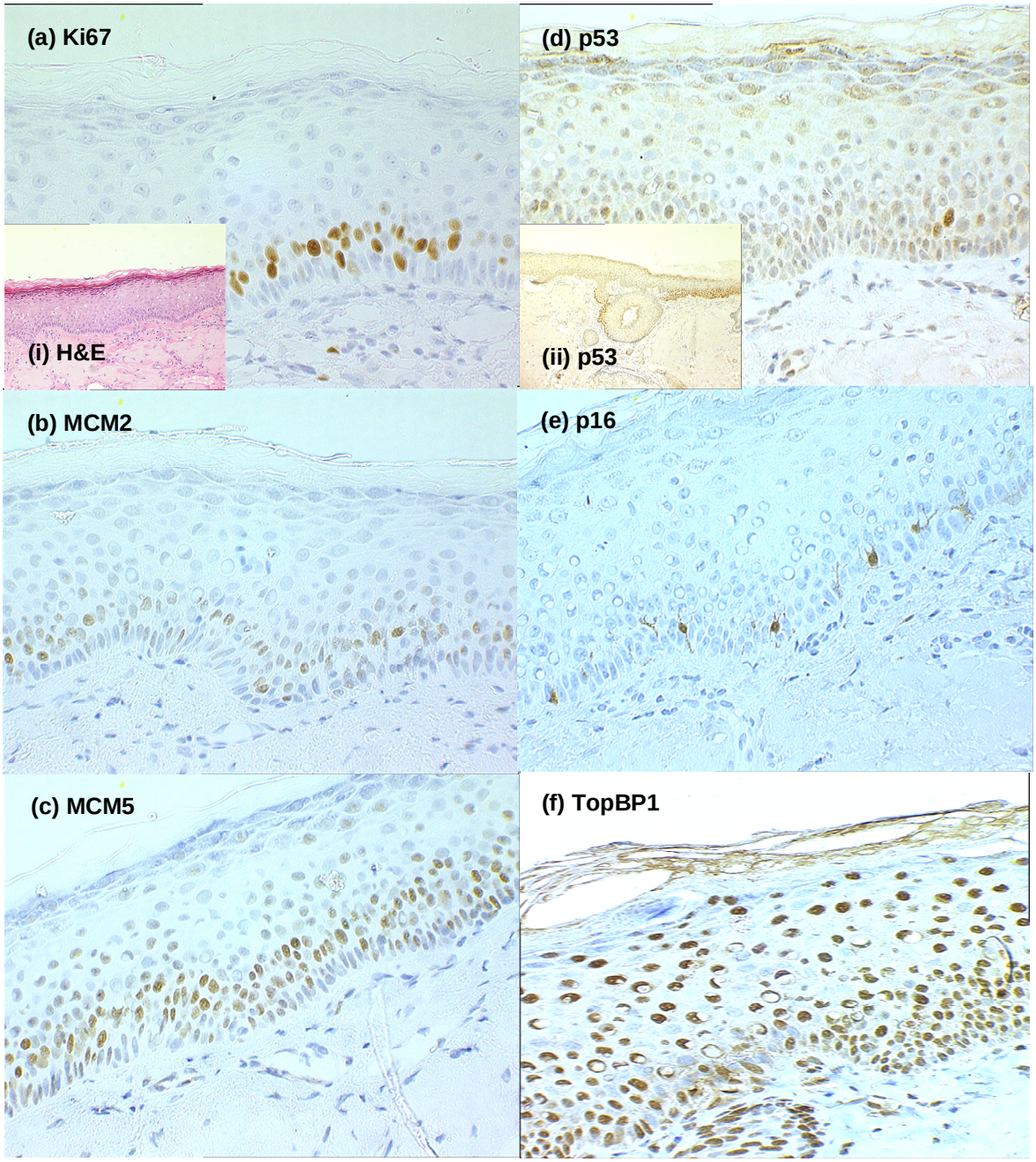

Figure 19 BetaPV negative actinic keratosis.

Sections stained with (i) H&E and antibody directed against (a) Ki67, (b) MCM2, (c) MCM5, (d)&(ii) p53, (e) p16 and (f) TopBP1. Ki67, MCM2, MCM5, TopBP1 staining is present through the full thickness of the lesion. Focal p53 (see inset) is present within the lesion. Original magnification (insets) x 5; (a)-(f) x 20.

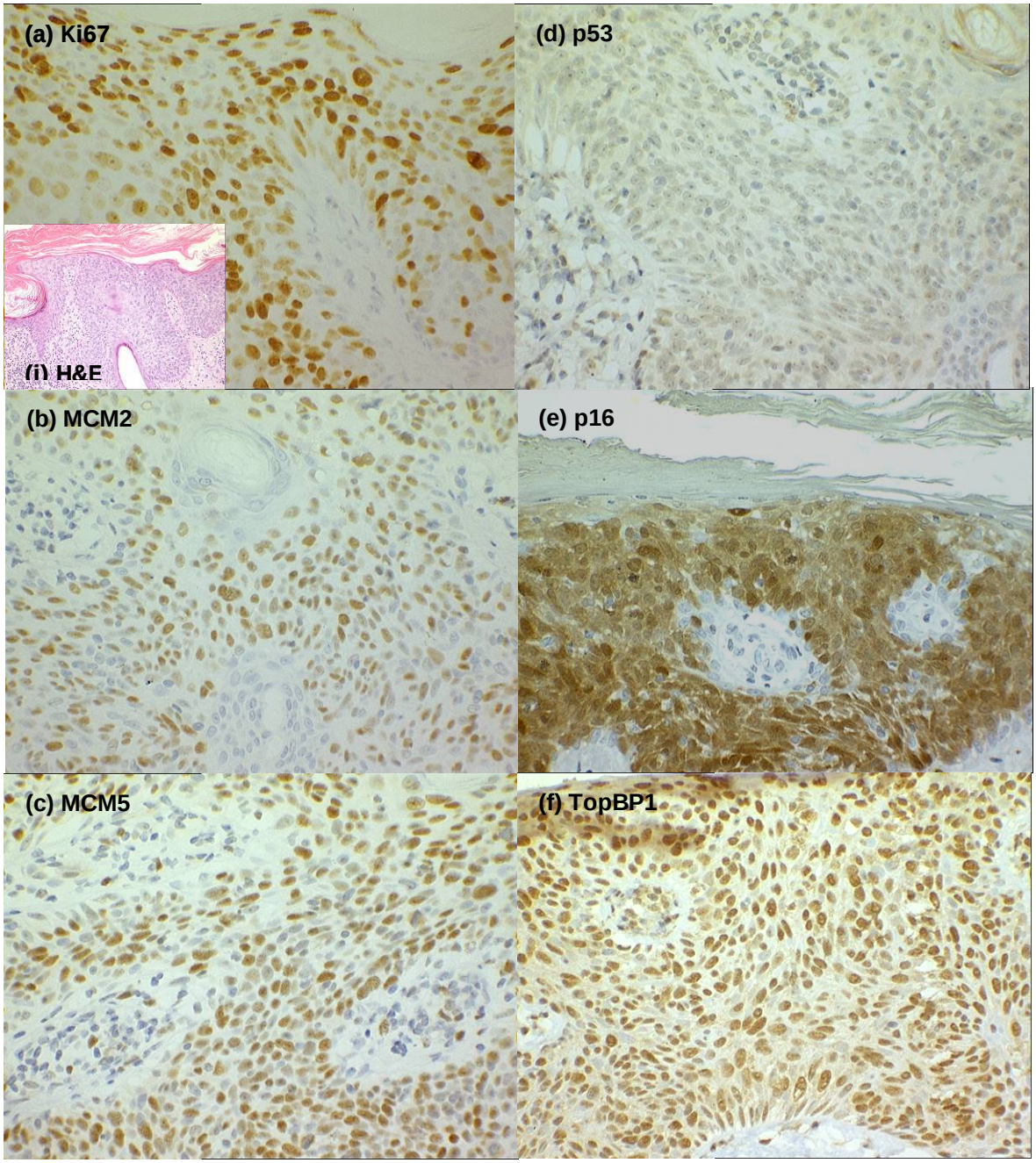

Figure 20 BetaPV positive intra-epidermal carcinoma.

Sections stained with (i) H&E and antibody directed against (a) Ki67, (b) MCM2, (c) MCM5, (d) p53, (e) p16 and (f) TopBP1. Original magnification (i) x 5; (a)-(f) x 20.

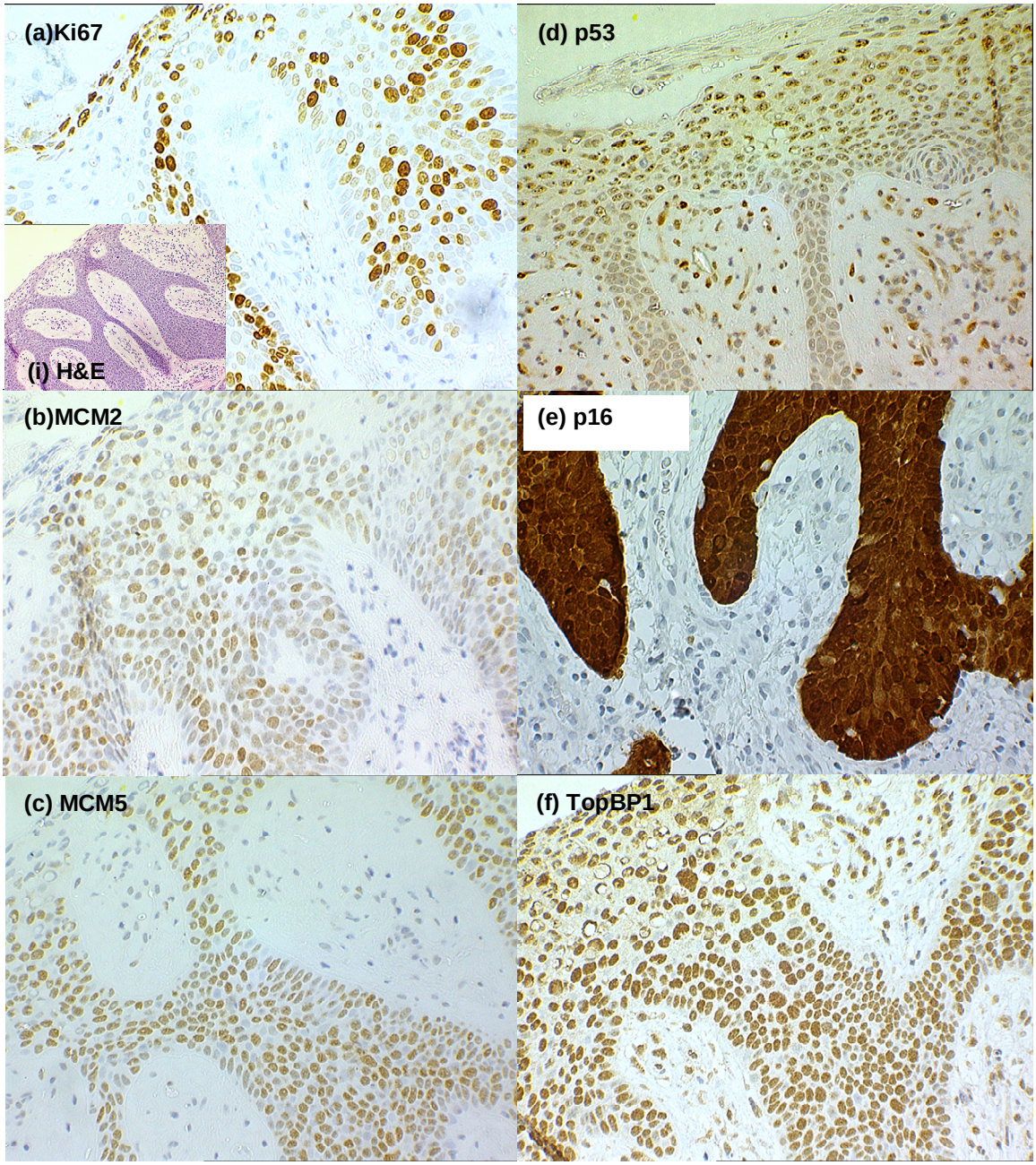

Figure 21 BetaPV negative intra-epidermal carcinoma.

Sections of a betaPV negative intra-epidermal carcinoma stained with (i) H&E and antibody directed against (a) Ki67, (b) MCM2, (c) MCM5, (d) p53, (e) p16 and (f) TopBP1. Ki67, MCM2, MCM5, P53 and TopBP1 staining is present through the full thickness of the lesion. p16 staining is present in an intense band through the full thickness of the lesion. Original magnification (i) x 5; (a)-(f) x 20.

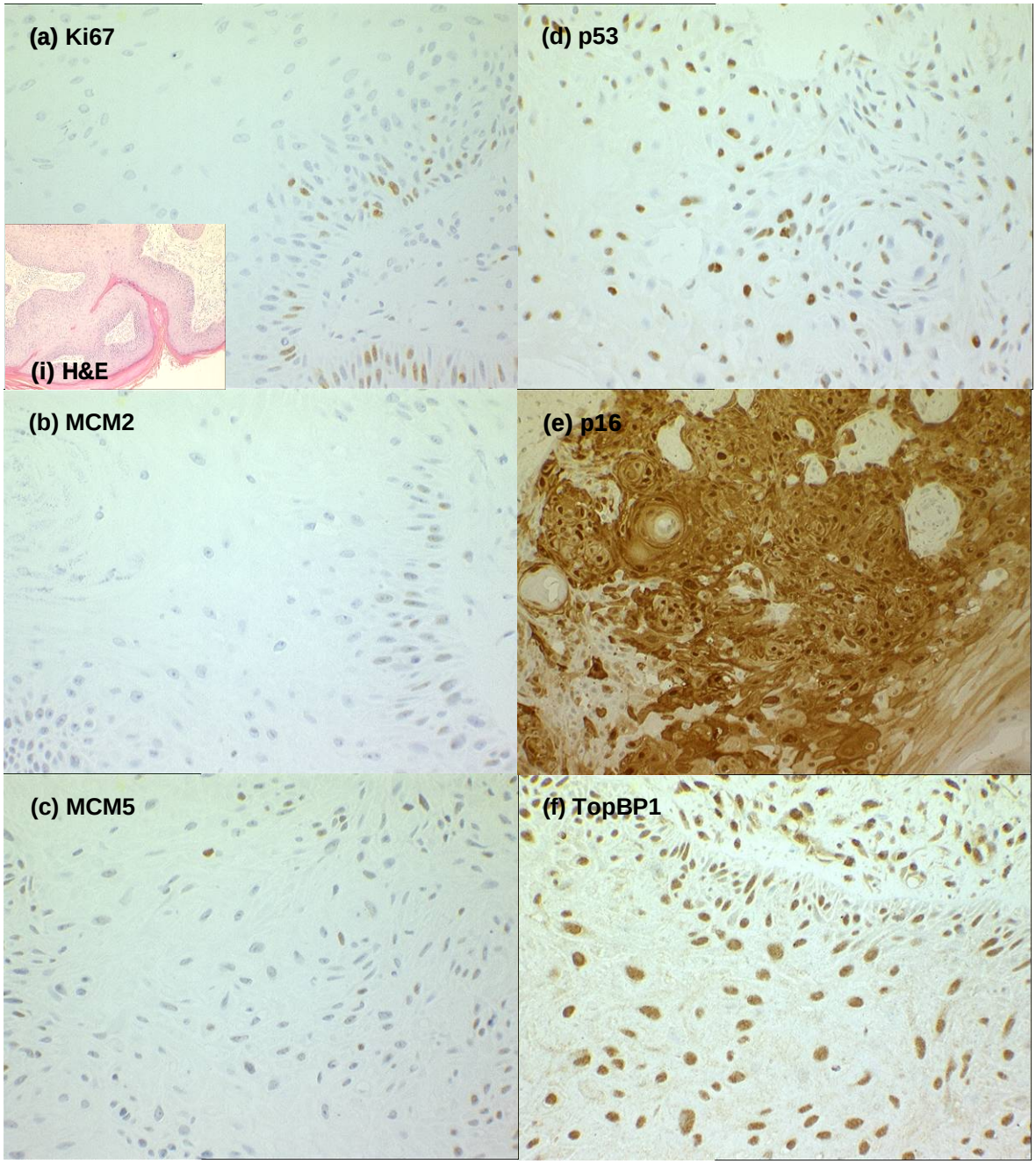

Figure 22 BetaPV positive squamous cell carcinoma (Low Grade).

Sections stained with (i) H&E and antibody directed against (a) Ki67, (b) MCM2, (c) MCM5, (d) p53, (e) p16 and (f) TopBP1. Original magnification (i) x 5; (a)-(f) x 20.

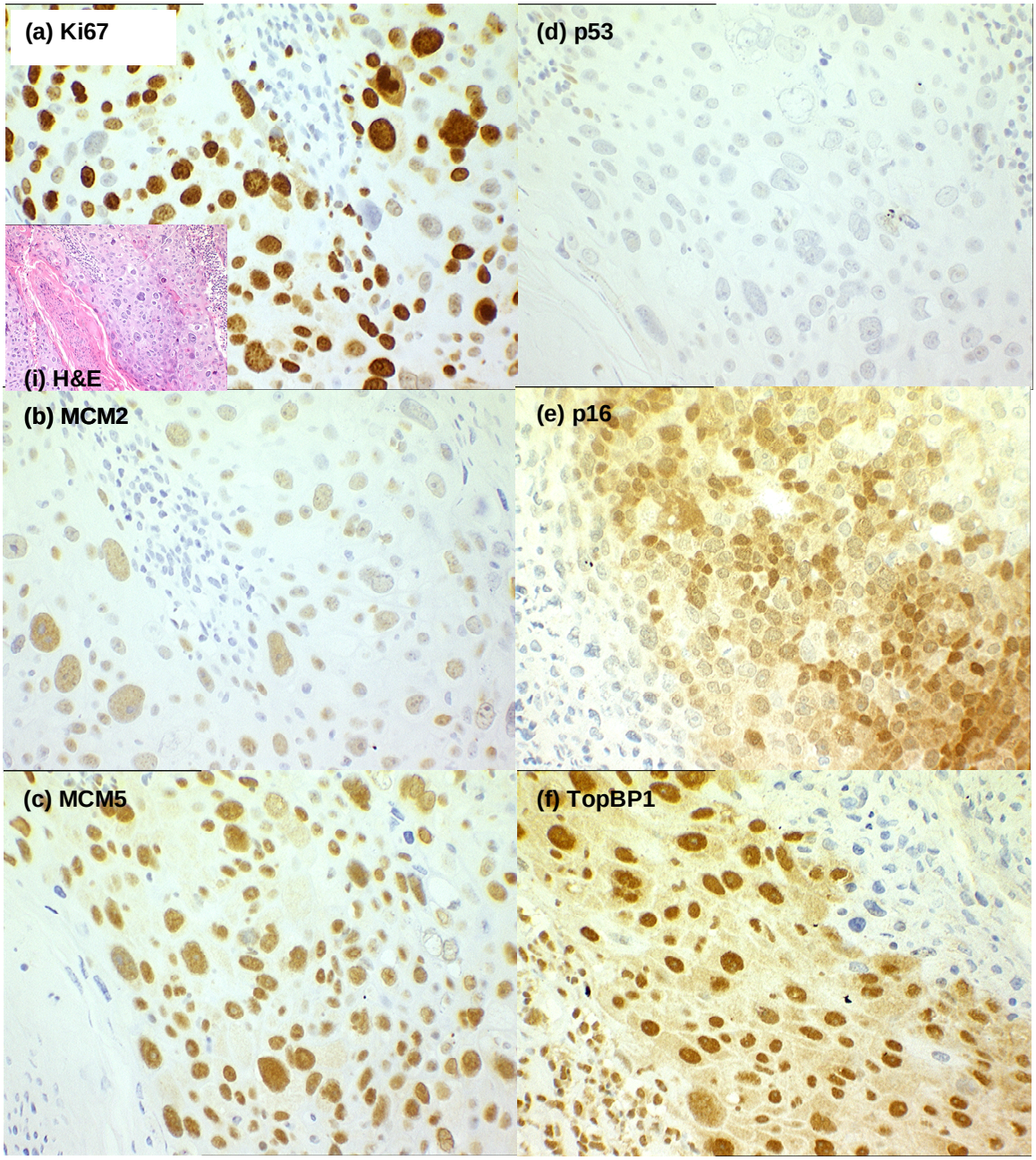

Figure 23 BetaPV negative squamous cell carcinoma (High Grade).

Sections stained with (i) H&E and antibody directed against (a) Ki67, (b) MCM2, (c) MCM5, (d) p53, (e) p16 and (f) TopBP1. Ki67, MCM2 and MCM5 are present through the full thickness of the lesion. p53 staining is not evident in the photographed area of the section but was present focally elsewhere. p16 staining, although less intense than that seen in Figure 16(e), is present in a band like distribution through the full thickness of the lesion. TopBP1 staining is both nuclear and cytoplasmic. Original magnification (i) x 5; (a)-(f) x 20.

3.3.4 Discussion

Ki67 protein is expressed in nuclei at all stages of the cell cycle except G0 and is a useful marker of proliferating/cycling cells (304). Previous studies of Ki67 expression in normal skin and a variety of both HPV typed and un-typed skin lesions found no correlation between Ki67 expression and proliferative state, risk of SCC progression or presence of HPV(305-309). Our results are in keeping with lack of correlation between Ki67 and HPV status in NMSC.

The family of MCM proteins 2-7 are components of the prereplicative complex essential for the initiation of DNA replication. Expression of MCM proteins is lost as the cell differentiates or is quiescent, thus the MCM proteins are a marker of cell proliferation (302). Antibodies to MCM proteins have been shown to improve detection of abnormal cells in Papanicolaou cervical smears and are more sensitive than anti-Ki67 antibody (302). Previous studies of MCM proteins in the skin showed a trend for a greater detection of proliferating cells with antibody directed against MCM5 protein compared to MCM 2 protein as seen in this study(310). Furthermore, expression of MCM proteins is, as expected, higher in poorly differentiated SCC compared to well differentiated lesions and staining is absent in the well differentiated cells adjacent to keratin pearls (310;311). Our study did not find an association between MCM protein expression and presence or absence of HPV.

The tumour suppressor gene, p53 is located on the short arm of chromosome 17p13.1. It is the most commonly mutated gene in human cancers. Cellular damage as a result of exposure of skin to UVR both induces wild type p53 and results in UV signature p53 mutations(312). Expression of wild type p53 protein initiates DNA repair mechanisms or induces cell cycle arrest or apoptosis. HPV infected cells must avoid p53 induced cell cycle arrest or apoptosis in order to replicate. Cervical cancer associated high risk mucosal HPV types do so through the action of the viral protein E6 which induces p53 degradation via the ubiquitin-proteasome pathway(137). BetaPV E6 protein does not degrade p53 via this pathway but can target the pro-apoptotic factor Bak for degradation thus avoiding apoptosis in a p53-independent manner (313;314). Several studies have examined the relationship between p53 staining in NMSC and presence of HPV and have found no relationship (307;315-317). Our samples were

comprehensively examined for betaPV and also found no correlation between betaPV presence and p53 staining.

P53 antibodies do not distinguish between mutated or wild type p53. In our samples we may have expected to see both over-expression of wild type p53 as a reflection of UVR exposure and mutated p53 as this is commonly found in all cancers. Furthermore betaPV E6 does not degrade p53 and therefore p53 may not have been a useful marker to examine for different expression patterns between HPV positive and negative lesions. Had they been available, antibodies to Bak may have been more useful as BetaPV E6 can target back in a p53 independent manner.

p16, encoded by the CDKN2a gene on 9p21, competes with cyclin D to bind CDK4/6 to prevent inactivation of pRb (318;319). The E7 oncoprotein from high-risk HPV types inactivates pRb resulting, by negative feedback, in over-expression of inactive p16 which is a marker to detect high risk mucosal PV infected cervical lesions (320). It has been shown that the HPV-38E7 protein has the ability to inactivate pRb therefore over expression of p16 in cutaneous lesions might be expected in betaPV infected samples. Previous studies of non-HPV typed skin lesions have shown p16 is absent in normal skin/benign controls and variably over-expressed in NMSC (305;321-323). Correlation of p16 expression and HPV presence has previously been found inconclusive due to small numbers (324;325). Our study did not find any correlation between p16 expression and betaPV infection. Although p16 has proven a useful marker in high risk mucosal HPV infected cervical lesions, because betaPV E7 does not inactivate pRb it may not be helpful in distinguishing between betaPV positive and negative skin cancers as has been shown in this case. Furthermore, p16 expression is often aberrant in skin cancers independent of HPV status again suggesting that p16 may not be useful in distinguishing between betaPV positive and negative skin cancers.

The marker TopBP1 has not been previously incorporated into studies of NMSC and betaPV. TopBP1 was included in this study as it has recently been shown to be aberrantly expressed in a significant percentage of breast cancers and is also essential for signalling DNA damage following UVR (248;254). The role of TopBP1 in activating the DNA damage signalling pathway through ATR following UVR

suggests this protein has a key role in maintaining genomic integrity in skin cells (254;256). Aberrant expression of TopBP1 in skin would therefore compromise the ability of the cells to respond appropriately to UVR and could be important in the development of NMSC. Furthermore, TopBP1 has been shown to be an interacting partner for the HPV-16 replication protein E2 (219). Our results showed aberrant expression of TopBP1 in a sub-set of NMSC although there was no association with presence of betaPV.

3.3.5.1 Conclusion

We have analysed by immunohistochemistry the expression patterns of cell cycle markers in a set of 100 nonmelanoma skin cancers typed for the presence of betaPV. We have shown over-expression of Ki67, MCM2, MCM5, p53 and p16 in a significant number of skin tumours compared to normal skin.

We have identified aberrant TopBP1 staining in skin tumours compared to normal skin - the first time that abnormal TopBP1 expression has been demonstrated in skin cancers.

We found no correlation between staining patterns and the presence or absence of HPV and the data shown do not support a role for HPV in NMSC. Although p53 and p16 are useful markers in HPV infected cervical lesions, they have not aided the distinction between HPV infected skin cancers. This is because UV results in over-expression of p53, both wild type and mutated. Furthermore, betaPV E6 does not degrade p53 but can target Bak for degradation thus avoiding apoptosis in a p53 independent manner. Antibodies to Bak, had they been available may have been a more useful biomarker to investigate. Similarly p16 may also be abnormally expressed in skin cancers and is not helpful ion distinguishing between betaPV positive and negative lesions as betaPV E7 does not bind pRb.

Had there been a difference in biomarker expression in betaPV positive and negative lesions, the results would have been validated by extending the study to examine the expression of these markers in other betaPV positive and negative lesions such as viral warts or seborrhoeic keratoses. This would have helped distinguish whether the patterns seen were a reflection of betaPV infection on replication alone or as part of malignant transformation. Another limitation of the study was the small numbers. A larger study would be required

to determine if other factors such as infection with specific types, e.g. HPV-5, -8 and -38, are the determining factor.

Chapter 3.4 The effect of TopBP1 on expression of viral proteins.

3.4.1 Interaction between E2 and TopBP1.

All the work in this chapter was carried out by Lorna Mackintosh unless stated otherwise.

Previous work in the Morgan laboratory identified TopBP1 as a cellular interacting partner for HPV-16E2 using a yeast-two hybrid screen (245). We propose that HPV replication in eukaryotic cells occurs via direct recruitment of TopBP1 to the E1-E2 complex resulting in DNA polymerase loading and initiation of replication.

To test this hypothesis we wished to generate a mutant of E2 that does not bind TopBP1 and then test the replication potential of this mutant. To do this, first the interaction between E2 and TopBP1 was mapped (Figure 24 A and B). The entire TopBP1 protein was screened in overlapping fragments as *in vitro* translated proteins for interaction with a fusion protein GST-E2 2-229. Amino acids 2-229 on the E2 protein is the interaction domain used to identify the TopBP1-E2 interaction. Three interaction domains were identified on TopBP1, amino acids 19-86, 586-606 and 818-888 (Figure 24 A).

To further map the domain on E2 that interacts with the domains on TopBP1, GST deletion mutant proteins of E2 were made and binding tested against three TopBP1 fragments each containing one of the TopBP1-E2 binding domains as described. The core interaction domain was thus mapped to between amino acids 50 and 110. This domain retained several amino acids that could be possible TopBP1 contact residues, some of which are 100% conserved between all E2 proteins (Figure 24 B) (Work carried out by M. Donaldson).

A

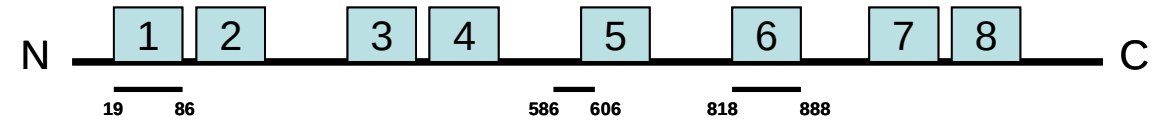

B

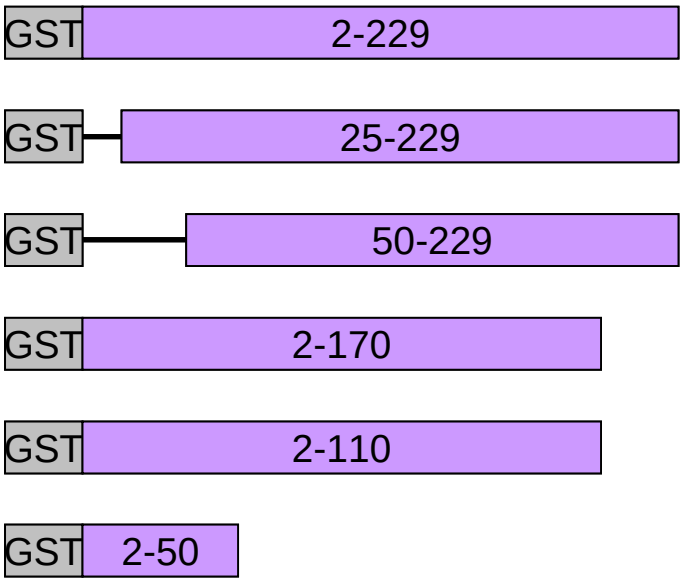

TopBP1 2-258	TopBP1 586-700	TopBP1 776-1292
+++	+++	+++
+++	+++	+++
+++	+++	++
++	+++	+++
+	++	++
-	-	-

Figure 24 A complex interaction between HPV-16 E2 and TopBP1.

A. Schematic representation of the TopBP1 protein illustrating the three E2 interaction domains identified (represented by thick black lines). The blue boxes numbered one to eight represent BRCT domains.

B. The domain on E2 that interacts with the domains on TopBP1 was further mapped with GST deletion mutant proteins. A schematic representation of the proteins is illustrated with the grey boxes representing GST and the purple boxes the E2 fragment. The table on the right shows the binding affinity between each of the GST-E2 deletion mutant proteins and three TopBP1 fragments each of which contains a TopBP1-E2 interaction domain. From this it was clear the region on E2 responsible for TopBP1 binding lay between amino acids 50-110.

Before generating an E2 mutant, the potential E2/TopBP1 contact residues were further narrowed down. To do this, amino acids on the E2 protein with previously assigned functions were eliminated.

Previous studies have characterised HPV16-E2 residues between amino acids 50 and 110 involved in transcriptional activity (transcription/Brd4 binding sites), E1 interaction sites as well as those predicted to be required for E2 structure. Mutation of amino acid residues may generate an E2 mutant with a compromised function; however mutation of certain residues generates an E2 mutant that fails to function in any tested assay suggesting that the residue was critical for the structure and function of the E2 protein. Such residues, identified from published studies, were deemed multiply defective. The locations of these known sites are illustrated in Figure 25.

TopBP1 is not required for E2 transcription function (261) and we predict a triple complex between E2-E1-TopBP1 for replication. Therefore the E2 residues required for E1 interaction should be distinct from those required for TopBP1 interaction. Therefore E2 residues required for transcription function and E1 interaction were eliminated. Also eliminated were residues shown to be multiply defective and those required for E2 structure and therefore could not be mutated. (Work carried out by M. Donaldson).

The residual amino acids not involved in any of the above functions are shown in Figure 25. These amino acids were mutated in pairs and with adjacent residues.

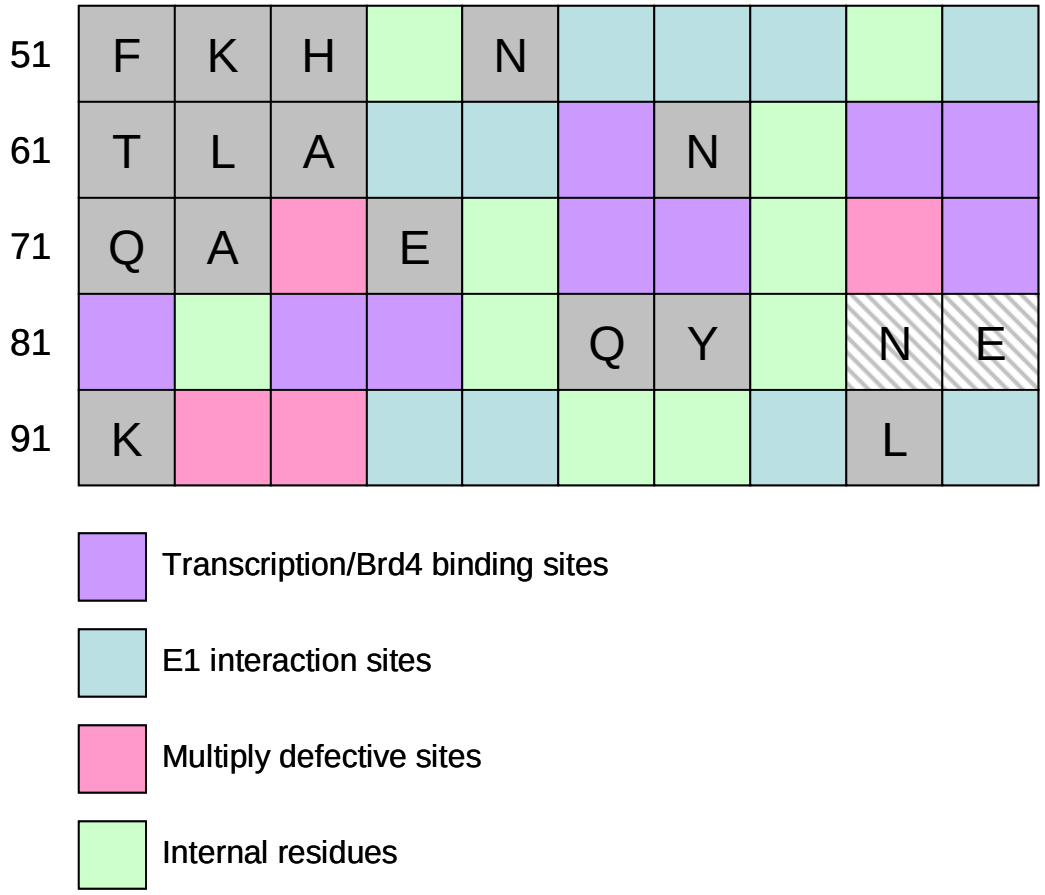

Figure 25 Selection of candidate residues for TopBP1 interaction.

E2 residues required for transcription function (purple) and E1 interaction (blue) were eliminated. Also eliminated were residues shown to be multiply defective (pink) and those required for E2 structure and therefore could not be mutated (green). This left the amino acids shown (grey). The two shaded residues represent amino acid residues 89 and 90.

3.4.2 Generation of an E2 mutant that does not bind TopBP1

HPV-16E2 mutants were generated by site directed mutagenesis of candidate amino acids residues in pairs with adjacent residues. Mutation of amino acid residues 89 and 90 (shaded residues, Figure 25), generated an E2 mutant (N89Y E90V) that failed to bind TopBP1 as demonstrated by co-immunoprecipitation between the mutant and TopBP1 (not shown) (work done by M. Donaldson).

To further characterise this mutant, single amino acid mutations were generated by site directed mutagenesis (2.2.4.11). The following HPV-16E2 mutants were generated N89Y, E90A and E90V with primers MDP264/265, MDP262/263 and MDP260/261 respectively. All mutants generated were sequenced as described (2.2.4.12) to ensure that the correct mutation had been inserted.

3.4.3 Replication efficiency of HPV16E2 wild type and mutants

In order to test the hypothesis that an E2 mutant that failed to bind TopBP1 would result in compromised replication of the HPV-16 genome in vivo, replication assays were performed in the 293T cell line (2.2.5.4).

293T cells were transiently transfected as described (2.2.5.2.1) with 100pg pOri (HPV-16 origin of replication) and 5μg HPV-16E1 plus 1ng or 10ng of HPV-16E2 wild type or mutants. Cells were harvested four days following transfection and the amount of replicated HPV DNA was assessed by quantitative PCR (2.2.4.9).

The results are shown in Figure 26 A and B and demonstrate that while the N89Y mutant replicates in a similar fashion to wild type E2, the presence of mutations N89YE90V and E90V result in reduced replication of HPV DNA. The reduction in replication compared to wild type is statistically significant for the N89YE90V mutant at both 1ng and 10ng ($p<0.05$) however for the single E90V mutant, there is no difference to wild type at the 1ng titration but at statistically significant reduction ($p<0.05$) at the 10ng titration.

A

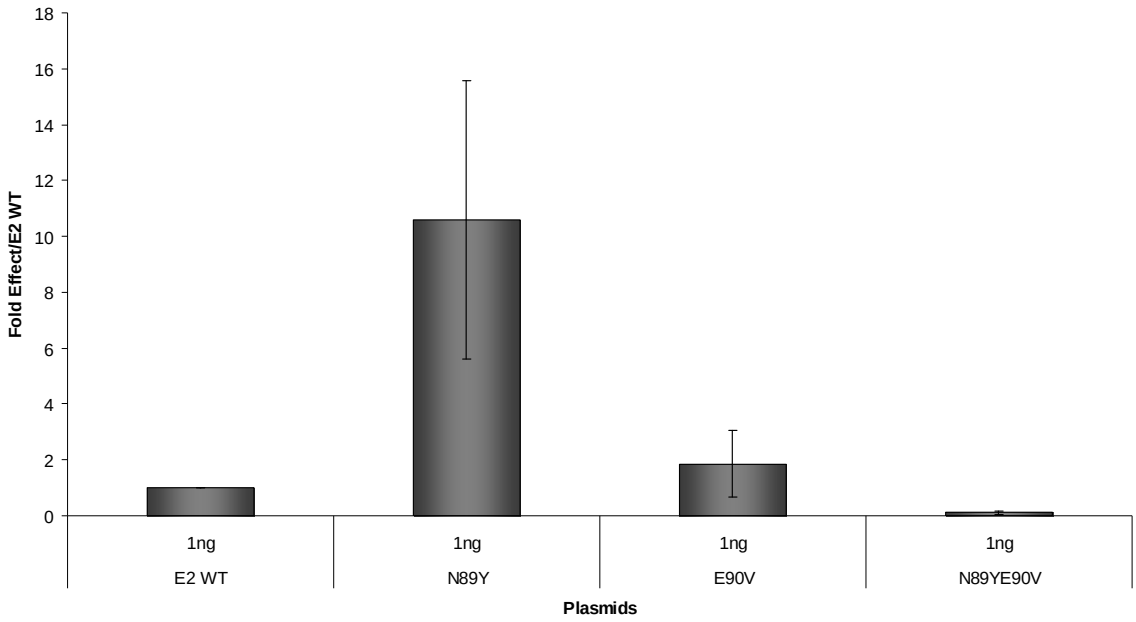

Plasmids		Mean Replication			Fold Effect/E2 WT 1ng					
		A	B	C	A	B	C	Mean	S.E.M.	p value
Cells only		0	0	0						
E2WT	1ng	0.61	0.13	1.26	1.00	1.00	1.00	1.00	0.00	
N89Y	1ng	0.44	2.12	18.42	0.71	16.49	14.58	10.60	4.98	0.12579
E90V	1ng	2.55	0.03	1.44	4.18	0.22	1.14	1.85	1.20	0.51790
N89YE90V	1ng	0.03	0.03	0.06	0.05	0.22	0.05	0.11	0.05	0.00008

B

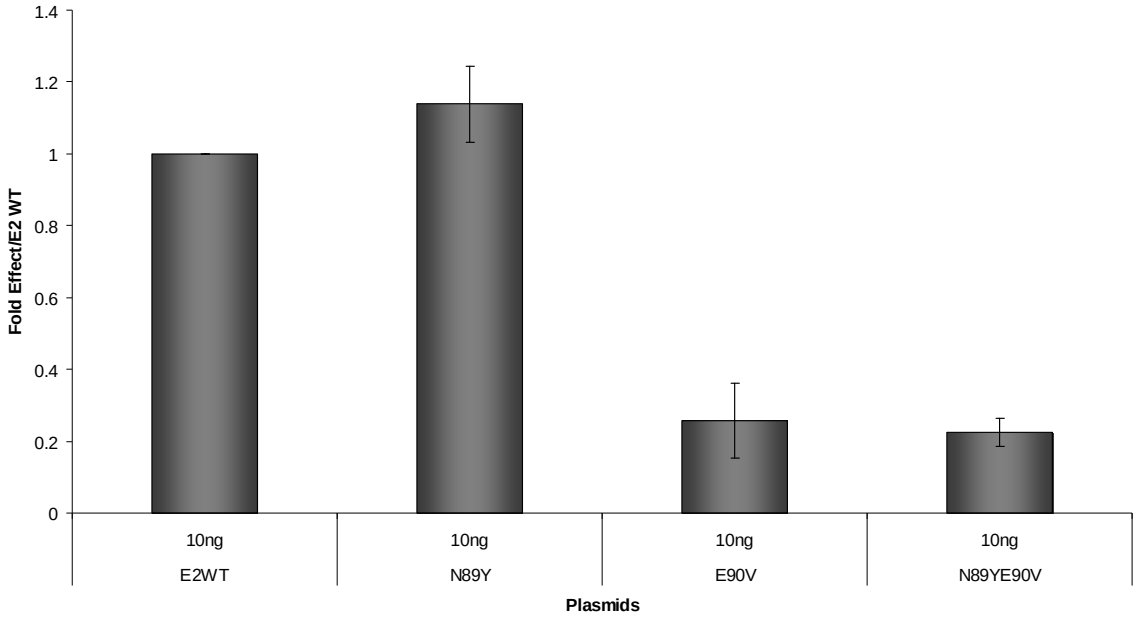

Plasmids		Mean Replication			Fold Effect/E2 WT 1ng					
		A	B	C	A	B	C	Mean	S.E.M.	p value
E2WT	10ng	2.22	2.97	33.62	1.00	1.00	1.00	1.00	0.00	
N89Y	10ng	2.52	2.85	44.43	1.14	0.96	1.32	1.14	0.11	0.25946
E90V	10ng	0.35	0.45	15.58	0.16	0.15	0.46	0.26	0.10	0.00197
N89YE90V	10ng	0.66	0.48	7.28	0.30	0.16	0.22	0.22	0.04	0.00004

Figure 26 A and B Replication activity of HPV-16 wild type and mutants.

293T cells were transfected with HPV-16E2 wild type and mutants. Each experiment was carried out in triplicate.

A. Replication is expressed as the fold effect in replication over E2 wild type 1ng.

B. Replication is expressed as the fold effect in replication over E2 wild type 10ng

The graphs shows the mean of three experiments +/- S.E.M. (standard error of the mean).

Results from each experiment (A-C) are shown in the tables below each graph. Variation between replicates A-C reflects variation in the efficiency of transient transfection. Control plates with cells only, pOri or pOri+E1 were included to ensure there was no contamination (results shown for cells only). Each PCR reaction was performed in triplicate; the amount of replication shown is the mean of three wells.

3.4.4 HPV-16E2 mutants binding to TopBP1 and HPV-16E1

The results shown above demonstrate that the N89YE90V mutant exhibits a compromised replication phenotype. The N89YE90V mutant is significantly compromised compared to wild type E2 at both 1ng and 10ng, the E90V mutant is significantly compromised at 10ng and the N89Y mutant replicated like wild type. To investigate whether the single point mutations of the E2 protein E90V, E90A and N89Y failed to bind TopBP1 similar to the double mutation N90YE90V, a co-immunoprecipitation was carried out between the E2 mutants and TopBP1. The results demonstrate failure of N89YE90V and E90V to bind TopBP1. HPV16E2 mutants E90A and N89Y bind TopBP1 similar to wild type E2. The results are shown in Figure 27.

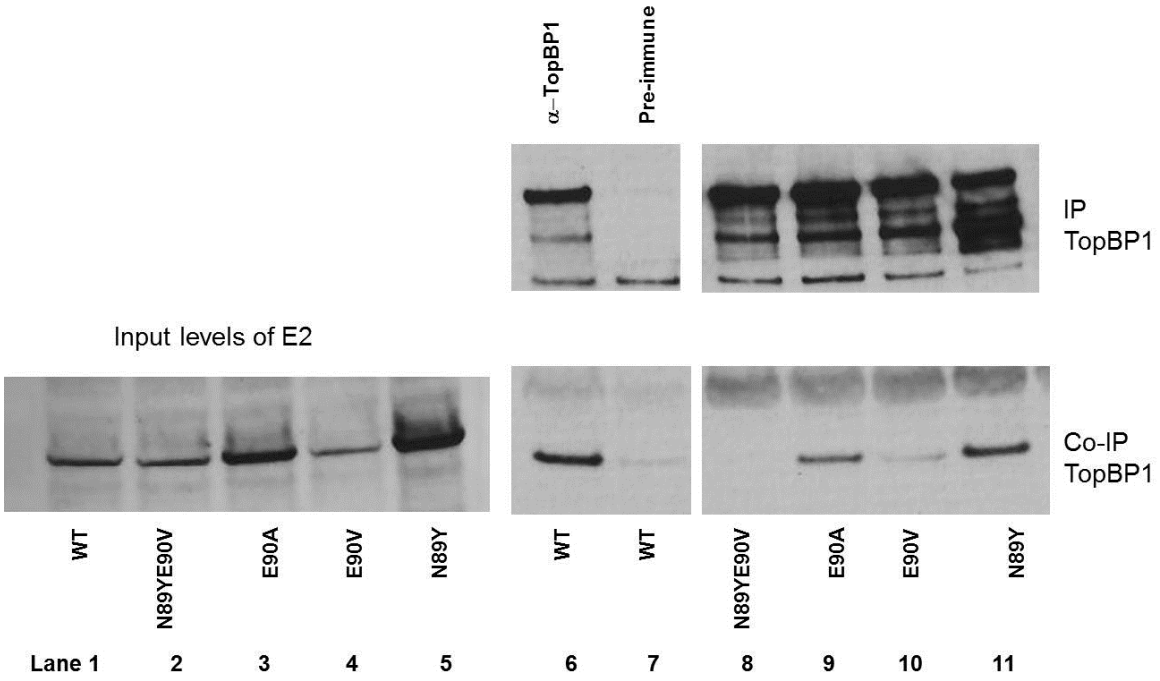

Figure 27 Western Blot of 293T protein extracts expressing HPV16E2 wild type (WT) or mutants N89YE90V, E90A, E90V and N89Y.

The lower panels are probed with the E2 antibody and the left hand panel (lanes 1 to 5) shows the level of input E2 protein (this represented 10% of the protein used in the co-immunoprecipitation experiment). The upper panels represent TopBP1 levels; there are no input levels shown as these are often difficult to detect (lanes 1 to 5). In Lane 6 the results of co-immunoprecipitation with the TopBP1 antibody and wild type E2 are shown. It is clear that in the lower panel a significant level of E2 protein is co-immunoprecipitated with TopBP1. Lane 7 represents the same experiment with pre-immune serum from the rabbit used to raise the TopBP1 antibody; neither TopBP1 nor E2 is immunoprecipitated (the faint E2 band detected is due to residual binding to the sepharose beads). Lanes 8-11 show the results of the co-immunoprecipitations of the E2 mutants by TopBP1; it is clear that TopBP1 has been immunoprecipitated in every sample (top panel) while E2 is co-immunoprecipitated in the E90A and N89Y samples. N89YE90V and E90V E2 mutants fail to co-immunoprecipitate with TopBP1.

Replication occurs in S phase of the cell cycle and this laboratory has previously shown the E2 protein is stabilised in S phase(326).

To test if the N89YE90V mutant was also stabilised in S phase, 293T cells, transfected with wild type HPV-16E2 or HPV-16E2N89YE90V were treated with the DNA polymerase inhibitor Aphidicolin (5μg/ml) for 16 hours to synchronise the cells. This treatment arrests the cells at the G1/S phase transition of the cell cycle. The drug was then removed, allowing for cell cycle progression into S phase and the cells were harvested at 2 and 4 hours. Protein extracts were prepared and TopBP1 and E2 protein levels investigated by Western Blotting. The results are shown in Figure 28A and illustrate that TopBP1 and wild type E2 are stabilised in S phase however N89YE90V is not (work done by M. Donaldson).

As the N89YE90V E2 mutant is not stabilised in S phase a Co-IP of the interaction between TopBP1 and N89YE90V was carried out in S phase. It can be seen that wild type E2 binds TopBP1 in untreated, Aphidicolin arrested and released cells, the strongest interaction is observed, as expected, 4 hours after release when both TopBP1 and E2 are stabilised. The N89YE90V mutant does not bind TopBP1 either in untreated cells or in S phase (Figure 28B) (work done by E. Dornan).

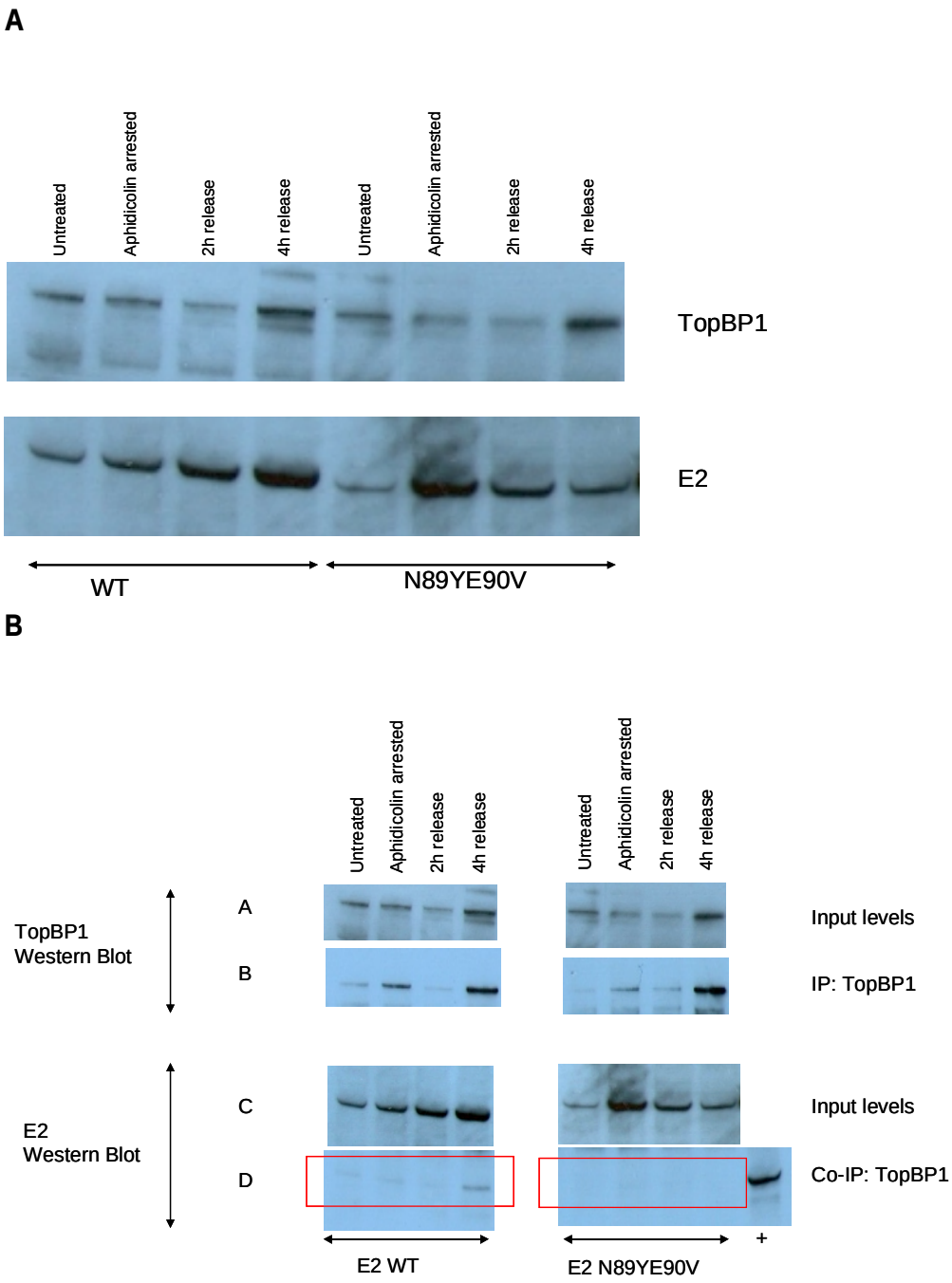

Figure 28 S phase stability of E2 and CoIP with TopBP1

A. Western Blot of 293T protein extracts, untreated, arrested with Aphidicolin and 2 and 4 hours following removal of the drug (2h release, 4h release). The upper panels demonstrate that TopBP1 is stabilised in S phase. The lower panels show stabilisation of wild type E2 in S phase as demonstrated by an increased density band at both 2 and 4 hours whereas in cells transfected with the mutant E2 N89YE90V, there is no stabilisation.

B. 293T cells were transfected with 16E2 wild type or N89YE90V treated with Aphidicolin for 16 hours then released and harvested 2 and 4 hours later. The Western Blots of the inputs are shown (panels A and C). The IP with TopBP1 shows increased levels of TopBP1 at 4 hrs post release (panel B). The CoIP between E2 and TopBP1 (panel D) shows that E2 is pulled down in untreated and Aphidicolin treated cells and in S phase (2h and 4h) however the N89YE90V mutant does not bind TopBP1 either in untreated cells or in S phase. The positive control lane (+), panel D demonstrates that the E2 antibody is working.

In order to demonstrate that compromised replication function of the E2 mutant was not due to lack of binding to E1, a co-immunoprecipitation experiment was carried out between the E2 mutant and E1. The E1 plasmid was tagged with the HA epitope to allow for detection by Western Blotting.

293T cells were transiently transfected with E2 alone or co-transfected with E1HA. E2 wild type or E2 N89YE90V was transfected along with two negative control experiments, no E2 or E2E39A, an E2 mutant that fails to bind E1. A Co-IP experiment was then carried out and the resultant cell lysates separated by SDS-PAGE gel electrophoresis and probed by Western Blotting for HA and E2.

The results of the Co-immunoprecipitation are shown in Figure 29. (Work carried out by E. Dornan).

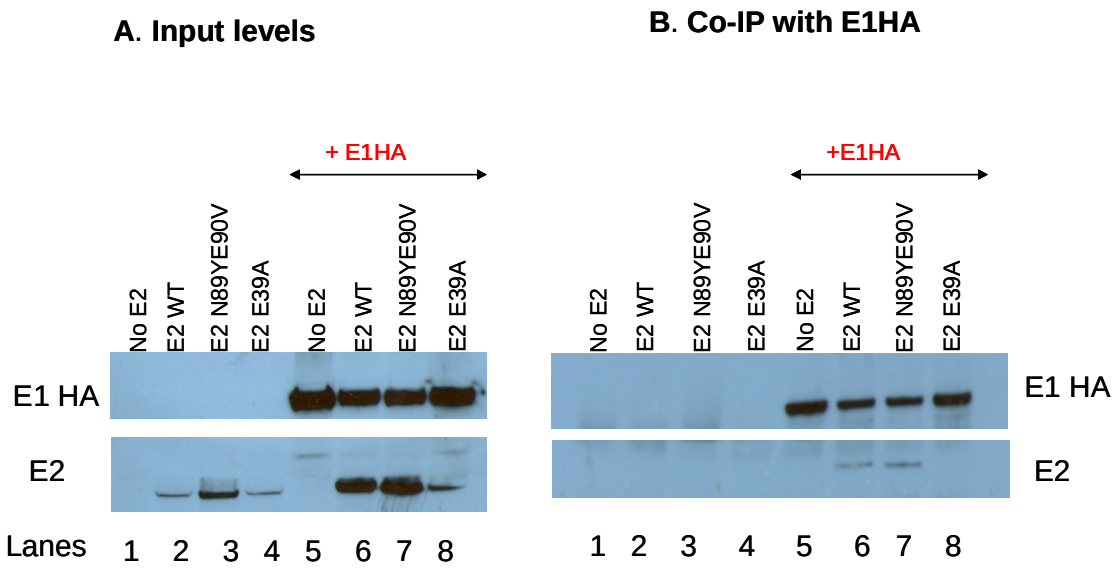

Figure 29 Co-IP of HPV-16E2 and HPV-16E1HA

A. Input levels.

Lanes 1-4 are 293T cell extracts transfected with E2 or controls in the absence of E1HA. As expected no bands are observed when the lysates are probed by Western Blotting with the HA antibody (upper panels). The lower panels demonstrate the input levels of E2 with no band seen in lane 1 (no E2) which acts as a negative control.

Lanes 5-8 show the input levels where E2 was co-transfected with E1HA. As expected, HA bands are clearly seen when the Western Blot is probed with the HA antibody (upper panels). The lower panels again show the presence of E2 in all but the negative control lane (5). In the presence of E1HA, the E2 bands are stronger as E2 is stabilised by E1.

B. Co-IP with E1HA

Lanes 1-4 show 293T lysates transfected with E2 alone. As expected no bands are seen with the HA antibody (upper panels) and E2 is not pulled down (lower panels).

In lanes 5-8 the IP with E1HA shows the HA bands in each lane indicating that the lysates are co-transfected with E1HA and that the HA antibody is working (upper panels). The lower panels show the Co-IP. When probed for E2, no E2 band is seen in lane 5 (negative control) however, E1HA pulls down both wild type E2 (lane 6) and the E2N89YE90V mutant (lane 7). E1 does not pull down E2E39A (lane8) as expected as this E2 mutant does not bind E1.

3.4.5 Transcriptional activity of HPV-16E2 mutants

In order to demonstrate that compromised replication is not due to altered transcription of the HPV-16E2 mutant, luciferase assays were carried out in the 293T cell line with the ptK6E2 promoter plasmid.

The ptk6E2 plasmid consists of an HSV tk promoter which has six consecutive E2 binding sites. E2 binds at these sites and drives the expression of the luciferase reporter gene (269). Measurement of luciferase activity thus acts as a surrogate marker for the transcriptional activity of E2. A schematic representation of the ptK6E2 plasmid is illustrated in Figure 30.

Figure 30 Schematic representation of the ptk6E2 plasmid.

A schematic representation of the ptk6E2 plasmid illustrating six E2 binding sites, the tk promoter from HSV1 and the luciferase reporter gene.

Luciferase assays were performed in the 293T cell line. 293T cells transiently transfected with 1μg of ptK6E2 and 1ng, 10ng, 100ng and 1μg of HPV-16E2 wild type and mutants were harvested two days following transfection and luciferase activity was measured as described (2.2.5.5).

Each experiment was carried out in triplicate and the results are shown in Figure 31.

The HPV-16E2 N89YE90V mutant demonstrates a significant reduction in transcriptional activity compared to wild type at 10ng (p 0.0307) but is not significantly different at the 1ng, 100ng and 1μg titrations. No significant differences in transcriptional activity of the HPV-16E2 N89Y or E90V mutants compared to wild type E2 were observed. This suggests that the reduced replication activity observed with the E2 mutant N89YE90V is not due to mis-folding of the protein. However it is interesting to note that the pattern of transcriptional activation observed with the N89YE90V mutant is different to that seen with wild type E2 or the N89Y and E90V E2 mutants. Furthermore, transcriptional activity is present at lower levels than seen with the N89Y and E90V mutants, the reason for this observation is not currently clear but could be related to the inability to bind TopBP1.

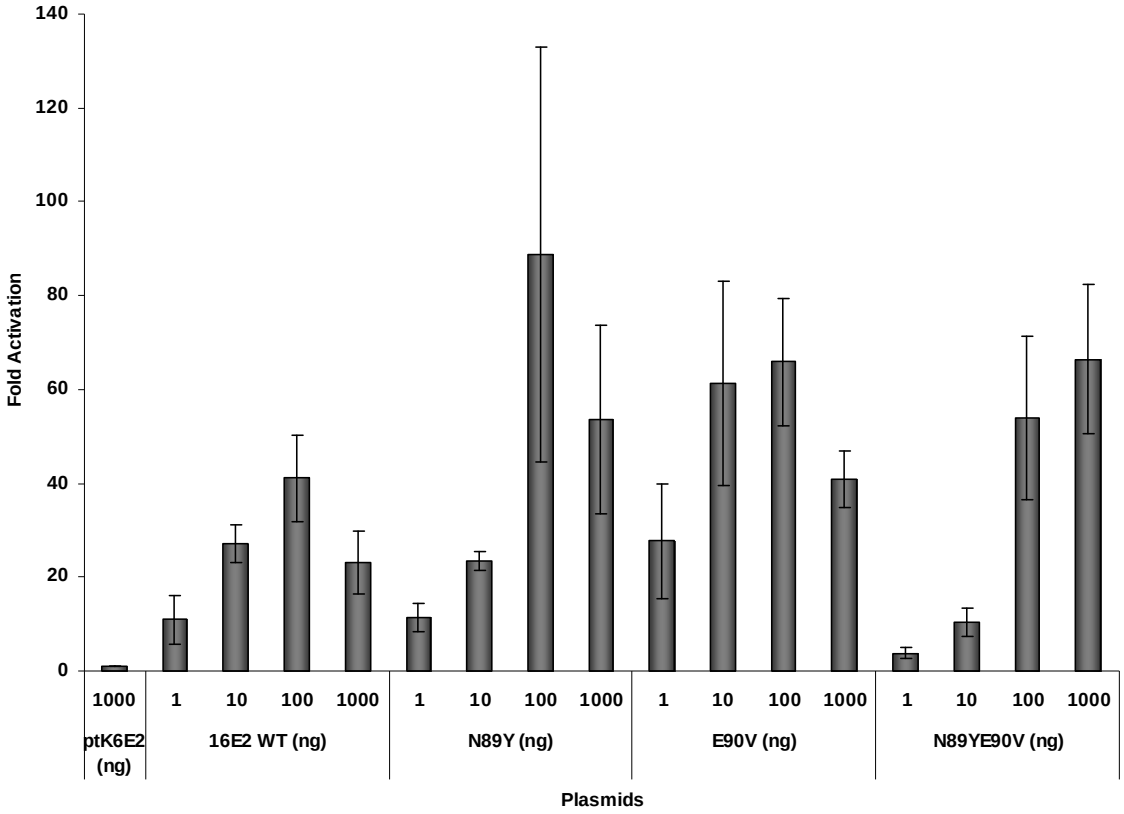

Plasmids		Mean Luminescence			Fold Activation /ptK6E2					
		A	B	C	A	B	C	Mean	S.E.M	P value
Cells only	x	2.45	0.89	5.63						
pGL3 Control	1μg	2056.02	919.07	5710.50						
pGL3 Basic	1μg	3.09	3.95	13.82						
ptK6E2	1μg	2.52	2.08	3.15	1.00	1.00	1.00	1.00	0.00	
16E2 WT	1ng	14.17	44.62	18.04	5.63	21.48	5.73	10.94	5.27	
	10ng	48.02	66.90	93.75	19.06	32.20	29.75	27.01	4.04	
	100ng	60.71	90.56	174.95	24.10	43.59	55.52	41.07	9.17	
	1μg	77.28	20.17	91.45	30.68	9.71	29.02	23.14	6.74	
N89Y	1ng	15.71	35.12	35.41	6.24	16.91	11.24	11.46	3.09	0.9367
	10ng	49.41	51.24	82.83	19.62	24.66	26.29	23.52	2.01	0.4825
	100ng	141.15	70.80	555.35	56.04	34.08	176.25	88.79	44.24	0.3500
	1μg	97.32	59.74	294.20	38.64	28.76	93.37	53.59	20.12	0.2241
E90V	1ng	20.41	51.97	157.55	8.10	25.01	50.00	27.71	12.18	0.2749
	10ng	58.07	205.19	195.60	23.05	98.77	62.08	61.30	21.89	0.1978
	100ng	126.82	193.00	171.85	50.35	92.90	54.54	65.93	13.56	0.2030
	1μg	120.83	60.08	144.05	47.97	28.92	45.72	40.87	6.02	0.1209
N89YE90V	1ng	7.66	12.50	7.84	3.04	6.02	2.49	3.85	1.10	0.2578
	10ng	11.05	26.42	44.76	4.39	12.72	14.20	10.44	3.06	0.0307
	100ng	49.44	136.48	241.45	19.63	65.69	76.63	53.98	17.49	0.5484
	1μg	124.33	107.04	309.10	49.36	51.52	98.10	66.33	15.92	0.0666

Figure 31 Transcriptional activation of HPV-16E2 wild type and mutants in 293T cells.

Luciferase activity, is expressed as the fold activity over that seen with the ptK6E2 promoter alone. Each experiment was carried out in triplicate and the graph shows the mean results of three experiments +/- S.E.M. (standard error of the mean). Results from each experiment (A-C) are shown in the table. Control plates (cells only, pGL3Control and pGL3Basic, ptK6E2 promoter) were included for each experiment. Each replicate was carried out in duplicate; mean luminescence is the mean from each set of duplicates. Variation between replicates reflects variation in the efficiency of transient transfection.

3.4.6 Stability of HPV-16E2 proteins

Compromised replication of HPV DNA could result from altered stability of the E2 protein when the E2 gene is mutated. In order to determine whether the E2 mutant proteins differed in stability from wild type E2 protein, the 293T cell line was transiently transfected with E2 wild type or mutants and a Cycloheximide treatment time course experiment was carried out (2.2.5.6). Cell culture plates were treated with Cycloheximide and harvested at different time-points to determine the half life of the wild type and mutated E2 protein. Equal amounts of the resultant protein lysates were separated by protein gel electrophoresis and analysed by Western Blotting. Blots were probed for E2 (TVG261) and γ-tubulin as a loading control. The experiment was repeated three times and a representative Western Blot is shown in Figure 32. There is variable expression of E2 wild type and mutants however there does not appear to be any major differences in any of the mutants in comparison to wild type E2.

To confirm this, Western Blots from the three repeats were scanned and analysed using Image J software (rsbweb.nih.gov/ij/). Following normalisation of the intensity of each E2 protein band to the corresponding γ-tubulin band, the E2 protein band density at each time point was expressed relative to the E2 protein band density pre-Cycloheximide treatment. The results are illustrated in Figure 33 and confirm that there are no significant differences in the half lives of the E2 mutants in comparison to wild type E2. The protein half lives were Wild Type, 6.08 hours, N89YE90V, 8.39 hours, N89Y, 9.36 hours, E90V, 7.60 hours.

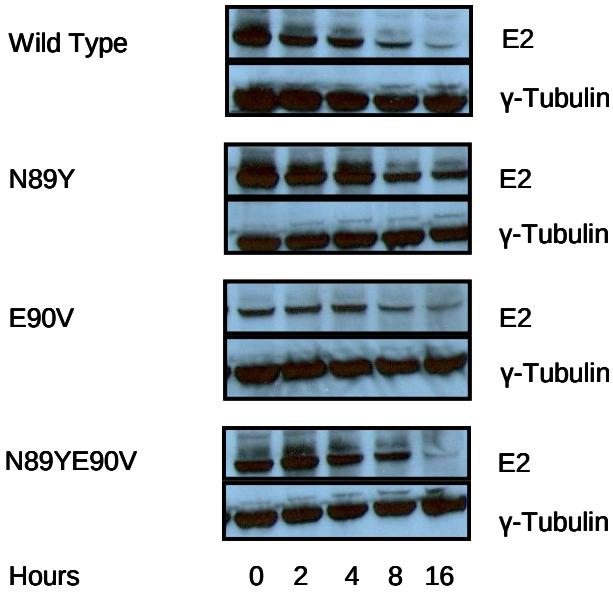

Figure 32 Stability of HPV-16E2 wild type and mutants in transiently transfected 293T cell line.

Cells transfected with wild type HPV-16E2 or mutants N89Y, E90V or N89YE90V were treated with Cycloheximide and harvested at 0, 2, 4, 8 and 16 hours post treatment. The resultant protein lysates were separated by SDS-PAGE electrophoresis and analysed by Western Blotting. Blots were probed for both E2 (TVG 261 antibody) (upper panels) and γ-tubulin as a loading control. The experiment was repeated three times and a representative Western Blot is shown.

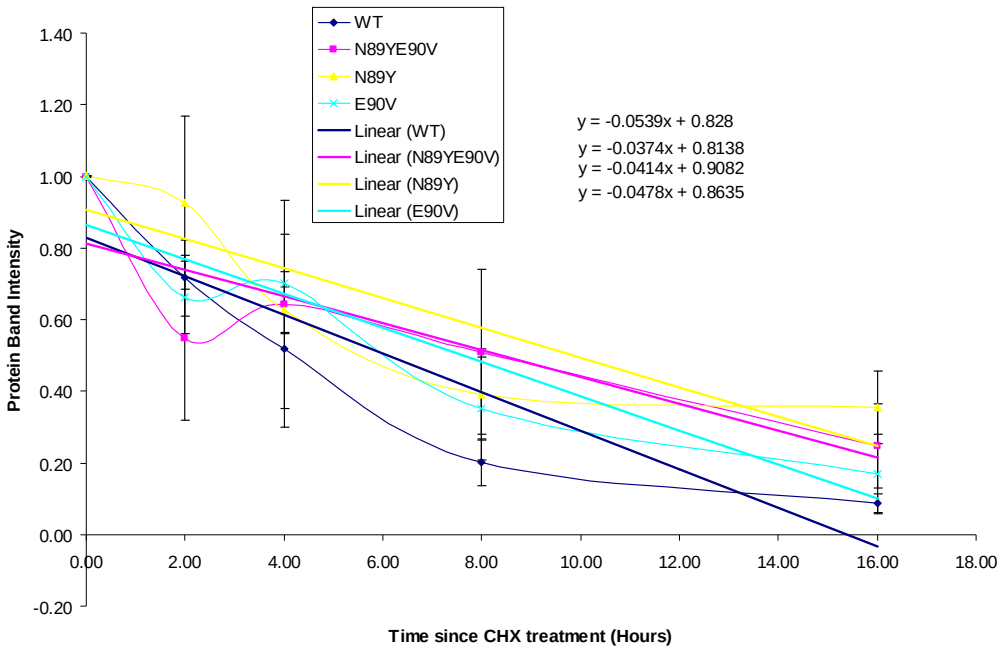

Figure 33 Graph of E2 protein band density over time since Cycloheximide treatment.

Western Blots from three experiments Cycloheximide time course experiments were scanned and the protein band density analysed using the Image J software.

HPV-16E2 wild type is represented by the blue line and the N89Y, yellow, E90V, turquoise and N89YE90V pink. For each time point, the density of the E2 protein band was normalised to the corresponding protein band intensity for γ-tubulin. For E2 WT and each E2 mutant, the density of the E2 protein band pre Cycloheximide treatment was taken as 100% and all subsequent time points expressed relative to the pre-treatment levels. The results shown are the mean of three experiments +/- S.E.M.

For each protein, a linear trendline (shown in the corresponding colour) and the equation of the line is shown allowing calculation of the half life of each protein. The half lives were, WT, 6.08; N89YE90V, 8.39; N89Y, 9.86 and E90V, 7.60 hours.

To confirm these results, the Cycloheximide treatment time course was repeated in the U2OS cell line that had been stably transfected with HPV-16E2 wild type (U2OS B3 cell line) and HPV-16E2 N89YE90V (U2OS 4.1 cell line).

A Cycloheximide treatment time course experiment was carried out as described (2.2.5.6). Equal amounts of the resultant protein lysates were separated by protein gel electrophoresis and analysed by Western Blotting. Blots were probed for E2 (TVG261) and γ-tubulin as a loading control. The experiment was repeated three times and a representative Western Blot is shown in Figure 34.

It can be seen that wild type E2 expression in the B3 cell line is more pronounced that E2 N89YE90V expression in the 4.1 cell line however there does not appear to be any difference in the overall half life of either protein. Western Blots from the three repeats were scanned and analysed using Image J software (rsbweb.nih.gov/ij/) as described above. The results are illustrated in Figure 35. The half life of both wild type E2 and E2N89YE90V are however similar, the half life of the wild type E2 being 10.94 hours and the half life of N89YE90V being 8.22 hours.

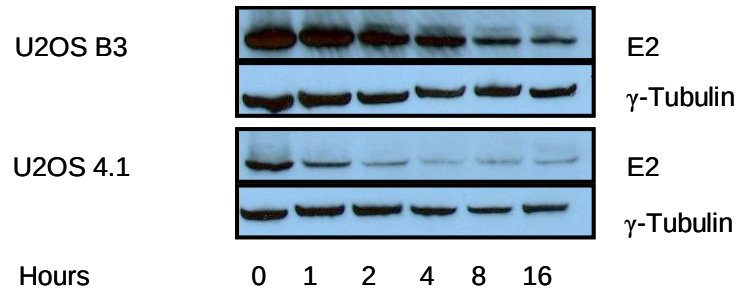

Figure 34 Stability of HPV-16E2 wild type and E2N89YE90V in stably transfected cell lines U2OS B3 and U2OS 4.1.

U2OS B3 and 4.1 cells were treated with Cycloheximide and harvested at 0, 1, 2, 4, 8, 16 and 24 hours post treatment. The resultant protein lysates were separated by SDS-PAGE electrophoresis and analysed by Western Blotting. Blots were probed for both E2 (TVG 261 antibody) (upper panels) and γ-tubulin as a loading control (lower panels). The experiment was repeated three times and a single representative Western Blot is shown.

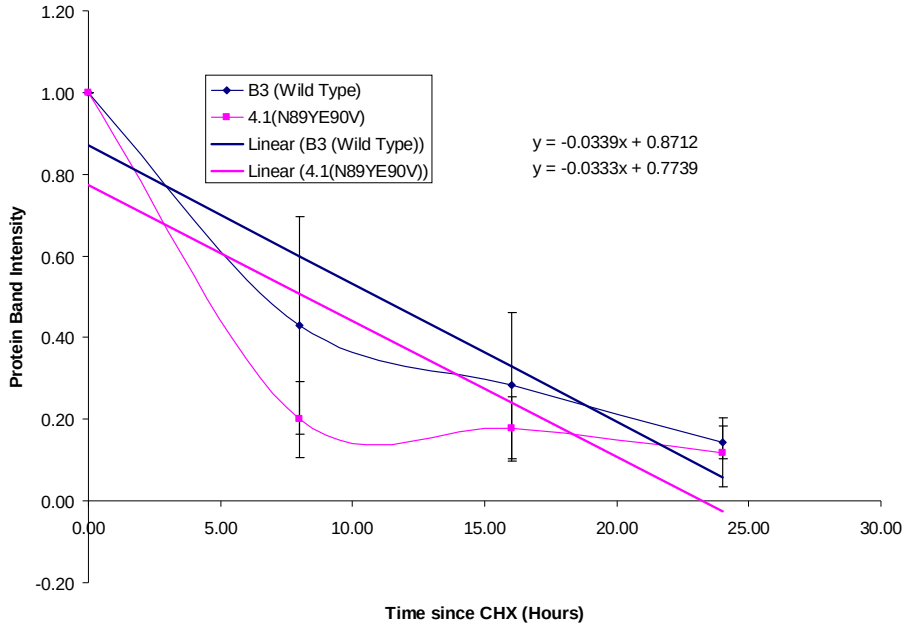

Figure 35 Graph of E2 protein band density over time since Cycloheximide treatment.

Western Blots from three Cycloheximide time course experiments were scanned and the protein band density analysed using the Image J software. The B3 cell line is represented by the blue line and the 4.1 cells by the pink line. For each time point, the density of the E2 protein band was normalised to the corresponding protein band intensity for γ-tubulin. The density of the E2 protein band pre Cycloheximide treatment was taken as 100% and all subsequent time points expressed relative to the pre-treatment levels. The results shown are the mean of three experiments +/- S.E.M.

For each protein, a linear trendline (shown in the corresponding colour) and the equation of the line is shown allowing calculation of the half life of each protein. The half lives were, WT,10.94; N89YE90V, 8.22 hours.

3.4.7 Generation of E2 mutants in an alternative HPV type.

The results have demonstrated that generation of a mutant E2 that fails to bind TopBP1 has resulted in a compromised replication phenotype. We wished to see if these results could be replicated in another HPV type. For these experiments HPV-8 was chosen. HPV-8 belongs to the genus Betapapillomaviruses and has been identified in SCC from patients with EV and in NMSC from both immunocompetent and immunocompromised individuals.

The amino acid at position 90 on the E2 gene is highly conserved between species. An amino acid alignment illustrating this is shown in Figure 36. It can be seen that amino acid 90 is conserved across HPV-16, -18 (high risk mucosal types), HPV-6, -11 (low risk mucosal types) and HPV-8, -5 (betaPV types).

```
HPV16           ----METLCQRLNVCQDKILTHYENDSTDLRDHIDYWKQMRLECAIYYKAREMGFKHINH 56
HPV18           MQTPKETLSERLSALQDKIIDHYENDSKDIDSQIQYWQLIRWENAIFFAAREHGIQTLNH 60
HPV11           ----MEAIAKRLDACQDQLLELYEENSIDIHKHIMHWKCIRLESVLLHKAKQMGLSHIGL 56
HPV6            ----MEAIAKRLDACQEQLLELYEENSTDLHKHVLHWKCMRHESVLLYKAKQMGLSHIGM 56
HPV8            ----MENLSERFNVLQDQLMNIYEAAEQTLEAQIAHWLLLRKEAVLLYFARQKGITRIGY 56
HPV5            ----MENLSERFNALQDQLMNIYEAAEQTLQAQIKHWQTLRKEPVLLYYAREKGVTRLGY 56

HPV16           QVVPTLAVSKNKALQAIELQLTLETIYNSQYSNEKWTLQDVSLEVYLTAPTGCIKKHGYT 116
HPV18           QVVPAYNISKSKAHKAIELQMALQGLAQSAYKTEDWTLQDTCEELWNTEPTHCFKKGGQT 120
HPV11           QVVPPLTVSETKGHNAIEMQMHLESLAKTQYGVEPWTLQDTSYEMWLTPPKRCFKKQGNT 116
HPV6            QVVPPLKVSEAKGHNAIEMQMHLESLLRTEYSMEPWTLQETSYEMWQTPPKRCFKKRGKT 116
HPV8            QPVPPLAVSEAKAKQAIGIMLQLQSLQKSEFADEPWTLVDTSIETYKNAPENHFKKGATP 116
HPV5            QPVPVKAVSETKAKEAIAMVLQLESLQTSDFAHEPWTLVDTSIETFRSAPEGHFKKGPLP 116
```

Figure 36 Amino acid alignment.

Amino acid alignment showing conservation of amino acid at position 90 on the E2 gene in HPV-16, -18, -11, -6, -8 and -5.

To investigate the TopBP1 /E2 interaction in HPV-8, the following plasmids were received as kind gifts from B.Akgul. p-8-1 containing the HPV-8 origin of replication; pCE1: HPV-8E1 in pCB6; pCE2: HPV-8E2 in pCB6; pCMV2-Flag: empty vector and pCMV2-HPV-8E2-Flag: containing the E2 open reading frame ligated into the EcoR1 and BamH1 sites of pCMV2-Flag.

For clarity from here on p-8-1 will be known as HPV-8ori, pCE1 as HPV-8E1 and pCE2 as HPV-8E2.

There are no available antibodies for the detection of HPV-8E2 and detection therefore relies on the presence of an epitope detectable with commercially available antibodies.

pCMV2-HPV-8E2-Flag (1, 2 and 5μg) was transiently transfected into 293T cells. Equal amounts of the resultant protein lysates and controls were separated by SDS-PAGE gel electrophoresis and analysed by Western Blotting. The blot was probed with Anti-Flag antibody (SIGMA F7425) at different concentrations and conditions but it was not possible to detect the Flag epitope (data not shown). The pCMV2-HPV-8E2Flag plasmid was sequenced by ABI cycle sequencing as described (2.2.4.12) with primer MDP271 (2.4.10.7). Sequencing revealed that the Flag epitope was present however it was out of alignment with the multiple cloning site in pCMV2 and this was thought to be the explanation for the inability to detect the plasmid by Western Blotting. To test the function of pCMV2-HPV-8E2-Flag further, increasing amounts of HPV-8E2-Flag plasmid were tested in a replication assay using the non-flag tagged plasmid, HPV-8E2 as a control. pCMV-HPV-8E2-Flag could not replicate (data not shown) therefore this plasmid was not used in any further experiments.

To overcome this problem and to allow detection of HPV-8E2 by Western Blotting a myc epitope was attached to HPV-8E2 by cloning. HPV-8E2 was amplified by platinum Pfx DNA polymerase PCR (2.2.4.11.1) with primers LMP7 and LMP8 (2.1.4.10.8). The PCR product was cleaned up using the QiaQuick PCR purification kit. The PCR product and plasmid vector p16E1-myc, clone 3 (2.1.4.9) and restriction digested (2.2.4.5.2) with EcoR1 and BamH1. Restriction digest products were purified and gel extracted (2.2.4.5.2) before treating the cut vector with phosphatase as described (2.2.4.5.3). The digested insert and vector were ligated (2.2.4.5.4) and the chemically competent bacteria

transformed with the resultant ligation product (2.2.4.6). Small scale preparation of the resultant plasmid was performed (miniprep procedure, 2.2.4.8) and the DNA was sequenced as described (2.2.4.12) with primer MDP271 (2.4.10.7). Sequencing revealed that HPV-8E2 had been correctly cloned into the myc tagged vector (data not shown).

To check expression of HPV-8E2myc, 0, 1 and 5μg of plasmid was transiently transfected into 293T cells. Cells were harvested 48 hours following transfection. The resultant protein lysates were separated by SDS-PAGE gel electrophoresis and analysed by Western Blotting. The blot was probed with anti-myc antibody (9E10,1:2000 dilution, AbCam). HPV-8E2myc protein could be clearly detected (Figure 37).

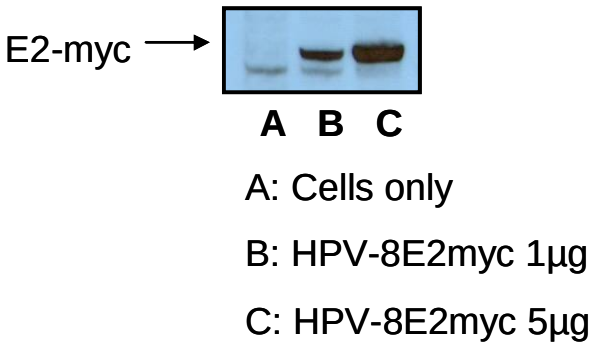

Figure 37 Detection of myc tagged HPV-8E2 protein by Western Blotting.

Western Blot was probed with anti-myc antibody at a 1:2000 dilution. HPV-8E2 protein is approximately 55KDa and the myc tag and multiple cloning site are approximately 2KDa. A 57KDa protein band is visible on the Western Blot.

3.4.8 Replication efficiency of HPV-8E2 mutants

We hypothesised that the HPV-8E2 mutants would behave in a similar fashion to the HPV-16E2 mutants and exhibit a compromised replication phenotype.

HPV8-E2 mutants were generated in HPV-8E2 and HPV-8E2myc by site directed mutagenesis as described (2.2.4.11). The following HPV-8E2 mutants were generated, D89A, E90A, E90V and D89AE90V (equivalent to N89Y, E90A, E90V and N89YE90V in HPV-16E2) using primers LMP11/12, MDP 272/273, MDP270/271 and LMP13/14 respectively (2.1.4.10). The resultant plasmids were amplified and sequenced as described (2.2.4.12) to ensure that the desired mutations had been made correctly (data not shown).

A DNA probe and primer set for detection of HPV-8 origin of replication was designed (2.1.4.10.3). This was tested by preparing a standard curve of serial dilutions of HPV-8ori and assessing the quantity by PCR reaction. A standard curve was obtained indicating that the probe and primer set were efficient at detecting HPV-8ori (data not shown).

293T cells transiently transfected with 100pg pOri (HPV-8 origin of replication) and 5μg HPV8E1 plus 1ng, 10ng or 100ng of HPV-8E2 wild type or mutants were harvested four days following transfection (2.2.5.4) and the amount of replicated HPV DNA was assessed by quantitative PCR (2.2.4.9). Initial experiments were carried out using the HPV-8E2myc wild type and mutant plasmids however, similar to the findings when testing pCMV-HPV-8E2-Flag, replication was severely compromised when using HPV-8E2-myc plasmids in comparison with HPV-8E2 plasmids. Replication assays were therefore performed using only the HPV-8E2 wild type and mutant plasmids. The experiments were carried out on three occasions and the results are illustrated in Figure 38 A-C.

The results demonstrate that there is a trend for the HPV-8E2 D89A mutant to replicate more efficiently than wild type HPV-8E2, this is significant at 1ng ($p=0.067$) but is not significantly different at the 10ng and 100ng doses. The HPV-8E2 E90A replicated in a similar fashion to wild type E2. Both the HPV-8E2 E90V and D89AE90V mutant exhibit severely compromised replication and this is significant at 1, 10 and 100ng titrations ($p<0.05$). This pattern of reduced

replication is similar to that observed with HPV-16E2 E90V and N89YE90V mutants; however the reduction in replication is more significant with the HPV-8E2 mutants.

A

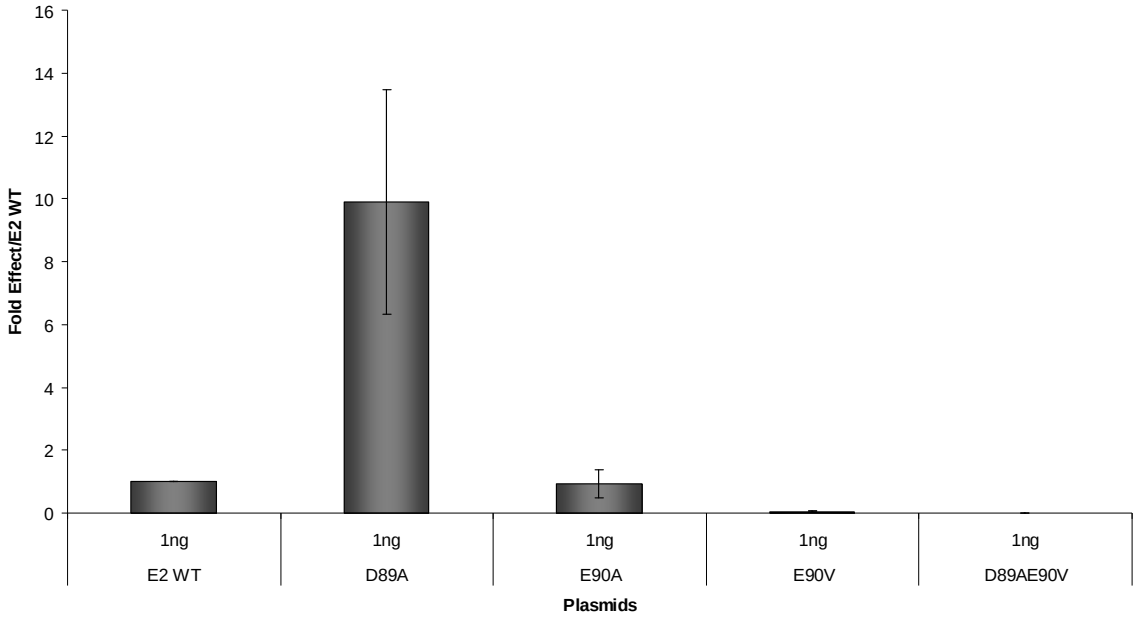

Plasmids		Mean Replication			Fold Effect/E2 WT 1ng					
		A	B	C	A	B	C	Mean	S.E.M.	p value
Cells only		0.00	0.00	0.00						
E2 WT	1ng	0.27	0.03	0.00	1.00	1.00	1.00	1.00	0.00	
D89A	1ng	1.09	0.32	0.00	4.00	9.38	16.35	9.91	3.58	0.067336
E90A	1ng	0.38	0.00	0.00	1.39	0.06	1.33	0.93	0.43	0.874932
E90V	1ng	0.02	0.00	0.00	0.07	0.07	0.00	0.05	0.02	0.000002
D89AE90V	1ng	0.00	0.00	0.00	0.02	0.00	0.00	0.01	0.01	<0.0000001

B

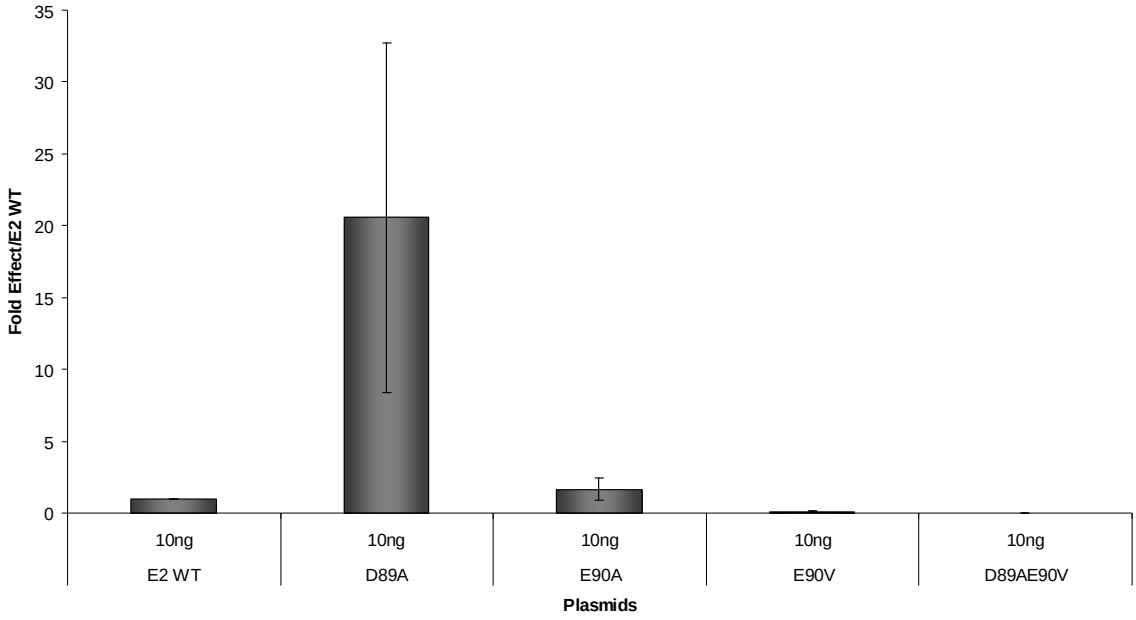

Plasmids		Mean Replication			Fold Effect/E2 WT 10ng					
		A	B	C	A	B	C	Mean	S.E.M.	p value
E2 WT	10ng	12.10	0.65	0.01	1.00	1.00	1.00	1.00	0.00	
D89A	10ng	20.65	10.88	0.44	1.71	16.74	43.23	20.56	12.15	0.182364
E90A	10ng	3.84	1.04	0.03	0.32	1.61	3.01	1.65	0.78	0.453665
E90V	10ng	1.89	0.07	0.00	0.16	0.11	0.01	0.09	0.04	0.000032
D89AE90V	10ng	0.21	0.00	0.00	0.02	0.00	0.00	0.01	0.01	<0.0000001

C

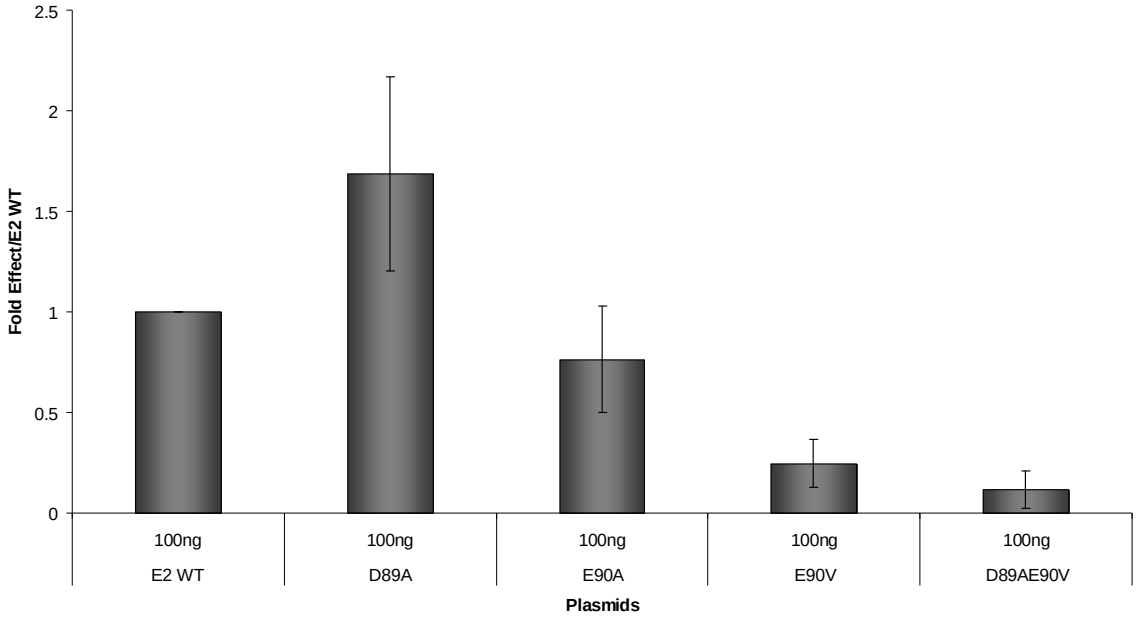

Plasmids		Mean Replication			Fold Effect/E2 WT 100ng					
		A	B	C	A	B	C	Mean	S.E.M.	p value
E2 WT	100ng	26.69	6.61	0.72	1.00	1.00	1.00	1.00	0.00	
D89A	100ng	26.51	17.27	1.05	0.99	2.61	1.45	1.69	0.48	0.227230
E90A	100ng	18.85	8.23	0.25	0.71	1.24	0.34	0.76	0.26	0.419252
E90V	100ng	12.34	1.48	0.04	0.46	0.22	0.05	0.24	0.12	0.000184
D89AE90V	100ng	7.97	0.34	0.00	0.30	0.05	0.00	0.12	0.09	0.000655

Figure 38 Replication activity of HPV-8E2 wild type and mutants

293T cells were transfected with HPV-8E2 wild type and mutants. Each experiment was carried out in triplicate.

A. Replication is expressed as the fold effect in replication over E2 wild type 1ng

B. Replication is the fold effect over E2 wild type 10ng

C. Replication is the fold effect over E2 wild type 100ng

Each graph shows the mean of three experiments +/- S.E.M. (standard error of the mean).

Results from each experiment (A-C) are shown in the tables below each graph. Variation between replicates A-C reflects variation in the efficiency of transient transfection. Control plates with cells only, pOri or pOri+E1 were included to ensure there was no contamination (results shown for cells only in Table A). Each PCR reaction was performed in triplicate; the amount of replication shown is the mean of three wells.

3.4.9 Transcription efficiency of HPV8E2 mutants

To confirm that these mutants are still functional, luciferase assays were carried out similarly to the HPV-16E2 mutants. 293T cells were transiently transfected with increasing concentrations of HPV-8E2 wild type or HPV-8E2 mutants and the ptk6E2 plasmid as described (2.2.5.5). Although the ptK6E2 promoter has 6 HPV-16E2 binding sites, we hypothesised that due to the similarities between the HPV-16E2 and HPV-8E2 genomes, HPV-8E2 would bind to the ptK6E2 promoter.

The results are shown in Figure 39. There is a non-significant trend for increased transcriptional activity of the HPV-8E2 D89A mutant, similar to the non-significant trend for increased transcriptional activity observed with the HPV-16E2 N89Y mutant. There are significant increases in transcriptional activity for both the HPV-8E2 E90A and E90V mutants at the 100ng titration but no significant differences at the 1ng, 10ng or 1μg titrations. The results therefore demonstrate that transcriptional activity of the HPV-8E2 mutants is not compromised in comparison to wild type HPV-8E2 and suggest that the compromised replication seen with the HPV-8E2 mutant D89AE90V is not due to a fundamental structural defect in the protein.

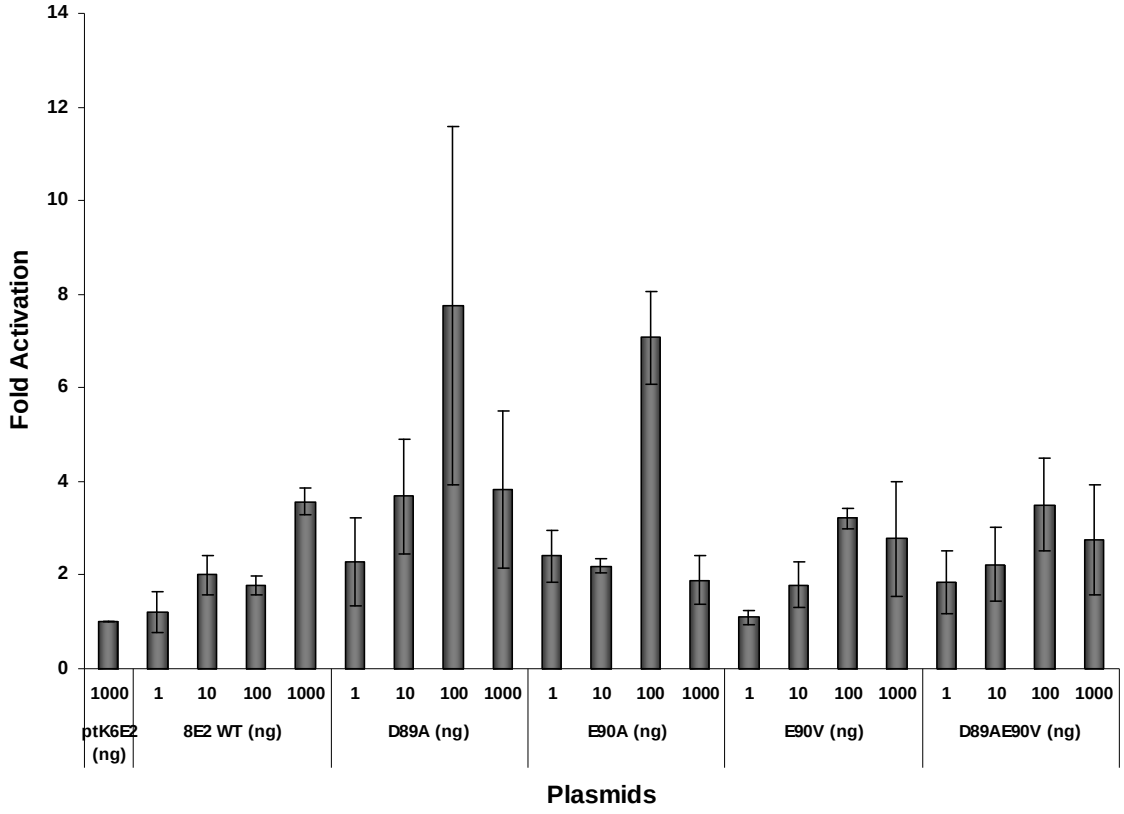

		Mean Luminescence			Fold Activation/ptK6E2					
Plasmids		**A**	**B**	**C**	**A**	**B**	**C**	**Mean**	**S.E.M**	**P value**
Cells only	x	27.11	6.22	16.66						
pGL3 Control	1μg	25447.86	6193.23	15820.54						
pGL3 Basic	1μg	87.97	11.85	49.91						
ptK6E2	1μg	18.80	3.07	10.94	1.00	1.00	1.00	1.00	0.00	
8E2 WT	1ng	13.05	6.40	9.72	0.69	2.09	0.89	1.22	0.44	
	10ng	47.08	3.60	25.34	2.50	1.17	2.32	2.00	0.42	
	100ng	38.01	4.20	21.10	2.02	1.37	1.93	1.77	0.20	
	1μg	60.65	12.71	36.68	3.23	4.15	3.35	3.58	0.29	
D89A	1ng	21.35	12.78	17.07	1.14	4.17	1.56	2.29	0.95	0.36507
	10ng	41.34	18.71	30.02	2.20	6.10	2.75	3.68	1.22	0.26143
	100ng	58.48	46.97	52.72	3.11	15.32	4.82	7.75	3.82	0.19290
	1μg	33.83	21.86	27.84	1.80	7.13	2.55	3.82	1.67	0.88993
E90A	1ng	32.74	10.78	21.76	1.74	3.51	1.99	2.41	0.55	0.16616
	10ng	44.49	5.83	25.16	2.37	1.90	2.30	2.19	0.15	0.68522
	100ng	110.49	27.72	69.10	5.88	9.04	6.32	7.08	0.99	0.00628
	1μg	23.93	8.91	16.42	1.27	2.91	1.50	1.89	0.51	0.04560
E90V	1ng	17.43	4.20	10.82	0.93	1.37	0.99	1.10	0.14	0.79350
	10ng	22.65	8.45	15.55	1.20	2.76	1.42	1.79	0.49	0.76578
	100ng	55.52	11.21	33.37	2.95	3.66	3.05	3.22	0.22	0.00851
	1μg	24.48	15.84	20.16	1.30	5.17	1.84	2.77	1.21	0.55221
D89AE90V	1ng	19.28	9.82	14.55	1.03	3.20	1.33	1.85	0.68	0.47962
	10ng	23.99	11.59	17.79	1.28	3.78	1.63	2.23	0.78	0.80828
	100ng	43.38	16.75	30.06	2.31	5.46	2.75	3.51	0.99	0.16048
	1μg	25.25	15.60	20.43	1.34	5.09	1.87	2.77	1.17	0.53888

Figure 39 Transcriptional activity of HPV-8E2 WT and mutants.

293T cells transiently expressing 1μg of ptK6E2 and 1ng, 10ng, 100ng or 1μg of HPV8E2 wild type and mutants were harvested two days following transfection and luciferase activity measured. Each experiment was carried out in triplicate. Luciferase activity is expressed as the fold activity over that seen with the ptK6E2 promoter alone. The results show the mean of three experiments +/- S.E.M. (standard error of the mean). Control plates with cells only, positive and negative controls pGL3control and pGL3Basic and the ptK6E2 promoter were included for each experiment. Each replicate was carried out in duplicate;

mean luminescence is the mean from each set of duplicates. Variation between replicates reflects variation in the efficiency of transient transfection.

3.4.10 Discussion

HPV replication is a possible therapeutic target that may be utilised for the development of anti-viral therapies. Disruption of the viral E1 /E2 interaction has not proven clinically useful thus far. Interactions between E1 and E2 with host proteins are possible alternative therapeutic targets. Little is known about the host cellular proteins that E1-E2 interact with in order to initiate viral DNA replication. Previous work in the Morgan laboratory has demonstrated that HPV-16E2 interacts with the cellular protein TopBP1 (219;245;261) and with HPV-16E1 (unpublished data).

We hypothesised that viral DNA replication occurs via direct recruitment of TopBP1 to the E1-E2 complex resulting in DNA polymerase loading and initiation of replication.

The first step towards testing this hypothesis was to map the interaction between TopBP1 and the HPV-16E2 DNA binding domain. Amino acids 50-110 of E2 were identified as being responsible for the interaction with TopBP1. Selection of candidate residues within this region followed by mutational analysis identified that when amino acids 89 and 90 were mutated, HPV-16 E2 failed to interact with TopBP1.

The work carried out in this Chapter has examined the TopBP1 E2 interaction. A double HPV16-E2 mutant was generated, N89YE90V and tested alongside single point mutations N89Y, E90A and E90V. We have confirmed that HPV-16E2 N89YE90V fails to bind TopBP1 by co-immunoprecipitation and have shown that the single mutant E90V is sufficient to disrupt binding while mutants E90A and N89Y bind like wild type E2.

To test the function of these HPV-16E2 mutants, replication assays were carried out and we have demonstrated that HPV-16E2 N89YE90V has a compromised replication phenotype whilst the replication efficiency of the single E2 mutations are not significantly altered compared to wild type E2 suggesting the double mutation is important to interrupt function.

The transcriptional activity of the HPV-16E2 mutants was tested by luciferase assays and the both the double and single mutants were functional suggesting that compromised replication is not due to a fundamental structural alteration of the E2 protein. However it is noted that there are subtle differences in the pattern of transcriptional activation seen with HPV-16E2 N89YE90V the reasons for which are currently unclear. Although TopBP1 clearly is not essential for transcription of E2 it but could be involved in its regulation.

Finally, demonstration that there are no significant differences in the half life of the HPV-16E2 mutants when compared to wild type suggests that alteration in protein stability is not responsible for the alteration in replication that observed with HPV-16E2 N89YE90V.

Interaction between E1-E2 and host cellular proteins are likely to be conserved across HPV types an important factor when considering the development of an anti-viral therapy. Therefore it was important to generate mutants of E2 in another HPV type and for this HPV-8 was chosen. The work on HPV-8E2 has demonstrated that generation of a mutant at amino acids 80 and 90 results in compromised replication of HPV-8E2. Furthermore, we have demonstrated, as in HPV-16 that this is not due to a fundamental alteration in the protein as the transcriptional activity of the HPV8E2 mutants is preserved. Interestingly replication is significantly altered in HPV-8E2 with the single amino acid mutations at position 90 but not position 89, this was not demonstrated in HPV-16 and it is possible that in some HPV types, a single amino acid substitution is sufficient to induce an altered replication phenotype.

In summary, we propose that TopBP1 interacts with E2 forming a TopBP1/E2/E1 complex which binds polymerase α and initiated viral DNA replication (Figure 40). By generating a mutant of E2 in HPV types -16 and -8 which fails to bind TopBP1, we propose that TopBP1 does not form a triple complex with E2/E1, polymerase α is not recruited and there is no initiation of viral DNA replication. This interaction is a potential future target for anti-viral therapies aimed at disruption of viral DNA replication.

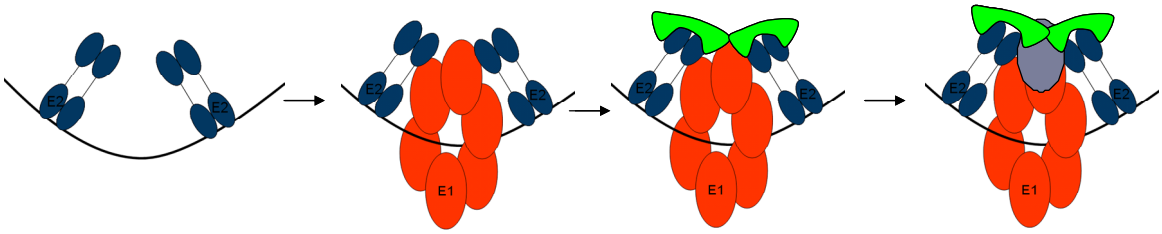

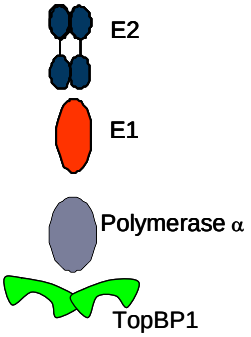

E2 protein forms homodimers and binds to the origin of replication

↓

E1 is recruited to the origin via a protein-protein interaction with E2

↓

E2 interacts with TopBP1 which binds to the E1/E2 complex

↓

TopBP1 binds and loads polymerase α

↓

Initiation of viral DNA replication

Figure 40 Schematic representation of the TopBP1/E1/E2 interaction.

The origin of replication is represented by the black line, E2 by the blue ovals, E1 by the red ovals, TopBP1 is shown in green and polymerase α by the grey oval. A proposed sequence of events that leads to initiation of viral DNA replication is shown in the text box.

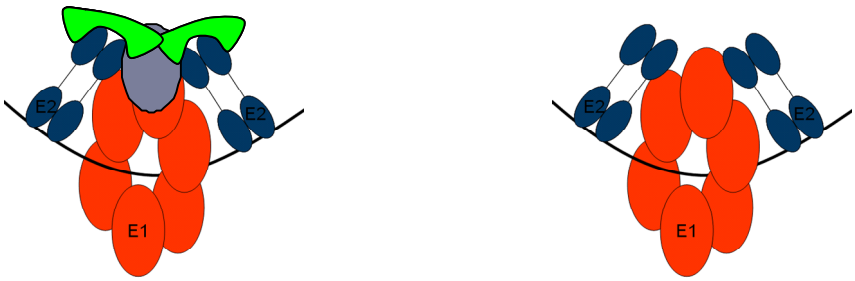

E2 Wild type

Recruits TopBP1

Binds polymerase α

Initiation of viral DNA replication

E2 N89YE90V

X Failure to efficiently recruit TopBP1

X Failure to efficiently recruit polymerase α

X Failure to efficiently initiate viral DNA replication

Figure 41 Schematic representation of disruption of the TopBP1 /E2/E1 interaction following generation of a mutant E2.

The proposed consequences of generation of an E2 mutant that fails to bind TopBP1. Figure legend as for Figure 16.

Chapter 3.5 The effect of TopBP1 on the cellular UV DNA damage response.

The expression of TopBP1 throughout the normal epidermis suggested that it may be involved in mediating the cellular response to UV irradiation due to its known role in activating ATR (256), the DNA damage response kinase. As TopBP1 is also a transcription factor, we hypothesised that TopBP1 may be involved in mediating the transcriptional response to UVR. To investigate this, we adopted a siRNA approach to knock down TopBP1 and then irradiate TopBP1 depleted cells before running a gene expression microarray analysis comparing wild type and TopBP1 depleted cells that were either UV irradiated or undamaged.

To perform a gene expression microarray analysis and allow comparison between the different experimental groups it was essential to firstly determine the dose of UVB that induced cellular DNA damage but allowed cell survival.

Secondly, it was essential to choose a cell line that would continue to cycle in the absence of TopBP1. TopBP1 is involved in DNA replication; it interacts with DNA polymerase ε (250) and directly associates with chromatin during DNA replication(260) suggesting that TopBP1 may play an essential role in DNA replication. In previous studies, when TopBP1 was knocked down in U2OS and Saos-2 cells, siTopBP1 treated cells arrested at G1 phase, again suggesting that TopBP1 is essential for DNA replication(327). Previous work in the Morgan laboratory investigated the effect of TopBP1 knockdown on cell replication in HEK293T, U2OS, MRC5, MCF7 and HeLa cell lines. MTT assays demonstrated that MRC5 and HeLa cells stopped growing 24 and 36 hours respectively following TopBP1 knockdown however, there was no effect on growth of the MCF7, 293T and U2OS cell lines over a four day period (Roni Wright – unpublished data).

The HaCat cell line, a spontaneously transformed human epithelial cell line derived from human adult skin which is immortal but non-tumorigenic and exhibits normal differentiation was chosen for this investigation (328). The initial experiments described in this chapter were to determine the dose of UVB that induced cellular DNA damage but allowed cell survival and to determine the effect of TopBP1 depletion on cellular replication.

3.5.1 The effect of UVB irradiation and TopBP1 knockdown in the HaCaT cell line.

To determine a dose of UVB that would induce cellular DNA damage in the HaCaT line, cells grown in monolayer were irradiated with increasing doses of UVB (2.2.5.7). Total cell lysates were harvested 30 minutes following irradiation and equal amounts of protein were separated by SDS-PAGE gel electrophoresis, the resultant Western Blot was probed for phosphorylated Chk1. Figure 42A shows that cellular DNA damage, determined by the induction of phosphorylated Chk1, was detected when cells were irradiated with UVB at doses of 0.004 J/cm^2 and above.

To determine the dose of UVB that would induce cellular DNA damage but allow cell survival, crystal violet colony survival assays were carried out over 14 days as described (2.2.5.8). In these assays, HaCaT cells grown in monolayer were mock irradiated or irradiated with increasing doses of UVB 0.004 to 0.030 J/cm^2 . Thirty minutes following irradiation, 500 cells from each plate were re-seeded in triplicate. At 14 days following irradiation, surviving colonies were stained with crystal violet and counted. The experiment was carried out in triplicate. As shown in Figure 42B, following a UVB dose of 0.004J/cm^2, 60% of colonies survived compared to those mock irradiated.

A.

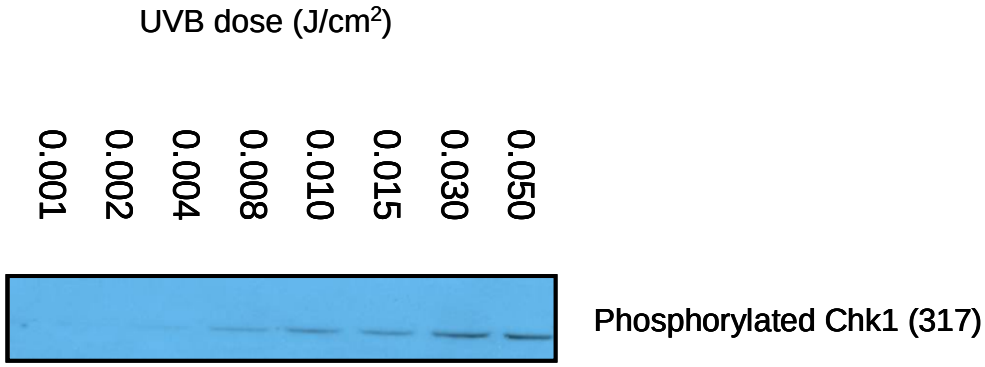

B.

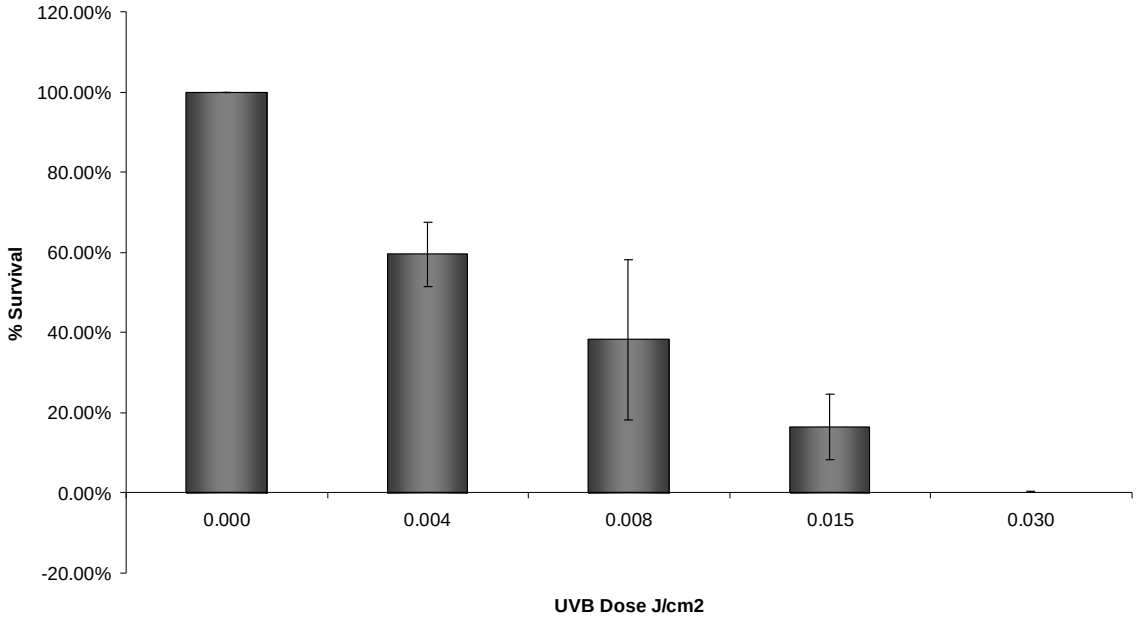

Figure 42 Effect of UVB irradiation on the HaCaT cell line

A. Phospho-Chk1 expression levels following UVB irradiation.

HaCaT cells grown in monolayer were irradiated with increasing doses of UVB. Induction of phosphorylated Chk1 antibody is seen following UVB doses of 0.004 J/cm^2 and above.

B. Crystal violet colony survival assay of HaCaT cells following UVB irradiation.

The results are the mean of the triplicates for each UVB dose +/- S.E.M. The colonies present following mock irradiation were expressed as 100%, the number of colonies in each subsequent UVB dose is expressed as percentage survival compared to mock irradiation.

TopBP1 was knocked down in HaCaT cells using specific small interfering RNA (siRNA) targeted against TopBP1 (2.1.4.10.1). siRNA treatment was delivered to cells by transient transfection using the lipofectamine 2000™ method (2.2.5.2.2). For all experiments using siRNA targeted against TopBP1 (siTopBP1), untreated cells, mock transfected cells (using lipofectamine only) and siRNA oligonucleotides against luciferase were included as experimental controls. Seventy-two hours following transfection, equal amounts of total cell lysates were separated by SDS-PAGE gel electrophoresis and the resultant Western Blot probed for the presence of TopBP1 with γ-tubulin as a loading control. As shown in Figure 43, a greater than 90% knockdown efficiency of TopBP1 was achieved.

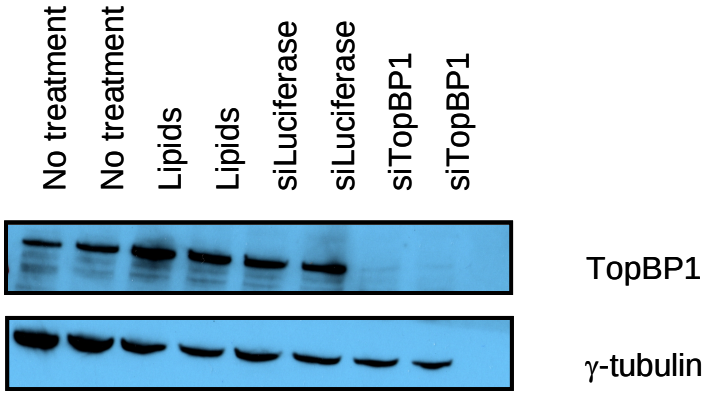

Figure 43 TopBP1 expression levels in HaCaT cells following siRNA treatment.

HaCaT cells were transiently transfected with siTopBP1 or siLuciferase, mock transfected (lipids only) or received no treatment. Total cell lysates were harvested 72 hours following transfection and equal amounts of protein were separated on a SDS-PAGE gel. The resultant Western Blot was probed for the presence of TopBP1 and γ-Tubulin as a loading control. This experiment was repeated a minimum of three times and a single representative Western Blot is shown.

To determine whether TopBP1 depleted HaCaT cells would continue to replicate, cell growth assays (2.2.5.9) were carried out in siTopBP1 treated HaCaTs and controls. The results are shown in Figure 44A.

The assays were carried out over four days. Cell lysates were harvested to demonstrate TopBP1 expression over the four days and were harvested at the same time as the cell growth assay readings (0, 48 and 96 hours). The expression of TopBP1 at 0, 48 and 96 hours is shown in Figure 44B and it is clear that the knockdown of TopBP1 was efficient and persisted at 96 hours.

Cell growth assays were carried out twice in triplicate. The results show a 25-fold increase in cell growth in untreated HaCaT cells over four days. TopBP1 depleted HaCaTs did not grow indicating that TopBP1 is essential for replication on the HaCaT cell line. si-Luciferase treatment and mock transfection have a modest effect on cell growth reducing the fold difference in cell growth to 20 and 12 fold respectively and this probably reflects toxicity from the lipofectamine treatment reducing cell growth in comparison to untreated cells.

A.

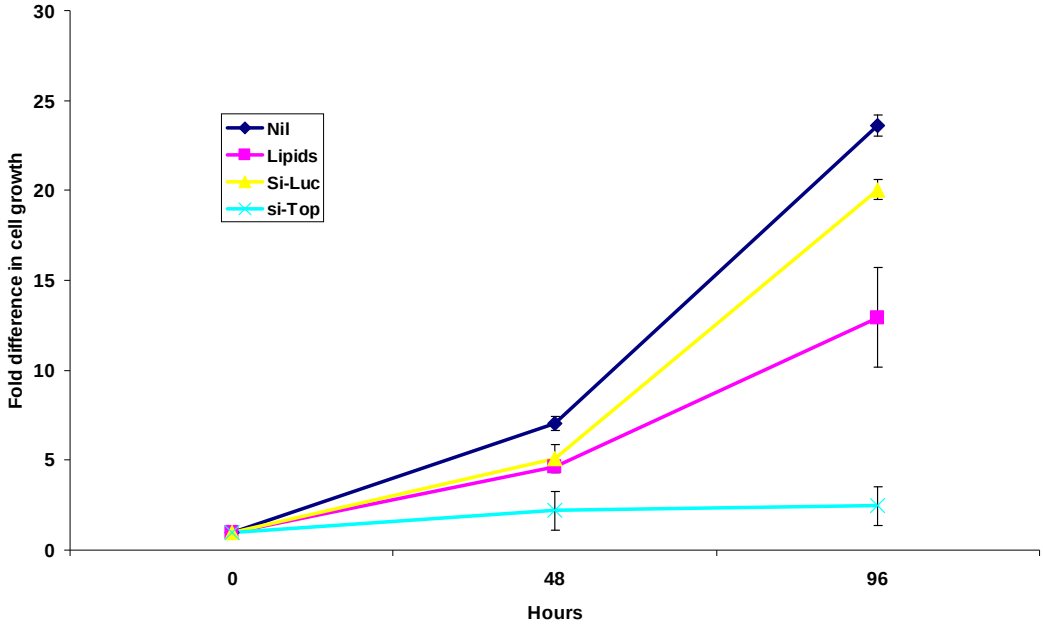

B.

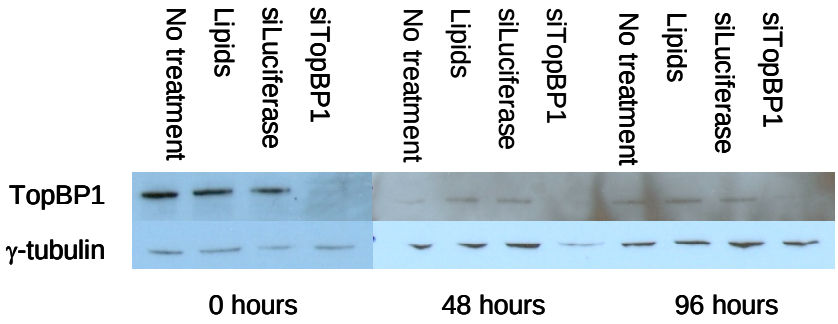

Figure 44 Effect of TopBP1 depletion on the HaCaT cell line

A. Cell Growth Assay of siRNA treated HaCaT cells.

Each experiment was carried out twice and in triplicate. The results shown are the mean of the triplicates and the mean of two experiments +/- S.E.M.

B. TopBP1 expression levels following siRNA treatment.

Cell lysates were harvested at the time points on the Cell Growth Assay as indicated, separated by SDS PAGE gel electrophoresis and the resultant blot probed for TopBP1 with γ-tubulin as a loading control. The Western Blot shown is a representative blot from one of the two experiments.

3.5.2 TopBP1 is not essential for replication in MCF7 cells

As the HaCaT cell line was unable to survive in culture when TopBP1 was depleted, an alternative cell line was required. Previous work in this laboratory has demonstrated that three alternative cell lines are able to grow in the absence of TopBP1, MCF7, U2OS and 293T cells. MCF7 cells are an epithelial cell line derived from a human breast cancer cells and were chosen as the cell line for further work in this chapter.

TopBP1 was depleted in MCF7 cells using siRNA targeted against TopBP1, siRNA-luciferase and mock transfected cells (lipofectamine only) were included as experimental controls. Cell growth in these cells was then measured using a MTT (3-(4,5-Dimethylthiazol-2-yl)-2,5-diphenyltetrazolium bromide) cell viability assay. The MTT assay provides a direct measure of metabolically active cells in culture, the yellow MTT substrate is reduced in the mitochondria of metabolically active cells to form insoluble purple formazan crystals which are then solubilised in DMSO and the absorbance reading at 570nm gives a direct measure of cell viability. The results of the MTT assay are shown in Figure 45 and demonstrate that there was no reduction in cell growth when TopBP1 was depleted compared to siLuciferase and mock transfection controls. Cell lysates were harvested at the same time points as the MTT assay readings were taken, the lysates analysed by Western Blotting and confirmed that the TopBP1 depletion was efficient throughout the duration of the experiment (data not shown). (MTT assay carried out by R.Wright).

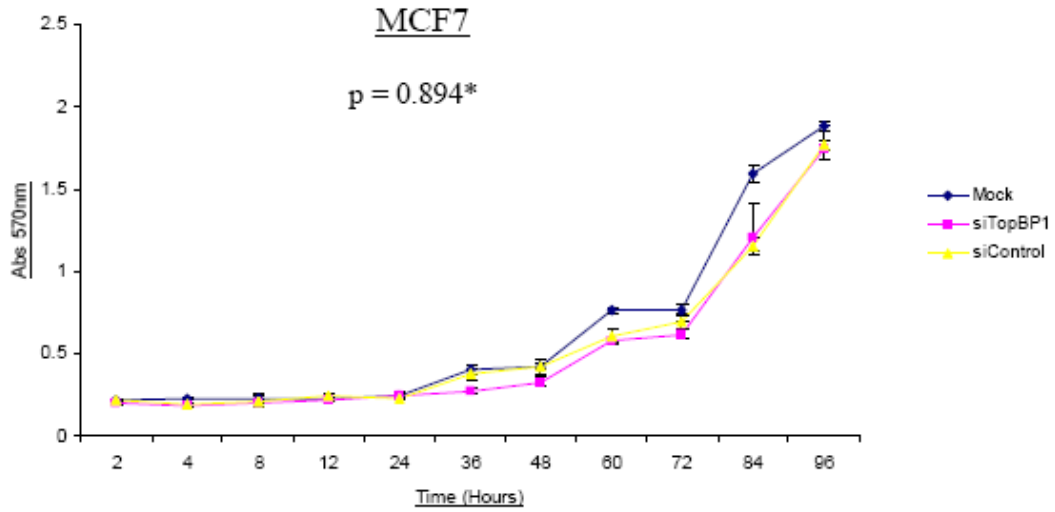

Figure 45 TopBP1 is not essential for cell growth in the MCF7 cell line.

MCF7 cells were treated with siTopBP1, siLuciferase or mock treated and the cell viability assay measure using the MTT assay. The experiment was carried out three times in duplicate and the results show the mean +/- S.E.M for the three experiments. Comparing results for siLuciferase against siTopBP1 using a Student paired T-Test showed there was no significant difference between the growth of siLuciferase and siTopBP1 treated cells (p=0.894) indicating that TopBP1 is not essential for growth in MCF7 cells.

3.5.3 The effect of UVB irradiation and TopBP1 knockdown in the MCF7 cell line.

To determine a dose of UVB which would induce cellular DNA damage in the MCF7 cell line, cells grown in monolayer were irradiated with increasing doses of UVB (2.2.5.7). Total cell lysates were harvested 30 minutes following irradiation and equal amounts of protein separated by SDS-PAGE gel electrophoresis. The resultant Western Blot probed for phosphoChk1 (ser317). As shown in Figure 46A an antibody band is just discernible at 0.002J/cm^2 indicating that this is the minimal dose with which to induce DNA damage in MCF7 cells.

To determine a dose of UVB that would induce DNA damage but allow MCF cells to survive in culture, crystal violet colony survival assays were performed (2.2.5.8). In these assays, carried out three times in triplicate, MCF7 cells grown in monolayer were mock irradiated or irradiated with increasing doses of UVB. Thirty minutes following irradiation, 1000 cells from each experiment were seeded in triplicate. All colonies were visualised with crystal violet 14 days following irradiation and counted. As shown in Figure 46B, when MCF7 cells were treated with 0.002J/cm^2 of UVB, 65% of colonies survived compared with cells that were mock irradiated.

A.

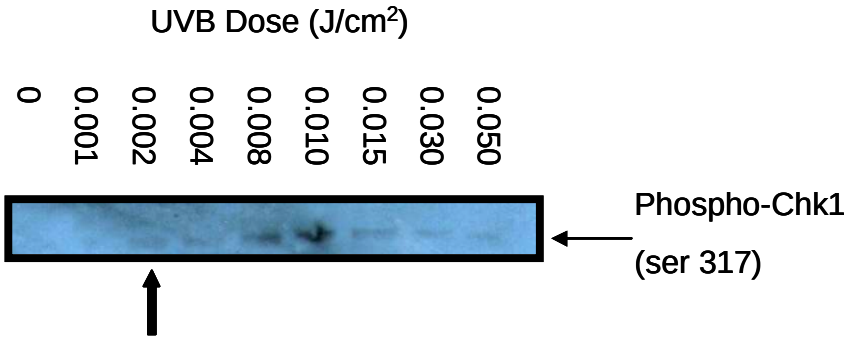

B.

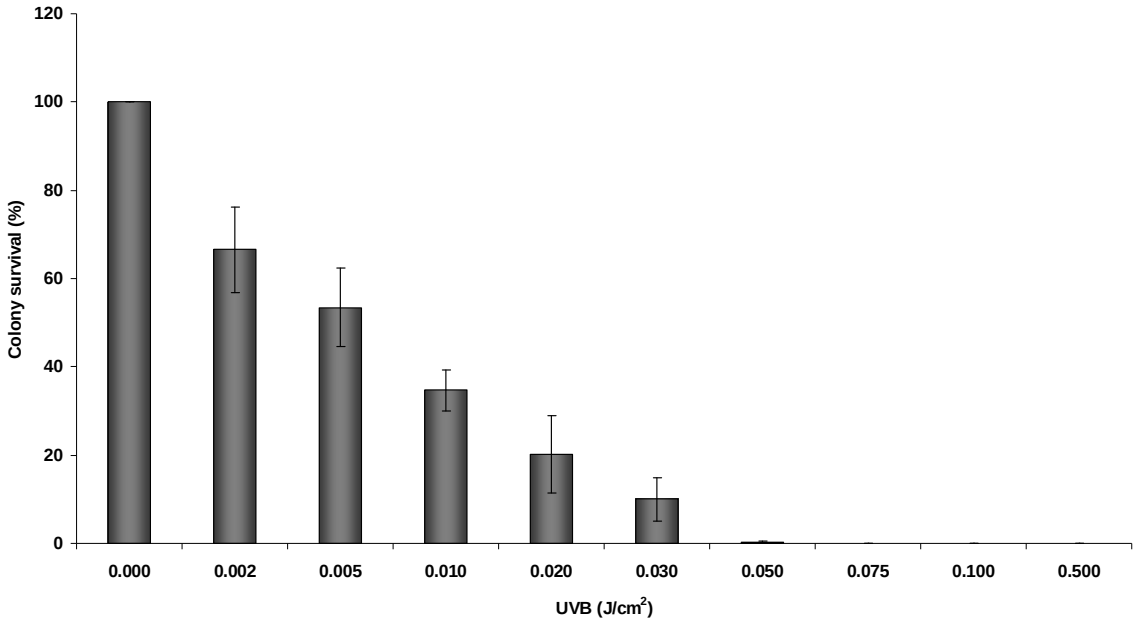

Figure 46 MCF7 cells treated with increasing doses of UVB.

A. Western Blot probed for phospho-Chk1. A faint antibody band is seen following irradiation with 0.002J/cm^2 of UVB.

B. Crystal violet colony survival assay of UVB irradiated MCF7 cells. The number of colonies following irradiation was expressed as percentage survival relative to colonies following mock irradiation only (taken as 100%). The experiment was performed on three occasions in triplicate. The graph shows the mean of three experiments +/- S.E.M.

TopBP1 was depleted in MCF7 cells using siRNA targeted against TopBP1 using the lipofectamine 2000™ transient transfection method (2.2.5.2.2). As before, for all siRNA experiments, untreated, mock transfected (lipofectamine only) and siLuciferase treated cells were included as experimental controls. Seventy two hours following transfection, total cell lysates were harvested, equal amounts separated by SDS-PAGE gel electrophoresis and the resultant Western Blot probed for TopBP1 with γ-tubulin as a loading control. As shown in Figure 47, a greater than 90% knockdown efficiency of TopBP1 was achieved.

A cell growth assay in siRNA treated MCF7 cells was not performed as previous work in this laboratory demonstrated that MCF7 cells are able to grow over a four day period in the absence of TopBP1 (as previously shown in Figure 45).

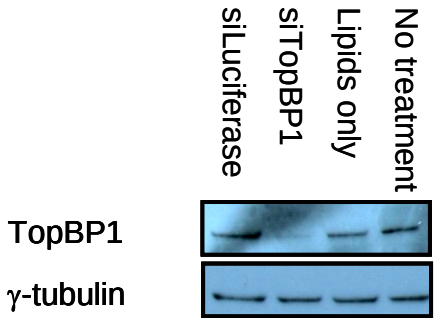

Figure 47 TopBP1 expression levels following siRNA treatment of MCF7 cells.

MCF7 were untreated, mock transfected (lipids only) or siRNA treated with siTopBP1 or siLuciferase. Protein lysates were separated by SDS-PAGE gel electrophoresis and analysed by Western Blotting with antibody directed against TopBP1 and γ-tubulin as loading control.

3.5.4 Experimental design and controls for gene expression microarray.

In order to investigate the genes involved in the cellular UV damage response that are regulated by TopBP1, a gene expression microarray experiment was performed. MCF7 cells were chosen for this experiment as these cells continue to replicate following TopBP1 depletion.

The experimental design is illustrated in Figure 48. Four samples were prepared in tandem and the experiment repeated three times resulting in 12 RNA samples for microarray analysis. MCF7 cells were treated with siLuciferase or siTopBP1 and plated in monolayer. After 48hours, samples were mock irradiated or irradiated with 0.002J/cm^2 of UVB. 30 minutes following UVB irradiation, cells were harvested for RNA using the Qiagen RNAeasy extraction kit as described (2.2.5.10). RNA was prepared in duplicate, one set of samples for microarray analysis and one set stored at -80°C for future use.

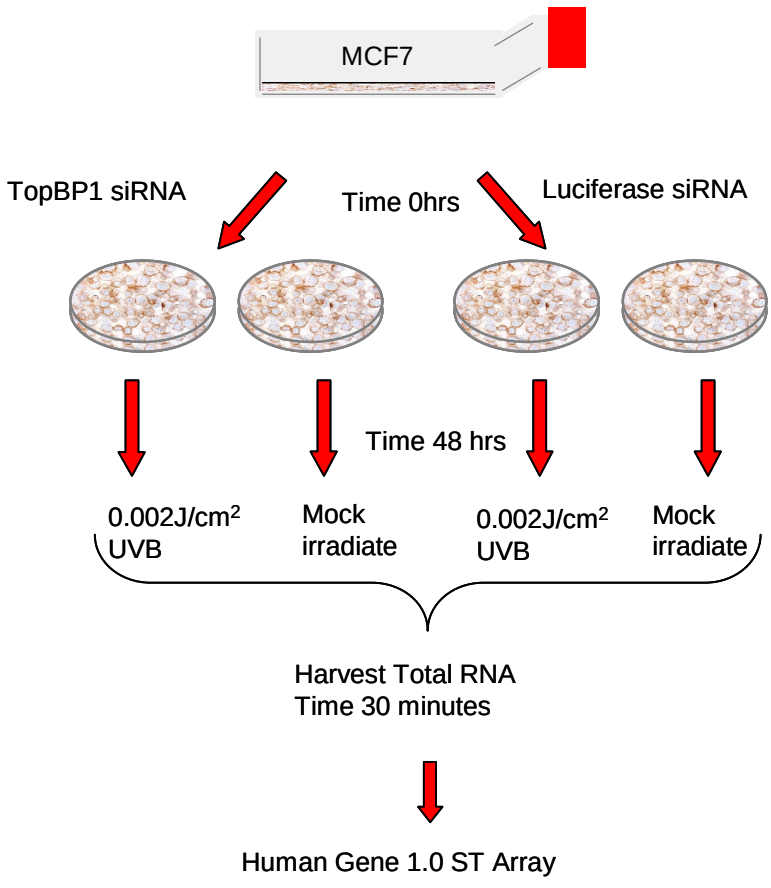

Figure 48 Experimental design of gene expression microarray analysis experiment.

For each experimental repeat, eight extra plates of MCF7 cells were included as experimental controls for determining the efficiency of TopBP1 knockdown (untreated, mock transfected, siLuciferase and siTopBP1). 30 minutes after irradiation or mock irradiation, these plates were harvested for protein as described (2.2.5.3), equal amounts of protein lysate were separated by SDS-PAGE gel electrophoresis and analysed by Western Blotting. The resultant blot was probed for TopBP1 with γ-tubulin as a loading control. These controls were included for each of the three experimental repeats. A single representative Western Blot is illustrated in Figure 49.

There is a clear reduction in TopBP1 expression in siTopBP1 treated cells. siLuciferase had no effect on TopBP1 expression compared to controls (no treatment/mock transfection.

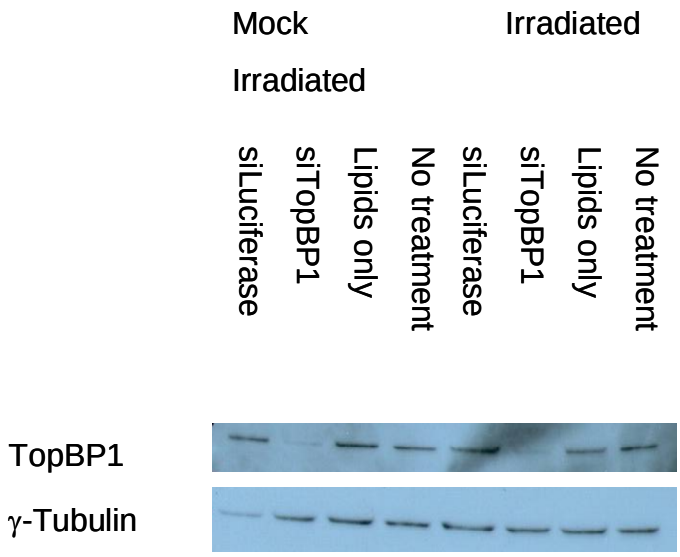

Figure 49 Western Blot showing TopBP1 expression levels in MCF7 cells.

Lysates were harvested at the same time as RNA for the microarray experiment.

3.5.5 RNA quality control

The concentrations and quality of the 12 RNA samples was then further analysed by Julie Galbraith (Sir Henry Welcome Functional genomics Facility (SHWFGF), University of Glasgow) on a 2100 Agilent Bioanalyzer to check the quantity and quality of RNA samples. The RNA concentrations of each sample are shown in Table 17. A summary of the quality control analysis is shown in Figure 50. To be suitable for microarray, the RIN value of the sample should be between 7 and 10.

Sample Name	Concentration of RNA (ng/μl)
6A	179
9A	190
12A	237
15A	179
6B	150
9B	97
12B	109
15B	79
6C	272
9C	257*
12B	129
15B	138

Table 17 RNA concentration of microarray samples.

*** Sample 9C was replaced with a duplicate sample from the same experimental repeat due to degradation of the sample.**

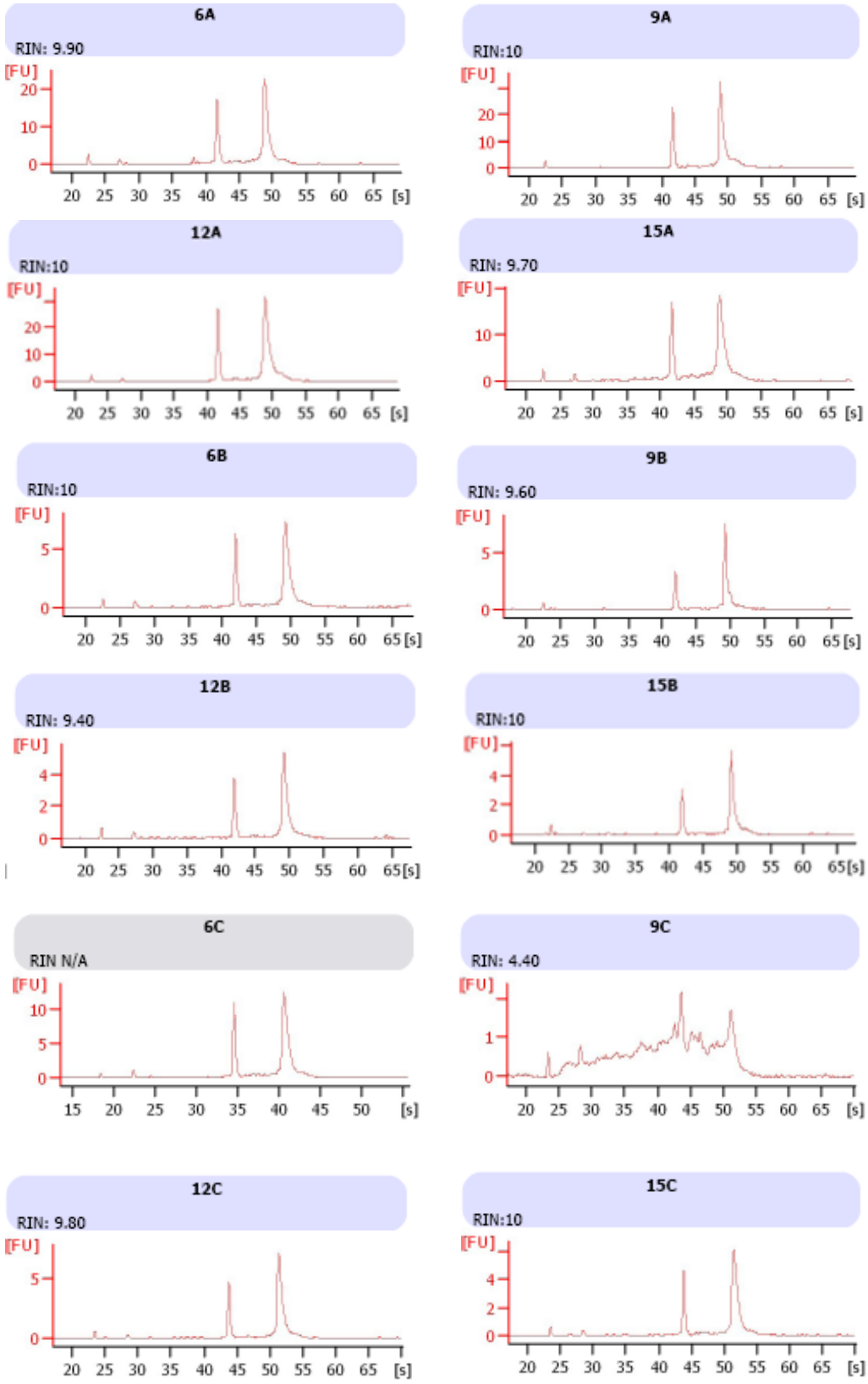

Figure 50 Quality of RNA samples for microarray.

Sample 9C exhibited degradation (RIN 4.40) and was therefore replaced with the duplicate sample from the same repeat. The quality of the duplicate sample was suitable for the microarray (data not shown).

3.5.6 Data analysis and quality controls

The RNA was prepared as described above and the quantity and quality of the RNA assessed as described. cDNA was prepared using the GeneChip® cDNA synthesis and amplification kit (Affymetrix) (Julie Galbraith, SHWFGF).

HuGene-1_0-st-v1 arrays were used for hybridisation and analysis (NetAffx release: 31 (2009-11-16). Hybridisation was performed with Affxmetrix GeneChip® Hybridisation Oven 640, the arrays were washed with Affymetrix fluidic Station 400 and subsequently scanned with the Affxmetrix GeneChip® Scanner 3000 7G.

The raw data in the form of Affxmetrix CEL files were generated with Affymetrix GeneChip® Operating Software (GCOS) and subsequent analysis was carried out with Partek® Genomic Suite™ (Partek Inc., St.Louis, MO, USA) (http://www.partek.com/). This analysis was carried out by Dr Pawel Herzyk, SHWFGF.

Normalization of all 12 chips was done using the GC-RMA (Robust Multichip Average) method (329), to correct the background levels for all probe sets reducing non-specific binding signals. The RNA was prepared in three sets of replicates, prepared on three different occasions. It is assumed that there will be bias between each set of replicates, known as the systematic replicate effect or batch effect. The batch effect was removed by ANOVA allowing all three sets of replicates to be combined and analysed together. Once the batch effect is removed the PCA analysis shows that the TopBP1 wild type and TopBP1 knockdown samples cluster together and both groups can be clearly separated from each other (Figure 51). The PCA analysis also shows that the Control samples (mock irradiated) and Damage samples (UVB irradiated) also cluster together and can be separated however the distinction between this set of samples is less distinct (Figure 52) suggesting that the effect of TopBP1 knock down on the cells is much bigger than the effect of UVB damage.

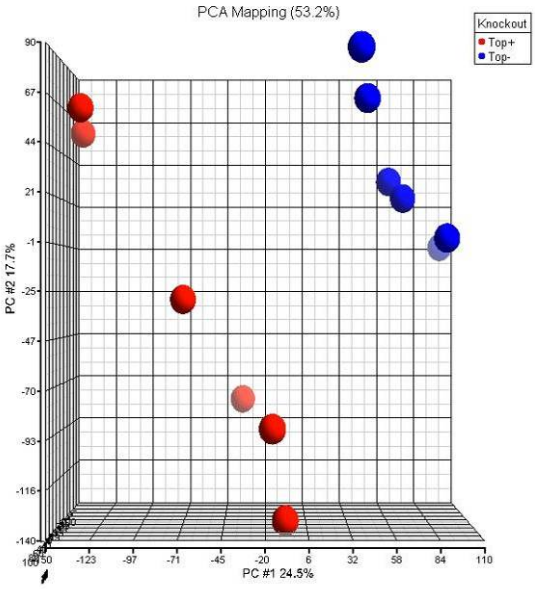

Figure 51 PCA analysis of clustering of TopBP1 wild type samples and TopBP1 knockdown samples following removal of batch effect.

The six TopBP1 wild type samples are represented by the red dots and the six TopBP1 knockdown samples are in blue. There is clear separation between the two groups of samples.

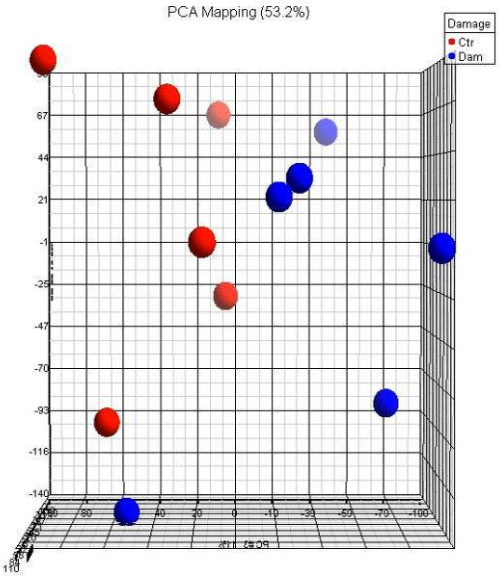

Figure 52 PCA analysis of clustering of mock irradiated (control samples) and UVB treated (Damaged) samples following removal of the batch effect.

The six control samples are represented by the red dots and the six Damage samples are shown in blue. Here it can be seen that there is clustering within each set of samples however the distinction between Control and damage samples is less distinct when compared to the TopBP1 wild type versus TopBP1 knockdown samples shown above suggesting that TopBP1 knockdown produced a greater effect on the cells than UVB irradiation.

3.5.7 Differentially expressed gene sets

Three sets of differentially expressed genes were generated from the microarray data using 2-way ANOVA. Only genes that had a p-value of less than 0.05 were included (confirming reproducibility in the three sets of replicates) and only those in which the change in expression was either increased or decreased 1.5 fold were included. Three lists of differentially expressed genes were generated.

1. Genes de-regulated by the absence of TopBP1 (Table 18).

2. Genes de-regulated by UVR damage (Table 19).

3. Genes de-regulated by UVR damage in the absence of TopBP1 (Table 20).

TABLE 18

18A DOWN REGULATED GENES

Transcript ID	Gene ID// Gene	p-value	Fold
8090772	NM_007027 // TOPBP1 // topoisomerase (DNA) II binding protein 1 // 3q22.1 // 110	6.39E-09	-5.09096
7979658	NM_002083 // GPX2 // glutathione peroxidase 2 (gastrointestinal) // 14q24.1 // 2	2.22E-05	-2.90938
8025429	NM_005968 // HNRNPM // heterogeneous nuclear ribonucleoprotein M // 19p13.3-p13.	1.40E-08	-2.87617
7979204	NM_006832 // FERMT2 // fermitin family homolog 2 (Drosophila) // 14q22.1 // 1097	6.68E-07	-2.61178
8024111	NM_004368 // CNN2 // calponin 2 // 19p13.3 // 1265 /// NM_201277 // CNN2 // calp	6.09E-06	-2.56983
8085033	NM_001136049 // LMLN // leishmanolysin-like (metallopeptidase M8 family) // 3q29	1.00E-06	-2.5537
8150906	NM_017813 // IMPAD1 // inositol monophosphatase domain containing 1 // 8q12.1 //	1.25E-05	-2.48823
7937508	NM_004357 // CD151 // CD151 molecule (Raph blood group) // 11p15.5 // 977 /// NM	3.89E-05	-2.22592
8063835	NM_144703 // LSM14B // LSM14B, SCD6 homolog B (S. cerevisiae) // 20q13.33 // 149	1.71E-05	-2.17166
7996677	NM_005796 // NUTF2 // nuclear transport factor 2 // 16q22.1 // 10204 /// ENST000	9.12E-06	-2.17075
8093826	NM_000683 // ADRA2C // adrenergic, alpha-2C-, receptor // 4p16 // 152 /// ENST00	1.25E-05	-2.16779
8102848	NM_030648 // SETD7 // SET domain containing (lysine methyltransferase) 7 // 4q28	1.03E-07	-2.1253
8150908	NM_017813 // IMPAD1 // inositol monophosphatase domain containing 1 // 8q12.1 //	2.14E-06	-2.11617
8091446	NM_053024 // PFN2 // profilin 2 // 3q25.1-q25.2 // 5217 /// NM_002628 // PFN2 //	4.56E-08	-2.0553
8079966	NM_004636 // SEMA3B // sema domain, immunoglobulin domain (Ig), short basic doma	0.000132646	-1.99527
7952046	NM_144765 // MPZL2 // myelin protein zero-like 2 // 11q24 // 10205 /// NM_005797	5.45E-07	-1.9824
8129071	NM_002031 // FRK // fyn-related kinase // 6q21-q22.3 // 2444 /// ENST00000368626	2.99E-06	-1.97654
8020323	NM_003799 // RNMT // RNA (guanine-7-) methyltransferase // 18p11.22-p11.23 // 87	1.06E-06	-1.95476
8110589	NM_015455 // CNOT6 // CCR4-NOT transcription complex, subunit 6 // 5q35.3 // 574	2.49E-07	-1.94066
7926385	NM_003473 // STAM // signal transducing adaptor molecule (SH3 domain and ITAM mo	9.00E-06	-1.93198
8138466	NM_182762 // MACC1 // metastasis associated in colon cancer 1 // 7p21.1 // 34638	4.71E-06	-1.91981
7913319	NM_003760 // EIF4G3 // eukaryotic translation initiation factor 4 gamma, 3 // 1p	2.20E-07	-1.90524
7915882	NM_014774 // KIAA0494 // KIAA0494 // 1pter-p22.1 // 9813 /// ENST00000371933 //	1.03E-07	-1.87497
7927658	NM_003338 // UBE2D1 // ubiquitin-conjugating enzyme E2D 1 (UBC4/5 homolog, yeast	2.57E-06	-1.87267
8102342	NM_024090 // ELOVL6 // ELOVL family member 6, elongation of long chain fatty aci	0.000327338	-1.86828
8050007	NM_012293 // PXDN // peroxidasin homolog (Drosophila) // 2p25 // 7837 /// ENST00	1.17E-05	-1.86341
7999553	NM_018340 // CPPED1 // calcineurin-like phosphoesterase domain containing 1 // 1	1.23E-06	-1.86206
7931728	NM_015155 // LARP4B // La ribonucleoprotein domain family, member 4B // 10p15.3	2.34E-07	-1.85228
7937612	NM_002458 // MUC5B // mucin 5B, oligomeric mucus/gel-forming // 11p15.5 // 72789	0.00145544	-1.8473
7967149	NM_016237 // ANAPC5 // anaphase promoting complex subunit 5 // 12q24.31 // 51433	2.81E-07	-1.83394
8044499	NM_005415 // SLC20A1 // solute carrier family 20 (phosphate transporter), member	3.61E-07	-1.83069
8068593	NM_005239 // ETS2 // v-ets erythroblastosis virus E26 oncogene homolog 2 (avian)	6.00E-05	-1.82779
8078227	NM_003884 // KAT2B // K(lysine) acetyltransferase 2B // 3p24 // 8850 /// ENST000	6.68E-06	-1.80333
7942896	NM_173556 // CCDC83 // coiled-coil domain containing 83 // 11q14.1-q14.2 // 2200	1.13E-06	-1.80293
8158424	NM_001127244 // LRRC8A // leucine rich repeat containing 8 family, member A // 9	1.31E-07	-1.78651
8042503	NM_002357 // MXD1 // MAX dimerization protein 1 // 2p13-p12 // 4084 /// ENST0000	3.19E-05	-1.78559
7917148	NM_022831 // AIDA // axin interactor, dorsalization associated // 1q41 // 64853	2.33E-06	-1.77011
8002692	NM_006885 // ZFHX3 // zinc finger homeobox 3 // 16q22.3-q23.1 // 463 /// NM_0011	0.000429008	-1.77004
7913655	NM_002167 // ID3 // inhibitor of DNA binding 3, dominant negative helix-loop-hel	1.79E-05	-1.7651
7993478	NM_004996 // ABCC1 // ATP-binding cassette, sub-family C (CFTR/MRP), member 1 //	0.000206196	-1.76493
7951077	NM_144665 // SESN3 // sestrin 3 // 11q21 // 143686 /// ENST00000278499 // SESN3	5.76E-05	-1.75309
8114287	NM_004598 // SPOCK1 // sparc/osteonectin, cwcv and kazal-like domains proteoglyc	8.92E-06	-1.74847
8000948	NM_004765 // BCL7C // B-cell CLL/lymphoma 7C // 16p11 // 9274 /// ENST0000021511	9.98E-06	-1.73895
7931683	NM_014974 // DIP2C // DIP2 disco-interacting protein 2 homolog C (Drosophila) //	5.70E-05	-1.7363
7959102	NM_014365 // HSPB8 // heat shock 22kDa protein 8 // 12q24.23 // 26353 /// ENST00	4.60E-05	-1.72777
8122818	BC011348 // C6orf211 // chromosome 6 open reading frame 211 // 6q25.1 // 79624 /	1.84E-05	-1.72524
8013112	NM_016084 // RASD1 // RAS, dexamethasone-induced 1 // 17p11.2 // 51655 /// ENST0	0.00346768	-1.72474
7948814	NM_001079559 // HNRNPUL2 // heterogeneous nuclear ribonucleoprotein U-like 2 //	7.02E-08	-1.72188
7963353	NM_002281 // KRT81 // keratin 81 // 12q13 // 3887 /// ENST00000327741 // KRT81 /	6.11E-06	-1.72157
8101916	NM_152292 // RG9MTD2 // RNA (guanine-9-) methyltransferase domain containing 2 /	3.03E-05	-1.71802
8095751	NM_015393 // PARM1 // prostate androgen-regulated mucin-like protein 1 // 4q13.3	7.05E-06	-1.71451
8088550	NM_198859 // PRICKLE2 // prickle homolog 2 (Drosophila) // 3p14.1 // 166336 ///	0.000155896	-1.7132
7982597	NM_003246 // THBS1 // thrombospondin 1 // 15q15 // 7057 /// ENST00000260356 // T	1.57E-05	-1.711
8169969	NM_032458 // PHF6 // PHD finger protein 6 // Xq26.3 // 84295 /// NM_001015877 //	2.01E-06	-1.7096
7921970	NM_000696 // ALDH9A1 // aldehyde dehydrogenase 9 family, member A1 // 1q23.1 //	8.58E-06	-1.7088
8009183	NM_203351 // MAP3K3 // mitogen-activated protein kinase kinase kinase 3 // 17q23	0.000165054	-1.70617

TABLE 18 continued

Transcript ID	Gene ID// Gene	p-value	Fold
8116921	NM_001955 // EDN1 // endothelin 1 // 6p24.1 // 1906 /// NM_001168319 // EDN1 //	0.000303041	-1.70393
8144078	NM_000193 // SHH // sonic hedgehog homolog (Drosophila) // 7q36 // 6469 /// ENST	3.35E-05	-1.70162
7958275	NM_018082 // POLR3B // polymerase (RNA) III (DNA directed) polypeptide B // 12q2	1.81E-05	-1.69853
8020308	NM_181481 // C18orf1 // chromosome 18 open reading frame 1 // 18p11.2 // 753 ///	6.20E-05	-1.69795
8172035	NM_006520 // DYNLT3 // dynein, light chain, Tctex-type 3 // Xp21 // 6990 /// ENS	8.18E-05	-1.69675
8140730	NM_024315 // C7orf23 // chromosome 7 open reading frame 23 // 7q21.1-q21.2 // 79	5.36E-06	-1.69438
8105506	NM_020928 // ZSWIM6 // zinc finger, SWIM-type containing 6 // 5q12.1 // 57688 //	3.99E-05	-1.69366
8047127	NM_001130158 // MYO1B // myosin IB // 2q12-q34 // 4430 /// NM_012223 // MYO1B //	5.18E-07	-1.69216
8156770	NM_024642 // GALNT12 // UDP-N-acetyl-alpha-D-galactosamine:polypeptide N-acetylg	0.000111382	-1.6878
8145227	NM_001160036 // RHOBTB2 // Rho-related BTB domain containing 2 // 8p21.3 // 2322	0.000222107	-1.68662
8092541	NM_139248 // LIPH // lipase, member H // 3q27 // 200879 /// ENST00000296252 // L	7.70E-05	-1.68217
7908940	NM_001001396 // ATP2B4 // ATPase, Ca++ transporting, plasma membrane 4 // 1q32.1	0.000132259	-1.68175
8175121	NM_001555 // IGSF1 // immunoglobulin superfamily, member 1 // Xq25 // 3547 /// N	3.02E-07	-1.68148
8089584	NM_015412 // C3orf17 // chromosome 3 open reading frame 17 // 3q13.2 // 25871 //	6.50E-05	-1.67967
7980744	NM_004755 // RPS6KA5 // ribosomal protein S6 kinase, 90kDa, polypeptide 5 // 14q	2.76E-05	-1.67582
7984517	NM_015554 // GLCE // glucuronic acid epimerase // 15q23 // 26035 /// ENST0000026	0.000106967	-1.67182
7938834	NM_182964 // NAV2 // neuron navigator 2 // 11p15.1 // 89797 /// NM_145117 // NAV	2.92E-05	-1.66855
7918913	NM_001542 // IGSF3 // immunoglobulin superfamily, member 3 // 1p13 // 3321 /// N	8.12E-05	-1.66139
8115397	NM_032385 // C5orf4 // chromosome 5 open reading frame 4 // 5q31-q32 // 10826 //	0.000500769	-1.66075
7987405	NM_005739 // RASGRP1 // RAS guanyl releasing protein 1 (calcium and DAG-regulate	4.11E-05	-1.66012
8106122	NM_002270 // TNPO1 // transportin 1 // 5q13.2 // 3842 /// NM_153188 // TNPO1 //	2.36E-06	-1.65862
8017162	NM_016125 // RNFT1 // ring finger protein, transmembrane 1 // 17q23.1 // 51136 /	6.78E-05	-1.65858
8146637	NM_152758 // YTHDF3 // YTH domain family, member 3 // 8q12.3 // 253943 /// ENST0	2.52E-05	-1.65389
8160670	NM_004925 // AQP3 // aquaporin 3 (Gill blood group) // 9p13 // 360 /// ENST00000	0.000299763	-1.65389
8139500	NM_022748 // TNS3 // tensin 3 // 7p12.3 // 64759 /// ENST00000398879 // TNS3 //	0.00013197	-1.65304
8006531	NM_144975 // SLFN5 // schlafen family member 5 // 17q12 // 162394 /// ENST000002	1.42E-05	-1.65039
8091954	NM_014498 // GOLIM4 // golgi integral membrane protein 4 // 3q26.2 // 27333 ///	7.80E-05	-1.64988
7939368	NM_017583 // TRIM44 // tripartite motif-containing 44 // 11p13 // 54765 /// ENST	0.00163902	-1.64891
8007272	NM_025233 // COASY // CoA synthase // 17q12-q21 // 80347 /// NM_001042530 // COA	0.000129145	-1.64236
8057599	NM_006287 // TFPI // tissue factor pathway inhibitor (lipoprotein-associated coa	8.99E-05	-1.63737
8039086	NR_002938 // LOC284379 // solute carrier family 7 (cationic amino acid transport	0.000149906	-1.6356
8149551	NM_015310 // PSD3 // pleckstrin and Sec7 domain containing 3 // 8pter-p23.3 // 2	0.000443744	-1.63477
7897236	NM_003636 // KCNAB2 // potassium voltage-gated channel, shaker-related subfamily	0.000112593	-1.63194
7933619	NM_147156 // SGMS1 // sphingomyelin synthase 1 // 10q11.2 // 259230 /// ENST0000	8.49E-06	-1.62816
7980616	NM_007039 // PTPN21 // protein tyrosine phosphatase, non-receptor type 21 // 14q	0.000428432	-1.62417
7989323	NM_004330 // BNIP2 // BCL2/adenovirus E1B 19kDa interacting protein 2 // 15q22.2	0.000106569	-1.61747
7961489	NM_016312 // WBP11 // WW domain binding protein 11 // 12p12.3 // 51729 /// ENST0	1.23E-05	-1.61495
7929596	NM_032440 // LCOR // ligand dependent nuclear receptor corepressor // 10q24 // 8	4.09E-05	-1.6103
7973962	BC062480 // STELLAR // germ and embryonic stem cell enriched protein STELLA // 1	0.0197989	-1.6096
8085220	NM_133480 // TADA3 // transcriptional adaptor 3 // 3p25.3 // 10474 /// NM_006354	0.000182069	-1.60777
8161945	NM_152573 // RASEF // RAS and EF-hand domain containing // 9q21.32 // 158158 ///	2.89E-05	-1.60603
7932407	NM_001004470 // ST8SIA6 // ST8 alpha-N-acetyl-neuraminide alpha-2,8-sialyltransf	0.000232003	-1.606
8106479	NM_004866 // SCAMP1 // secretory carrier membrane protein 1 // 5q13.3-q14.1 // 9	6.20E-07	-1.6054
7904843	NM_002614 // PDZK1 // PDZ domain containing 1 // 1q21 // 5174 /// NR_003377 // P	6.00E-08	-1.60507
8109428	NR_024084 // SAP30L // SAP30-like // 5q33.2 // 79685 /// NM_024632 // SAP30L //	3.84E-05	-1.59272
7971134	NM_025138 // C13orf23 // chromosome 13 open reading frame 23 // 13q13.3 // 80209	3.47E-05	-1.58922
8024323	NM_138393 // REEP6 // receptor accessory protein 6 // 19p13.3 // 92840 /// ENST0	8.16E-06	-1.58453
7927529	NM_002443 // MSMB // microseminoprotein, beta- // 10q11.2 // 4477 /// NM_138634	0.00183337	-1.58333
8090162	NM_002213 // ITGB5 // integrin, beta 5 // 3q21.2 // 3693 /// ENST00000296181 //	1.49E-05	-1.58276
7928308	NM_019058 // DDIT4 // DNA-damage-inducible transcript 4 // 10pter-q26.12 // 5454	0.0010453	-1.58227
8129562	NM_001901 // CTGF // connective tissue growth factor // 6q23.1 // 1490 /// ENST0	0.00747396	-1.58163
7950447	NM_182969 // XRRA1 // X-ray radiation resistance associated 1 // 11q13.4 // 1435	2.27E-06	-1.5789
8148059	NM_022783 // DEPDC6 // DEP domain containing 6 // 8q24.12 // 64798 /// ENST00000	0.000297358	-1.5773
8170400	ENST00000432041 // FLJ16423 // hypothetical LOC642889 // Xq28 // 642889 /// AK13	7.01E-06	-1.57616
7974387	NM_145251 // STYX // serine/threonine/tyrosine interacting protein // --- // 681	6.69E-06	-1.5758
8008819	NM_001005404 // YPEL2 // yippee-like 2 (Drosophila) // 17q22 // 388403 /// ENST0	0.000790589	-1.5755
7958600	NM_033121 // ANKRD13A // ankyrin repeat domain 13A // 12q24.11 // 88455 /// ENST	5.13E-05	-1.57325
8095009	NM_001040402 // DCUN1D4 // DCN1, defective in cullin neddylation 1, domain conta	7.07E-06	-1.57262
8157125	NM_002874 // RAD23B // RAD23 homolog B (S. cerevisiae) // 9q31.2 // 5887 /// ENS	1.38E-07	-1.57194

TABLE 18 continued

Transcript ID	Gene ID// Gene	p-value	Fold
8040587	NM_014971 // EFR3B // EFR3 homolog B (S. cerevisiae) // 2p23.3 // 22979 /// ENST	3.20E-05	-1.56481
7923489	NM_021633 // KLHL12 // kelch-like 12 (Drosophila) // 1q32.1 // 59349 /// ENST000	4.73E-06	-1.56154
7904082	XM_001716411 // LOC128322 // similar to nuclear transport factor 2 // 1p13.2 //	0.000789383	-1.56154
7912292	NM_032368 // LZIC // leucine zipper and CTNNBIP1 domain containing // 1p36.22 //	4.55E-06	-1.56056
7929932	NM_030929 // KAZALD1 // Kazal-type serine peptidase inhibitor domain 1 // 10q24.	0.000536639	-1.56022
8063814	NM_144703 // LSM14B // LSM14B, SCD6 homolog B (S. cerevisiae) // 20q13.33 // 149	0.000301547	-1.55853
8157264	NM_001860 // SLC31A2 // solute carrier family 31 (copper transporters), member 2	6.24E-05	-1.55772
7927972	NM_004896 // VPS26A // vacuolar protein sorting 26 homolog A (S. pombe) // 10q21	1.13E-05	-1.55754
8035445	NM_005354 // JUND // jun D proto-oncogene // 19p13.2 // 3727 /// ENST00000252818	7.67E-05	-1.55282
8166442	NM_014888 // FAM3C // family with sequence similarity 3, member C // 7q31 // 104	9.16E-05	-1.55254
7926851	NR_024557 // WAC // WW domain containing adaptor with coiled-coil // --- // 5132	0.000220327	-1.55251
7959751	NM_152437 // ZNF664 // zinc finger protein 664 // 12q24.31 // 144348 /// ENST000	0.000102201	-1.55094
8175177	NM_018388 // MBNL3 // muscleblind-like 3 (Drosophila) // Xq26.2 // 55796 /// NM_	8.23E-05	-1.54903
8058091	NM_015265 // SATB2 // SATB homeobox 2 // 2q33 // 23314 /// NM_001172517 // SATB2	2.62E-05	-1.5479
8144802	NM_006207 // PDGFRL // platelet-derived growth factor receptor-like // 8p22-p21.	0.000320649	-1.54771
8136614	NM_018238 // AGK // acylglycerol kinase // 7q34 // 55750 /// ENST00000355413 //	8.11E-06	-1.54738
8121076	NM_006813 // PNRC1 // proline-rich nuclear receptor coactivator 1 // 6q15 // 109	6.48E-05	-1.54362
7944285	NM_001655 // ARCN1 // archain 1 // 11q23.3 // 372 /// NM_001142281 // ARCN1 // a	6.15E-07	-1.54335
7915870	NM_022745 // ATPAF1 // ATP synthase mitochondrial F1 complex assembly factor 1 /	8.92E-05	-1.54078
8168472	NM_000052 // ATP7A // ATPase, Cu++ transporting, alpha polypeptide // Xq13.2-q13	6.59E-06	-1.54052
8132964	NM_015411 // SUMF2 // sulfatase modifying factor 2 // 7q11.1 // 25870 /// NM_001	0.00030698	-1.53773
8151890	NM_033285 // TP53INP1 // tumor protein p53 inducible nuclear protein 1 // 8q22 /	0.000803295	-1.53578
7934979	NM_014391 // ANKRD1 // ankyrin repeat domain 1 (cardiac muscle) // 10q23.31 // 2	0.000539834	-1.5357
7908072	NM_005562 // LAMC2 // laminin, gamma 2 // 1q25-q31 // 3918 /// NM_018891 // LAMC	0.00156595	-1.53398
7946228	NM_000391 // TPP1 // tripeptidyl peptidase I // 11p15 // 1200 /// ENST0000029942	0.00153193	-1.53108
8161192	NM_194328 // RNF38 // ring finger protein 38 // 9p13 // 152006 /// NM_194330 //	5.34E-05	-1.53089
8113073	NM_020801 // ARRDC3 // arrestin domain containing 3 // 5q14.3 // 57561 /// ENST0	1.90E-05	-1.52953
7975779	NM_005252 // FOS // FBJ murine osteosarcoma viral oncogene homolog // 14q24.3 //	0.00494673	-1.52724
8142540	NM_014888 // FAM3C // family with sequence similarity 3, member C // 7q31 // 104	5.36E-05	-1.52709
8110721	NM_024786 // ZDHHC11 // zinc finger, DHHC-type containing 11 // 5p15.33 // 79844	0.0029148	-1.52618
7975344	NM_018375 // SLC39A9 // solute carrier family 39 (zinc transporter), member 9 //	1.03E-05	-1.5248
7903742	NM_000850 // GSTM4 // glutathione S-transferase mu 4 // 1p13.3 // 2948 /// NR_02	0.00153528	-1.52399
8097801	NM_001109977 // FAM160A1 // family with sequence similarity 160, member A1 // 4q	0.000670545	-1.52213
8162744	NM_003389 // CORO2A // coronin, actin binding protein, 2A // 9q22.3 // 7464 ///	0.000264467	-1.52058
8026490	NR_015379 // UCA1 // urothelial cancer associated 1 (non-protein coding) // 19p1	0.00440711	-1.51997
8152845	BC017297 // FAM49B // family with sequence similarity 49, member B // 8q24.21 //	6.58E-06	-1.51677
7966259	NM_016433 // GLTP // glycolipid transfer protein // 12q24.11 // 51228 /// ENST00	0.000473221	-1.51625
7931081	NM_021622 // PLEKHA1 // pleckstrin homology domain containing, family A (phospho	0.000172979	-1.5161
8117120	NM_001546 // ID4 // inhibitor of DNA binding 4, dominant negative helix-loop-hel	0.00515598	-1.5111
8046306	NM_015530 // GORASP2 // golgi reassembly stacking protein 2, 55kDa // 2q31.1-q31	1.55E-06	-1.51069
8067206	BC137482 // CTCFL // CCCTC-binding factor (zinc finger protein)-like // 20q13.31	0.0102587	-1.51022
8098041	NM_018342 // TMEM144 // transmembrane protein 144 // 4q32.1 // 55314 /// ENST000	8.32E-06	-1.50876
8123181	NM_000876 // IGF2R // insulin-like growth factor 2 receptor // 6q26 // 3482 ///	0.000108385	-1.50558
8153497	NM_182706 // SCRIB // scribbled homolog (Drosophila) // 8q24.3 // 23513 /// NM_0	0.00030922	-1.50287
8090866	NR_024400 // ANAPC13 // anaphase promoting complex subunit 13 // 3q22.2 // 25847	0.000121744	-1.50274
7902687	NM_001554 // CYR61 // cysteine-rich, angiogenic inducer, 61 // 1p31-p22 // 3491	0.00781138	-1.50257
7903507	NM_001010883 // FAM102B // family with sequence similarity 102, member B // 1p13	5.10E-06	-1.5003

TABLE 18 continued

18B UP REGULATED GENES

Transcript ID	Gene ID// Gene	p-value	Fold
8154135	NM_004170 // SLC1A1 // solute carrier family 1 (neuronal/epithelial high affinit	1.33E-07	2.3755
8053733	NM_020382 // SETD8 // SET domain containing (lysine methyltransferase) 8 // 12q2	5.08E-08	2.34297
7991777	NM_001008393 // C4orf46 // chromosome 4 open reading frame 46 // 4q32.1 // 20172	0.000231828	2.25829
8107868	NM_020240 // CDC42SE2 // CDC42 small effector 2 // 5q23.3-q31.1 // 56990 /// NM_	8.33E-07	2.09077
8075322	NM_001037666 // GATSL3 // GATS protein-like 3 // 22q12 // 652968 /// CR456449 //	1.13E-05	2.05567
7973433	NM_182908 // DHRS2 // dehydrogenase/reductase (SDR family) member 2 // 14q11.2 /	1.75E-05	2.02608
7959574	NM_020382 // SETD8 // SET domain containing (lysine methyltransferase) 8 // 12q2	3.33E-05	1.97277
8043413	NM_144563 // RPIA // ribose 5-phosphate hosphati A // 2p11.2 // 22934 /// ENST0	2.08E-05	1.96329
7908766	NM_006335 // TIMM17A // translocase of inner mitochondrial membrane 17 homolog A	8.55E-07	1.93699
8114691	NM_003883 // HDAC3 // histone deacetylase 3 // 5q31 // 8841 /// ENST00000305264	1.80E-06	1.8618
8171561	NM_006089 // SCML2 // sex comb on midleg-like 2 (Drosophila) // Xp22 // 10389 //	3.70E-05	1.85549
8103431	NM_001008393 // C4orf46 // chromosome 4 open reading frame 46 // 4q32.1 // 20172	0.000117264	1.85146
8156826	NM_004612 // TGFBR1 // transforming growth factor, beta receptor 1 // 9q22 // 70	8.49E-06	1.84841
8107847	ENST00000334562 // KIAA1024L // KIAA1024-like // 5q23.3 // 100127206	1.06E-05	1.83643
8134091	NM_012129 // CLDN12 // claudin 12 // 7q21 // 9069 /// ENST00000287916 // CLDN12	8.73E-08	1.82784
7996393	NM_001755 // CBFB // core-binding factor, beta subunit // 16q22.1 // 865 /// NM_	6.44E-07	1.82325
8059642	NM_152527 // SLC16A14 // solute carrier family 16, member 14 (monocarboxylic aci	0.00209908	1.82021
8092534	NM_080652 // TMEM41A // transmembrane protein 41A // 3q27.2 // 90407 /// ENST000	8.20E-05	1.79431
8036840	NM_001626 // AKT2 // v-akt murine thymoma viral oncogene homolog 2 // 19q13.1-q1	1.72E-05	1.79034
7998233	NM_021259 // TMEM8A // transmembrane protein 8A // 16p13.3 // 58986 /// ENST0000	1.07E-06	1.78626
8054771	NM_025181 // SLC35F5 // solute carrier family 35, member F5 // 2q14.1 // 80255 /	2.56E-06	1.78541
7925492	NM_014322 // OPN3 // opsin 3 // 1q43 // 23596 /// NM_003679 // KMO // kynurenine	2.96E-05	1.77957
8079346	NM_014016 // SACM1L // SAC1 suppressor of actin mutations 1-like (yeast) // 3p21	3.24E-06	1.77796
8117045	NM_001143942 // RBM24 // RNA binding motif protein 24 // 6p22.3 // 221662 /// NM	3.42E-05	1.76691
8045795	NM_002239 // KCNJ3 // potassium inwardly-rectifying channel, subfamily J, member	2.69E-05	1.76548
7912239	NM_024980 // GPR157 // G protein-coupled receptor 157 // 1p36.23 // 80045 /// EN	7.95E-05	1.75029
7947784	NM_032389 // ARFGAP2 // ADP-ribosylation factor GTPase activating protein 2 // 1	6.98E-06	1.75017
7899737	NM_003757 // EIF3I // eukaryotic translation initiation factor 3, subunit I // 1	5.77E-06	1.7403
8173999	NM_212559 // XKRX // XK, Kell blood group complex subunit-related, X-linked // X	5.03E-05	1.72866
7919591	AB096683 // FAM72D // family with sequence similarity 72, member D // 1q21.1 //	2.18E-06	1.72287
8153201	NM_012154 // EIF2C2 // eukaryotic translation initiation factor 2C, 2 // 8q24 //	2.20E-06	1.71968
7970577	NM_005932 // MIPEP // mitochondrial intermediate peptidase // 13q12 // 4285 ///	3.13E-05	1.71844
8040190	NM_198182 // GRHL1 // grainyhead-like 1 (Drosophila) // 2p25.1 // 29841 /// ENST	4.48E-08	1.70688
7967002	NM_001080855 // PXN // paxillin // 12q24.31 // 5829 /// NM_002859 // PXN // paxi	7.81E-07	1.69777
8117535	NM_021064 // HIST1H2AG // histone cluster 1, H2ag // 6p22.1 // 8969 /// L19778 /	0.00010364	1.69602
8107133	NM_000919 // PAM // peptidylglycine alpha-amidating monooxygenase // 5q14-q21 //	1.27E-05	1.69235
8159220	NM_014279 // OLFM1 // olfactomedin 1 // 9q34.3 // 10439 /// NM_006334 // OLFM1 /	0.000397312	1.68799
7927710	NM_001786 // CDK1 // cyclin-dependent kinase 1 // 10q21.1 // 983 /// NM_033379 /	0.000252271	1.68718
8011275	NM_024086 // METT10D // methyltransferase 10 domain containing // 17p13.3 // 790	6.88E-05	1.65271
7917954	NM_001013660 // FRRS1 // ferric-chelate reductase 1 // 1p21.2 // 391059 /// ENST	0.000112193	1.64623
7999834	NM_015161 // ARL6IP1 // ADP-ribosylation factor-like 6 interacting protein 1 //	4.76E-08	1.64334
8032265	NM_203304 // MEX3D // mex-3 homolog D (C. elegans) // 19p13.3 // 399664 /// NM_0	4.36E-06	1.64321
8027323	NM_033468 // ZNF257 // zinc finger protein 257 // 19q13 // 113835 /// ENST000004	0.00274997	1.63847
8052626	NM_016516 // VPS54 // vacuolar protein sorting 54 homolog (S. cerevisiae) // 2p1	0.000111432	1.63182
8054769	AY427952 // PS1TP4 // HBV preS1-transactivated protein 4 // --- // 414327	0.000536096	1.63178
8042705	NM_006062 // SMYD5 // SMYD family member 5 // 2p13.2 // 10322 /// ENST0000038950	9.22E-06	1.62314
7954077	NM_020853 // KIAA1467 // KIAA1467 // 12p13.1 // 57613 /// ENST00000197268 // KIA	9.58E-05	1.61565
7951614	NM_002716 // PPP2R1B // protein hosphatise 2, regulatory subunit A, beta // 11q	1.27E-07	1.61138
8089072	NM_000097 // CPOX // coproporphyrinogen oxidase // 3q12 // 1371 /// ENST00000264	6.24E-05	1.61112
7914194	NM_014280 // DNAJC8 // DnaJ (Hsp40) homolog, subfamily C, member 8 // 1p35.3 //	0.000491171	1.61012
7946559	NM_001017998 // GNG10 // guanine nucleotide binding protein (G protein), gamma 1	3.72E-05	1.60788
7990269	BC111368 // C15orf59 // chromosome 15 open reading frame 59 // 15q24.1 // 388135	0.000964013	1.60403
7971027	NM_013338 // ALG5 // asparagine-linked glycosylation 5, dolichyl-phosphate beta-	0.000203071	1.60269
8124423	NM_003518 // HIST1H2BG // histone cluster 1, H2bg // 6p21.3 // 8339	0.00124977	1.59843
7985752	NR_026869 // NCRNA00052 // non-protein coding RNA 52 // 15q25.3 // 145978	6.37E-05	1.58282
8039928	AB096683 // FAM72D // family with sequence similarity 72, member D // 1q21.1 //	7.82E-06	1.58218

TABLE 18 continued

Transcript ID	Gene ID// Gene	p-value	Fold
7974366	NM_000956 // PTGER2 // prostaglandin E receptor 2 (subtype EP2), 53kDa // 14q22	0.000189853	1.57839
7904452	AB096683 // FAM72D // family with sequence similarity 72, member D // 1q21.1 //	0.000118303	1.57268
7924888	NM_033445 // HIST3H2A // histone cluster 3, H2a // 1q42.13 // 92815 /// ENST0000	0.00897968	1.56991
8073032	NM_020243 // TOMM22 // translocase of outer mitochondrial membrane 22 homolog (y	3.69E-05	1.56862
8003875	NM_001124758 // SPNS2 // spinster homolog 2 (Drosophila) // 17p13.2 // 124976 //	4.41E-05	1.56603
8146900	NM_001011720 // XKR9 // XK, Kell blood group complex subunit-related family, mem	1.54E-06	1.56537
8073645	NM_015380 // SAMM50 // sorting and assembly machinery component 50 homolog (S. c	8.88E-05	1.5613
8117614	NM_003527 // HIST1H2BO // histone cluster 1, H2bo // 6p22-p21.3 // 8348 /// ENST	0.0131485	1.56068
7909146	AB096683 // FAM72D // family with sequence similarity 72, member D // 1q21.1 //	0.00010545	1.55733
8045974	NM_001178015 // SLC4A10 // solute carrier family 4, sodium bicarbonate transport	0.000839872	1.54946
8107356	NM_152624 // DCP2 // DCP2 decapping enzyme homolog (S. cerevisiae) // 5q22.2 //	5.06E-06	1.54821
7928937	NM_004897 // MINPP1 // multiple inositol-polyphosphate phosphatase 1 // 10q23 //	3.28E-05	1.54749
7961983	NM_016551 // TM7SF3 // transmembrane 7 superfamily member 3 // 12q11-q12 // 5176	1.22E-06	1.54637
8065817	NM_000178 // GSS // glutathione synthetase // 20q11.2 // 2937 /// ENST0000021695	2.46E-05	1.54258
8092177	NM_001146276 // NCEH1 // neutral cholesterol ester hydrolase 1 // 3q26.31 // 575	2.07E-06	1.54218
8034482	NM_001136196 // TNPO2 // transportin 2 // 19p13.2 // 30000 /// NM_001136195 // T	2.47E-05	1.5397
8094278	NM_022346 // NCAPG // non-SMC condensin I complex, subunit G // 4p15.33 // 64151	9.05E-05	1.53822
8005501	NM_001135036 // FAM18B2 // family with sequence similarity 18, member B2 // 17p1	1.61E-05	1.53736
7963577	NM_032840 // SPRYD3 // SPRY domain containing 3 // 12q13.13 // 84926 /// ENST000	4.97E-05	1.53569
7965918	NM_001031701 // NT5DC3 // 5'-nucleotidase domain containing 3 // 12q22-q23.1 //	8.89E-05	1.53552
8068361	NM_006933 // SLC5A3 // solute carrier family 5 (sodium/myo-inositol cotransporte	0.000175137	1.53297
7951422	NM_032424 // KIAA1826 // KIAA1826 // 11q22 // 84437 /// ENST00000301919 // KIAA1	0.000116541	1.53185
7931479	NM_005539 // INPP5A // inositol polyphosphate-5-phosphatase, 40kDa // 10q26.3 //	8.26E-05	1.53091
8135587	NM_001233 // CAV2 // caveolin 2 // 7q31.1 // 858 /// NM_198212 // CAV2 // caveol	1.18E-06	1.5305
7969374	NM_024808 // C13orf34 // chromosome 13 open reading frame 34 // 13q22.1 // 79866	4.55E-05	1.52665
7969626	NM_180989 // GPR180 // G protein-coupled receptor 180 // 13q32.1 // 160897 /// E	2.54E-07	1.52548
8176286	NM_018390 // PLCXD1 // phosphatidylinositol-specific phospholipase C, X domain c	0.000411832	1.52251
7999079	NM_001116 // ADCY9 // adenylate cyclase 9 // 16p13.3 // 115 /// ENST00000294016	4.63E-05	1.51751
7941587	NM_182553 // CNIH2 // cornichon homolog 2 (Drosophila) // 11q13.2 // 254263 ///	3.97E-05	1.51471
7942679	NM_018367 // ACER3 // alkaline ceramidase 3 // 11q13.5 // 55331 /// ENST00000278	1.98E-05	1.51269
7905733	NM_006118 // HAX1 // HCLS1 associated protein X-1 // 1q21.3 // 10456 /// NM_0010	1.29E-06	1.50972
7983811	NM_004855 // PIGB // phosphatidylinositol glycan anchor biosynthesis, class B //	2.20E-05	1.50703
8148124	NM_022045 // MTBP // Mdm2, transformed 3T3 cell double minute 2, p53 binding pro	0.000433133	1.50643
7989501	NM_001218 // CA12 // carbonic anhydrase XII // 15q22 // 771 /// NM_206925 // CA1	8.39E-06	1.50605
7943218	NM_015368 // PANX1 // pannexin 1 // 11q21 // 24145 /// ENST00000227638 // PANX1	7.26E-05	1.50466
8007643	NM_001145080 // C17orf104 // chromosome 17 open reading frame 104 // 17q21.31 //	0.000331352	1.50311
8111220	NM_004934 // CDH18 // cadherin 18, type 2 // 5p15.2-p15.1 // 1016 /// NM_0011676	0.000457046	1.50198
8036351	BC052603 // ZNF850P // zinc finger protein 850 (pseudogene) // 19q13.12 // 34289	3.43E-05	1.50197
8059854	NM_005737 // ARL4C // ADP-ribosylation factor-like 4C // 2q37.1 // 10123 /// ENS	2.11E-05	1.50096

Table 18 Genes down regulated (A) and up regulated (B) by the absence of TopBP1

List of 162 genes that were down regulated and 95 genes that were up regulated in the TopBP1 knockdown cells compared to controls.

TABLE 19

19A DOWN REGULATED GENES

Transcript ID	Gene ID//Gene	p-value	Fold
8165672	L23320 // RFC1 // replication factor C (activator 1) 1, 145kDa // 4p14-p13 // 59	0.0029891	-1.86885
8156571	NR_029665 // MIR27B // microRNA 27b // 9q22.32 // 407019 /// AF043897 // C9orf3	0.017733	-1.64005
8090529	NM_198490 // RAB43 // RAB43, member RAS oncogene family // 3q21.3 // 339122 ///	0.000895159	-1.63546

17B UP REGULATED GENES

Transcript ID	Gene ID//Gene	p-value	Fold
8116921	NM_001955 // EDN1 // endothelin 1 // 6p24.1 // 1906 /// NM_001168319 // EDN1 //	0.000342525	2.08968
8108370	NM_001964 // EGR1 // early growth response 1 // 5q31.1 // 1958 /// ENST000002399	0.00831533	1.99951
7941707	NM_006328 // RBM14 // RNA binding motif protein 14 // 11q13.2 // 10432 /// BC007	0.044985	1.89393
8129562	NM_001901 // CTGF // connective tissue growth factor // 6q23.1 // 1490 /// ENST0	0.00860706	1.87448
8144228	AK094159 // FLJ36840 // hypothetical LOC645524 // --- // 645524	0.0274894	1.8458
7975779	NM_005252 // FOS // FBJ murine osteosarcoma viral oncogene homolog // 14q24.3 //	0.00608993	1.77322
8131263	X58060 // SNORD13P2 // small nucleolar RNA, C/D box 13 pseudogene 2 // 7p22.1 //	0.0476685	1.77105
7955589	NM_002135 // NR4A1 // nuclear receptor subfamily 4, group A, member 1 // 12q13 /	0.0116315	1.76044
7896754	AK290103 // LOC100287934 // similar to hCG2042721 // 1p36.33 // 100287934 /// EN	0.0342072	1.73316
7909990	AK290103 // LOC100287934 // similar to hCG2042721 // 1p36.33 // 100287934 /// EN	0.0348099	1.70884
7938366	BX641032 // WEE1 // WEE1 homolog (S. pombe) // 11p15.3-p15.1 // 7465	0.0214025	1.69439
8053797	ENST00000456556 // LOC400986 // protein immuno-reactive with anti-PTH polyclonal	0.0249957	1.68428
8069511	NR_027270 // C21orf81 // ankyrin repeat domain 20 family, member A3 pseudogene /	0.021898	1.6783
7952451	BC040288 // LOC100130428 // IGYY565 // 11q24.2 // 100130428	0.0488411	1.66138
8138592	AB052759 // TRA2A // transformer 2 alpha homolog (Drosophila) // 7p15.3 // 29896	0.0165506	1.62935
7937612	NM_002458 // MUC5B // mucin 5B, oligomeric mucus/gel-forming // 11p15.5 // 72789	0.0287124	1.56548
8115831	NM_004417 // DUSP1 // dual specificity phosphatase 1 // 5q34 // 1843 /// ENST000	0.00560495	1.53586
7952986	NM_213655 // HSN2 // hereditary sensory neuropathy, type II // 12p13.3 // 378465	0.0302536	1.52215
7938364	BX641032 // WEE1 // WEE1 homolog (S. pombe) // 11p15.3-p15.1 // 7465	0.0273611	1.51529
8149720	NM_004430 // EGR3 // early growth response 3 // 8p23-p21 // 1960 /// ENST0000031	0.0292799	1.50607

Table 19 Genes down regulated (A) and up regulated (B) by UVR damage.

List of three genes that were down regulated and 20 genes that were up regulated in UV irradiated cells compared to controls.

TABLE 20

20A DOWN REGULATED GENES

Transcript ID	Gene ID//Gene	p-value	Fold
8052669	NM_014755 // SERTAD2 // SERTA domain containing 2 // 2p14 // 9792 /// ENST000003	0.0185909	-1.50349

20B UP REGULATED GENES

Transcript ID	Gene ID//Gene	p-value	Fold
8152506	NM_207506 // SAMD12 // sterile alpha motif domain containing 12 // 8q24.12 // 40	0.00430001	1.51212
7985555	NM_024580 // EFTUD1 // elongation factor Tu GTP binding domain containing 1 // 1	0.0290991	1.55648
8116921	NM_001955 // EDN1 // endothelin 1 // 6p24.1 // 1906 /// NM_001168319 // EDN1 //	0.00411235	1.57695
7955589	NM_002135 // NR4A1 // nuclear receptor subfamily 4, group A, member 1 // 12q13 /	0.0269104	1.58396
7967486	NM_025140 // CCDC92 // coiled-coil domain containing 92 // 12q24.31 // 80212 ///	0.00276351	1.59316
7975779	NM_005252 // FOS // FBJ murine osteosarcoma viral oncogene homolog // 14q24.3 //	0.00355786	1.89949
8108370	NM_001964 // EGR1 // early growth response 1 // 5q31.1 // 1958 /// ENST000002399	0.00843497	1.9951

Table 20 Genes down regulated (A) and up regulated (B) by UVR in the absence of TopBP1.

List of one gene down regulated and seven genes up regulated by UVR in the absence of TopBP1.

3.5.8 Analysis of micro-array data

To characterise the microarray data further, the data were analysed with the Ingenuity Pathway Analysis (IPA) software, a web based software application designed to analyse data derived from gene expression microarray analysis and other sources (www.ingenuity.com). IPA is based on the Ingenuity Knowledge Base, which is a repository of biological interactions and functional annotations created from millions of individually modelled relationships between proteins, genes, drugs, and diseases. These modelled relationships are derived from published literature and the Knowledge Base is updated manually on a weekly basis according to strict protocols. IPA is a widely accepted tool that has been widely published in peer reviewed articles.

The three lists of altered genes generated by the microarray analysis were uploaded separately into the IPA software and analysed using the IPA Core Analysis function. The Functional Analysis identifies biological functions and diseases that are significantly represented in the respective gene sets and uses a Fisher's Exact Test to generate p values for significance measurement. The Pathways are known metabolic and signalling pathways compiled from literature analysis.

The biological functions and diseases are listed in the order of significance. The number of differentially expressed genes from the dataset that are involved in each function/disease are listed and the function of that gene described.

3.5.8.1 Pathway analysis of genes altered by the absence of TopBP1

The expression of 257 genes was significantly altered in MCF7 TopBP1 knockdown cells compared to controls (Table 18). The genes listed in Table 18 were analysed for functional gene sets and disease gene sets using the Ingenuity Pathway Analysis (IPA) software and this identified significant changes in 62 different biological functions and diseases.

The ten most significantly altered functions and diseases are illustrated in Figure 53 in order of significance. The genes down or up regulated in each function /disease are listed in Table 21.

The ten most significantly altered functions and diseases shown in Figure 53 tended to involve the highest numbers of differentially expressed genes, however, in this large gene set, a further nine significantly altered functions and diseases were identified, involving eight or more differentially expressed genes. These further nine functions/diseases are illustrated in Figure 54 in order of significance and the genes down or up regulated in each function/disease are listed in Table 22.

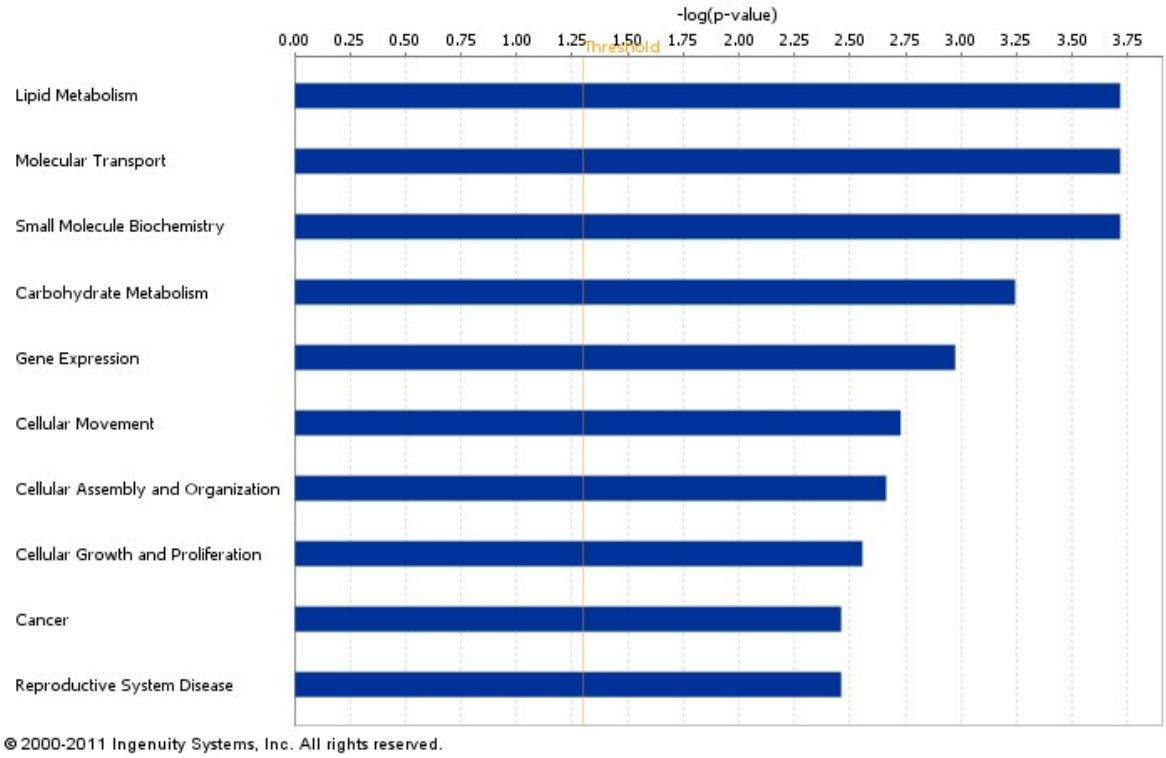

Figure 53 Top ten functions/diseases altered by genes regulated by the absence of TopBP1.

62 diseases/functions were significantly altered in this dataset. The ten most significantly altered are shown here. The threshold for significance (indicated by the orange line) is the log of the p-value 0.05.

Function / Disease	p- values	No. of genes	Altered genes
Lipid Metabolism	1.92E-04-4.34E-02	9	GLTP, LIPH, ACER3, THBS1, ABCC1, PTGER2, AGK, SGMS1, SACM1L
Molecular Transport	1.92E-04-4.11E-02	8	GLTP, TNPO2, ATP7A, THBS1, ABCC1, AGK, ATP2B4, SLC31A2
Small Molecule Biochemistry	1.92E-04-4.34E-02	15	LIPH, MINPP1, THBS1, COASY, ALDH9A1, NUTF2, CDK1, SGMS1, SACM1L, GLTP, ATP7A, ACER3, ABCC1, PTGER2, AGK
Carbohydrate Metabolism	5.71E-04-2.76E-02	6	ATP7A, LIPH, THBS1, ABCC1, AGK, SACM1L
Gene Expression	1.06E-03-4.11E-02	12	FOS, DYNLT3, TADA3, TGFBR1, HDAC3, TOPBP1, PNRC1, ETS2, JUND, DCP2, ID3, CDK1
Cellular Movement	1.87E-03-4.11E-02	16	CNN2, AKT2, PXN, TGFBR1, CTGF, THBS1, HAX1, LAMC2, ID3, CDK1, EDN1, RASGRP1, AGK, CYR61, ITGB5, CD151
Cellular Assembly and Organisation	2.17E-03-4.11E-02	7	CTGF, EDN1, THBS1, CAV2, LAMC2, ITGB5, CDK1
Cellular Growth and Proliferation	2.78E-03-4.87E-02	27	CTGF, TGFBR1, HSPB8, ETS2, GSS, SGMS1, EDN1, PXDN, RHOBTB2, JUND, SEMA3B, ZFHX3, AKT2, THBS1, PFN2, EIF2C2, ID3, HNRNPM, IGF2R, CDK1, FOS, HDAC3, EIF3I (includes EG:8668), ANAPC5, RPS6KA5, PTGER2, CYR61
Cancer	3.46E-03-4.81E-02	**54**	SHH, TGFBR1, CTGF, ABCC1, PXDN, JUND, ITGB5, ZFHX3, SCAMP1, AKT2, TP53INP1, DDIT4, TOPBP1, THBS1, PDGFRL, FERMT2, EIF4G3, SLC1A1, C6ORF211, ELOVL6, MEX3D, KAT2B, PSD3, HDAC3, C18ORF1, PTGER2, CYR61, TFPI, MSMB, PTPN21, CD151, HAX1, HSPB8, AQP3, ARL4C, EDN1, PNRC1, MXD1, RHOBTB2, LIPH, PXN, MIPEP, EIF2C2, OLFM1, LAMC2, UBE2D1, SLC5A3, IGF2R, CDK1, FOS, GPX2, ADRA2C, PPP2R1B, ID4
Reproductive System Disease	3.46E-03-4.11E-02	23	PXN, AKT2, TGFBR1, CTGF, DDIT4, TOPBP1, THBS1, FERMT2, HSPB8, C6ORF211, ELOVL6, FOS, PSD3, HDAC3, EDN1, PNRC1, RHOBTB2, PXDN, ADRA2C, JUND, PTGER2, CYR61, PPP2R1B

Table 21 List of altered genes in the top ten functions/diseases illustrated in Figure 53.

Top ten biological functions/diseases altered by genes de-regulated by the absence of TopBP1. Genes which were up regulated are shown in red, down regulated genes are shown in blue. The diseases/functions in which TopBP1 (always down regulated in this dataset) was involved are highlighted in yellow.

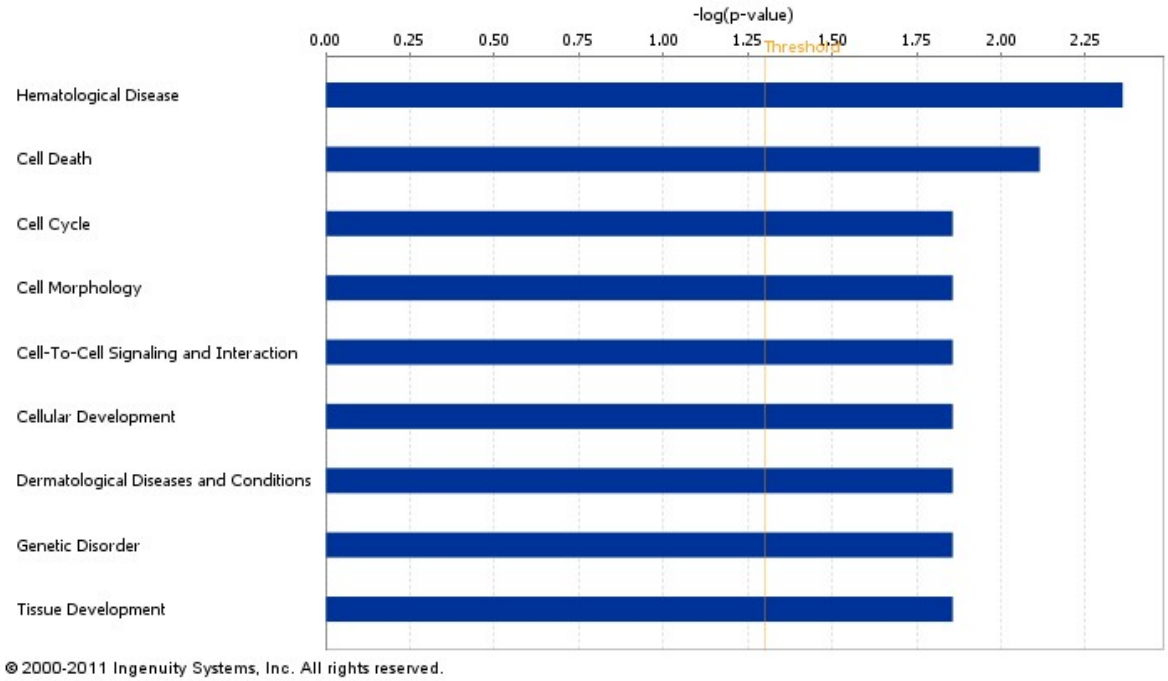

Figure 54 Further functions/diseases altered by genes de-regulated by the absence of TopBP1.

A further nine functions/diseases in which more than 8 altered genes were involved are illustrated. The threshold for significance (indicated by the orange line) is the log of the p-value 0.05.

Function / Disease	p- values	No. of genes	Altered genes
Haematological Disease	4.36E-03-2.81E-02	19	AKT2, CTGF, THBS1, HAX1, UBE2D1, GSS, CDK1, NUTF2, HDAC3, EDN1, ABCC1, PXDN, ADRA2C, PTGER2, TFPI, LRRC8A, ID4, ITGB5, CD151
Cell Death	7.68E-03-3.39E-02	28	CNN2, SHH, CTGF, HSPB8, ETS2, SGMS1, AQP3, TADA3, EDN1, ABCC1, RHOBTB2, CBFB, SEMA3B, ITGB5, RAD23B, DEPDC6 (includes EG:64798), AKT2, TP53INP1, TOPBP1, THBS1, IGF2R, CDK1, BNIP2, FOS, ANKRD1, HDAC3, GPX2, CYR61
Cell Cycle	1.39E-02-4.11E-02	8	EDN1, THBS1, GORASP2, ANAPC5, AGK, ID3, CDK1, ZFHX3
Cell Morphology	1.39E-02-4.11E-02	8	SLC20A1, AQP3, AKT2, EDN1, THBS1, CDC42SE2, VPS26A, CD151
Cell-To-Cell Signalling and Interaction	1.39E-02-4.36E-02	14	PXN, AKT2, CTGF, THBS1, IGSF1, MPZL2, KCNAB2, LAMC2, RASGRP1, SEMA3B, SPOCK1, CYR61, ITGB5, CD151
Cellular Development	1.39E-02-4.11E-02	17	SHH, AKT2, CTGF, THBS1, HSPB8, ETS2, IGF2R, SGMS1, CDK1, FOS, HDAC3, EDN1, RHOBTB2, CDC42SE2, PTGER2, CYR61, CD151
Dermatological Diseases and Conditions	1.39E-02-4.81E-02	8	SHH, LIPH, HDAC3, GPX2, SLC1A1, KRT81 (includes EG:3887), CDK1, CD151
Genetic Disorder	1.39E-02-4.11E-02	10	SHH, LIPH, CTGF, TGFBR1, THBS1, TPP1, RPIA, LRRC8A, KRT81 (includes EG:3887), CD151
Tissue Development	1.39E-02-4.36E-02	12	AKT2, PXN, CTGF, THBS1, RASGRP1, IGSF1, MPZL2, CYR61, SPOCK1, LAMC2, ITGB5, CD151

Table 22 List of altered genes in the functions/diseases illustrated in Figure 54.

Further nine biological functions/diseases altered by genes de-regulated by the absence of TopBP1. Genes which were up regulated are shown in red, down regulated genes are shown in blue. The diseases/functions in which TopBP1 (always down regulated in this dataset) was involved are highlighted in yellow.

3.5.8.2 Pathway analysis of genes de-regulated by UV damage

The expression of 23 genes was significantly altered in MCF7 cells following UV damage compared to controls (Table 19). The genes listed in Table 19 were analysed for functional gene sets and disease gene sets using the Ingenuity Pathway Analysis (IPA) software and this identified significant changes in 50 different biological functions and diseases.

The ten most significantly altered functions and diseases are illustrated in Figure 55 in order of significance. The genes down or up regulated in each function /disease are listed in Table 23.

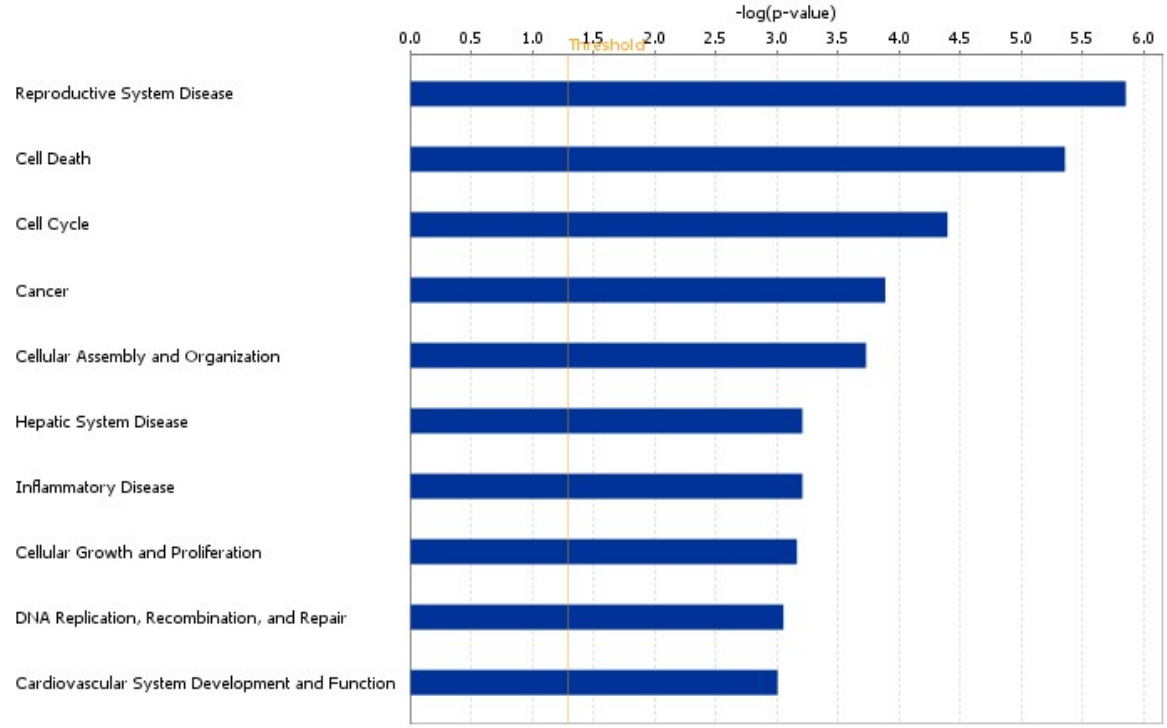

Figure 55 Top ten functions/diseases altered by genes de-regulated by UVR.

50 diseases/functions were significantly altered in this dataset. The ten most significantly altered are shown here. The threshold for significance (indicated by the orange line) is the log of the p-value 0.05.

Function / Disease	p- values	No. of genes	Altered genes
Reproductive System Disease	1.39E-06-2.14E-02	7	FOS, CTGF, EDN1, DUSP1, WEE1, EGR1, NR4A1
Cell Death	4.37E-06-4.98E-02	7	FOS, CTGF, EDN1, DUSP1, EGR1, WEE1, NR4A1
Cell Cycle	4E-05-2.23E-02	5	FOS, EDN1, DUSP1, WEE1, NR4A1
Cancer	1.29E-04-2.14E-02	9	TRA2A, FOS, CTGF, EDN1, DUSP1, WEE1, EGR1, WNK1, NR4A1
Cellular Assembly and Organization	1.85E-04-2.23E-02	3	CTGF, EDN1, RFC1
Hepatic System Disease	6.15E-04-2.38E-03	2	CTGF, NR4A1
Inflammatory Disease	6.15E-04-2.71E-02	4	FOS, CTGF, WNK1, NR4A1
Cellular Growth and Proliferation	6.81E-04-3.47E-02	7	TRA2A, FOS, CTGF, EDN1, WEE1, EGR1, NR4A1
DNA Replication, Recombination, and Repair	8.79E-04-2.28E-02	5	FOS, EDN1, DUSP1, NR4A1, RFC1
Cardiovascular System Development and Function	9.8E-04-3.19E-02	2	EDN1, NR4A1

Table 23 List of altered genes in the top ten functions/diseases illustrated in Figure 55.

Top ten biological functions/diseases altered by genes de-regulated by UVR. Genes which were up regulated are shown in red, down regulated genes are shown in blue.

3.5.8.3 Pathway analysis of genes de-regulated by UV damage in the absence of TopBP1

The expression of eight genes was significantly altered in MCF7 TopBP1 knockdown cells following UV damage compared to controls (Table 20). The genes listed in Table 20 were analysed for functional gene sets and disease gene sets using the Ingenuity Pathway Analysis (IPA) software and this identified significant changes in 45 different biological functions and diseases.

The ten most significantly altered functions and diseases are illustrated in Figure 56 in order of significance. The genes down or up regulated in each function /disease are listed in Table 24.

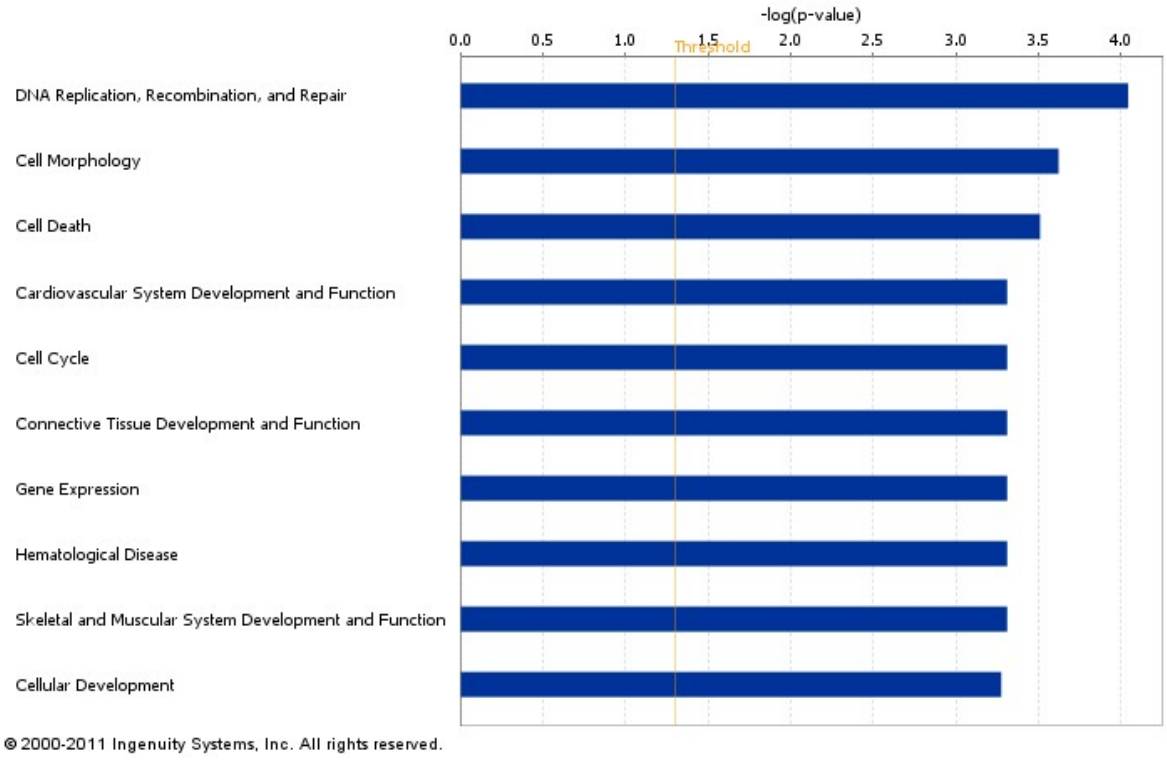

Figure 56 Top ten functions/diseases altered by genes de-regulated by UVR in the absence of TopBP1.

45 diseases/functions were significantly altered in this dataset. The ten most significantly altered are shown here. The threshold for significance (indicated by the orange line) is the log of the p-value 0.05.

Function / Disease	p- values	No. of genes	Altered genes
DNA Replication, Recombination, and Repair	9.08E-05-6.84E-03	3	FOS, EDN1, NR4A1
Cell Morphology	2.4E-04-1.61E-02	2	EDN1, NR4A1
Cell Death	3.1E-04-4.99E-02	4	FOS, EDN1, EGR1, NR4A1
Cardiovascular System Development and Function	4.9E-04-2.62E-02	2	EDN1, NR4A1
Cell Cycle	4.9E-04-2.8E-02	3	FOS, EDN1, NR4A1
Connective Tissue Development and Function	4.9E-04-2.94E-03	1	EDN1
Gene Expression	4.9E-04-2.19E-02	2	FOS, EGR1
Haematological Disease	4.9E-04-4.9E-04	1	EDN1
Skeletal and Muscular System Development and Function	4.9E-04-2.71E-02	2	FOS, EDN1
Cellular Development	5.32E-04-3.24E-02	4	FOS, EDN1, EGR1, NR4A1

Table 24 List of altered genes in the top ten functions/diseases illustrated in Figure 56.

Top ten biological functions/diseases altered by genes de-regulated by UVR in the absence of TopBP1. Genes which were up regulated are shown in red, down regulated genes are shown in blue.

3.5.9 Discussion

3.5.9.1 Summary of Experimental Design

The results in Chapter 3.5 have shown that the HaCaT cell line was unable to grow in the absence of TopBP1. This is in keeping with previously published results suggesting that TopBP1 is essential for cell growth and replication on cultured cells (330). However, previous work in this laboratory had shown that TopBP1 was essential for growth in the MRC5 and HeLa cell lines but the 293T, MCF7 and U2OS cell lines were able to survive in culture for a four day period following knockdown of TopBP1 (R. Wright, unpublished data).

The MCF7 cell line was chosen for these experiments and it was demonstrated that DNA damage could be induced in this cell line following irradiation with 0.002J/cm^2 of UVB (Figure 46). Furthermore, the results demonstrate that TopBP1 could be efficiently knocked down in MCF7 cells by siRNA as shown in Figure 47.

3.5.9.2 Microarray Results

3.5.9.2.1 Genes de-regulated by the absence of TopBP1

The list of genes altered in the absence of TopBP1 and the biological functions/diseases in which they are involved highlight the functions that TopBP1 is known to be involved in.

In the 19 altered biological functions/ diseases listed in Figures 53 and 54, TopBP1 has already been shown to have a role in six of them including cancer, cellular growth and proliferation, gene expression, reproductive system disease, cell death and cell cycle.

Cancer: TopBP1 is known to be involved in cancer, particularly breast cancer. TopBP1 protein has been shown by immunohistochemistry to be aberrantly expressed in a significant number of breast cancers compared to normal breast tissue controls (248) and, in a separate study, those with over expression of TopBP1 were shown to have a more aggressive breast cancer phenotype and reduced survival (331) . A heterozygous Arg309Cys variant in the TopBP1 gene

has been associated with a slightly elevated risk for familial breast and/or ovarian cancer (249).

Cell Growth and Proliferation: TopBP1 is involved in cellular DNA replication. TopBP1 interacts with DNA polymerase ε, a polymerase essential for DNA replication and repair (250). TopBP1 monitors the replication; TopBP1 is essential for an intact S phase an displays a key role in monitoring genome integrity throughout S phase(260). Furthermore, TopBP1 recruits the replication pre-initiation complex to chromatin (330).

The seventh and eighth BRCT domains of TopBP1 interact with the DNA binding domain of p53 leading to inhibition of p53 promoter binding activity. By actively repressing p53, TopBP1 keeps p53 at a low level under physiological conditions and allows a normal G1/S transition. However, over expression of TopBP1 leads to inhibition of p53 target gene expression and therefore inhibition of p53 mediated apoptosis and G1 arrest as a response to DNA damage (331). Therefore through its interaction with p53, TopBP1 appears to be essential for normal cell growth and proliferation however aberrant expression of TopBP1 may enhance DNA damage and contribute to the malignant phenotype by inhibition of p53.

TopBP1 is involved in cell growth and proliferation via its involvement in the DNA damage/repair response. TopBP1 is recruited to sites of DNA damage (250) possibly by direct interaction with damaged DNA (247) and/or via recruitment by Rad9 (251;252). TopBP1 signals the detection of DNA damage by interacting with the ATR/ATRIP complex thus activating ATR and allowing phosphorylation of downstream targets of ATR such as Chk1(253-257).

Gene Expression: TopBP1 is a transcriptional regulator, it can regulate the transcription of p53 as described above (331) and is a transcriptional repressor of E2F1 (262). The sixth BRCT domain on TopBP1 interacts with the amino terminus of E2F1 by recruiting Brg1/Brm chromatin-remodelling complex (263). TopBP1 mediated repression of E2F1 is crucial in the control of E2F1 dependent apoptosis during normal cell growth and DNA damage (263).

Reproductive System Disease: TopBP1 is involved in reproductive system disease via its involvement in both breast and ovarian cancers as described earlier. TopBP1 has also been shown to be an interacting partner with HPV-16 E2

(219) and thus may be included in this disease gene set through its potential involvement in the HPV infection and the pathogenesis of cervical cancer**.**

Cell Death: TopBP1 is known to be involved in cell death through its interactions with the p53 regulated apoptotic pathway as described above. Furthermore it has been shown that SiTopBP1 treated cells arrest at G1(330).

Cell Cycle: As described above, TopBP1 is known to be involved in the regulation of the cell cycle via its interaction with E2F1.

3.5.9.2.2 Genes de-regulated by UVR

UV induces dimerization of adjacent pyrimidines on DNA to form cyclobutane pyrimidine dimers (CPD) and 6-4 pyrimidone photoproducts (6-4PP). UVB induces characteristic mutations at di-pyrimidine sites (C to T transitions) and these UVB signature mutations have been detected in p53 genes from SCC (3). UVB induced DNA damage activates the DNA damage response pathway as damage is sensed by the phosphoinositide 3 kinase (PI3K) related proteins kinases (PIKKs) including ATM (ataxia telangiectasia mutated) and ATR (ATM and RAD3 related). ATM and ATR are the major regulators of the DNA damage response pathway and act to phosphorylate downstream targets that regulate the cell cycle, DNA replication, DNA repair and apoptosis (reviewed in (258;332)).

Five of the top ten altered biological functions/diseases identified with this gene set by the IPA analysis were the main functions/diseases that we would expect UV to be involved in, namely cell death, cell cycle, cancer, cellular growth and proliferation and DNA replication, recombination and repair.

The list of differentially expressed genes induced by UVR damage contained only 23 genes. The relatively small gene number observed in this study may be due to the UV dose that was utilised to damage cells. We used a low UV dosage system, designed to induce DNA damage, as shown by induction of phosphorylated Chk1 but a dose that would allow cell survival, essential to allow for the microarray analysis. Furthermore, cells were harvested 30 minutes following UV irradiation and while it is anticipated that this would be sufficient time to allow for UVR induced changes in gene expression, it is conceivable that a longer period of

time between UV treatment and cell harvesting may have generated a larger number of altered genes.

3.5.9.2.3 Genes de-regulated by UVR in the absence of TopBP1.

The final set of differentially expressed genes, genes de-regulated by UVR in the absence of TopBP1 contained only eight significantly altered genes.

UV induced DNA damage activates the DNA damage response pathway primarily through activation of ATR (reviewed in (258;332)). TopBP1 interacts with the ATR-ATRIP complex, activating ATR and allowing phosphorylation of downstream targets such as Chk1 (253-257). The small number of differentially expressed genes in this gene set may be due to lack of TopBP1 and therefore reduced activation of ATR and its downstream targets.

There were three genes up regulated by UVR both in the presence and absence of UVR: EGR1, FOS and NR4A1 – suggesting that these genes are regulated by UVR independently of TopBP1.

Chapter 4: Discussion

4.1. Conclusions, Summary and Future Prospects

The scope of work carried out in this thesis ranges from a clinical and epidemiological study through two investigations utilising patient samples, finishing with two molecular experimental chapters. For this reason, the findings have been discussed in detail at the end of each results chapter.

Chapter 3.1 describes the results of a clinical and epidemiological study of the West of Scotland renal transplant population. Chapters 3.2 and 3.3 describe two investigations utilising tissue samples from this population, firstly by HPV genotyping the samples and secondly examining the same samples by immunohistochemistry to determine expression of cell cycle biomarkers.

The study of the epidemiology of NMSC in the West of Scotland renal transplant population is the largest study of this kind to be carried out in Scottish RTRs. The results demonstrated that the incidence of nonmelanoma skin cancer in our population was lower than that seen in other geographical areas with higher UV exposure such as Australia and interestingly was also lower than that previously reported in other areas of the UK. The results also demonstrate a different pattern of skin cancer with a change in the BCC:SCC ratio but no reversal, a finding that has been reported infrequently from other studies from Southern Europe but not from the UK (30;31). It will be interesting to determine whether this pattern changes with continued follow up of this cohort over time. The data also demonstrate that with changing immunosuppressive regimes such as introduction of ciclosporin and the move from dual to triple therapy, duration of time between transplantation and the development of a first skin cancer has shortened. While this largely retrospective data must be interpreted with caution, the results are in keeping with what is currently known about immunosuppressants and skin cancer risk. With the advent of newer immunosuppressants such as the mTORi it may be that skin cancer incidences fall although other factors that tend towards increased skin cancer incidences such as older age at transplantation and longer duration of graft survival are likely to increase. In our population there were too few patients currently on mTORi to establish if these newer agents have led to a reduced incidence of skin cancer in our population and continued prospective collection of data is necessary to address this question.

A skin cancer database intrinsically linked to the renal patient electronic record has been established along with a vital clinical service which has achieved the objectives of providing rapid access to Dermatology services to RTRs in the West of Scotland and establishing links with renal and transplant medicine. Ongoing prospective data collection will facilitate future research in this population.

From this clinical and epidemiological study an investigation was carried out utilising patient samples from this population. Normal skin and skin cancers samples were collected and examined for the presence of betaPV. This investigation utilised a novel technique for examining for all betaPV types and this technique has since been widely used for studies of betaPV prevalence in both IC and IS patients. Use of a single technique across studies may allow more accurate comparisons of betaPV prevalence between studies, an important factor in determining whether any single type(s) of betaPV prevails in NMSC. Our study identified betaPV presence in 47.1% of paraffin-embedded tissue samples and 18.2% of normal skin samples. This may add support to the literature that suggests betaPV has a role in NMSC. The detection of betaPV in our samples was lower than we had anticipated. Emerging studies using this technique have detected betaPV in 80-90% of samples. Our lower detection rates may reflect the use of archival material where the quality of the DNA extracted may be poorer quality and more difficult to amplify. A higher prevalence of betaPV was present in frozen tissue (84.6% of skin cancers and 57.1% of normal skin samples) suggesting that the use of frozen tissue would be optimal.

BetaPV carriage is ubiquitous and detection of betaPV DNA in normal skin and skin cancers in both immunocompetent and immunosuppressed populations using many detection methods including the PCR-RHA assay has failed to establish a hierarchy of risk for different betaPV types and their relationship to cutaneous SCC. Another approach to investigate the relationship between betaPV and NMSC is to measure betaPV antibodies in the sera of NMSC cases and controls. Serological responses to betaPV may suggest a clinically significant past or present infection whereas detection of betaPV DNA may be a reflection of the ubiquitous nature of betaPV DNA and not represent active infection. Conversely, it is possible that development of an SCC may lead to a positive serological response as could a cancer related event such as severe sunburn, a concept known as reverse causality. The factors which predict a serological response to

betaPV are not known and therefore the significance of positive serology is not well defined. Recently a study combined both approaches; DNA detection, utilising the skin beta HPV prototype research assay (Diassay BV, Rijswijk, The Netherlands) to detect betaPV DNA in eyebrow hairs and multiplex serology to detect antibody responses. Using concordant DNA detection and antibodies, this study identified a significant association HPV-36 infection and cutaneous SCC in OTRs and a trend towards positive associations for HPV-5, -9 and -24(117). It may have been helpful to incorporate serology into the investigation described in this thesis. Future large epidemiological studies utilising this combined approach may be helpful in determining the association between betaPV and SCC.

In this investigation, a wide spectrum of betaPV genotypes were isolated, the most common types being HPV-24,-36, -38, -15, -5 and -80 but no one type predominated in keeping with the current literature. The body of evidence suggesting that betaPV is important in cutaneous carcinogenesis is increasing but a causal link has not yet been established. We hypothesised that one way to establish a link between HPV and NMSC would be to examine the genotyped lesions by immunohistochemistry to determine if there were differences in biomarker expression between HPV positive and HPV negative lesions. Such differences have been observed in HPV positive and negative cervical lesions. The results of this part of the investigation are described in Chapter 3.3. We examined the expression of a number of biomarkers (Ki67, MCM2, MCM5, p53 and P16) and found them to be over-expressed in comparison to normal skin however there was no relationship between the expression of any of these markers and the presence or absence of HPV. It may be that the number of lesions examined (100) was too small to detect any differences between the two groups or it is possible that only infection with certain betaPV types would alter biomarkers expression and to determine this larger sample numbers would be required. Furthermore, whereas in cervical lesions, altered expression of biomarkers relates to disease state and HPV status, in skin lesions, biomarkerexpression, in particular p53 and p16, may also be altered by the effects of UVR thus making linking interpretation of staining patterns to HPV increasingly complex. Had alternative antibodies such as Bak been available they would have been a preferable biomarker to p53.

A novel marker, TopBP1 was included in the panel of biomarkers examined. TopBP1 expression was investigated because aberrant expression of TopBP1 protein has been demonstrated in breast cancers and polymorphisms in the TopBP1 gene have been identified in a sub-set of familial breast and ovarian cancers. TopBP1 expression in other cancer types has not been previously investigated. TopBP1 is a DNA damage response protein that is essential for signalling DNA damage following UVR. Therefore aberrant expression of TopBP1 in skin might compromise the cells ability to respond to UV damage thus contributing to carcinogenesis. Furthermore, TopBP1 is an interacting partner for HPV16 E2. For these reasons we wished to determine if the expression of TopBP1 differed between HPV positive and negative skin cancers. The results showed that TopBP1 expression was aberrant in a sub-set of skin cancers; however there was no association with presence or absence of betaPV. Aberrant TopBP1 expression in NMSC is a novel finding however the determining factor for this was not identified. A larger sample number would be required to determine whether it was related to infection with specific betaPV types.

From this novel finding of aberrant TopBP1 expression in skin cancers, a molecular study of TopBP1 and its interaction with HPV was carried out. This was first performed with HPV 16 and the work extended to the betaPV HPV-8. The final two experimental chapters focused on TopBP1, its interaction with HPV and role in UVR induced DNA damage.

HPV replication is a possible therapeutic target that could be utilised for the development of anti-viral therapies. TopBP1 interacts with HPV-16E2 and with HPV-16E1. We hypothesised that viral DNA replication occurs via direct recruitment of TopBP1 to the E1-E2 complex resulting in DNA polymerase loading and initiation of viral DNA replication.

The amino acid at residue 90 on the E2 protein is highly conserved across HPV types; however previous studies have not demonstrated a phenotype associated with mutation at this residue. The results in Chapter 3.4 describe the generation of a HPV-16E2 protein mutated at residues 89 and 90 on the E2 transcriptional/replication domain that does not bind TopBP1, HPV-16E2N89YE90V.The results demonstrate that viral DNA replication is compromised when this E2 mutant is tested in replication assays. Furthermore,

replication is also compromised with a single mutation at residue 90 (E90V). We have also demonstrated that all of the proteins activate transcription suggesting that this altered replication phenotype is not due to mis-folding or altered stability of the proteins. The results then demonstrate that generation of an equivalent double mutant at residues 89 and 90 on the HPV-8E2 gene HPV-8E2D89AE90V generates the same phenotype and with HPV-8E2, the single mutant E90V, also results in compromised replication. This is a novel finding and it is possible that this could be used for the development of drugs that target viral replication. The importance of this finding is that such drugs may work across virus types, which is highly relevant for skin cancer in which no single virus predominates.

In the final experimental Chapter 3.5 we further examined the role of TopBP1 in skin cancer by conducting a microarray analysis of genes differentially expressed in TopBP1 knockdown cells that were damaged by UV. TopBP1 is a protein that is linked to DNA metabolism more than any other; it is involved in DNA damage and repair responses, in DNA replication and in transcription. TopBP1 is found throughout the epidermis in normal skin. Aberrant TopBP1 expression and poymorphisms in the TopBP1 gene have previously been described in breast and ovarian cancers. We hypothesised that TopBP1 might be involved in mediating the cellular DNA damage response to UVR through it's known role as a transcription factor and specifically through activation of ATR. Little is known of the functions of TopBP1 as a transcription factor. Whilst we confirmed that TopBP1 is involved in a number of cellular processes, only a small gene set were significantly differentially expressed following UVR both in the presence and absence of TopBP1 thereby the data were inconclusive. The experiment was designed to induce a damage response in the cells and not a death response which would induce alterations in a different gene set such as those involved in apoptosis and death signalling. A dose of 0.002J/cm^2 was chosen as it had been shown to produce damage by induction of phosphorylated -Chk1. With hindsight it is likely that the dose chosen was too low and a higher dose such as 0.008J/cm^2 may have induced more DNA damage yet still permitted survival of the MCF7 cells. It is likely that the lower UVB dose used was insufficient thereby resulting in too few genes being significantly differentially expressed. An alternative explanation could be that the time between damaging the cells and harvesting was too short (30 minutes) and perhaps a longer time would have

yielded a greater number of altered genes. Had there been no time or financial constraints then it would have been desirable to repeat the experiment utilising a higher UVB dose.

4.2 Future prospects

The clinical and epidemiological parts of this work will continue in the future as data continues to be collected prospectively. This may facilitate the involvement of our patient population in future studies with particular interest in determining factors that influence the development and outcome of skin cancer in this population such as immunosuppression and betaPV.

The data support the hypothesis that the E2-TopBP1 interaction is essential for viral replication and we hypothesise that this interaction will be essential for the viral life cycle. To confirm this, further work is being carried out in association with Professor Lou Laimins, Northwestern University, expert in HPV life cycle studies (333-335). This system involves introducing mutations into the whole HPV genome, e.g. HPV16E2 N89YE90V and transfecting the genomes into primary keratinocytes. The cells may then be "rafted" to produce living skin equivalents or grown in monolayer and differentiation induced by the addition of calcium. The genome (wild type or mutated) is established in non-differentiated cells and then amplifies as differentiation is induced in the cells, mimicking a natural infection. In this way, the effect of mutations introduced into the genome on the viral life cycle may be measured.

We predicted that viral DNA containing the HPV16E2 N89YE90V mutation would not replicate thus confirming the results of our studies *in vivo*. Initial results of the life cycle studies have confirmed this. In monolayer wild type HPV16 E2 genomes replicate as demonstrated by the detection of episomal DNA. In cells transfected with HPV-16 genomes containing either the single or double mutations in the E2 gene, E90V or N89Y E90V, no episomal DNA is detected indicating that the presence of these mutations result in failure to replicate viral DNA (unpublished data, not shown).

The results of the work described in this thesis suggest that introduction of mutations E90V or N89YE90V on the HPV-16 E2 gene generate an E2 mutant that

fails to bind TopBP1 and that failure to bind TopBP1 results in compromised replication of viral DNA and failure to establish viral maintenance of infection. This discovery is potentially very important for the development of therapies that target viral DNA replication and may be developed for the treatment of HPV associated disease.

Future studies will confirm whether a single mutation at amino acid 90 is sufficient to disrupt the E2/TopBP1 interaction or if a double mutation across residues 89 and 90 is required. Amino acid 90 is always conserved across HPV types whereas amino acid 89 is not which would suggest that a mutation at residue 90 might be sufficient to disrupt the interaction. The data from the HPV-16 mutants show that both single and double mutants fail to bind TopBP1 in vivo and, result in compromised replication, however, replication is more severely compromised with the double mutant and can be seen at both 1ng and 10ng titrations. In the life cycle studies, both the E90V and N89YE90V mutants demonstrate the same phenotype and this is a more sensitive assay than the replication assays suggesting that E90V alone may be sufficient. The data generated by the HPV-8E2 mutants in replication assays support the hypothesis that a single amino acid substitution is sufficient as that both the E90V and the D89YE90V mutants have a severely compromised replication phenotype. Previous work generating a single amino acid substitution at position 90 on the E2 gene failed to generate a phenotype however the substitution was Glutamine to an Alanine (271). We have also shown that HPV-16E90A binds TopBP1 like wild type in vitro and also replicates like wild type in replication assays (data not shown). Our HPV-8 data demonstrate that the E90A mutant behaves like wild type E2 in replication assays. It is interesting that the substitution of amino acid 90 to a Valine generates a phenotype whereas an Alanine does not. This may be due to the properties of Valine which is hydrophobic and may thus interfere with interaction at or around this site with greater efficiency than an Alanine substitution and this can be due to the site within the folded protein. Importantly, our data show that the introduction of a Valine substitution does not alter the folding of the protein. To further examine the interaction and to elucidate the reasons for this, which will be vital for the development of drugs, we will generate a crystal structure of the E2/TopBP1 interaction. The first step in this process is to make TopBP1 protein and the results are shown in Figures 57 and 58 below (work performed by L. Mackintosh). The proteins have now gone to

our collaborators in (Dr Brian Smith, University of Glasgow) to generate these proteins on a large scale and the crystal structure of the TopBP1/E2 interaction will then be generated by collaborators at St Andrews University.

Further work in this laboratory will confirm the results of TopBP1/E2 interaction in other virus types such as HPV-18, a pathogen in cervical cancer and HPV-6, (genital warts).

The work will ultimately facilitate the development of anti-viral therapies that target HPV DNA replication by disrupting the E2/TopBP1 interaction.

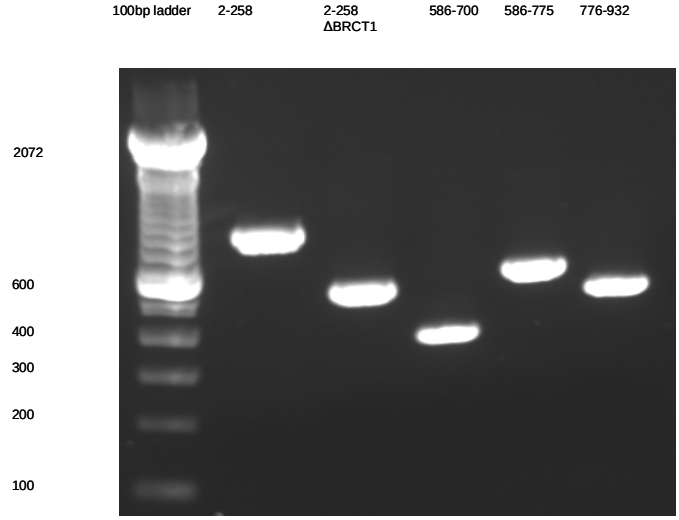

Figure 57 Agarose gel of TopBP1-GST fusion proteins.

To make the TopBP1-GST fusion proteins that will be used to generate a crystal structure of the TopBP1/HPV-16E2 interaction, primers were designed amplify fragments of the TopBP1 genes from template DNA (TopBP1-myc and TopBP1ΔBRCT1). The fragments amplified by PCR were TopBP1 (2-258; 2-258ΔBRCT1, 586-700, 586-775 and 776-932). The PCR products were run on an Agarose gel (above) which confirmed the DNA was of the expected size. TopBP1 fragments were then cloned into the GST containing vector, pGEX-4T-2 between the BamH1 and Xho1 restriction sites. DH5α bacteria were transformed with the TopBP1-GST fusion plasmids, plasmid DNA was purified and the proteins prepared and purified as described (2.2.4.17).

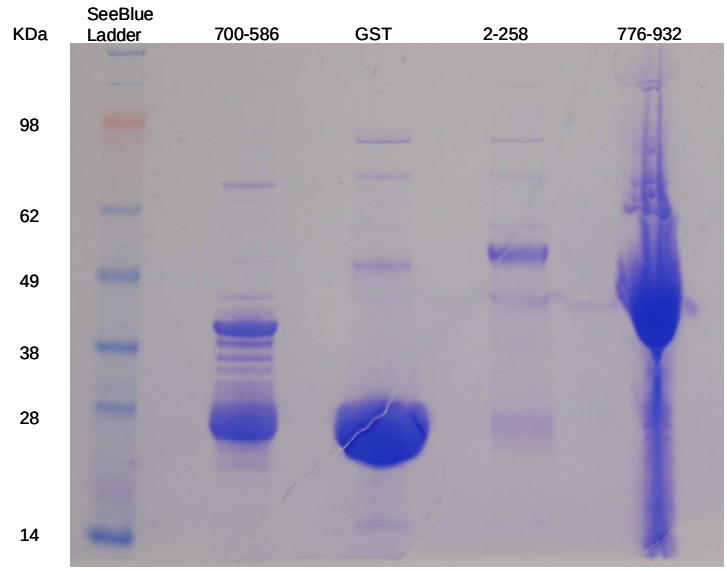

Figure 58 TopBP1-GST fusion proteins stained with Coomassie Blue.

Three TopBP1-GST proteins were chosen for induction (2-258, 700-586 and 776-932). After large scale production and purification, proteins were separated by SDS-PAGE gel electrophoresis and visualised by Coomassie Blue staining of the gel as described (2.2.4.18).

List of References

Bibliography

(1) National Institute for Health and Clinical Excellence. Improving outcomes for patients with skin tumours including melanoma. 2006.
Ref Type: Online Source

(2) IARC monographs on the evaluation of carcinogenic risks to humans. Solar and ultraviolet radiation. http://monographs iarc fr/ENG/Monographs/vol55/mono55 pdf 199255Available from: URL: http://monographs.iarc.fr/ENG/Monographs/vol55/mono55.pdf

(3) Brash DE, Ziegler A, Jonason AS, Simon JA, Kunala S, Leffell DJ. Sunlight and sunburn in human skin cancer: p53, apoptosis, and tumor promotion. J Investig Dermatol Symp Proc 1996 Apr;1(2):136-42.

(4) Cleaver JE. Cancer in xeroderma pigmentosum and related disorders of DNA repair. Nat Rev Cancer 2005 Jul;5(7):564-73.

(5) Epstein EH. Basal cell carcinomas: attack of the hedgehog. Nat Rev Cancer 2008 Oct;8(10):743-54.

(6) Ziegler A, Jonason AS, Leffell DJ, Simon JA, Sharma HW, Kimmelman J, et al. Sunburn and p53 in the onset of skin cancer. Nature 1994 Dec 22;372(6508):773-6.

(7) Soufir N, Moles JP, Vilmer C, Moch C, Verola O, Rivet J, et al. P16 UV mutations in human skin epithelial tumors. Oncogene 1999 Sep 23;18(39):5477-81.

(8) Brown VL, Harwood CA, Crook T, Cronin JG, Kelsell DP, Proby CM. p16INK4a and p14ARF tumor suppressor genes are commonly inactivated in cutaneous squamous cell carcinoma. J Invest Dermatol 2004 May;122(5):1284-92.

(9) Ananthaswamy HN, Pierceall WE. Molecular alterations in human skin tumors. Prog Clin Biol Res 1992;376:61-84.

(10) Scrivener Y, Grosshans E, Cribier B. Variations of basal cell carcinomas according to gender, age, location and histopathological subtype. Br J Dermatol 2002 Jul;147(1):41-7.

(11) Gailani MR, Stahle-Backdahl M, Leffell DJ, Glynn M, Zaphiropoulos PG, Pressman C, et al. The role of the human homologue of Drosophila patched in sporadic basal cell carcinomas. Nat Genet 1996 Sep;14(1):78-81.

(12) Ziegler A, Leffell DJ, Kunala S, Sharma HW, Gailani M, Simon JA, et al. Mutation hotspots due to sunlight in the p53 gene of nonmelanoma skin cancers. Proc Natl Acad Sci U S A 1993 May 1;90(9):4216-20.

(13) Giglia-Mari G, Sarasin A. TP53 mutations in human skin cancers. Hum Mutat 2003 Mar;21(3):217-28.

(14) Miranda B, Matesanz R. International issues in transplantation. Setting the scene and flagging the most urgent and controversial issues. Ann N Y Acad Sci 1998 Dec 30;862:129-43.

(15) Hariharan S, Johnson CP, Bresnahan BA, Taranto SE, McIntosh MJ, Stablein D. Improved graft survival after renal transplantation in the United States, 1988 to 1996. N Engl J Med 2000 Mar 2;342(9):605-12.

(16) Adami J, Gabel H, Lindelof B, Ekstrom K, Rydh B, Glimelius B, et al. Cancer risk following organ transplantation: a nationwide cohort study in Sweden. Br J Cancer 2003 Oct 6;89(7):1221-7.

(17) Kasiske BL, Snyder JJ, Gilbertson DT, Wang C. Cancer after kidney transplantation in the United States. Am J Transplant 2004 Jun;4(6):905-13.

(18) Birkeland SA, Storm HH, Lamm LU, Barlow L, Blohme I, Forsberg B, et al. Cancer risk after renal transplantation in the Nordic countries, 1964-1986. Int J Cancer 1995 Jan 17;60(2):183-9.

(19) Penn I, First MR. Merkel's cell carcinoma in organ recipients: report of 41 cases. Transplantation 1999 Dec 15;68(11):1717-21.

(20) Buell JF, Trofe J, Hanaway MJ, Beebe TM, Gross TG, Alloway RR, et al. Immunosuppression and Merkel cell cancer. Transplant Proc 2002 Aug;34(5):1780-1.

(21) Penn I. Posttransplant malignancies. Transplant Proc 1999 Feb;31(1-2):1260-2.

(22) Hartevelt MM, Bavinck JN, Kootte AM, Vermeer BJ, Vandenbroucke JP. Incidence of skin cancer after renal transplantation in The Netherlands. Transplantation 1990 Mar;49(3):506-9.

(23) Cohen EB, Komorowski RA, Clowry LJ. Cutaneous complications in renal transplant recipients. Am J Clin Pathol 1987 Jul;88(1):32-7.

(24) Hardie IR, Strong RW, Hartley LC, Woodruff PW, Clunie GJ. Skin cancer in Caucasian renal allograft recipients living in a subtropical climate. Surgery 1980 Feb;87(2):177-83.

(25) Hollenbeak CS, Todd MM, Billingsley EM, Harper G, Dyer AM, Lengerich EJ. Increased incidence of melanoma in renal transplantation recipients. Cancer 2005 Nov 1;104(9):1962-7.

(26) Jensen P, Hansen S, Moller B, Leivestad T, Pfeffer P, Geiran O, et al. Skin cancer in kidney and heart transplant recipients and different long-term immunosuppressive therapy regimens. J Am Acad Dermatol 1999 Feb;40(2 Pt 1):177-86.

(27) Lindelof B, Sigurgeirsson B, Gabel H, Stern RS. Incidence of skin cancer in 5356 patients following organ transplantation. Br J Dermatol 2000 Sep;143(3):513-9.

(28) Bouwes Bavinck JN, Hardie DR, Green A, Cutmore S, MacNaught A, O'Sullivan B, et al. The risk of skin cancer in renal transplant recipients

in Queensland, Australia. A follow-up study. Transplantation 1996 Mar 15;61(5):715-21.

(29) Webb MC, Compton F, Andrews PA, Koffman CG. Skin tumours posttransplantation: a retrospective analysis of 28 years' experience at a single centre. Transplant Proc 1997 Feb;29(1-2):828-30.

(30) Fuente MJ, Sabat M, Roca J, Lauzurica R, Fernandez-Figueras MT, Ferrandiz C. A prospective study of the incidence of skin cancer and its risk factors in a Spanish Mediterranean population of kidney transplant recipients. Br J Dermatol 2003 Dec;149(6):1221-6.

(31) Marcen R, Pascual J, Tato AM, Teruel JL, Villafruela JJ, Fernandez M, et al. Influence of immunosuppression on the prevalence of cancer after kidney transplantation. Transplant Proc 2003 Aug;35(5):1714-6.

(32) Caforio AL, Fortina AB, Piaserico S, Alaibac M, Tona F, Feltrin G, et al. Skin cancer in heart transplant recipients: risk factor analysis and relevance of immunosuppressive therapy. Circulation 2000 Nov 7;102(19 Suppl 3):III222-III227.

(33) Espana A, Redondo P, Fernandez AL, Zabala M, Herreros J, Llorens R, et al. Skin cancer in heart transplant recipients. J Am Acad Dermatol 1995 Mar;32(3):458-65.

(34) Ong CS, Keogh AM, Kossard S, Macdonald PS, Spratt PM. Skin cancer in Australian heart transplant recipients. J Am Acad Dermatol 1999 Jan;40(1):27-34.

(35) Ramsay HM, Fryer AA, Hawley CM, Smith AG, Nicol DL, Harden PN. Factors associated with nonmelanoma skin cancer following renal transplantation in Queensland, Australia. J Am Acad Dermatol 2003 Sep;49(3):397-406.

(36) Ramsay HM, Fryer AA, Hawley CM, Smith AG, Harden PN. Non-melanoma skin cancer risk in the Queensland renal transplant population. Br J Dermatol 2002 Nov;147(5):950-6.

(37) Wisgerhof HC, Edelbroek JR, de Fijter JW, Haasnoot GW, Claas FH, Willemze R, et al. Subsequent squamous- and basal-cell carcinomas in kidney-transplant recipients after the first skin cancer: cumulative incidence and risk factors. Transplantation 2010 May 27;89(10):1231-8.

(38) Euvrard S, Kanitakis J, Decullier E, Butnaru AC, Lefrancois N, Boissonnat P, et al. Subsequent skin cancers in kidney and heart transplant recipients after the first squamous cell carcinoma. Transplantation 2006 Apr 27;81(8):1093-100.

(39) Liddington M, Richardson AJ, Higgins RM, Endre ZH, Venning VA, Murie JA, et al. Skin cancer in renal transplant recipients. Br J Surg 1989 Oct;76(10):1002-5.

(40) Euvrard S, Kanitakis J, Pouteil-Noble C, Dureau G, Touraine JL, Faure M, et al. Comparative epidemiologic study of premalignant and malignant

epithelial cutaneous lesions developing after kidney and heart transplantation. J Am Acad Dermatol 1995 Aug;33(2 Pt 1):222-9.

(41) Blohme I, Larko O. Premalignant and malignant skin lesions in renal transplant patients. Transplantation 1984 Feb;37(2):165-7.

(42) Chuang TY, Popescu NA, Su WP, Chute CG. Squamous cell carcinoma. A population-based incidence study in Rochester, Minn. Arch Dermatol 1990 Feb;126(2):185-8.

(43) Berg D, Otley CC. Skin cancer in organ transplant recipients: Epidemiology, pathogenesis, and management. J Am Acad Dermatol 2002 Jul;47(1):1-17.

(44) Le ML, Hollowood K, Gray D, Bordea C, Wojnarowska F. Melanomas in renal transplant recipients. Br J Dermatol 2006 Mar;154(3):472-7.

(45) Chang Y, Cesarman E, Pessin MS, Lee F, Culpepper J, Knowles DM, et al. Identification of herpesvirus-like DNA sequences in AIDS-associated Kaposi's sarcoma. Science 1994 Dec 16;266(5192):1865-9.

(46) Penn I. Sarcomas in organ allograft recipients. Transplantation 1995 Dec 27;60(12):1485-91.

(47) Mbulaiteye SM, Engels EA. Kaposi's sarcoma risk among transplant recipients in the United States (1993-2003). Int J Cancer 2006 Dec 1;119(11):2685-91.

(48) Serraino D, Piselli P, Angeletti C, Minetti E, Pozzetto A, Civati G, et al. Risk of Kaposi's sarcoma and of other cancers in Italian renal transplant patients. Br J Cancer 2005 Feb 14;92(3):572-5.

(49) Qunibi W, Akhtar M, Sheth K, Ginn HE, Al-Furayh O, DeVol EB, et al. Kaposi's sarcoma: the most common tumor after renal transplantation in Saudi Arabia. Am J Med 1988 Feb;84(2):225-32.

(50) Hojo M, Morimoto T, Maluccio M, Asano T, Morimoto K, Lagman M, et al. Cyclosporine induces cancer progression by a cell-autonomous mechanism. Nature 1999 Feb 11;397(6719):530-4.

(51) Kelly GE, Meikle W, Sheil AG. Effects of immunosuppressive therapy on the induction of skin tumors by ultraviolet irradiation in hairless mice. Transplantation 1987 Sep;44(3):429-34.

(52) O'Donovan P, Perrett CM, Zhang X, Montaner B, Xu YZ, Harwood CA, et al. Azathioprine and UVA light generate mutagenic oxidative DNA damage. Science 2005 Sep 16;309(5742):1871-4.

(53) MacDonald AS. Cancer and transplantation intersect at the mammalian target of rapamycin. Transplantation 2007 Sep 27;84(6):682-4.

(54) Koehl GE, Andrassy J, Guba M, Richter S, Kroemer A, Scherer MN, et al. Rapamycin protects allografts from rejection while simultaneously attacking tumors in immunosuppressed mice. Transplantation 2004 May 15;77(9):1319-26.

(55) Feng H, Shuda M, Chang Y, Moore PS. Clonal integration of a polyomavirus in human Merkel cell carcinoma. Science 2008 Feb 22;319(5866):1096-100.

(56) Munoz N, Bosch FX, de SS, Herrero R, Castellsague X, Shah KV, et al. Epidemiologic classification of human papillomavirus types associated with cervical cancer. N Engl J Med 2003 Feb 6;348(6):518-27.

(57) Gissmann L, deVilliers EM, zur HH. Analysis of human genital warts (condylomata acuminata) and other genital tumors for human papillomavirus type 6 DNA. Int J Cancer 1982 Feb 15;29(2):143-6.

(58) Gissmann L, Diehl V, Schultz-Coulon HJ, zur HH. Molecular cloning and characterization of human papilloma virus DNA derived from a laryngeal papilloma. J Virol 1982 Oct;44(1):393-400.

(59) Naghashfar Z, McDonnell PJ, McDonnell JM, Green WR, Shah KV. Genital tract papillomavirus type 6 in recurrent conjunctival papilloma. Arch Ophthalmol 1986 Dec;104(12):1814-5.

(60) Orth G, Jablonska S, Favre M, Croissant O, Obalek S, Jarzabek-Chorzelska M, et al. Identification of papillomaviruses in butchers' warts. J Invest Dermatol 1981 Feb;76(2):97-102.

(61) Jablonska S, Orth G, Obalek S, Croissant O. Cutaneous warts. Clinical, histologic, and virologic correlations. Clin Dermatol 1985 Oct;3(4):71-82.

(62) Melton JL, Rasmussen JE. Clinical manifestations of human papillomavirus infection in nongenital sites. Dermatol Clin 1991 Apr;9(2):219-33.

(63) Rubben A, Krones R, Schwetschenau B, Grussendorf-Conen EI. Common warts from immunocompetent patients show the same distribution of human papillomavirus types as common warts from immunocompromised patients. Br J Dermatol 1993 Mar;128(3):264-70.

(64) IARC monographs on the evaluation of carcinogenic risks to humans. Human Papillomaviruses. http://monographs iarc fr/ENG/Monographs/vol90/index php 200790 (2007)Available from: URL: http://monographs.iarc.fr/ENG/Monographs/vol90/index.php

(65) IARC monographs on the evaluation of carcinogenic risks to humans. Human Papillomaviruses. http://monographs iarc fr/ENG/Monographs/vol64/index php 199564 (1995)Available from: URL: http://monographs.iarc.fr/ENG/Monographs/vol64/index.php

(66) de Villiers EM, Fauquet C, Broker TR, Bernard HU, zur HH. Classification of papillomaviruses. Virology 2004 Jun 20;324(1):17-27.

(67) Ramoz N, Rueda LA, Bouadjar B, Montoya LS, Orth G, Favre M. Mutations in two adjacent novel genes are associated with epidermodysplasia verruciformis. Nat Genet 2002 Dec;32(4):579-81.

(68) Majewski S, Jablonska S. Epidermodysplasia verruciformis as a model of human papillomavirus-induced genetic cancer of the skin. Arch Dermatol 1995 Nov;131(11):1312-8.

(69) Jablonska S, Majewski S. Epidermodysplasia verruciformis: immunological and clinical aspects. Curr Top Microbiol Immunol 1994;186:157-75.

(70) Boyle J, MacKie RM, Briggs JD, Junor BJ, Aitchison TC. Cancer, warts, and sunshine in renal transplant patients. A case-control study. Lancet 1984 Mar 31;1(8379):702-5.

(71) Harwood CA, Surentheran T, McGregor JM, Spink PJ, Leigh IM, Breuer J, et al. Human papillomavirus infection and non-melanoma skin cancer in immunosuppressed and immunocompetent individuals. J Med Virol 2000 Jul;61(3):289-97.

(72) Meyer T, Arndt R, Nindl I, Ulrich C, Christophers E, Stockfleth E. Association of human papillomavirus infections with cutaneous tumors in immunosuppressed patients. Transpl Int 2003 Mar;16(3):146-53.

(73) Shamanin V, zur HH, Lavergne D, Proby CM, Leigh IM, Neumann C, et al. Human papillomavirus infections in nonmelanoma skin cancers from renal transplant recipients and nonimmunosuppressed patients. J Natl Cancer Inst 1996 Jun 19;88(12):802-11.

(74) Stark LA, Arends MJ, McLaren KM, Benton EC, Shahidullah H, Hunter JA, et al. Prevalence of human papillomavirus DNA in cutaneous neoplasms from renal allograft recipients supports a possible viral role in tumour promotion. Br J Cancer 1994 Feb;69(2):222-9.

(75) Stockfleth E, Nindl I, Sterry W, Ulrich C, Schmook T, Meyer T. Human papillomaviruses in transplant-associated skin cancers. Dermatol Surg 2004 Apr;30(4 Pt 2):604-9.

(76) Barr BB, Benton EC, McLaren K, Bunney MH, Smith IW, Blessing K, et al. Human papilloma virus infection and skin cancer in renal allograft recipients. Lancet 1989 Jan 21;1(8630):124-9.

(77) Berkhout RJ, Bouwes Bavinck JN, Ter SJ. Persistence of human papillomavirus DNA in benign and (pre)malignant skin lesions from renal transplant recipients. J Clin Microbiol 2000 Jun;38(6):2087-96.

(78) de Jong-Tieben LM, Berkhout RJ, Smits HL, Bouwes Bavinck JN, Vermeer BJ, Van Der Woude FJ, et al. High frequency of detection of epidermodysplasia verruciformis-associated human papillomavirus DNA in biopsies from malignant and premalignant skin lesions from renal transplant recipients. J Invest Dermatol 1995 Sep;105(3):367-71.

(79) de Jong-Tieben LM, Berkhout RJ, Ter SJ, Vermeer BJ, de Fijter JW, Bruijn JA, et al. The prevalence of human papillomavirus DNA in benign keratotic skin lesions of renal transplant recipients with and without a history of skin cancer is equally high: a clinical study to assess risk factors for keratotic skin lesions and skin cancer. Transplantation 2000 Jan 15;69(1):44-9.

(80) de Villiers EM, Lavergne D, McLaren K, Benton EC. Prevailing papillomavirus types in non-melanoma carcinomas of the skin in renal allograft recipients. Int J Cancer 1997 Nov 4;73(3):356-61.

(81) Tieben LM, Berkhout RJ, Smits HL, Bouwes Bavinck JN, Vermeer BJ, Bruijn JA, et al. Detection of epidermodysplasia verruciformis-like human papillomavirus types in malignant and premalignant skin lesions of renal transplant recipients. Br J Dermatol 1994 Aug;131(2):226-30.

(82) Forslund O, Iftner T, Andersson K, Lindelof B, Hradil E, Nordin P, et al. Cutaneous human papillomaviruses found in sun-exposed skin: Beta-papillomavirus species 2 predominates in squamous cell carcinoma. J Infect Dis 2007 Sep 15;196(6):876-83.

(83) Biliris KA, Koumantakis E, Dokianakis DN, Sourvinos G, Spandidos DA. Human papillomavirus infection of non-melanoma skin cancers in immunocompetent hosts. Cancer Lett 2000 Dec 8;161(1):83-8.

(84) Caldeira S, Zehbe I, Accardi R, Malanchi I, Dong W, Giarre M, et al. The E6 and E7 proteins of the cutaneous human papillomavirus type 38 display transforming properties. J Virol 2003 Feb;77(3):2195-206.

(85) Iftner A, Klug SJ, Garbe C, Blum A, Stancu A, Wilczynski SP, et al. The prevalence of human papillomavirus genotypes in nonmelanoma skin cancers of nonimmunosuppressed individuals identifies high-risk genital types as possible risk factors. Cancer Res 2003 Nov 1;63(21):7515-9.

(86) Pfister H, Fuchs PG, Majewski S, Jablonska S, Pniewska I, Malejczyk M. High prevalence of epidermodysplasia verruciformis-associated human papillomavirus DNA in actinic keratoses of the immunocompetent population. Arch Dermatol Res 2003 Dec;295(7):273-9.

(87) Struijk L, Hall L, van der Meijden E, Wanningen P, Bavinck JN, Neale R, et al. Markers of cutaneous human papillomavirus infection in individuals with tumor-free skin, actinic keratoses, and squamous cell carcinoma. Cancer Epidemiol Biomarkers Prev 2006 Mar;15(3):529-35.

(88) Asgari MM, Kiviat NB, Critchlow CW, Stern JE, Argenyi ZB, Raugi GJ, et al. Detection of human papillomavirus DNA in cutaneous squamous cell carcinoma among immunocompetent individuals. J Invest Dermatol 2008 Jun;128(6):1409-17.

(89) de KM, Quint W, Struijk L, Kleter B, Wanningen P, van Doorn LJ, et al. Evaluation of a novel highly sensitive, broad-spectrum PCR-reverse hybridization assay for detection and identification of beta-papillomavirus DNA. J Clin Microbiol 2006 May;44(5):1792-800.

(90) Patel AS, Karagas MR, Perry AE, Nelson HH. Exposure profiles and human papillomavirus infection in skin cancer: an analysis of 25 genus beta-types in a population-based study. J Invest Dermatol 2008 Dec;128(12):2888-93.

(91) Plasmeijer EI, Neale RE, Buettner PG, de Koning MN, Ter SJ, Quint WG, et al. Betapapillomavirus infection profiles in tissue sets from cutaneous squamous cell-carcinoma patients. Int J Cancer 2010 Jun 1;126(11):2614-21.

(92) Antonsson A, Forslund O, Ekberg H, Sterner G, Hansson BG. The ubiquity and impressive genomic diversity of human skin papillomaviruses suggest

a commensalic nature of these viruses. J Virol 2000 Dec;74(24):11636-41.

(93) Boxman IL, Berkhout RJ, Mulder LH, Wolkers MC, Bouwes Bavinck JN, Vermeer BJ, et al. Detection of human papillomavirus DNA in plucked hairs from renal transplant recipients and healthy volunteers. J Invest Dermatol 1997 May;108(5):712-5.

(94) Harwood CA, Surentheran T, Sasieni P, Proby CM, Bordea C, Leigh IM, et al. Increased risk of skin cancer associated with the presence of epidermodysplasia verruciformis human papillomavirus types in normal skin. Br J Dermatol 2004 May;150(5):949-57.

(95) Hazard K, Karlsson A, Andersson K, Ekberg H, Dillner J, Forslund O. Cutaneous human papillomaviruses persist on healthy skin. J Invest Dermatol 2007 Jan;127(1):116-9.

(96) Antonsson A, Erfurt C, Hazard K, Holmgren V, Simon M, Kataoka A, et al. Prevalence and type spectrum of human papillomaviruses in healthy skin samples collected in three continents. J Gen Virol 2003 Jul;84(Pt 7):1881-6.

(97) Boxman IL, Russell A, Mulder LH, Bavinck JN, Schegget JT, Green A. Case-control study in a subtropical Australian population to assess the relation between non-melanoma skin cancer and epidermodysplasia verruciformis human papillomavirus DNA in plucked eyebrow hairs. The Nambour Skin Cancer Prevention Study Group. Int J Cancer 2000 Apr 1;86(1):118-21.

(98) Boxman IL, Russell A, Mulder LH, Bavinck JN, Ter SJ, Green A. Association between epidermodysplasia verruciformis-associated human papillomavirus DNA in plucked eyebrow hair and solar keratoses. J Invest Dermatol 2001 Nov;117(5):1108-12.

(99) Struijk L, Bouwes Bavinck JN, Wanningen P, van der Meijden E, Westendorp RG, Ter SJ, et al. Presence of human papillomavirus DNA in plucked eyebrow hairs is associated with a history of cutaneous squamous cell carcinoma. J Invest Dermatol 2003 Dec;121(6):1531-5.

(100) Termorshuizen F, Feltkamp MC, Struijk L, de Gruijl FR, Bavinck JN, van LH. Sunlight exposure and (sero)prevalence of epidermodysplasia verruciformis-associated human papillomavirus. J Invest Dermatol 2004 Jun;122(6):1456-62.

(101) de Koning MN, Struijk L, Bavinck JN, Kleter B, Ter SJ, Quint WG, et al. Betapapillomaviruses frequently persist in the skin of healthy individuals. J Gen Virol 2007 May;88(Pt 5):1489-95.

(102) Bouwes Bavinck JN, Neale RE, Abeni D, Euvrard S, Green AC, Harwood CA, et al. Multicenter study of the association between betapapillomavirus infection and cutaneous squamous cell carcinoma. Cancer Res 2010 Dec 1;70(23):9777-86.

(103) Casabonne D, Michael KM, Waterboer T, Pawlita M, Forslund O, Burk RD, et al. A prospective pilot study of antibodies against human

papillomaviruses and cutaneous squamous cell carcinoma nested in the Oxford component of the European Prospective Investigation into Cancer and Nutrition. Int J Cancer 2007 Oct 15;121(8):1862-8.

(104) Favre M, Majewski S, Noszczyk B, Maienfisch F, Pura A, Orth G, et al. Antibodies to human papillomavirus type 5 are generated in epidermal repair processes. J Invest Dermatol 2000 Mar;114(3):403-7.

(105) Feltkamp MC, Broer R, di Summa FM, Struijk L, van der Meijden E, Verlaan BP, et al. Seroreactivity to epidermodysplasia verruciformis-related human papillomavirus types is associated with nonmelanoma skin cancer. Cancer Res 2003 May 15;63(10):2695-700.

(106) Karagas MR, Nelson HH, Sehr P, Waterboer T, Stukel TA, Andrew A, et al. Human papillomavirus infection and incidence of squamous cell and basal cell carcinomas of the skin. J Natl Cancer Inst 2006 Mar 15;98(6):389-95.

(107) Bouwes Bavinck JN, Stark S, Petridis AK, Marugg ME, Ter SJ, Westendorp RG, et al. The presence of antibodies against virus-like particles of epidermodysplasia verruciformis-associated humanpapillomavirus type 8 in patients with actinic keratoses. Br J Dermatol 2000 Jan;142(1):103-9.

(108) Masini C, Fuchs PG, Gabrielli F, Stark S, Sera F, Ploner M, et al. Evidence for the association of human papillomavirus infection and cutaneous squamous cell carcinoma in immunocompetent individuals. Arch Dermatol 2003 Jul;139(7):890-4.

(109) Stark S, Petridis AK, Ghim SJ, Jenson AB, Bouwes Bavinck JN, Gross G, et al. Prevalence of antibodies against virus-like particles of Epidermodysplasia verruciformis-associated HPV8 in patients at risk of skin cancer. J Invest Dermatol 1998 Oct;111(4):696-701.

(110) Steger G, Olszewsky M, Stockfleth E, Pfister H. Prevalence of antibodies to human papillomavirus type 8 in human sera. J Virol 1990 Sep;64(9):4399-406.

(111) Casabonne D, Waterboer T, Michael KM, Pawlita M, Lally A, Mitchell L, et al. The sero-epidemiology of human papillomavirus among Caucasian transplant recipients in the UK. Infect Agent Cancer 2009;4:13.

(112) Dang C, Koehler A, Forschner T, Sehr P, Michael K, Pawlita M, et al. E6/E7 expression of human papillomavirus types in cutaneous squamous cell dysplasia and carcinoma in immunosuppressed organ transplant recipients. Br J Dermatol 2006 Jul;155(1):129-36.

(113) Forslund O, Lindelof B, Hradil E, Nordin P, Stenquist B, Kirnbauer R, et al. High prevalence of cutaneous human papillomavirus DNA on the top of skin tumors but not in "Stripped" biopsies from the same tumors. J Invest Dermatol 2004 Aug;123(2):388-94.

(114) Plasmeijer EI, Neale RE, de Koning MN, Quint WG, McBride P, Feltkamp MC, et al. Persistence of betapapillomavirus infections as a risk factor for actinic keratoses, precursor to cutaneous squamous cell carcinoma. Cancer Res 2009 Dec 1;69(23):8926-31.

(115) Majewski S, Jablonska S, Orth G. Epidermodysplasia verruciformis. Immunological and nonimmunological surveillance mechanisms: role in tumor progression. Clin Dermatol 1997 May;15(3):321-34.

(116) Weissenborn SJ, Nindl I, Purdie K, Harwood C, Proby C, Breuer J, et al. Human papillomavirus-DNA loads in actinic keratoses exceed those in non-melanoma skin cancers. J Invest Dermatol 2005 Jul;125(1):93-7.

(117) Proby CM, Harwood CA, Neale RE, Green AC, Euvrard S, Naldi L, et al. A case-control study of betapapillomavirus infection and cutaneous squamous cell carcinoma in organ transplant recipients. Am J Transplant 2011 Jul;11(7):1498-508.

(118) Ghittoni R, Accardi R, Hasan U, Gheit T, Sylla B, Tommasino M. The biological properties of E6 and E7 oncoproteins from human papillomaviruses. Virus Genes 2010 Feb;40(1):1-13.

(119) Doorbar J. Molecular biology of human papillomavirus infection and cervical cancer. Clin Sci (Lond) 2006 May;110(5):525-41.

(120) Bedell MA, Hudson JB, Golub TR, Turyk ME, Hosken M, Wilbanks GD, et al. Amplification of human papillomavirus genomes in vitro is dependent on epithelial differentiation. J Virol 1991 May;65(5):2254-60.

(121) Stanley MA, Browne HM, Appleby M, Minson AC. Properties of a non-tumorigenic human cervical keratinocyte cell line. Int J Cancer 1989 Apr 15;43(4):672-6.

(122) Pett M, Coleman N. Integration of high-risk human papillomavirus: a key event in cervical carcinogenesis? J Pathol 2007 Aug;212(4):356-67.

(123) Wentzensen N, Vinokurova S, von Knebel DM. Systematic review of genomic integration sites of human papillomavirus genomes in epithelial dysplasia and invasive cancer of the female lower genital tract. Cancer Res 2004 Jun 1;64(11):3878-84.

(124) Corden SA, Sant-Cassia LJ, Easton AJ, Morris AG. The integration of HPV-18 DNA in cervical carcinoma. Mol Pathol 1999 Oct;52(5):275-82.

(125) Cullen AP, Reid R, Campion M, Lorincz AT. Analysis of the physical state of different human papillomavirus DNAs in intraepithelial and invasive cervical neoplasm. J Virol 1991 Feb;65(2):606-12.

(126) Pirami L, Giache V, Becciolini A. Analysis of HPV16, 18, 31, and 35 DNA in pre-invasive and invasive lesions of the uterine cervix. J Clin Pathol 1997 Jul;50(7):600-4.

(127) Melsheimer P, Vinokurova S, Wentzensen N, Bastert G, von Knebel DM. DNA aneuploidy and integration of human papillomavirus type 16 e6/e7 oncogenes in intraepithelial neoplasia and invasive squamous cell carcinoma of the cervix uteri. Clin Cancer Res 2004 May 1;10(9):3059-63.

(128) Dowhanick JJ, McBride AA, Howley PM. Suppression of cellular proliferation by the papillomavirus E2 protein. J Virol 1995 Dec;69(12):7791-9.

(129) Munger K, Baldwin A, Edwards KM, Hayakawa H, Nguyen CL, Owens M, et al. Mechanisms of human papillomavirus-induced oncogenesis. J Virol 2004 Nov;78(21):11451-60.

(130) zur HH. Papillomaviruses and cancer: from basic studies to clinical application. Nat Rev Cancer 2002 May;2(5):342-50.

(131) Alvarez-Salas LM, DiPaolo JA. Molecular approaches to cervical cancer therapy. Curr Drug Discov Technol 2007 Oct;4(3):208-19.

(132) Thomas M, Pim D, Banks L. The role of the E6-p53 interaction in the molecular pathogenesis of HPV. Oncogene 1999 Dec 13;18(53):7690-700.

(133) Vogelstein B, Lane D, Levine AJ. Surfing the p53 network. Nature 2000 Nov 16;408(6810):307-10.

(134) Slee EA, O'Connor DJ, Lu X. To die or not to die: how does p53 decide? Oncogene 2004 Apr 12;23(16):2809-18.

(135) Vousden KH, Lu X. Live or let die: the cell's response to p53. Nat Rev Cancer 2002 Aug;2(8):594-604.

(136) Huibregtse JM, Scheffner M, Howley PM. A cellular protein mediates association of p53 with the E6 oncoprotein of human papillomavirus types 16 or 18. EMBO J 1991 Dec;10(13):4129-35.

(137) Scheffner M, Werness BA, Huibregtse JM, Levine AJ, Howley PM. The E6 oncoprotein encoded by human papillomavirus types 16 and 18 promotes the degradation of p53. Cell 1990 Dec 21;63(6):1129-36.

(138) Werness BA, Levine AJ, Howley PM. Association of human papillomavirus types 16 and 18 E6 proteins with p53. Science 1990 Apr 6;248(4951):76-9.

(139) Hiller T, Poppelreuther S, Stubenrauch F, Iftner T. Comparative analysis of 19 genital human papillomavirus types with regard to p53 degradation, immortalization, phylogeny, and epidemiologic risk classification. Cancer Epidemiol Biomarkers Prev 2006 Jul;15(7):1262-7.

(140) Lechner MS, Laimins LA. Inhibition of p53 DNA binding by human papillomavirus E6 proteins. J Virol 1994 Jul;68(7):4262-73.

(141) Butz K, Denk C, Ullmann A, Scheffner M, Hoppe-Seyler F. Induction of apoptosis in human papillomaviruspositive cancer cells by peptide aptamers targeting the viral E6 oncoprotein. Proc Natl Acad Sci U S A 2000 Jun 6;97(12):6693-7.

(142) Sorenson CM. Bcl-2 family members and disease. Biochim Biophys Acta 2004 Mar 1;1644(2-3):169-77.

(143) Thomas M, Banks L. Inhibition of Bak-induced apoptosis by HPV-18 E6. Oncogene 1998 Dec 10;17(23):2943-54.

(144) Jackson S, Harwood C, Thomas M, Banks L, Storey A. Role of Bak in UV-induced apoptosis in skin cancer and abrogation by HPV E6 proteins. Genes Dev 2000 Dec 1;14(23):3065-73.

(145) Klingelhutz AJ, Foster SA, McDougall JK. Telomerase activation by the E6 gene product of human papillomavirus type 16. Nature 1996 Mar 7;380(6569):79-82.

(146) Shay JW, Wright WE. Senescence and immortalization: role of telomeres and telomerase. Carcinogenesis 2005 May;26(5):867-74.

(147) Massimi P, Gammoh N, Thomas M, Banks L. HPV E6 specifically targets different cellular pools of its PDZ domain-containing tumour suppressor substrates for proteasome-mediated degradation. Oncogene 2004 Oct 21;23(49):8033-9.

(148) Kim SK. Polarized signaling: basolateral receptor localization in epithelial cells by PDZ-containing proteins. Curr Opin Cell Biol 1997 Dec;9(6):853-9.

(149) Gardiol D, Kuhne C, Glaunsinger B, Lee SS, Javier R, Banks L. Oncogenic human papillomavirus E6 proteins target the discs large tumour suppressor for proteasome-mediated degradation. Oncogene 1999 Sep 30;18(40):5487-96.

(150) Kiyono T, Hiraiwa A, Fujita M, Hayashi Y, Akiyama T, Ishibashi M. Binding of high-risk human papillomavirus E6 oncoproteins to the human homologue of the Drosophila discs large tumor suppressor protein. Proc Natl Acad Sci U S A 1997 Oct 14;94(21):11612-6.

(151) Thomas M, Laura R, Hepner K, Guccione E, Sawyers C, Lasky L, et al. Oncogenic human papillomavirus E6 proteins target the MAGI-2 and MAGI-3 proteins for degradation. Oncogene 2002 Aug 1;21(33):5088-96.

(152) Munger K, Werness BA, Dyson N, Phelps WC, Harlow E, Howley PM. Complex formation of human papillomavirus E7 proteins with the retinoblastoma tumor suppressor gene product. EMBO J 1989 Dec 20;8(13):4099-105.

(153) McLaughlin-Drubin ME, Munger K. The human papillomavirus E7 oncoprotein. Virology 2009 Feb 20;384(2):335-44.

(154) Frolov MV, Dyson NJ. Molecular mechanisms of E2F-dependent activation and pRB-mediated repression. J Cell Sci 2004 May 1;117(Pt 11):2173-81.

(155) Munger K, Howley PM. Human papillomavirus immortalization and transformation functions. Virus Res 2002 Nov;89(2):213-28.

(156) Cobrinik D, Dowdy SF, Hinds PW, Mittnacht S, Weinberg RA. The retinoblastoma protein and the regulation of cell cycling. Trends Biochem Sci 1992 Aug;17(8):312-5.

(157) Boyer SN, Wazer DE, Band V. E7 protein of human papilloma virus-16 induces degradation of retinoblastoma protein through the ubiquitin-proteasome pathway. Cancer Res 1996 Oct 15;56(20):4620-4.

(158) Hwang SG, Lee D, Kim J, Seo T, Choe J. Human papillomavirus type 16 E7 binds to E2F1 and activates E2F1-driven transcription in a retinoblastoma protein-independent manner. J Biol Chem 2002 Jan 25;277(4):2923-30.

(159) Rihet S, Lorenzato M, Clavel C. Oncogenic human papillomaviruses and ploidy in cervical lesions. J Clin Pathol 1996 Nov;49(11):892-6.

(160) Cottage A, Dowen S, Roberts I, Pett M, Coleman N, Stanley M. Early genetic events in HPV immortalised keratinocytes. Genes Chromosomes Cancer 2001 Jan;30(1):72-9.

(161) Hashida T, Yasumoto S. Induction of chromosome abnormalities in mouse and human epidermal keratinocytes by the human papillomavirus type 16 E7 oncogene. J Gen Virol 1991 Jul;72 (Pt 7):1569-77.

(162) White AE, Livanos EM, Tlsty TD. Differential disruption of genomic integrity and cell cycle regulation in normal human fibroblasts by the HPV oncoproteins. Genes Dev 1994 Mar 15;8(6):666-77.

(163) Duensing S, Munger K. The human papillomavirus type 16 E6 and E7 oncoproteins independently induce numerical and structural chromosome instability. Cancer Res 2002 Dec 1;62(23):7075-82.

(164) Winkler B, Crum CP, Fujii T, Ferenczy A, Boon M, Braun L, et al. Koilocytotic lesions of the cervix. The relationship of mitotic abnormalities to the presence of papillomavirus antigens and nuclear DNA content. Cancer 1984 Mar 1;53(5):1081-7.

(165) Bettencourt-Dias M, Glover DM. Centrosome biogenesis and function: centrosomics brings new understanding. Nat Rev Mol Cell Biol 2007 Jun;8(6):451-63.

(166) Duensing S, Duensing A, Crum CP, Munger K. Human papillomavirus type 16 E7 oncoprotein-induced abnormal centrosome synthesis is an early event in the evolving malignant phenotype. Cancer Res 2001 Mar 15;61(6):2356-60.

(167) Hildesheim A, Schiffman MH, Gravitt PE, Glass AG, Greer CE, Zhang T, et al. Persistence of type-specific human papillomavirus infection among cytologically normal women. J Infect Dis 1994 Feb;169(2):235-40.

(168) Malmgaard L. Induction and regulation of IFNs during viral infections. J Interferon Cytokine Res 2004 Aug;24(8):439-54.

(169) Chang YE, Laimins LA. Microarray analysis identifies interferon-inducible genes and Stat-1 as major transcriptional targets of human papillomavirus type 31. J Virol 2000 May;74(9):4174-82.

(170) Nees M, Geoghegan JM, Hyman T, Frank S, Miller L, Woodworth CD. Papillomavirus type 16 oncogenes downregulate expression of interferon-responsive genes and upregulate proliferation-associated and NF-kappaB-responsive genes in cervical keratinocytes. J Virol 2001 May;75(9):4283-96.

(171) Park JS, Kim EJ, Kwon HJ, Hwang ES, Namkoong SE, Um SJ. Inactivation of interferon regulatory factor-1 tumor suppressor protein by HPV E7 oncoprotein. Implication for the E7-mediated immune evasion mechanism in cervical carcinogenesis. J Biol Chem 2000 Mar 10;275(10):6764-9.

(172) Ronco LV, Karpova AY, Vidal M, Howley PM. Human papillomavirus 16 E6 oncoprotein binds to interferon regulatory factor-3 and inhibits its transcriptional activity. Genes Dev 1998 Jul 1;12(13):2061-72.

(173) Caldeira S, Filotico R, Accardi R, Zehbe I, Franceschi S, Tommasino M. p53 mutations are common in human papillomavirus type 38-positive non-melanoma skin cancers. Cancer Lett 2004 Jun 8;209(1):119-24.

(174) Elbel M, Carl S, Spaderna S, Iftner T. A comparative analysis of the interactions of the E6 proteins from cutaneous and genital papillomaviruses with p53 and E6AP in correlation to their transforming potential. Virology 1997 Dec 8;239(1):132-49.

(175) Jackson S, Storey A. E6 proteins from diverse cutaneous HPV types inhibit apoptosis in response to UV damage. Oncogene 2000 Jan 27;19(4):592-8.

(176) Giampieri S, Garcia-Escudero R, Green J, Storey A. Human papillomavirus type 77 E6 protein selectively inhibits p53-dependent transcription of proapoptotic genes following UV-B irradiation. Oncogene 2004 Jul 29;23(34):5864-70.

(177) Accardi R, Dong W, Smet A, Cui R, Hautefeuille A, Gabet AS, et al. Skin human papillomavirus type 38 alters p53 functions by accumulation of deltaNp73. EMBO Rep 2006 Mar;7(3):334-40.

(178) Thomas M, Banks L. Human papillomavirus (HPV) E6 interactions with Bak are conserved amongst E6 proteins from high and low risk HPV types. J Gen Virol 1999 Jun;80 (Pt 6):1513-7.

(179) Giampieri S, Storey A. Repair of UV-induced thymine dimers is compromised in cells expressing the E6 protein from human papillomaviruses types 5 and 18. Br J Cancer 2004 Jun 1;90(11):2203-9.

(180) Iftner T, Elbel M, Schopp B, Hiller T, Loizou JI, Caldecott KW, et al. Interference of papillomavirus E6 protein with single-strand break repair by interaction with XRCC1. EMBO J 2002 Sep 2;21(17):4741-8.

(181) Akgul B, Garcia-Escudero R, Ghali L, Pfister HJ, Fuchs PG, Navsaria H, et al. The E7 protein of cutaneous human papillomavirus type 8 causes invasion of human keratinocytes into the dermis in organotypic cultures of skin. Cancer Res 2005 Mar 15;65(6):2216-23.

(182) Schaper ID, Marcuzzi GP, Weissenborn SJ, Kasper HU, Dries V, Smyth N, et al. Development of skin tumors in mice transgenic for early genes of human papillomavirus type 8. Cancer Res 2005 Feb 15;65(4):1394-400.

(183) Pfefferle R, Marcuzzi GP, Akgul B, Kasper HU, Schulze F, Haase I, et al. The human papillomavirus type 8 E2 protein induces skin tumors in transgenic mice. J Invest Dermatol 2008 Sep;128(9):2310-5.

(184) Dong W, Kloz U, Accardi R, Caldeira S, Tong WM, Wang ZQ, et al. Skin hyperproliferation and susceptibility to chemical carcinogenesis in transgenic mice expressing E6 and E7 of human papillomavirus type 38. J Virol 2005 Dec;79(23):14899-908.

(185) Michel A, Kopp-Schneider A, Zentgraf H, Gruber AD, de Villiers EM. E6/E7 expression of human papillomavirus type 20 (HPV-20) and HPV-27 influences proliferation and differentiation of the skin in UV-irradiated SKH-hr1 transgenic mice. J Virol 2006 Nov;80(22):11153-64.

(186) Bouvard V, Matlashewski G, Gu ZM, Storey A, Banks L. The human papillomavirus type 16 E5 gene cooperates with the E7 gene to stimulate proliferation of primary cells and increases viral gene expression. Virology 1994 Aug 15;203(1):73-80.

(187) Valle GF, Banks L. The human papillomavirus (HPV)-6 and HPV-16 E5 proteins co-operate with HPV-16 E7 in the transformation of primary rodent cells. J Gen Virol 1995 May;76 (Pt 5):1239-45.

(188) Leechanachai P, Banks L, Moreau F, Matlashewski G. The E5 gene from human papillomavirus type 16 is an oncogene which enhances growth factor-mediated signal transduction to the nucleus. Oncogene 1992 Jan;7(1):19-25.

(189) Leptak C, Cajal S, Kulke R, Horwitz BH, Riese DJ, Dotto GP, et al. Tumorigenic transformation of murine keratinocytes by the E5 genes of bovine papillomavirus type 1 and human papillomavirus type 16. J Virol 1991 Dec;65(12):7078-83.

(190) Ashrafi GH, Tsirimonaki E, Marchetti B, O'Brien PM, Sibbet GJ, Andrew L, et al. Down-regulation of MHC class I by bovine papillomavirus E5 oncoproteins. Oncogene 2002 Jan 10;21(2):248-59.

(191) Marchetti B, Ashrafi GH, Tsirimonaki E, O'Brien PM, Campo MS. The bovine papillomavirus oncoprotein E5 retains MHC class I molecules in the Golgi apparatus and prevents their transport to the cell surface. Oncogene 2002 Nov 7;21(51):7808-16.

(192) Ashrafi GH, Haghshenas MR, Marchetti B, O'Brien PM, Campo MS. E5 protein of human papillomavirus type 16 selectively downregulates surface HLA class I. Int J Cancer 2005 Jan 10;113(2):276-83.

(193) Zhang B, Li P, Wang E, Brahmi Z, Dunn KW, Blum JS, et al. The E5 protein of human papillomavirus type 16 perturbs MHC class II antigen maturation in human foreskin keratinocytes treated with interferon-gamma. Virology 2003 May 25;310(1):100-8.

(194) Doorbar J, Campbell D, Grand RJ, Gallimore PH. Identification of the human papilloma virus-1a E4 gene products. EMBO J 1986 Feb;5(2):355-62.

(195) Peh WL, Middleton K, Christensen N, Nicholls P, Egawa K, Sotlar K, et al. Life cycle heterogeneity in animal models of human papillomavirus-associated disease. J Virol 2002 Oct;76(20):10401-16.

(196) Nakahara T, Peh WL, Doorbar J, Lee D, Lambert PF. Human papillomavirus type 16 E1circumflexE4 contributes to multiple facets of the papillomavirus life cycle. J Virol 2005 Oct;79(20):13150-65.

(197) Wilson R, Fehrmann F, Laimins LA. Role of the E1--E4 protein in the differentiation-dependent life cycle of human papillomavirus type 31. J Virol 2005 Jun;79(11):6732-40.

(198) Wilson R, Ryan GB, Knight GL, Laimins LA, Roberts S. The full-length E1E4 protein of human papillomavirus type 18 modulates differentiation-dependent viral DNA amplification and late gene expression. Virology 2007 Jun 5;362(2):453-60.

(199) Fang L, Budgeon LR, Doorbar J, Briggs ER, Howett MK. The human papillomavirus type 11 E1/\E4 protein is not essential for viral genome amplification. Virology 2006 Aug 1;351(2):271-9.

(200) Davy CE, Jackson DJ, Wang Q, Raj K, Masterson PJ, Fenner NF, et al. Identification of a G(2) arrest domain in the E1 wedge E4 protein of human papillomavirus type 16. J Virol 2002 Oct;76(19):9806-18.

(201) Knight GL, Grainger JR, Gallimore PH, Roberts S. Cooperation between different forms of the human papillomavirus type 1 E4 protein to block cell cycle progression and cellular DNA synthesis. J Virol 2004 Dec;78(24):13920-33.

(202) Nakahara T, Nishimura A, Tanaka M, Ueno T, Ishimoto A, Sakai H. Modulation of the cell division cycle by human papillomavirus type 18 E4. J Virol 2002 Nov;76(21):10914-20.

(203) Raj K, Berguerand S, Southern S, Doorbar J, Beard P. E1 empty set E4 protein of human papillomavirus type 16 associates with mitochondria. J Virol 2004 Jul;78(13):7199-207.

(204) Doorbar J, Ely S, Sterling J, McLean C, Crawford L. Specific interaction between HPV-16 E1-E4 and cytokeratins results in collapse of the epithelial cell intermediate filament network. Nature 1991 Aug 29;352(6338):824-7.

(205) Rogel-Gaillard C, Pehau-Arnaudet G, Breitburd F, Orth G. Cytopathic effect in human papillomavirus type 1-induced inclusion warts: in vitro analysis of the contribution of two forms of the viral E4 protein. J Invest Dermatol 1993 Dec;101(6):843-51.

(206) Roberts S, Ashmole I, Johnson GD, Kreider JW, Gallimore PH. Cutaneous and mucosal human papillomavirus E4 proteins form intermediate filament-like structures in epithelial cells. Virology 1993 Nov;197(1):176-87.

(207) Campo MS, Roden RB. Papillomavirus prophylactic vaccines: established successes, new approaches. J Virol 2010 Feb;84(3):1214-20.

(208) Ozbun MA, Meyers C. Human papillomavirus type 31b E1 and E2 transcript expression correlates with vegetative viral genome amplification. Virology 1998 Sep 1;248(2):218-30.

(209) Chow LT, Broker TR. Mechanisms and Regulation of DNA Replication. In: Campo MS, editor. Papillomavirus Research : From Natural History to Vaccines and Beyond. Caister Academic Press; 2006. p. 53-71.

(210) Stenland A. DNA Replication of Papillomaviruses. In: DiMaio D, editor. The Papillomaviruses. 1 ed. Springer; 2007. p. 145-74.

(211) Sedman J, Stenlund A. The papillomavirus E1 protein forms a DNA-dependent hexameric complex with ATPase and DNA helicase activities. J Virol 1998 Aug;72(8):6893-7.

(212) Masterson PJ, Stanley MA, Lewis AP, Romanos MA. A C-terminal helicase domain of the human papillomavirus E1 protein binds E2 and the DNA polymerase alpha-primase p68 subunit. J Virol 1998 Sep;72(9):7407-19.

(213) Muller F, Sapp M. Domains of the E1 protein of human papillomavirus type 33 involved in binding to the E2 protein. Virology 1996 May 1;219(1):247-56.

(214) Conger KL, Liu JS, Kuo SR, Chow LT, Wang TS. Human papillomavirus DNA replication. Interactions between the viral E1 protein and two subunits of human dna polymerase alpha/primase. J Biol Chem 1999 Jan 29;274(5):2696-705.

(215) Loo YM, Melendy T. Recruitment of replication protein A by the papillomavirus E1 protein and modulation by single-stranded DNA. J Virol 2004 Feb;78(4):1605-15.

(216) Hamid NA, Brown C, Gaston K. The regulation of cell proliferation by the papillomavirus early proteins. Cell Mol Life Sci 2009 May;66(10):1700-17.

(217) de Prat-Gay G, Gaston K, Cicero DO. The papillomavirus E2 DNA binding domain. Front Biosci 2008;13:6006-21.

(218) Mohr IJ, Clark R, Sun S, Androphy EJ, MacPherson P, Botchan MR. Targeting the E1 replication protein to the papillomavirus origin of replication by complex formation with the E2 transactivator. Science 1990 Dec 21;250(4988):1694-9.

(219) Boner W, Taylor ER, Tsirimonaki E, Yamane K, Campo MS, Morgan IM. A Functional interaction between the human papillomavirus 16 transcription/replication factor E2 and the DNA damage response protein TopBP1. J Biol Chem 2002 Jun 21;277(25):22297-303.

(220) Francis DA, Schmid SI, Howley PM. Repression of the integrated papillomavirus E6/E7 promoter is required for growth suppression of cervical cancer cells. J Virol 2000 Mar;74(6):2679-86.

(221) Nishimura A, Ono T, Ishimoto A, Dowhanick JJ, Frizzell MA, Howley PM, et al. Mechanisms of human papillomavirus E2-mediated repression of viral oncogene expression and cervical cancer cell growth inhibition. J Virol 2000 Apr;74(8):3752-60.

(222) Demeret C, Garcia-Carranca A, Thierry F. Transcription-independent triggering of the extrinsic pathway of apoptosis by human papillomavirus 18 E2 protein. Oncogene 2003 Jan 16;22(2):168-75.

(223) Desaintes C, Goyat S, Garbay S, Yaniv M, Thierry F. Papillomavirus E2 induces p53-independent apoptosis in HeLa cells. Oncogene 1999 Aug 12;18(32):4538-45.

(224) Bastien N, McBride AA. Interaction of the papillomavirus E2 protein with mitotic chromosomes. Virology 2000 Apr 25;270(1):124-34.

(225) Parish JL, Bean AM, Park RB, Androphy EJ. ChlR1 is required for loading papillomavirus E2 onto mitotic chromosomes and viral genome maintenance. Mol Cell 2006 Dec 28;24(6):867-76.

(226) You J, Croyle JL, Nishimura A, Ozato K, Howley PM. Interaction of the bovine papillomavirus E2 protein with Brd4 tethers the viral DNA to host mitotic chromosomes. Cell 2004 Apr 30;117(3):349-60.

(227) Zheng PS, Brokaw J, McBride AA. Conditional mutations in the mitotic chromosome binding function of the bovine papillomavirus type 1 E2 protein. J Virol 2005 Feb;79(3):1500-9.

(228) Roden RBSaVRP. Impact of PV-like Particle Technology. In: Campo MS, editor. Papillomavirus research from natural history to vaccines and beyond. 1 ed. Caister Academic press; 2006. p. 279-310.

(229) Evans TG, Bonnez W, Rose RC, Koenig S, Demeter L, Suzich JA, et al. A Phase 1 study of a recombinant viruslike particle vaccine against human papillomavirus type 11 in healthy adult volunteers. J Infect Dis 2001 May 15;183(10):1485-93.

(230) Harro CD, Pang YY, Roden RB, Hildesheim A, Wang Z, Reynolds MJ, et al. Safety and immunogenicity trial in adult volunteers of a human papillomavirus 16 L1 virus-like particle vaccine. J Natl Cancer Inst 2001 Feb 21;93(4):284-92.

(231) Nardelli-Haefliger D, Wirthner D, Schiller JT, Lowy DR, Hildesheim A, Ponci F, et al. Specific antibody levels at the cervix during the menstrual cycle of women vaccinated with human papillomavirus 16 virus-like particles. J Natl Cancer Inst 2003 Aug 6;95(15):1128-37.

(232) Romanowski B, de Borba PC, Naud PS, Roteli-Martins CM, De Carvalho NS, Teixeira JC, et al. Sustained efficacy and immunogenicity of the human papillomavirus (HPV)-16/18 AS04-adjuvanted vaccine: analysis of a randomised placebo-controlled trial up to 6.4 years. Lancet 2009 Dec 12;374(9706):1975-85.

(233) Villa LL, Costa RL, Petta CA, Andrade RP, Ault KA, Giuliano AR, et al. Prophylactic quadrivalent human papillomavirus (types 6, 11, 16, and 18) L1 virus-like particle vaccine in young women: a randomised double-blind placebo-controlled multicentre phase II efficacy trial. Lancet Oncol 2005 May;6(5):271-8.

(234) Villa LL, Costa RL, Petta CA, Andrade RP, Paavonen J, Iversen OE, et al. High sustained efficacy of a prophylactic quadrivalent human papillomavirus types 6/11/16/18 L1 virus-like particle vaccine through 5 years of follow-up. Br J Cancer 2006 Dec 4;95(11):1459-66.

(235) Harper DM, Franco EL, Wheeler C, Ferris DG, Jenkins D, Schuind A, et al. Efficacy of a bivalent L1 virus-like particle vaccine in prevention of infection with human papillomavirus types 16 and 18 in young women: a randomised controlled trial. Lancet 2004 Nov 13;364(9447):1757-65.

(236) Harper DM, Franco EL, Wheeler CM, Moscicki AB, Romanowski B, Roteli-Martins CM, et al. Sustained efficacy up to 4.5 years of a bivalent L1 virus-like particle vaccine against human papillomavirus types 16 and 18: follow-up from a randomised control trial. Lancet 2006 Apr 15;367(9518):1247-55.

(237) Schiller JT, Castellsague X, Villa LL, Hildesheim A. An update of prophylactic human papillomavirus L1 virus-like particle vaccine clinical trial results. Vaccine 2008 Aug 19;26 Suppl 10:K53-K61.

(238) Jagu S, Karanam B, Gambhira R, Chivukula SV, Chaganti RJ, Lowy DR, et al. Concatenated multitype L2 fusion proteins as candidate prophylactic pan-human papillomavirus vaccines. J Natl Cancer Inst 2009 Jun 3;101(11):782-92.

(239) Slupetzky K, Gambhira R, Culp TD, Shafti-Keramat S, Schellenbacher C, Christensen ND, et al. A papillomavirus-like particle (VLP) vaccine displaying HPV16 L2 epitopes induces cross-neutralizing antibodies to HPV11. Vaccine 2007 Mar 1;25(11):2001-10.

(240) Hellner K, Munger K. Human Papillomaviruses As Therapeutic Targets in Human Cancer. J Clin Oncol 2011 Jan 10.

(241) Welters MJ, Kenter GG, Piersma SJ, Vloon AP, Lowik MJ, Berends-van der Meer DM, et al. Induction of tumor-specific CD4+ and CD8+ T-cell immunity in cervical cancer patients by a human papillomavirus type 16 E6 and E7 long peptides vaccine. Clin Cancer Res 2008 Jan 1;14(1):178-87.

(242) Kenter GG, Welters MJ, Valentijn AR, Lowik MJ, Berends-van der Meer DM, Vloon AP, et al. Vaccination against HPV-16 oncoproteins for vulvar intraepithelial neoplasia. N Engl J Med 2009 Nov 5;361(19):1838-47.

(243) Faucher AM, White PW, Brochu C, Grand-Maitre C, Rancourt J, Fazal G. Discovery of small-molecule inhibitors of the ATPase activity of human papillomavirus E1 helicase. J Med Chem 2004 Jan 1;47(1):18-21.

(244) Fradet-Turcotte A, Archambault J. Recent advances in the search for antiviral agents against human papillomaviruses. Antivir Ther 2007;12(4):431-51.

(245) Boner W, Morgan IM. Novel cellular interacting partners of the human papillomavirus 16 transcription/replication factor E2. Virus Res 2002 Dec;90(1-2):113-8.

(246) Yamane K, Kawabata M, Tsuruo T. A DNA-topoisomerase-II-binding protein with eight repeating regions similar to DNA-repair enzymes and to a cell-cycle regulator. Eur J Biochem 1997 Dec 15;250(3):794-9.

(247) Yamane K, Tsuruo T. Conserved BRCT regions of TopBP1 and of the tumor suppressor BRCA1 bind strand breaks and termini of DNA. Oncogene 1999 Sep 16;18(37):5194-203.

(248) Going JJ, Nixon C, Dornan ES, Boner W, Donaldson MM, Morgan IM. Aberrant expression of TopBP1 in breast cancer. Histopathology 2007 Mar;50(4):418-24.

(249) Karppinen SM, Erkko H, Reini K, Pospiech H, Heikkinen K, Rapakko K, et al. Identification of a common polymorphism in the TopBP1 gene associated with hereditary susceptibility to breast and ovarian cancer. Eur J Cancer 2006 Oct;42(15):2647-52.

(250) Makiniemi M, Hillukkala T, Tuusa J, Reini K, Vaara M, Huang D, et al. BRCT domain-containing protein TopBP1 functions in DNA replication and damage response. J Biol Chem 2001 Aug 10;276(32):30399-406.

(251) Furuya K, Poitelea M, Guo L, Caspari T, Carr AM. Chk1 activation requires Rad9 S/TQ-site phosphorylation to promote association with C-terminal BRCT domains of Rad4TOPBP1. Genes Dev 2004 May 15;18(10):1154-64.

(252) Greer DA, Besley BD, Kennedy KB, Davey S. hRad9 rapidly binds DNA containing double-strand breaks and is required for damage-dependent topoisomerase II beta binding protein 1 focus formation. Cancer Res 2003 Aug 15;63(16):4829-35.

(253) Hashimoto Y, Tsujimura T, Sugino A, Takisawa H. The phosphorylated C-terminal domain of Xenopus Cut5 directly mediates ATR-dependent activation of Chk1. Genes Cells 2006 Sep;11(9):993-1007.

(254) Kumagai A, Lee J, Yoo HY, Dunphy WG. TopBP1 activates the ATR-ATRIP complex. Cell 2006 Mar 10;124(5):943-55.

(255) Liu S, Bekker-Jensen S, Mailand N, Lukas C, Bartek J, Lukas J. Claspin operates downstream of TopBP1 to direct ATR signaling towards Chk1 activation. Mol Cell Biol 2006 Aug;26(16):6056-64.

(256) Mordes DA, Glick GG, Zhao R, Cortez D. TopBP1 activates ATR through ATRIP and a PIKK regulatory domain. Genes Dev 2008 Jun 1;22(11):1478-89.

(257) Yan S, Lindsay HD, Michael WM. Direct requirement for Xmus101 in ATR-mediated phosphorylation of Claspin bound Chk1 during checkpoint signaling. J Cell Biol 2006 Apr 24;173(2):181-6.

(258) Shiloh Y. ATM and related protein kinases: safeguarding genome integrity. Nat Rev Cancer 2003 Mar;3(3):155-68.

(259) Van Hatten RA, Tutter AV, Holway AH, Khederian AM, Walter JC, Michael WM. The Xenopus Xmus101 protein is required for the recruitment of Cdc45 to origins of DNA replication. J Cell Biol 2002 Nov 25;159(4):541-7.

(260) Kim JE, McAvoy SA, Smith DI, Chen J. Human TopBP1 ensures genome integrity during normal S phase. Mol Cell Biol 2005 Dec;25(24):10907-15.

(261) Donaldson MM, Boner W, Morgan IM. TopBP1 regulates human papillomavirus type 16 E2 interaction with chromatin. J Virol 2007 Apr;81(8):4338-42.

(262) Liu K, Lin FT, Ruppert JM, Lin WC. Regulation of E2F1 by BRCT domain-containing protein TopBP1. Mol Cell Biol 2003 May;23(9):3287-304.

(263) Liu K, Luo Y, Lin FT, Lin WC. TopBP1 recruits Brg1/Brm to repress E2F1-induced apoptosis, a novel pRb-independent and E2F1-specific control for cell survival. Genes Dev 2004 Mar 15;18(6):673-86.

(264) Herold S, Wanzel M, Beuger V, Frohme C, Beul D, Hillukkala T, et al. Negative regulation of the mammalian UV response by Myc through association with Miz-1. Mol Cell 2002 Sep;10(3):509-21.

(265) Sjottem E, Rekdal C, Svineng G, Johnsen SS, Klenow H, Uglehus RD, et al. The ePHD protein SPBP interacts with TopBP1 and together they co-operate to stimulate Ets1-mediated transcription. Nucleic Acids Res 2007;35(19):6648-62.

(266) Wright RH, Dornan ES, Donaldson MM, Morgan IM. TopBP1 contains a transcriptional activation domain suppressed by two adjacent BRCT domains. Biochem J 2006 Dec 15;400(3):573-82.

(267) Boukamp P, Petrussevska RT, Breitkreutz D, Hornung J, Markham A, Fusenig NE. Normal keratinization in a spontaneously immortalized aneuploid human keratinocyte cell line. J Cell Biol 1988 Mar;106(3):761-71.

(268) Taylor ER, Boner W, Dornan ES, Corr EM, Morgan IM. UVB irradiation reduces the half-life and transactivation potential of the human papillomavirus 16 E2 protein. Oncogene 2003 Jul 17;22(29):4469-77.

(269) Vance KW, Campo MS, Morgan IM. An enhanced epithelial response of a papillomavirus promoter to transcriptional activators. J Biol Chem 1999 Sep 24;274(39):27839-44.

(270) Bouvard V, Storey A, Pim D, Banks L. Characterization of the human papillomavirus E2 protein: evidence of trans-activation and trans-repression in cervical keratinocytes. EMBO J 1994 Nov 15;13(22):5451-9.

(271) Sakai H, Yasugi T, Benson JD, Dowhanick JJ, Howley PM. Targeted mutagenesis of the human papillomavirus type 16 E2 transactivation domain reveals separable transcriptional activation and DNA replication functions. J Virol 1996 Mar;70(3):1602-11.

(272) Kadaja M, Sumerina A, Verst T, Ojarand M, Ustav E, Ustav M. Genomic instability of the host cell induced by the human papillomavirus replication machinery. EMBO J 2007 Apr 18;26(8):2180-91.

(273) Taylor ER, Morgan IM. A novel technique with enhanced detection and quantitation of HPV-16 E1- and E2-mediated DNA replication. Virology 2003 Oct 10;315(1):103-9.

(274) Akgul B, Karle P, Adam M, Fuchs PG, Pfister HJ. Dual role of tumor suppressor p53 in regulation of DNA replication and oncogene E6-promoter activity of epidermodysplasia verruciformis-associated human papillomavirus type 8. Virology 2003 Apr 10;308(2):279-90.

(275) Moosa MR, Gralla J. Skin cancer in renal allograft recipients--experience in different ethnic groups residing in the same geographical region. Clin Transplant 2005 Dec;19(6):735-41.

(276) Carroll RP, Ramsay HM, Fryer AA, Hawley CM, Nicol DL, Harden PN. Incidence and prediction of nonmelanoma skin cancer post-renal transplantation: a prospective study in Queensland, Australia. Am J Kidney Dis 2003 Mar;41(3):676-83.

(277) Naldi L, Fortina AB, Lovati S, Barba A, Gotti E, Tessari G, et al. Risk of nonmelanoma skin cancer in Italian organ transplant recipients. A registry-based study. Transplantation 2000 Nov 27;70(10):1479-84.

(278) Moloney FJ, Comber H, O'Lorcain P, O'Kelly P, Conlon PJ, Murphy GM. A population-based study of skin cancer incidence and prevalence in renal transplant recipients. Br J Dermatol 2006 Mar;154(3):498-504.

(279) Bordea C, Wojnarowska F, Millard PR, Doll H, Welsh K, Morris PJ. Skin cancers in renal-transplant recipients occur more frequently than previously recognized in a temperate climate. Transplantation 2004 Feb 27;77(4):574-9.

(280) Staples M, Marks R, Giles G. Trends in the incidence of non-melanocytic skin cancer (NMSC) treated in Australia 1985-1995: are primary prevention programs starting to have an effect? Int J Cancer 1998 Oct 5;78(2):144-8.

(281) Proby CM, Wisgerhof HC, Casabonne D, Green A, Harwood CA, Bouwes Bavinck JN. The epidemiology of transplant-associated keratinocyte cancers in different geographical regions. In: Stockfleth E, Ulrich C, Euvrard S, Proby C, Bouwes Bavinck JN, Geissler EK, editors. Skin Cancer After Organ Transplantation. Springer; 2009. p. 75-95.

(282) Dantal J, Hourmant M, Cantarovich D, Giral M, Blancho G, Dreno B, et al. Effect of long-term immunosuppression in kidney-graft recipients on cancer incidence: randomised comparison of two cyclosporin regimens. Lancet 1998 Feb 28;351(9103):623-8.

(283) Glover MT, Deeks JJ, Raftery MJ, Cunningham J, Leigh IM. Immunosuppression and risk of non-melanoma skin cancer in renal transplant recipients. Lancet 1997 Feb 8;349(9049):398.

(284) Kehinde EO, Petermann A, Morgan JD, Butt ZA, Donnelly PK, Veitch PS, et al. Triple therapy and incidence of de novo cancer in renal transplant recipients. Br J Surg 1994 Jul;81(7):985-6.

(285) Bouwes Bavinck JN, Stark S, Petridis AK, Marugg ME, Ter SJ, Westendorp RG, et al. The presence of antibodies against virus-like particles of epidermodysplasia verruciformis-associated humanpapillomavirus type 8 in patients with actinic keratoses. Br J Dermatol 2000 Jan;142(1):103-9.

(286) Feltkamp MC, Broer R, di Summa FM, Struijk L, van der Meijden E, Verlaan BP, et al. Seroreactivity to epidermodysplasia verruciformis-related human papillomavirus types is associated with nonmelanoma skin cancer. Cancer Res 2003 May 15;63(10):2695-700.

(287) Harwood CA, Surentheran T, Sasieni P, Proby CM, Bordea C, Leigh IM, et al. Increased risk of skin cancer associated with the presence of epidermodysplasia verruciformis human papillomavirus types in normal skin. Br J Dermatol 2004 May;150(5):949-57.

(288) Steger G, Olszewsky M, Stockfleth E, Pfister H. Prevalence of antibodies to human papillomavirus type 8 in human sera. J Virol 1990 Sep;64(9):4399-406.

(289) Berkhout RJ, Bouwes Bavinck JN, Ter SJ. Persistence of human papillomavirus DNA in benign and (pre)malignant skin lesions from renal transplant recipients. J Clin Microbiol 2000 Jun;38(6):2087-96.

(290) Winkelhorst JT, Brokelman WJ, Tiggeler RG, Wobbes T. Incidence and clinical course of de-novo malignancies in renal allograft recipients. Eur J Surg Oncol 2001 Jun;27(4):409-13.

(291) Penn I. Cancers of the anogenital region in renal transplant recipients. Analysis of 65 cases. Cancer 1986 Aug 1;58(3):611-6.

(292) Sheil AG, Flavel S, Disney AP, Mathew TH, Hall BM. Cancer incidence in renal transplant patients treated with azathioprine or cyclosporine. Transplant Proc 1987 Feb;19(1 Pt 3):2214-6.

(293) De CL, Slim AO, De GA, Muti G, Giacomoni A, Di BF, et al. Posttransplant lymphoproliferative disorders: report from a single center. Transplant Proc 2001 Aug;33(5):2815-6.

(294) Forslund O, Iftner T, Andersson K, Lindelof B, Hradil E, Nordin P, et al. Cutaneous human papillomaviruses found in sun-exposed skin: Beta-papillomavirus species 2 predominates in squamous cell carcinoma. J Infect Dis 2007 Sep 15;196(6):876-83.

(295) Pfister H. Chapter 8: Human papillomavirus and skin cancer. J Natl Cancer Inst Monogr 2003;(31):52-6.

(296) Hopfl R, Bens G, Wieland U, Petter A, Zelger B, Fritsch P, et al. Human papillomavirus DNA in non-melanoma skin cancers of a renal transplant recipient: detection of a new sequence related to epidermodysplasia verruciformis associated types. J Invest Dermatol 1997 Jan;108(1):53-6.

(297) de Villiers EM, Lavergne D, McLaren K, Benton EC. Prevailing papillomavirus types in non-melanoma carcinomas of the skin in renal allograft recipients. Int J Cancer 1997 Nov 4;73(3):356-61.

(298) Harwood CA, Surentheran T, McGregor JM, Spink PJ, Leigh IM, Breuer J, et al. Human papillomavirus infection and non-melanoma skin cancer in immunosuppressed and immunocompetent individuals. J Med Virol 2000 Jul;61(3):289-97.

(299) Pfister H, Fuchs PG, Majewski S, Jablonska S, Pniewska I, Malejczyk M. High prevalence of epidermodysplasia verruciformis-associated human papillomavirus DNA in actinic keratoses of the immunocompetent population. Arch Dermatol Res 2003 Dec;295(7):273-9.

(300) de Jong-Tieben LM, Berkhout RJ, Smits HL, Bouwes Bavinck JN, Vermeer BJ, van der Woude FJ, et al. High frequency of detection of epidermodysplasia verruciformis-associated human papillomavirus DNA in biopsies from malignant and premalignant skin lesions from renal transplant recipients. J Invest Dermatol 1995 Sep;105(3):367-71.

(301) Klaes R, Benner A, Friedrich T, Ridder R, Herrington S, Jenkins D, et al. p16INK4a immunohistochemistry improves interobserver agreement in the diagnosis of cervical intraepithelial neoplasia. Am J Surg Pathol 2002 Nov;26(11):1389-99.

(302) Williams GH, Romanowski P, Morris L, Madine M, Mills AD, Stoeber K, et al. Improved cervical smear assessment using antibodies against proteins that regulate DNA replication. Proc Natl Acad Sci U S A 1998 Dec 8;95(25):14932-7.

(303) Pirog EC, Baergen RN, Soslow RA, Tam D, DeMattia AE, Chen YT, et al. Diagnostic Accuracy of Cervical Low-Grade Squamous Intraepithelial Lesions Is Improved With MIB-1 Immunostaining. Am J Surg Pathol 2002 Jan;26(1):70-5.

(304) Gerdes J, Lemke H, Baisch H, Wacker HH, Schwab U, Stein H. Cell cycle analysis of a cell proliferation-associated human nuclear antigen defined by the monoclonal antibody Ki-67. J Immunol 1984 Oct;133(4):1710-5.

(305) Conscience I, Jovenin N, Coissard C, Lorenzato M, Durlach A, Grange F, et al. P16 is overexpressed in cutaneous carcinomas located on sun-exposed areas. Eur J Dermatol 2006 Sep;16(5):518-22.

(306) Onodera H, Nakamura S, Sugai T. Cell proliferation and p53 protein expressions in cutaneous epithelial neoplasms. Am J Dermatopathol 1996 Dec;18(6):580-8.

(307) Mitsuishi T, Kawana S, Kato T, Kawashima M. Human papillomavirus infection in actinic keratosis and bowen's disease: comparative study with expression of cell-cycle regulatory proteins p21(Waf1/Cip1), p53, PCNA, Ki-67, and Bcl-2 in positive and negative lesions. Hum Pathol 2003 Sep;34(9):886-92.

(308) Kanitakis J, Narvaez D, Euvrard S, Faure M, Claudy A. Proliferation markers Ki67 and PCNA in cutaneous squamous cell carcinomas: lack of prognostic value. Br J Dermatol 1997 Apr;136(4):643-4.

(309) Mansoor A, McKee PH, Simpson JA, McGuire B, Hobbs C. Prognostic significance of Ki-67 and p53 immunoreactivity in cutaneous squamous cell carcinomas. Am J Dermatopathol 1996 Aug;18(4):351-7.

(310) Freeman A, Morris LS, Mills AD, Stoeber K, Laskey RA, Williams GH, et al. Minichromosome maintenance proteins as biological markers of dysplasia and malignancy. Clin Cancer Res 1999 Aug;5(8):2121-32.

(311) Liu H, Takeuchi S, Moroi Y, Lin N, Urabe K, Kokuba H, et al. Expression of minichromosome maintenance 5 protein in proliferative and malignant skin diseases. Int J Dermatol 2007 Nov;46(11):1171-6.

(312) McNutt NS, Saenz-Santamaria C, Volkenandt M, Shea CR, Albino AP. Abnormalities of p53 protein expression in cutaneous disorders. Arch Dermatol 1994 Feb;130(2):225-32.

(313) Steger G, Pfister H. In vitro expressed HPV 8 E6 protein does not bind p53. Arch Virol 1992;125(1-4):355-60.

(314) Jackson S, Harwood C, Thomas M, Banks L, Storey A. Role of Bak in UV-induced apoptosis in skin cancer and abrogation by HPV E6 proteins. Genes Dev 2000 Dec 1;14(23):3065-73.

(315) O'Connor DP, Kay EW, Leader M, Murphy GM, Atkins GJ, Mabruk MJ. Altered p53 expression in benign and malignant skin lesions from renal transplant recipients and immunocompetent patients with skin cancer: correlation with human papillomaviruses? Diagn Mol Pathol 2001 Sep;10(3):190-9.

(316) Pelisson I, Chardonnet Y, Euvrard S, Schmitt D. Immunohistochemical detection of p53 protein in cutaneous lesions from transplant recipients harbouring human papillomavirus DNA. Virchows Arch 1994;424(6):623-30.

(317) Stark LA, Arends MJ, McLaren KM, Benton EC, Shahidullah H, Hunter JA, et al. Accumulation of p53 is associated with tumour progression in cutaneous lesions of renal allograft recipients. Br J Cancer 1994 Oct;70(4):662-7.

(318) Sherr CJ. Cancer cell cycles. Science 1996 Dec 6;274(5293):1672-7.

(319) Russo AA, Tong L, Lee JO, Jeffrey PD, Pavletich NP. Structural basis for inhibition of the cyclin-dependent kinase Cdk6 by the tumour suppressor p16INK4a. Nature 1998 Sep 17;395(6699):237-43.

(320) Klaes R, Benner A, Friedrich T, Ridder R, Herrington S, Jenkins D, et al. p16INK4a immunohistochemistry improves interobserver agreement in the diagnosis of cervical intraepithelial neoplasia. Am J Surg Pathol 2002 Nov;26(11):1389-99.

(321) Hodges A, Smoller BR. Immunohistochemical comparison of p16 expression in actinic keratoses and squamous cell carcinomas of the skin. Mod Pathol 2002 Nov;15(11):1121-5.

(322) Salama ME, Mahmood MN, Qureshi HS, Ma C, Zarbo RJ, Ormsby AH. p16INK4a expression in actinic keratosis and Bowen's disease. Br J Dermatol 2003 Nov;149(5):1006-12.

(323) Nilsson K, Svensson S, Landberg G. Retinoblastoma protein function and p16INK4a expression in actinic keratosis, squamous cell carcinoma in situ and invasive squamous cell carcinoma of the skin and links between p16INK4a expression and infiltrative behavior. Mod Pathol 2004 Dec;17(12):1464-74.

(324) Nindl I, Meyer T, Schmook T, Ulrich C, Ridder R, Audring H, et al. Human papillomavirus and overexpression of P16INK4a in nonmelanoma skin cancer. Dermatol Surg 2004 Mar;30(3):409-14.

(325) Willman JH, Heinz D, Golitz LE, Shroyer KR. Correlation of p16 and pRb expression with HPV detection in Bowen's disease. J Cutan Pathol 2006 Sep;33(9):629-33.

(326) Johansson C, Graham SV, Dornan ES, Morgan IM. The human papillomavirus 16 E2 protein is stabilised in S phase. Virology 2009 Nov 25;394(2):194-9.

(327) Jeon Y, Lee KY, Ko MJ, Lee YS, Kang S, Hwang DS. Human TopBP1 participates in cyclin E/CDK2 activation and preinitiation complex assembly during G1/S transition. J Biol Chem 2007 May 18;282(20):14882-90.

(328) Boukamp P, Petrussevska RT, Breitkreutz D, Hornung J, Markham A, Fusenig NE. Normal keratinization in a spontaneously immortalized aneuploid human keratinocyte cell line. J Cell Biol 1988 Mar;106(3):761-71.

(329) Irizarry RA, Bolstad BM, Collin F, Cope LM, Hobbs B, Speed TP. Summaries of Affymetrix GeneChip probe level data. Nucleic Acids Res 2003 Feb 15;31(4):e15.

(330) Jeon Y, Lee KY, Ko MJ, Lee YS, Kang S, Hwang DS. Human TopBP1 participates in cyclin E/CDK2 activation and preinitiation complex assembly during G1/S transition. J Biol Chem 2007 May 18;282(20):14882-90.

(331) Liu K, Bellam N, Lin HY, Wang B, Stockard CR, Grizzle WE, et al. Regulation of p53 by TopBP1: a potential mechanism for p53 inactivation in cancer. Mol Cell Biol 2009 May;29(10):2673-93.

(332) Cimprich KA, Cortez D. ATR: an essential regulator of genome integrity. Nat Rev Mol Cell Biol 2008 Aug;9(8):616-27.

(333) Melar-New M, Laimins LA. Human papillomaviruses modulate expression of microRNA 203 upon epithelial differentiation to control levels of p63 proteins. J Virol 2010 May;84(10):5212-21.

(334) Moody CA, Fradet-Turcotte A, Archambault J, Laimins LA. Human papillomaviruses activate caspases upon epithelial differentiation to induce viral genome amplification. Proc Natl Acad Sci U S A 2007 Dec 4;104(49):19541-6.

(335) Moody CA, Laimins LA. Human papillomaviruses activate the ATM DNA damage pathway for viral genome amplification upon differentiation. PLoS Pathog 2009 Oct;5(10):e1000605.